Regulation of Energy Mobilization in Rainbow Trout: Metabolic Fluxes and Signaling

Giancarlo G.M. Talarico

Thesis submitted to the University of Ottawa in partial fulfillment of the requirements for a Master's degree of Science in Biology

Department of Biology
Faculty of Science
University of Ottawa

Regulation of Energy Mobilization in Rainbow Trout: Metabolic Fluxes and Signaling

TABLE OF CONTENTS

ACKNOWLEDGEMENTS vi
ABSTRACT vii
RÉSUMÉ ix
LIST OF FIGURES AND TABLES xi
LIST OF ABBREVIATIONS xiv
Chapter 1: General Introduction 1
Rainbow trout as a research model in the comparative physiology of metabolic fuel selection 2
The importance of glucoregulation in metabolic fuel selection 2
Endogenous glucose production and regulation 4
Lactate as a metabolic fuel and its retention in white muscle 5
Lactate as a metabolic signal 6
Lipid mobilization and metabolism 8
Fatty acids as metabolic signals 10
Integrating whole-body fluxes with measurements of gene expression, protein signaling and enzyme activities 11
Thesis objectives 12
Chapter 2: Lactate signaling for fuel selection: Mobilization of energy reserves 15
Introduction 16
Methods 17
Animals 17
Catheterization 20
Glucose and glycerol kinetics (series 1 and 2) 20
Plasma sample analyses 22
Tissue measurements (series 3) 23
RNA extraction and gene expression 24
Western blotting 25
Enzyme activities 27
Calculations and statistics 29
Results 29
Series 1: Glucose kinetics 29
Series 2: Glycerol kinetics 30
Series 3: Gene expression, protein signaling and enzyme activities 40
Discussion 55
Lactate infusion protocol mimics strenuous exercise 55
High lactate does not inhibit fish lipolysis 56
High lactate reduces hepatic glucose production 58

Glucose, lactate and lipid oxidation 60
Differential oxidative fuel selection in red and white muscle 61
Lipolytic rate cannot be predicted from changes in glycerol concentration 63

Chapter 3: Mobilization of energy reserves during Intralipid infusion 64
Introduction 65
Methods 66
Animals 66
Catheterizations 69
Glycerol and glucose kinetics (series 1 and 2) 69
Plasma sample analyses 70
Tissue measurements (series 3) 71
Fatty acid analysis 72
RNA extraction and gene expression 73
Western blotting 75
Enzyme activities 76
Calculations and statistics 77
Results 79
Fatty acid composition of circulating lipids 79
Series 1: Glycerol kinetics 82
Series 2: Glucose kinetics 82
Series 3: Gene expression, protein signaling and enzyme activities 88
Discussion 102
Intralipid induces hyperlipidemia and alters fatty acid composition in trout 102
Effects of Intralipid on lipolytic rate 103
Suppression of endogenous lipid metabolism in response to Intralipid 104
How Intralipid modulates glycerol and lipid utilization 105
How Intralipid modulates glucose utilization 109

Chapter 4: General Conclusions and Future Directions 111
Insights into fuel mobilization and selection in rainbow trout 112
G-protein coupled receptors as molecular mediators of fuel selection 113
The molecular evolution of lactate and long chain fatty acid metabolite sensing in vertebrates with a focus on teleost fish 115
Novel insights into G-protein coupled receptors may explain hyperlipolysis in rainbow trout 135
Limitations 135
Future directions and final remarks 137

SUPPLEMENTAL 139
APPENDIX 149

The mammalian insulin antagonist S961 does not exhibit insulin receptor antagonism in rainbow trout *in vivo* 151
Abstract 152
Introduction 152
Methods 154
Animals 154
Feeding status experiment (series 1) 155
Insulin infusion experiment (series 2) 156
Western blot analysis of insulin signaling pathway 157
Glucose concentration analysis 157
In silico characterization of rainbow trout insulin receptor paralogues 158
Calculations and statistics 158
Results 159
Postprandial insulin signaling is not attenuated by S961 159
Bolus S961 injection and exogenous insulin do not attenuate insulin signaling and fail to increase circulating glucose concentration 160
In silico analysis reveals sequential duplication events of insulin receptor loci in teleost fish and conservation of key residues involved in insulin binding 161
Discussion 183
S961 does not induce signaling or metabolic changes indicative of insulin receptor antagonism in rainbow trout 183
In silico analysis identifies differences in the fish insulin receptor as a possible reason for the lack of S961 activity in rainbow trout 184
REFERENCES 188

ACKNOWLEDGEMENTS

I want to first and foremost thank my supervisors, Dr. Jean-Michel Weber and Dr. Jan Mennigen, for their exceptional guidance and mentorship during the years in their labs. Your constructive criticism and faith in my abilities inspired me to become a better biologist. I would also like to thank my committee members, Dr. Jenny Bruin and Dr. Katie Gilmour, for their valuable feedback and support. A special thanks go to Dr. Elie Farhat, Mais Jubouri and Dr. Elisa Thoral for their support and patience in teaching me the skills necessary for success. It has been a privilege to collaborate with Dr. Elie Farhat and Dr. Dapeng Zhang on chapters of my thesis in addition to other projects not included here. To all other current and former lab members, thank you for your help and support. Furthermore, I want to thank all the animal care personnel for ensuring the animals were well taken care of. Finally, I would like to especially thank my family for their love and continuous support through my pursuit of a Master's degree. My parents, Ross and Antonietta Talarico, have always inspired me to be confident and persevere in accomplishing my goals. I am incredibly lucky and blessed to have you as my parents.

ABSTRACT

Rainbow trout (*Oncorhynchus mykiss*) is an important freshwater fish whose glucose intolerance, white muscle lactate retention and high lipolytic inertia, have interested comparative physiologists for decades. Recent advancements in mammalian G-protein coupled receptor deorphanization research have identified many endogenous metabolites as regulators of energy metabolism, including lactate and long-chain fatty acids. In addition to being essential metabolic fuels, lactate and long-chain fatty acids regulate lipolysis and lipogenesis by binding to hydroxycarboxylic acid receptor 1 (HCAR1) and the free fatty acid receptors (FFAR1 and 4), respectively. Therefore, the goal of this thesis was to quantify the effects of exogenous lactate and lipids on glucose and fatty acid mobilization in rainbow trout and identify potential signaling mechanisms by monitoring the expression and activity of key glycolytic, gluconeogenic, lipolytic, lipogenic and β-oxidation targets in the liver, muscle and adipose tissue. In Chapter 2, *in vivo* measurements of metabolic fuel kinetics show that lactate (i) strongly reduced hepatic glucose production by substituting glucose for lactate and (ii) exhibited no lipolytic suppression suggesting HCAR1 signaling is weak in trout. In Chapter 3, *in vivo* measurements of energy mobilization show that Intralipid strongly induced lipolysis by saturating circulating lipases while transcriptional induction of gluconeogenesis compensates for the acute reduction in hepatic glucose production. Intralipid infusion increased total fatty acid concentration and altered fatty acid composition while suppressing lipid metabolism of trout liver and adipose tissue. In Chapter 4, I identify the presence (*hcar1* and *ffar1*) and absence (*ffar4*) of these G-protein coupled receptor genes in the rainbow trout genome and describe their evolutionary origins, using *in*

silico approaches of microsynteny, amino acid sequence similarity and critical residue conservation. However, their importance in fish physiology remains relatively unknown, thus future studies are warranted to further investigate such metabolic signals.

RÉSUMÉ

La truite arc-en-ciel (*Oncorhynchus mykiss*) est un poisson important d'eau douce dont l'intolérance au glucose, la rétention de lactate dans les muscles blancs et la forte inertie lipolytique, intéressent les physiologistes comparatifs depuis des décennies. Les progrès récents de la recherche sur la déorphanisation des récepteurs couplés aux protéines G des mammifères ont permis d'identifier de nombreux métabolites endogènes comme régulateurs du métabolisme énergétique, notamment le lactate et les acides gras à longue-chaîne. En plus d'être des carburants métaboliques essentiels, le lactate et les acides gras à longue-chaîne régulent la lipolyse et la lipogenèse en se liant au récepteur de l'acide hydroxycarboxylique 1 (HCAR1) et aux récepteurs des acides gras libres (FFAR1 et 4), respectivement. Par conséquent, l'objectif de cette thèse était de quantifier les effets du lactate et des lipides exogènes sur la mobilisation du glucose et des acides gras chez la truite arc-en-ciel et d'identifier les mécanismes de signallisation potentiels en surveillant l'expression et l'activité de cibles glycolytiques, gluconéogéniques, lipolytiques, lipogéniques et de β-oxydation clés dans le foie, le muscle et le tissu adipeux. Dans le deuxième chapitre, les mesures *in vivo* de la cinétique des carburants métaboliques montrent que le lactate (i) réduitsentfortement la production hépatique de glucose en substituant le glucose au lactate et (ii) ne présentent aucune suppression lipolytique suggérant que la signallisation HCAR1 est faible chez la truite. Dans le troisième chapitre, les mesures *in vivo* de la mobilisation énergétique montrent que l'Intralipide induit fortement la lipolyse en saturant les lipases circulantes tandis que l'induction transcriptionnelle de la gluconéogenèse compense la réduction aiguë de la production hépatique de glucose.

L’administration d’Intralipide augmente la concentration totale d’acides gras tout en ralentissant le métabolisme lipidique du foie et du tissu adipeux de la truite. Dans le quatrième chapitre, j'identifie la présence (*hcar1* et *ffar1*) et l'absence (*ffar4*) de ces gènes de récepteurs couplés aux protéines G dans le génome de la truite arc-en-ciel et je décris leurs origines évolutives, en utilisant des approches *in silico* de microsynténie, de similarité de séquence d'acides aminés et de conservation de résidus critiques. Cependant, leur importance dans la physiologie des poissons reste relativement inconnue, ce qui justifie de futures études pour approfondir la connaissance de ces signaux métaboliques.

LIST OF FIGURES AND TABLES

Chapter 2

Table 2.1. Physical characteristics and hematocrit of the rainbow trout used in lactate-infused experiments 19
Figure 2.1. Circulating glucose (A) and lactate concentrations (B) of rainbow trout while hepatic glucose production was quantified during exogenous lactate infusion 31
Figure 2.2. Effects of exogenous lactate on glucose specific activity (A) and hepatic glucose production (B) in rainbow trout 33
Figure 2.3. Circulating glycerol (A) and lactate concentrations (B) of rainbow trout while lipolytic rate was quantified and during exogenous lactate infusion 35
Figure 2.4. Effects of exogenous lactate on glycerol specific activity (A) and lipolytic rate (B) in rainbow trout 37
Table 2.2. Initial (baseline) and final values after 3 h of lactate administration for the kinetics experiments 39
Table 2.3. Plasma lactate, glucose and glycerol concentration for lactate-infused molecular experiment 41
Figure 2.5. Effects of exogenous lactate on the relative mRNA expression of *hcar1* 44
Figure 2.6. Effects of exogenous lactate on the relative mRNA expression of genes associated with carbohydrate metabolism 46
Figure 2.7. Effects of exogenous lactate on the relative mRNA expression of genes associated with lipid metabolism 48
Figure 2.8. Effects of exogenous lactate on the protein expression of liver Pck1 and muscle Glut4 51
Figure 2.9. Effects of exogenous lactate on the activity of enzymes involved in carbohydrate and lipid metabolism 53

Chapter 3

Table 3.1. Physical characteristics and hematocrit of rainbow trout used in Intralipid-infused experiments 68
Figure 3.1. Effects of Intralipid on circulating fatty acid concentration (A) and omega-3 omega-6 ratio (B) 80
Figure 3.2. Effects of Intralipid on circulating glycerol concentration (A), glycerol specific activity (B) and lipolytic rate (C) 83
Figure 3.3. Effects of Intralipid on circulating glucose concentration (A), glucose specific activity (B) and hepatic glucose production rate (C) 85
Table 3.2. Initial (baseline) and final values after 4 h of Intralipid administration for the kinetics experiments 87
Table 3.3. Plasma glucose and glycerol concentration for Intralipid-infused molecular experiment 89

Figure 3.4. Effects of Intralipid on the relative mRNA expression of genes associated with lipid metabolism 93
Figure 3.5. Effects of Intralipid on the relative mRNA expression of genes associated with carbohydrate metabolism 95
Figure 3.6. Effects of Intralipid on the protein expression of liver Pck1 and Fas in the liver and adipose tissue 98
Figure 3.7. Effects of Intralipid on the activity of enzymes involved in carbohydrate and lipid metabolism 100

Chapter 4

Figure 4.1. Genome-derived amino acid sequences of HCAR-like receptors from fish and other vertebrates were identified as HCAR1 receptors based on conserved critical residues 118
Figure 4.2. Proposed evolution of lactate (HCAR1) and long-chain fatty acid receptor (FFAR1 and FFAR4) in vertebrates 120
Figure 4.3. Genome sequence-derived microsynteny analysis of the *hcar1* locus in select Elasmobranchii + Actinopterygii (A) and Sarcopterygii (B) 121
Figure 4.4. Microsynteny analysis of the mammalian FFAR1 locus across selected vertebrate species 126
Figure 4.5. Overall amino acid sequence similarity of FFAR1(-like), FFAR2(-like) and FFAR3(-like) receptors across vertebrates in relevant loci 127
Figure 4.6. Conservation of amino acid residues critically involved in the mammalian FFAR1 binding pocket in protein sequences extrapolated from genome sequences of FFAR1 and neighboring FFAR-like genes across vertebrates 129
Figure 4.7. Genome sequence-derived microsynteny analysis of the *ffar4* locus in select Elasmobranchii + Actinopterygii (A) and Sarcopterygii (B) 131
Figure 4.8. Genome-derived amino acid sequences of FFAR4 from fish and other vertebrates 133
Figure 4.9. Phylogenetic analysis of *ffar4* (A) and neighboring genes *rbp4* (B) *cep551* (C) and *Igilb* (D) in relevant loci in key fish species 134

Supplemental

Table S2.1. *Real-time* RT-PCR primer sequences and reaction parameters of gene targets involved in glucose transport, glycolysis and gluconeogenesis 140
Table S2.2. *Real-time* RT-PCR primer sequences and reaction parameters of gene targets involved in lipolytic regulation, fatty acid oxidation, transport and synthesis in hyperlactatemic rainbow trout 141
Table S3.1. *Real-time* RT-PCR primer sequences and reaction parameters of gene targets involved in glucose transport, glycolysis and gluconeogenesis in hyperlactatemic rainbow trout 142

Table S3.2. *Real-time* RT-PCR primer sequences and reaction parameters of gene targets involved in TAG breakdown and synthesis, fatty acid oxidation, transport and synthesis in Intralipid-infused rainbow trout..... 143
Table S3.3. Intralipid fatty acid composition of NL, PL, NEFA..... 144
Table S3.4. Fatty acid composition of the total fatty acids from trout plasma expressed as a percentage of total fatty acids..... 145
Table S3.5. Fatty acid composition of NLs from trout plasma expressed as a percentage of total fatty acids..... 146
Table S3.6. Fatty acid composition of PLs from trout plasma expressed as a percentage of total fatty acids..... 147
Table S3.7. Fatty acid composition of NEFAs from trout plasma expressed as a percentage of total fatty acids..... 148

Appendix

Figure 5.1. Schematic representation of the experimental designs used to probe the efficacy of the mammalian insulin receptor antagonist S961 in attenuating key nodes of the hepatic and muscular rainbow trout insulin cell signalling pathway..... 163
Figure 5.2. Postprandial activation of hepatic Akt and S6 assessed by Western Blot quantification..... 165
Figure 5.3. Postprandial activation of muscle Akt and S6 assessed by Western Blot quantification..... 167
Figure 5.4. Postprandial blood glucose concentrations in caudal vein blood samples.169
Figure 5.5. Exogenous bovine insulin infusion dependent activation of hepatic Akt and S6 following bolus infusion of S961 antagonist at multiple concentrations. 171
Figure 5.6. Exogenous bovine insulin infusion dependent activation of muscle Akt and S6 following bolus infusion of S961 antagonist at multiple concentrations. 173
Figure 5.7. Exogenous bovine insulin infusion-dependent circulating glucose concentration following bolus infusion of S961 antagonist at multiple concentrations. 175
Figure 5.8. Alignment of human, rat, zebrafish, Atlantic salmon and rainbow trout insulin receptor amino acid sequences, NCBI genome sequence-derived insulin receptor amino acid sequence-derived phylogeny and insulin receptor microsynteny analysis.177
Figure 5.9. Alignment of human, rat, zebrafish, Atlantic salmon and rainbow trout insulin amino acid sequences, NCBI genome sequence-derived insulin amino acid sequence-derived phylogeny and insulin microsynteny analysis..... 179
Table 5.1. Physical characteristics and experimental parameters of four groups of rainbow trout used in the feeding status experiment..... 181
Table 5.2. Physical characteristics and experimental parameters of rainbow trout used in the insulin infusion experiment..... 182

LIST OF ABBREVIATIONS

16:0	Palmitic acid
16:1	Palmitoleic acid
17:0	Margaric acid; NL/NEFA internal standard
17:0 PC	Phosphatidylcholine; PL internal standard
18:0	Stearic acid
18:1	Oleic acid
18:2	Linoleic acid
20:0	Arachidic acid
20:2	Eicosadienoic acid
20:3	Dihomo-γ-liniolenic acid
20:4	Arachidonic acid
20:5	Eicosapentaenoic acid
22:0	Behenic acid
22:1	Erucic acid
22:3	Docosatrienoic acid
22:5	Docosapentaenoic acid
22:6	Docosahexaenoic acid
24:0	Lignoceric acid
Acryl/Bis	Acrylamide/bis-acrylamide
ANOVA	Analysis of variance
APS	Ammonium persulphate
atgl	Adipose triglyceride lipase gene
ATGL	Adipose triglyceride lipase
ATP	Adenosine triphosphate
BCA	Bicinchoninic acid
β-oxidation	Beta-oxidation
BL	Body lengths
Bq	Becquerel
BSA	Bovine serum albumin
cAMP	Cyclic adenosine monophosphate
CD36	Fatty acid translocase
cd36	Fatty acid translocase gene
cDNA	Complementary deoxyribonucleic acid
cpt1a	Carnitine palmitoyltransferase 1a gene
ddH_2O	Double-distilled water
dgat2	Diacylglycerol acyltransferase 2 gene
dGDP	Deoxyguanosine diphosphate
dH_2O	Distilled water

DNA	Deoxyribonucleic acid
DTT	Dithiothreitol
EDTA	Ethylenediaminetetraacetic acid
FA	Fatty acid
FAS	Fatty acid synthase
fas	Fatty acid synthase gene
Fas	Fatty acid synthase protein
FFAR1	Free fatty acid receptor 1 (GPR40)
ffar1	Free fatty acid receptor 1 gene
FFAR2	Free fatty acid receptor 2 (GPR43)
ffar2	Free fatty acid receptor 2 gene
FFAR3	Free fatty acid receptor 3 (GPR41)
ffar3	Free fatty acid receptor 3 gene
FFAR4	Free fatty acid receptor 4 (GPR120)
ffar4	Free fatty acid receptor 4 gene
g6pca	Glucose-6-phosphatase a gene
g6pcb1a	Glucose-6-phosphatase b1a gene
g6pcb1b	Glucose-6-phosphatase b1b gene
G6PDH	Glucose-6-phosphate dehydrogenase
GBq	Gigabecquerel
gcka	Glucokinase a gene
gckb	Glucokinase b gene
GK	Glucokinase
Glut4	Glucose transporter 4 protein
glut4a	Glucose transporter 4a gene
glut4b	Glucose transporter 4b gene
GPR	G-protein coupled receptor
HCAR1	Hydroxycarboxylic acid receptor 1 (GPR81)
hcar1	Hydroxycarboxylic acid receptor 1 gene
Hcar1	Hydroxycarboxylic acid receptor 1 protein
HCAR2	Hydroxycarboxylic acid receptor 2 (GPR109A)
HCAR3	Hydroxycarboxylic acid receptor 3 (GPR109B)
HCl	Hydrochloric acid
HDL	High-density lipoprotein
HK	Hexokinase
HOAD	3-hydroxyacyl dehydrogenase
hoad	3-hydroxyacyl dehydrogenase gene
HSL	Hormone-sensitive lipase
hsl	Hormone-sensitive lipase gene
KCl	Potassium chloride

KCN	Potassium cyanide
LCFA	Long-chain fatty acid
LDL	Low-density lipoprotein
LPL	Lipoprotein lipase
lpl	Lipoprotein lipase gene
mgat1	Monoacylglycerol acyltransferase 1 gene
$MgCl_2$	Magnesium chloride
$MgSO_4$	Magnesium sulphate
$MnCl_2$	Manganese chloride
mRNA	Messenger ribonucleic acid
MS-222	Tricaine methanesulfonate
n-3	Omega-3 polyunsaturated
n-6	Omega-6 polyunsaturated
N_2	Nitrogen
NaCl	Sodium chloride
NAD^+	Nicotinamide adenine dinucleotide
NADH	Nicotinamide adenine dinucleotide, reduced
$NADP^+$	Nicotinamide adenine dinucleotide phosphate
NADPH	Nicotinamide adenine dinucleotide phosphate, reduced
NaF	Sodium fluoride
$NaHCO_3$	Sodium bicarbonate
NEFA	Non-esterified fatty acid
NH_2NH_2	Hydrazine
NL	Neutral lipids
PBS	Phosphate buffered saline
PBST	Phosphate buffered saline and Tween 20
PCK	Phosphoenolpyruvate carboxykinase
pck1	Phosphoenolpyruvate carboxykinase 1 gene
Pck1	Phosphoenolpyruvate carboxykinase 1 protein
Pck2	Phosphoenolpyruvate carboxykinase 2 protein
pck2a	Phosphoenolpyruvate carboxykinase 2a gene
pck2b	Phosphoenolpyruvate carboxykinase 2b gene
PEP	Phosphoenolpyruvate
PKA	Protein kinase A
PL	Phospholipid
PLIN1	Perilipin 1
plin1	Perilipin 1 gene
R_a glucose	Rate of hepatic glucose production
R_a glycerol	Rate of glycerol production; lipolytic rate
RCF	Relative centrifugal force

RM-ANOVA	Repeated-measures two-way analysis of variance
RNA	Ribonucleic acid
RPM	Revolutions per minute
RT	Reverse transcriptase
RT-PCR	Reverse transcription polymerase chain reaction
s.e.m.	Standard error of the mean
SCFA	Short-chain fatty acid
SDS	Sodium dodecyl sulphate
srebp1c	Sterol regulatory element-binding protein 1c gene
TCA	Tricarboxylic acid
TEMED	Tetramethylethylenediamine
TGS	Tris glycine SDS
U	Unit of enzyme catalytic activity; 1 U = μmol min^{-1}
VLDL	Very low-density lipoprotein

Chapter 1: General Introduction

.

Rainbow trout as a research model in the comparative physiology of metabolic fuel selection

Rainbow trout (*Oncorhynchus mykiss*) is a salmonid species native to North America but over the past 150 years, has been introduced to water systems all over the world. The research focused on rainbow trout energy metabolism has received considerable funding due to the importance of this freshwater fish in industrial aquaculture. While, the study of energy metabolism in rainbow trout has interested comparative physiologists due to their (i) glucose intolerance and pronounced hyperglycemia in response to dietary carbohydrates (Legate et al., 2001; Petersen et al., 2017), (ii) white muscle lactate retention and poor MCT expression (Omlin and Weber, 2013; Wang et al., 1997) and (iii) high basal lipolytic and re-esterification rates (Bernard et al., 1999). In industrial aquaculture, the dietary requirements of this carnivorous species are currently met by fish meal. This practice is economically and ecologically unsustainable, thus the study of rainbow trout energy metabolism has global implications (Jubouri et al., 2021; Naylor et al., 2009). Therefore, significant efforts have been focused on the determination of underlying molecular and physiological mechanisms regulating trout carbohydrate and lipid metabolism.

The importance of glucoregulation in metabolic fuel selection

Comparative physiologists have been interested in salmonid glucose metabolism due to their inability to regulate glycemia (Enes et al., 2009; Legate et al., 2001; Polakof et al., 2012). In vertebrates, glucoregulation is mediated by catabolic glycolysis, oxidative phosphorylation and anabolic gluconeogenesis. Under aerobic conditions, the tricarboxylic acid (TCA) cycle mediates the complete oxidation of glucose through

glycolysis and oxidative phosphorylation. In this process, a series of reactions results in the oxidation of nicotinamide adenine dinucleotide which fuels mitochondrial oxidative phosphorylation to yield >30 adenosine triphosphate (ATP) molecules from a single molecule of glucose (Liemburg-Apers et al., 2011). Under anaerobic conditions, lack of oxygen prevents mitochondrial oxidative phosphorylation, therefore, the glycolytic pathway generates 2 ATP as well as lactate as a metabolic by-product (Liemburg-Apers et al., 2011). Mammals control circulating glucose through tight regulation of glucose disposal and utilization, while trout are traditionally recognized as poor glucose regulators due to their insensitivity to insulin (Enes et al., 2009; Petersen et al., 2017; Forbes et al., 2019).

In mammals, glucose acts as an essential fuel for the brain and contributes significantly to energy metabolism in working muscles (Gerich, 2010). During aerobic exercise, mammalian glucose fluxes increase 5-fold over resting values to meet energy requirements and carbohydrate oxidation can account for the majority of the metabolic rate (Romijn et al., 2000; Wahren et al., 1971; Weber et al., 1996). However, trout decrease glucose flux during prolonged swimming suggesting glucose oxidation is not the primary mode of energy production in working muscles (Choi and Weber, 2016; Shanghavi and Weber, 1999). These highlighted differences likely originate from differences in glucose transport and disposal. Glucose transporter 4 (Glut4) is of particular interest due to its high expression in tissues responsible for most glucose disposal, skeletal muscle (Capilla et al., 2002; Díaz et al., 2007; Liu et al., 2017). In teleosts, slower temporal responses of Glut4 expression and translocation along with a lower affinity of Glut4 for glucose may, in part, explain differences in glucoregulation

between mammals and fish (Capilla et al., 2002; Marín-Juez et al., 2013).

Endogenous glucose production and regulation

The liver plays a central role in the regulation of hepatic glucose production (R_a glucose) due to the contribution of two hepatic processes, gluconeogenesis and glycogenolysis (Haman et al., 1997a; Jones, 2016). Acute changes in circulating glucose are mainly regulated through glycogenolysis, while prolonged changes in glycemia rely on gluconeogenesis, especially as glycogen reserves become depleted (Bechmann et al., 2012; Chung et al., 2015; Zhang et al., 2019). In vertebrates, regulation of key gluconeogenic and glycogenolytic gene expression controls R_a glucose (Enes et al., 2009; Hatting et al., 2018; Méndez-Lucas et al., 2013). In vertebrates, endogenous gluconeogenic precursors such as lactate, glycerol and amino acids, compete as substrates for hepatic gluconeogenesis (Mauerwerk et al., 2020; Polakof et al., 2012; Rito et al., 2019; Zhang et al., 2019).

In all vertebrates, two isoforms of phosphoenolpyruvate carboxykinase, the cytosolic form (PCK1) and the mitochondrial form (PCK2) are expressed. Sequential genome duplication in rainbow trout has led to the expression of multiple *pck2* isoforms [phosphoenolpyruvate carboxykinase 2a (*pck2a*) and phosphoenolpyruvate carboxykinase 2b (*pck2b*)]. In mammals, both PCK isoforms contribute to gluconeogenesis, however, localization has given rise to differential precursor preference (Marandel et al., 2019; Méndez-Lucas et al., 2013). In the canonical linear gluconeogenic pathway, glycerol is an indiscriminate intermediate and its use is predicated on the expression of glycerol kinase, while, amino acids and pyruvate derivatives, including lactate are preferentially metabolized by PCK2 (Modaressi et al.,

1998) The regulation of R_a glucose in vertebrates is multifactorial and includes nutritional status, hormonal balance and exercise intensity and duration (Chung et al., 2015; Enes et al., 2009; Kirchner et al., 2008; Zhang et al., 2019). Glucose mobilization is reduced by exogenously administered glucose, alanine, insulin and propranolol as well as prolonged swimming and low temperature, but is stimulated by epinephrine (Choi and Weber, 2016; Forbes et al., 2019b; Haman et al., 1997b; Jubouri et al., 2021; Shanghavi and Weber, 1999; Weber and Shanghavi, 2000).

Lactate as a metabolic fuel and its retention in white muscle

Lactate is an energy intermediate that can be formed in tissues undergoing accelerated glycolysis and distributed throughout the body to be utilized as an oxidative fuel (Brooks, 2020; Brooks et al., 2022; Philp et al., 2005; Rooney and Trayhurn, 2011; Sun et al., 2017). In vertebrates, lactate production occurs continuously and at high rates during aerobic metabolism. While swimming, glycolytic muscle fibres produce lactate, which can accumulate in the circulation and be utilized by neighbouring oxidative fibres. In rainbow trout, oxidation is responsible for most lactate utilization observed during high intensity swimming, making aerobic metabolism essential for lactate elimination (Omlin et al., 2014). Rainbow trout have a high baseline of R_a lactate, likely as a continuous supply to highly aerobic tissues that favour lactate for oxidative metabolism (Omlin et al., 2014; Omlin and Weber, 2010; Teulier et al., 2013). In trout, higher lactate availability increases its utilization in peripheral tissues (Omlin et al., 2014). Of the many fates of circulating lactate, its role as an oxidative fuel dominates lactate utilization (Brooks, 2002; Brooks, 2020; Brooks et al., 2022; Girard and Milligan, 1992; Milligan and Girard, 1993; Pagnotta and Milligan, 1991).

Comparative physiologists have been interested in lactate metabolism in ectothermic muscles due to their unique behaviour compared to mammals (Weber, 2011; Weber et al., 2016). The energetic demands of skeletal muscles are dependent on both swimming intensity and duration. The oxidative muscle fibres of the red muscle are utilized at rest and for low-intensity swimming, while, the glycolytic fibres in the white muscle are reserved for explosive exercise (Domenici and Blake, 1997; Marras et al., 2013; McKenzie, 2011). Lactate efflux from exercising fish white muscle is 10 times slower than from mammalian muscle (Wang et al., 1997). Fish lactate transport across membranes has been characterized to be facilitated by four MCT isoforms denoted as MCT1a, MCT1b, MCT2 and MCT4 (Omlin and Weber, 2013). Lactate retention in fish white muscle can be explained by: (i) the poor expression of MCTs in trout compared to mammals and other trout tissues and (ii) the failure of exhaustive exercise to upregulate MCT isoform expression and thus lactate permeability in white muscle (Omlin and Weber, 2013). Thus, white muscle carbohydrate metabolism can be characterized as a quasi-closed system.

Lactate as a metabolic signal

Lactate is traditionally recognized as a glycolytic end-product, an oxidative fuel and a major gluconeogenic precursor. More recently, its role as an essential metabolic signaling molecule via G-protein coupled receptor (GPR) activation has been characterized in mammals. (Brooks, 2020; Brooks et al., 2022; Philp et al., 2005; Rooney and Trayhurn, 2011; Sun et al., 2017). GPRs form one of the largest protein families and are encoded by over 800 genes in mammals (Pierce et al., 2002). Over the last two decades, deorphanization studies have revealed many endogenous

metabolites make up the ligand profiles of previously orphaned GPRs and thereby re-interpreting their roles from simply substrates to regulators of energy metabolism. Recently, three GPRs structurally and phylogenetically related, have been classified as HCARs because they are activated by endogenous hydroxycarboxylic acids. Individual members include hydroxycarboxylic acid receptor 1, 2 and 3 (HCAR1, HCAR2 and HCAR3), formerly GPR81, GPR109A and GPR109B, respectively (Ahmed, 2011; Offermanns et al., 2011). All three receptors exhibit anti-lipolytic effects through the inhibition of the highly conserved protein kinase A (PKA) signaling pathway and thus function as metabolic sensors.

HCAR1 has been characterized in humans as a key binding target for lactate (Offermanns, 2014) and has recently been identified in fish (Kuei et al., 2011). Lactate activates HCAR1 (4-5 mM) within its physiological circulating concentration (1-20 mM), strongly suggesting that lactate is an endogenous ligand for HCAR1 (Cai et al., 2008; Kuei et al., 2011; Liu et al., 2009). The anti-lipolytic binding target for lactate, HCAR1, plays a key role in regulating mammalian fuel selection in adipose and intramuscular tissue from rodents and humans. This mechanism explains the relationship between high blood lactate and (i) TAG accumulation and (ii) low levels of circulating non-esterified fatty acids (NEFAs) (Chen et al., 2021; Li et al., 2022; Sun et al., 2016; Zhou et al., 2021). Studies on transgenic rodents have demonstrated that this anti-lipolytic effect is mediated by HCAR1 binding as HCAR1-deficient mice exhibited normal lipolysis compared to the wild-type (Ahmed et al., 2010). Due to its membership in the GPR family of receptors, HCAR1 activation triggers a signaling cascade which inhibits adenylyl cyclase activity and cyclic adenosine monophosphate (cAMP) production.

Inhibition of cAMP accumulation is consistent with the physiological evidence that lactate mediates lipolysis, given cAMP is a key mediator of lipolytic enzyme activity via the PKA signaling pathway. Given the global role of cAMP production and PKA activity in many metabolic pathways, their inhibition by HCAR1 may affect fuel selection (Ahmed et al., 2010; Rooney and Trayhurn, 2011). In contrast to its early portrayal as a metabolic waste product and fatigue agent, lactate is now considered an essential metabolic signaling molecule in mammals, however little is known about its effects in fish species (Kuei et al., 2011; Thomsen et al., 2019).

Lipid mobilization and metabolism

Lipids derived from the liver, muscle and adipose tissue are essential in energy distribution in vertebrates (Henderson and Tocher, 1987; Lauff and Wood, 1997; Weber, 2011). As a result of their high energy density, lipids, stored as TAG, make up the majority of energy reserves (Hurley et al., 1986; Weber, 2011). Due to their inability to traverse cell membranes, the mobilization of TAG out of intracellular reserves requires their (i) hydrolytic breakdown into its constituents, 3 NEFAs and 1 glycerol, or (ii) secretion in TAG-rich micelles known as lipoproteins. Vertebrates adopt various strategies for shuttling energy from lipids from tissues with high-lipid deposits to working muscles. Mammals transport most lipids as NEFAs bound to solubilizing proteins (albumin and NEFA binding proteins), while in rainbow trout, >90% of circulating lipids are lipoproteins of varying densities, including chylomicrons, very low-, low- and high-density lipoproteins (VLDL, LDL and HDL, respectively) (Babin and Vernier, 1989; Magnoni and Weber, 2007). The hydrolytic breakdown of intracellular TAGs is catalyzed by lipases in a process called lipolysis. The regulation of lipolytic genes, adipose

triglyceride lipase (*atgl*), hormone-sensitive lipase (*hsl*), perilipin 1 (*plin1*) and lipoprotein lipase (*lpl*), and the activities of their corresponding enzymes are crucial to mediating lipid mobilization and homeostasis (Ahmadian et al., 2009; Kittilson et al., 2011; Kostyniuk et al., 2019b; Ladu et al., 1991; Sheridan, 1988; Sohn et al., 2018). Lipids liberated from reserves through lipolysis can be oxidized for fuel during fasting or prolonged exercise or recycled through lipogenesis (Bou et al., 2016; Edens et al., 1990; Frayn, 2010; Tocher, 2003). In vertebrates, several genes are involved in lipid accumulation including lipogenic genes [fatty acid synthase (*fas*), sterol regulatory element-binding protein 1c (*srebp1c*) and diacylglycerol acyltransferase 2 (*dgat2*)] (Chitraju et al., 2019; Kostyniuk et al., 2018; Kostyniuk et al., 2019a; Ranganathan et al., 2006). Despite, lipolysis yielding 3 NEFAs and 1 glycerol, ratios of NEFA/glycerol fluxes measured in trout are ~1 (Bernard et al., 1999). Thus, most NEFA released through lipolysis is immediately re-esterified *in situ*, whereas glycerol metabolism occurs in peripheral tissues where glycerol kinase activity is higher (Lech, 1970).

In most vertebrates, lipids are the primary fuel when their metabolic rate is below 50% maximal oxygen consumption (Brooks, 1998; Terjung and Kaciuba-Usciłko, 1986; Wolfe et al., 1990). However, at higher exercise intensities the rate of ATP utilization exceeds the maximal rates of ATP production through lipid oxidation, thus, most vertebrates switch to oxidizing carbohydrates (Brooks, 1998; Hultman, 1995; McClelland, 2004; Roberts et al., 1996; van Loon et al., 2001; Weber, 2011). This crossover of metabolic fuels from lipid to carbohydrate is generally conserved across mammals (Weber, 2011). In contrast, migrating fish rely mostly on lipid oxidation for endurance swimming and irreversible protein catabolism in the latter stages of migration

(Weber, 2011). In fish, most lipids mobilized by lipolysis are re-esterified (Turenne and Weber, 2018).

Fatty acids as metabolic signals

GPRs deorphanization research over the past two decades has revealed NEFAs, as the ligand profile of the previously orphaned GPRs, GPR40, GPR43, GPR41 and GPR120 currently known as free fatty acid receptor (FFAR) 1, 2, 3 and 4, respectively (Briscoe et al., 2003; Brown et al., 2003; Hirasawa et al., 2005; Itoh et al., 2003). Though FFARs are characterized as such, individual ligand profiles depend on the length of the carbon chain. FFAR1 and 4 are activated by long-chain fatty acids (LCFAs), while FFAR2 and 3 are activated by short-chain fatty acids (SCFAs). SCFAs are lipids consisting of $\leq$6 carbons and as a group have various physiological functions. Endogenous SCFAs are sourced from bacterial fermentation of dietary fibre by the gut microbiota. Though the physiological roles of FFAR2 and 3 are varied, their high expression in epithelial cells of the intestinal tract suggests their involvement in appetite regulation (Andoh et al., 2003; Karaki et al., 2006). LCFAs are lipids consisting of $\geq$12 carbons and as an energy source, these lipids are supplied primarily by food intake, *de novo* synthesis and breakdown from lipids deposits. LCFAs are abundant in organisms in much higher quantities and have higher energy densities than their shorter counterparts (Ishizawa et al., 2015; Seidelin, 1995). Thus, LCFAs are characterized as an essential oxidative fuel and are often the focus of research regarding lipid metabolism.

Both saturated and unsaturated LCFAs can act as agonists for FFAR1 and 4 (Hirasawa et al., 2005). The strength of the agonistic effects of LCFAs on FFAR1

activity, as measured by changes in intracellular calcium concentration, increases with increasing carbon-chain length (Itoh et al., 2003). The physiological functions of FFAR1 and 4 appear strongly related to glucoregulation and lipid homeostasis. In mammals, FFAR1 is mainly responsive to dietary TAG-derived LCFAs liberated locally from postprandial chylomicrons and low-density lipoproteins by LPL (Psichas et al., 2017). FFAR4 expression is highest in adipocytes and increases during adipogenesis suggesting its plays an important role in adipocyte differentiation and maturation (Gotoh et al., 2007). FFAR4 dysfunction has also been reported to lead to obesity in mammals, while selective FFAR4 activation suppressed lipolysis primarily in adipose tissue (Ichimura et al., 2012; Satapati et al., 2017). More recently in mammalian adipose tissue, FFAR4 functions as a LCFA-activated, autocrine negative feedback regulator of lipolysis, likely by suppressing lipolytic enzymes, ATGL, HSL and PLIN1 (Anthonsen et al., 1998; Husted et al., 2020; Pagnon et al., 2012; Pollak et al., 2015; Strålfors et al., 1984). FFAR2 and 3 have received considerable attention in comparative rainbow trout research. However, the importance of LCFA to lipid metabolism makes FFAR1 and 4 more interesting candidates for metabolic research.

Integrating whole-body fluxes with measurements of gene expression, protein signaling and enzyme activities

Trout, like all multicellular life, continuously adjust rates of *in vivo* metabolite turnover to correspond with changes in metabolism (Weber and Zwingelstein, 1995). The double cannulation, continuous tracer infusion technique is designed to measure changes in metabolite fluxes in rainbow trout (Bernard et al., 1999; Haman et al., 1997a; Haman and Weber, 1996). The steady equation of Steele was derived to explain how

metabolites behave in a two-compartment model: plasma and tissues (Steele, 1959). R_a glucose and the rate of glycerol production (R_a glycerol) are calculated as follows using the steady state equation of Steele:

$$R_a = R_d = \frac{F}{SA}$$

Here R_a is the rate of appearance, R_d is the rate of disappearance, F is the infusion rate of either labelled glucose or glycerol and SA is the specific activity.

Though flux measurements can be mediated by circulating concentration, multiple permutations of R_a and R_d can lead to the same changes in concentration. Thus measuring fluxes are more informative than relying on changes in concentration (Kim et al., 2020). In addition, measuring *in vivo* metabolite fluxes rather than relying solely on measurements of messenger ribonucleic acid (mRNA) and protein abundance and enzymatic activity of key metabolic proteins is better for understanding metabolic status. Although changes in key metabolic indices can predict changes in metabolite fluxes an overreliance on these measurements may result in erroneous conclusions. Integrating *in vivo* kinetics with molecular measurements of mRNA and protein abundance and enzymatic activity, help us to understand the underlying mechanisms that lead to the observed changes in energy metabolism.

Thesis objectives

The main objective of this thesis is to investigate *in vivo* fuel mobilization in adult rainbow trout and how it plays a functional role in regulating key carbohydrate and lipid metabolic pathways. The integration of *in vivo* mobilization of glucose (the rate of hepatic glucose production: R_a glucose) and lipid reserves (the lipolytic rate or rate of glycerol production: R_a glycerol) with gene expression, protein abundance and enzyme

activity of key metabolic indices allows for a better mechanistic understanding of how metabolic fuel selection is regulated. This thesis is divided into 2 data chapters and a conclusion chapter, which corresponds to three specific objectives as follows.

1. To my knowledge, no prior studies have investigated the impact of lactate on *in vivo* R_a glucose (in fish) and R_a glycerol (in any species). Thus, in my first data chapter, I investigated the effects of exogenous lactate on R_a glucose and R_a glycerol in adult rainbow trout. Moreover, I sought to assess gene expression, protein abundance and enzyme activity of key markers of carbohydrate and lipid metabolism. I hypothesized rainbow trout (i) induce an HCAR1-mediated inhibition of lipolysis and (ii) exhibit an oxidative preference for lactate over glucose in response to elevated plasma lactate. I also hypothesized rainbow trout modulate gene expression, protein abundance and enzyme activity to support changes in glucose and glycerol mobilization.
2. For my second data chapter, I investigated the effects of the lipid emulsion, Intralipid, on R_a glucose and R_a glycerol in adult rainbow trout. Similarly, I sought to assess gene expression, protein abundance and enzyme activity of key markers of carbohydrate and lipid metabolism. I hypothesized rainbow trout induce (i) an increase in lipolysis and (ii) an inhibition in hepatic glucose production in response to elevated plasma lipids. I also hypothesized rainbow trout modulate gene expression, protein abundance and enzyme activity to support changes in glucose and glycerol mobilization.
3. In my conclusion chapter, I will revisit the results of my two data chapters and discuss metabolic fuel selection in rainbow trout. Moreover, I sought to assess

microsynteny, amino acid sequence similarity and critical residue conservation in binding pockets of vertebrate *hcar1*, *ffar1* and *ffar4* with an emphasis on teleosts. These GPRs were chosen due to their well-characterized roles in modulating mammalian energy homeostasis.

Chapter 2: Lactate signaling for fuel selection: Mobilization of energy reserves

This chapter is based on a manuscript titled “Lactate signaling for fuel selection: Mobilization of energy reserves in rainbow trout”

Written by
Giancarlo G.M. Talarico[1], Elisa Thoral[1,2], Elie Farhat[1], Loïc Teulier[2], Jan A. Mennigen[1] and Jean-Michel Weber[1]

[1] Biology Department, University of Ottawa, Canada
[2] Ecologie des Hydrosystèmes Naturels et Anthropisés, Université Claude Bernard Lyon 1, France

In preparation for
American Journal of Physiology

Author contributions: G.G.M.T., J.A.M. and J.-M.W. conception and design of research; G.G.M.T., E.T. and E.F. performed experiments; G.G.M.T., J.A.M. and J.-M.W. analyzed data, interpreted results and prepared figures; G.G.M.T. drafted the manuscript; G.G.M.T., J.A.M. and J.-M.W. edited, revised and approved the manuscript.

Introduction

In addition to its traditional roles as glycolytic end-product, oxidative fuel and gluconeogenic precursor, lactate is also recognized as an essential metabolic signal (Brooks, 2020; Brooks et al., 2022; Philp et al., 2005; Rooney and Trayhurn, 2011; Sun et al., 2017). HCAR1 was characterized in humans as a key binding target for lactate (Offermanns, 2014) and more recently also identified in fish (Kuei et al., 2011). HCAR1 signaling is known to play an important role in regulating mammalian fuel selection because it mediates the inhibition of lipolysis when circulating lactate levels are elevated by intense exercise (Ahmed et al., 2010; Cai et al., 2008; Liu et al., 2009).

Multiple factors affecting metabolic fuel selection have been characterized in fish, particularly rainbow trout (Weber et al., 2016). Glucose mobilization (the rate of hepatic glucose production: R_a glucose) is reduced by exogenous glucose or alanine (Choi and Weber, 2015; Jubouri et al., 2021) insulin (Forbes et al., 2019b), propranolol (Weber and Shanghavi, 2000), prolonged swimming (Shanghavi and Weber, 1999) and low temperature (Haman et al., 1997b), but it is stimulated by epinephrine (Weber and Shanghavi, 2000). The mobilization of lipid reserves (the lipolytic rate or rate of glycerol production: R_a glycerol) is also increased by epinephrine but inhibited by norepinephrine (Magnoni et al., 2008b). Surprisingly, lipolysis remains unaffected by endurance swimming (Bernard et al., 1999) or graded exercise up to critical speed (Turenne and Weber, 2018). Whether lactate signaling is involved in modulating fuel selection in fish is unknown. Therefore, this study aimed to explore how exogenous lactate modulates fuel selection *in vivo* by measuring its effects on hepatic glucose production and lipolytic rate in rainbow trout. Exogenous supply rather than swimming-induced hyperlactatemia

was selected here to avoid the confounding impact of the metabolic, hormonal, and neural changes caused by exercise itself and to focus on lactate as a signal. My goals were to quantify the effects of elevated lactate levels on: (i) R_a glucose and R_a glycerol, and (ii) strategic tissue parameters involved in lactate signaling or carbohydrate and lipid metabolism that could potentially explain the observed changes in glucose or glycerol kinetics. The selected tissue indices targeted key carbohydrate and lipid metabolic pathways including: glycolysis, gluconeogenesis, fatty acid (FA) oxidation, lipogenesis, lipolysis and fuel transport. The activity of these targets was quantified when a reliable assay for the fish protein could be implemented. When this was not the case, protein abundance or gene expression was measured depending on the availability of antibodies cross-reacting with the trout protein. I anticipated that lactate would cause a decrease in hepatic glucose production and the HCAR1-mediated inhibition of lipolysis as it does in mammals (Ahmed et al., 2010; Miller et al., 2002a). It was predicted that these trout responses would be reflected by corresponding changes in key regulatory proteins of carbohydrate and lipid metabolism.

Methods

Animals

Rainbow trout (*Oncorhynchus mykiss*), with a Fulton's condition factor of 1.12 ± 0.03 (N=34) (Blackwell et al., 2000) of both sexes were purchased from Linwood Acres Trout Farm (Campbellcroft, Ontario, Canada). Three groups of fish were used: (i) for *in vivo* measurements of glucose and (ii) glycerol kinetics, and (iii) for measurements of gene expression [*real-time* reverse transcription polymerase chain reaction (RT-PCR)], protein abundance (Western blots) and enzyme activities. The physical characteristics

of all experimental groups are presented in Table 2.1. The fish were held in a 1,200-litre flow-through tank supplied with dechloraminated Ottawa tap water at 13°C, on a 12 h:12 h light-dark photoperiod and were fed Profishnet floating fish pellets (Martin Mills, Elmira, ON, Canada) 5 days a week. They were acclimated to these conditions for a minimum of 3 weeks before experiments. The results presented are pooled male and female values because no significant sex differences were observed in this study. All the procedures were approved by the Animal Care Committee of the University of Ottawa (protocol BL-1625) and adhered to the guidelines established by the Canadian Council on Animal Care.

Table 2.1. Physical characteristics and hematocrit of the rainbow trout used during exogenous lactate administration.

	Glucose kinetics	Glycerol kinetics	Molecular experiments
Sample size	8	10	16
Body mass (g)	478 ± 25	661 ± 39	217 ± 7
Body length (cm)	34.8 ± 0.6	38.0 ± 0.8	27.6 ± 0.3
Fulton's condition factor (K)	1.13 ± 0.03	1.20 ± 0.03	1.04 ± 0.02
Hematocrit (%)	19.2 ± 1.6	19.6 ± 1.2	24.4 ± 0.8

Trout were used for (i) *in vivo* glucose kinetics measurements, (ii) *in vivo* glycerol kinetics measurements, or (iii) tissue gene expression, signaling and enzyme activity. Body mass and length were measured before the surgery. Hematocrit was measured on the second day, after recovery from the surgery to minimize blood loss. Mean values ± s.e.m. are presented.

Catheterization

Fish were anesthetized with 60 mg l^{-1} tricaine methanesulfonate (MS-222; DIN 02168510, Syndel Canada, Nanaimo BC, Canada) buffered with 0.2 g l^{-1} sodium bicarbonate ($NaHCO_3$; S6014, Sigma-Aldrich St Louis, MO, USA) and surgically fitted with 2 catheters (*in vivo* kinetics experiments) or a single catheter (tissue measurement experiments) (BTPE-50, Instech Laboratories, Plymouth Meeting, PA, USA) in the dorsal aorta (Haman and Weber, 1996). The catheters were kept patent by flushing with Cortland saline containing 50 U ml^{-1} heparin (H3393, Sigma-Aldrich). After catheterization, the fish were left to recover overnight in a 90-litre swim-tunnel (Loligo Systems, Viborg, Denmark) where *in vivo* measurements were carried out in resting animals kept at a water velocity of 0.5 body lengths (BL) s^{-1}. This weak current reduces stress and enhances the flow of water over the gills, but does not require swimming to maintain body position (Choi and Weber, 2015). The swim tunnel was supplied with 13°C aerated and dechloraminated Ottawa tap water.

Glucose and glycerol kinetics (series 1 and 2)

The rates of R_a glucose and R_a glycerol were measured by continuous infusion of [6-^{3}H] glucose [American Radiolabelled Chemicals, St. Louis, MO, USA; 2220 gigabecquerel (GBq) $mmol^{-1}$] and [2-^{3}H] glycerol (American Radiolabelled Chemicals; 925 GBq $mmol^{-1}$) respectively. This *in vivo* tracer method has been validated to quantify R_a glucose in fish (Haman et al., 1997a) and thoroughly tested for rainbow trout under a variety of physiological stresses (Choi and Weber, 2016; Haman et al., 1997b; Jubouri et al., 2021; Shanghavi and Weber, 1999; Weber et al., 2016). Similarly, the tracer method used to quantify R_a glycerol has been tested repeatedly for rainbow trout

(Bernard et al., 1999; Magnoni et al., 2008b; Turenne and Weber, 2018). Infusates were freshly prepared immediately before each experiment by drying an aliquot of the radiolabelled tracer under nitrogen (N_2) and resuspending in Cortland saline. For glucose kinetics, a priming dose of tracer equivalent to 180 min of infusion was injected as a bolus at the start of each infusion to reach isotopic steady state in <45 min. A priming dose was not necessary for glycerol kinetics because the high turnover rate relative to pool size allows for rapid equilibration of labelled glycerol within the glycerol pool. For each flux measurement, the infusate was administered continuously at ~1 ml h^{-1} (exact infusion rates were determined individually for each fish to correct for differences in body mass) using a calibrated syringe pump (Infuse/Withdraw Pump 11 Elite Syringe Pump, Harvard Apparatus, Holliston, MA, USA) as described in Jubouri et al., 2021. Infusion rates averaged 1523.3 ± 36.2 becquerel (Bq) kg^{-1} min^{-1} (N=8) for labelled glucose and 9226.9 ± 297.05 Bq kg^{-1} min^{-1} (N=10) for labelled glycerol. These trace amounts (labelled and unlabelled) had no effect on glucose or glycerol metabolism, only accounting for <0.0000001% of baseline endogenous R_a glucose and <0.00001% of the baseline endogenous R_a glycerol. Blood samples (~200 µl each) were drawn 50, 55 and 60 min after starting the tracer infusion to determine baseline glucose or glycerol kinetics, and every 20 min thereafter during exogenous lactate administration (L7022, Sigma-Aldrich; at a rate of 30 µmol kg^{-1} min^{-1}). This rate of lactate infusion is equivalent to twice the baseline endogenous rate of lactate appearance in circulation (Omlin and Weber, 2010). A previous study has shown that an equivalent infusion rate causes a gradual increase in blood lactate concentration to ~13 mM after 180 min (Omlin et al., 2014). The total amount of blood sampled from each

fish accounted for <10% of the total blood volume. Blood samples were immediately centrifuged to separate plasma [5 min; 13,000 revolutions per minute (RPM)] and stored at -20ºC until analyses.

Plasma sample analyses

Glucose and glycerol radioactivity was measured by scintillation counting (Beckman Coutler LS 6500, Fullerton, CA, USA) in Bio-Safe II scintillation fluid (111195; Research Products International Corp., Mount Prospect, IL, USA). To measure glucose radioactivity in series 1, plasma samples were prepared prior to the scintillation counting by drying 20 µl of each sample under N_2, eliminating tritiated H_2O, and resuspending in 1 ml distilled water (dH_2O). To measure glycerol radioactivity in series 2, plasma samples were prepared prior to the scintillation counting by eliminating glucose activity. Tritium from infused [2-^{3}H] glycerol partitions into circulating glycerol, glucose and H_2O (Bernard et al., 1999). Glucose activity was eliminated by incubating 40 µl of each sample with 1.11 mM ATP (A2383, Sigma-Aldrich) and 7 U ml^{-1} hexokinase (HK; H4502, Sigma-Aldrich) to phosphorylate and remove free tritiated glucose by ion-exchange column chromatography. The samples were passed through cation (DOWEX 50Wx8, hydrogen form; 44519, Sigma-Aldrich) and anion (DOWEX 1x8, formate form; 13858-U, Sigma-Aldrich) 200-400 mesh exchange resins in elution columns, separated with porous polyethylene frits (United Chemical Technologies, Bristol, PA, USA) as described in Turenne and Weber, 2018. Samples were washed through the elution column with 7 ml dH_2O allowing only labelled glycerol and tritiated H_2O to pass through. Eluates were dried overnight at 65°C under N_2 to eliminate tritiated H_2O. Residues were resuspended in 1 ml dH_2O and counted. A previous study determined that 10.6% of

labelled glycerol was lost during the ion-exchange separation by column chromatography, therefore, glycerol activity was corrected accordingly (Turenne and Weber, 2018).

Plasma lactate, glucose and glycerol concentrations were measured spectrophotometrically using a Spectra Max Plus 384 Microplate Spectrophotometer (Molecular Devices, Sunnyvale, CA, USA). Plasma lactate concentration was measured with 322 U ml^{-1} lactate dehydrogenase (L2500, Sigma-Aldrich) and a glycine buffer (G5418, Sigma-Aldrich) containing 0.446 mM nicotinamide adenine dinucleotide (NAD^+; N7004, Sigma-Aldrich). Plasma glucose concentration was determined with 7 U ml^{-1} HK and 0.1 U ml^{-1} glucose-6-phosphate dehydrogenase (G6PDH; G5885, Sigma-Aldrich) in a buffer containing 60 mM Trizma base (T6066, Sigma-Aldrich), 40 mM Tris-hydrochloric acid (HCl; TRS004, BioShop Canada Inc., Burlington, ON, Canada), 1.01 mM magnesium sulphate ($MgSO_4$; M7506, Sigma-Aldrich), 2.22 mM NAD^+ and 1.11 mM ATP. Plasma glycerol concentration was determined with 4 U ml^{-1} glycerol kinase (G6142, Sigma-Aldrich) and 8.7 U ml^{-1} glycerophosphate dehydrogenase (G6751, Sigma-Aldrich) in a buffer containing, 350 mM hydrazine (NH_2NH_2) base (225819, Sigma-Aldrich), 50 mM $NH_2NH_2 \cdot 2$ HCl (H6628, Sigma-Aldrich), 2 mM NAD^+ and 2 mM ATP. All concentrations were determined by measuring the absorbance of the reduced form of nicotinamide adenine dinucleotide (NADH) at 340 nm.

Tissue measurements (series 3)

To avoid analyzing radioactive tissues, these experiments were carried out on different fish than those used to measure glucose and glycerol kinetics. Saline (control group; N=8) or lactate (treatment group; N=8; 30 µmol kg^{-1} min^{-1}) was administered at

~1 ml h^{-1} for 180 min. Blood samples were taken prior to and following the 180 min infusion. The trout were euthanized by spinal cord transection and the whole liver, red muscle (along the lateral line) and white muscle (perpendicular to the dorsal fin) were collected and stored at -80°C until analyses.

RNA extraction and gene expression

Total ribonucleic acid (RNA) from the liver, red and white muscle was extracted by homogenizing 50 mg of tissue in TRIzol reagent (15596, Invitrogen, Burlington, ON, Canada) using a sonicator (Fisher Scientific Sonic Dismembrator model 100, San Diego, CA, USA). RNA concentration was quantified using a NanoDrop 2000c UV-Vis Spectrophotometer (Thermo-Fisher Scientific, Waltham, MA, USA) and samples were stored at -80°C. QuantiTect reverse transcriptase kit (205313, Qiagen, Toronto, ON, Canada) was used to generate complementary deoxyribonucleic acid (cDNA) using total RNA from liver, red and white muscle tissues following the manufacturer's protocol. A no-reverse transcriptase (RT) negative control (RT replaced with RNase-free H_2O) and a no-template negative control (RNA replaced with RNase-free H_2O) were included to check for genomic contamination as described in Jubouri et al., 2021. Two-step *real-time* RT-PCR assays were performed on a Bio-Rad CFX96 instrument (Bio-Rad, Mississauga, ON, Canada) to quantify relative fold-changes in mRNA abundances of key glycolytic genes [glucokinase a (*gcka*) and glucokinase b (*gckb*)], gluconeogenic genes [*pck1*, *pck2a*, *pck2b*, glucose-6-phosphatase a (*g6pca*), glucose-6-phosphatase b1a (*g6pcb1a*), and glucose-6-phosphatase b1b (*g6pcb1b*)] and glucose transporters [glucose transporter 4a (*glut4a*) and glucose transporter 4b (*glut4b*)]. Additionally, transcripts involved in lipid metabolism, specifically lipolytic regulation (*hcar1*, *hsl and*

lpl), FA oxidation [carnitine palmitoyltransferase 1a (*cpt1a*) and 3-hydroxyacyl dehydrogenase (*hoad*)], transport [fatty acid translocase (*cd36*)] and synthesis (*fas* and *srebp1c*) were quantified. For each assay, a standard curve consisting of serial dilutions of pooled cDNA samples was run in duplicate for each experiment. The total reaction volume was 20 µl, which consisted of 1 µl of diluted cDNA template, 1 µl of 10 nM specific forward and 1 µl of 10 nM specific reverse primer (Tables S2.1 and S2.2), 10 µl of SsoAdvanced Universal SYBR Green Supermix (1725275, Bio-Rad) and 7 µl of H_2O as described in Jubouri et al., 2021. *Real-time* RT-PCR cycling parameters were a 5 min activation step at 95°C, followed by 40 cycles consisting of a 20 s denaturation step at 95°C and a 30 s annealing and extension step at a primer-specific temperature (Tables S2.1 and S2.2). Negative controls (no-RT and no-template) were included in each assay to control for genomic contamination. After each run, melting curves were produced and monitored for single peaks to confirm the specificity of the reaction and the absence of primer dimers. All amplification efficiencies calculated from serially diluted 7-point standard curves were between 92.8-108.7%, with R^2 values >0.950 (Tables S2.1 and S2.2). Relative transcript abundance derived from standard curves was normalized using the NORMA-Gene approach (Heckmann et al., 2011). Finally, mRNA fold changes were calculated relative to the control group.

Western blotting

Total protein from the liver, red and white muscle tissue was extracted by homogenizing 100 mg of tissue in 400 µl of cold homogenization buffer using a sonicator as described in (Jubouri et al., 2021). The homogenization buffer (pH 8.0) contained 150 mM sodium chloride (NaCl; S9625, Sigma-Aldrich), 1% Triton X-100

(T9284, Sigma-Aldrich), 0.5% sodium deoxycholate (D6750, Sigma-Aldrich), 0.1% sodium dodecyl sulphate (SDS; SDS001, BioShop Canada Inc.), 50 mM Tris-HCl, 1 mM ethylenediaminetetraacetic acid (EDTA; E9884, Sigma-Aldrich), 100 mM sodium fluoride (NaF; 201154, Sigma-Aldrich), 4 mM sodium pyrophosphate (S6422, Sigma-Aldrich), 2 mM sodium orthovanadate (S6508, Sigma-Aldrich) and a protease inhibitor cocktail (A32953, Thermo Fisher Scientific). Homogenates were centrifuged [10 min; 15,000 relative centrifugal force (RCF)] at 4°C, the resulting supernatants were recovered and stored at -20°C. Protein concentrations were determined using bicinchoninic acid (BCA; B9643, Sigma-Aldrich) assay with bovine serum albumin (BSA; 05470, Sigma-Aldrich) as a standard. Protein samples were denatured (5 min; 95°C), reduced and diluted in 2X Laemmli buffer (S3401, Sigma-Aldrich) for a total amount of 25 µg protein in 20 µl of loading volume. Protein samples were loaded along with 5 µl of Page Ruler prestained protein ladder (26616, Thermo Fisher Scientific) in a 10% resolving gel [5 ml double-distilled water (ddH_2O), 2.5 ml buffer B [1.5 M Tris base (TRS003, BioShop Canada Inc.) and 0.04% SDS dissolved in dH_2O, pH 8.8], 2.5 ml 40% acrylamide/bis-acrylamide (Acryl/Bis; 1610148, Bio-Rad), 50 µl 10% ammonium persulphate (APS; A3678, Sigma-Aldrich) and 20 µl tetramethylethylenediamine (TEMED; 15524-010, Invitrogen)] and a 4% stacking gel [3.25 ml ddH_2O, 1.25 ml buffer C (0.5 M Tris and 0.04% SDS dissolved in dH_2O, pH 6.8), 0.5 ml 40% Acryl/Bis, 25 µl 10% APS and 10 µl TEMED] as described in Jubouri et al., 2021. Gels were placed in 1X Tris glycine SDS (TGS) running buffer consisting of 2.5 mM Tris base, 0.192 M glycine (GLN002, BioShop Canada Inc.) and 0.1% SDS dissolved in dH_2O. Proteins were migrated (2 h; 100 V) and blotted (2 h; 100 V) on nitrocellulose membrane (pore

size 0.2 µm, Bio-Rad Laboratories, Hercules, CA, USA) in 20% Western transfer buffer consisting of 250 mM Tris base, 1.92 M glycine dissolved in dH_2O. Membranes were then incubated in Odyssey blocking buffer (LI-COR Biosciences, Lincoln, NE, USA) for 1 h at room temperature.

Membranes were incubated overnight at 4°C in rabbit-raised Pck1 (A2036, ABclonal Technology, Woburn, MA, USA) or Glut4 (A7637, ABclonal Technology) antibodies (diluted 1:1000 in Odyssey blocking buffer), previously validated in rainbow trout (Jubouri et al., 2021). Following incubation in primary antibodies, membranes were washed with phosphate buffered saline and Tween 20 [phosphate buffered saline (PBS; P4417, Sigma-Aldrich) and 0.01% (v/v) Tween 20 (P9416, Sigma-Aldrich)] and incubated with IRDye 800 CW goat-anti-rabbit secondary antibody (diluted 1:5000 in Odyssey blocking buffer; 925-32211, LI-COR) for 1.5 h at room temperature on the shaker protected from light. Following incubation in secondary antibodies, membranes were washed with PBST followed by PBS as described in Jubouri et al., 2021. Membranes were visualized by infrared fluorescence using the Odyssey Imaging System (LI-COR Biosciences) and band intensity was quantified by Odyssey Infrared Imaging System software (v.3.0; LI-COR Biosciences). Protein intensities were normalized to Revert 700 Total Protein Stain (LI-COR Biosciences) intensity. Finally, fold changes were calculated relative to the control group.

Enzyme activities

Tissue homogenate was prepared by sonicating 100 mg of tissue in 1 ml of cold homogenization buffer. Homogenates were centrifuged (5 min; 2400 RCF) at 4°C, the resulting supernatants were recovered and stored at -80°C. The homogenization buffer

(pH 7.5) contained 25 mM Tris-HCl, 1 mM EDTA, 5 mM dithiothreitol (DTT; D0632, Sigma-Aldrich) and 0.05% Triton X-100. Protein concentrations were determined using Bradford reagent (B6916, Sigma-Aldrich) assay with BSA as a standard. Enzyme activity was determined kinetically at room temperature by measuring the oxidation of NADH or reduction of nicotinamide adenine dinucleotide phosphate ($NADP^+$) at 340 nm using a microplate reader, expressed as μmol min^{-1} g^{-1} protein and assayed in triplicate. Control reactions were run for 10 min for each enzyme assay after adding reagents. Background activity was subtracted from enzyme activity. The conditions of the individual enzyme assay were as detailed below (final concentration in the well). HK (EC 2.7.1.1) and glucokinase (GK; EC 2.7.1.2) assay mixture contained 300 mM imidazole (I202, Sigma-Aldrich, pH 8.1), 100 mM potassium chloride (KCl; P5405, Sigma-Aldrich), 10 mM magnesium chloride ($MgCl_2$; M8266, Sigma-Aldrich), 1 mM $NADP^+$ (N0505, Sigma-Aldrich), 5 U ml^{-1} G6PDH, 5 mM ATP and 5 or 50 mM glucose (G7021, Sigma-Aldrich; omitted for control) for HK and GK respectively. PCK (EC 4.1.1.32) reaction mixture contained 50 mM imidazole, 20 mM $NaHCO_3$, 1 mM manganese chloride ($MnCl_2$; 244589, Sigma-Aldrich), 0.5 mM phosphoenolpyruvate (PEP) · Na_3 (P7002, Sigma-Aldrich), 0.12 mM NADH (N8129, Sigma-Aldrich), 6 U ml^{-1} malate dehydrogenase and 0.2 mM deoxyguanosine diphosphate (dGDP; D9250, Sigma-Aldrich; omitted for control). HOAD (EC 1.1.1.35) reaction mixture contained 50 mM imidazole, 5 mM EDTA, 1 mM potassium cyanide (KCN; 2078101, Sigma -Aldrich), 0.05 mM NADH and 0.1 mM acetoacetyl CoA (A1625, Sigma-Aldrich; omitted for control).

Calculations and statistics

The Fulton's condition factor, *K*, was calculated using the equation,

$$K = \frac{10^5 \cdot m_b}{L^3}$$

Here m_b is body mass and *L* is fork length (Blackwell et al., 2000). Rates of *in vivo* R_a glucose and R_a glycerol were calculated over time using the steady-state equation of Steele (Steele, 1959). Statistical comparisons for metabolite kinetics (series 1 and 2) were performed using one-way repeated-measures two-way analysis of variance (RM-ANOVA) with the Dunnett's post hoc test to compare with mean baseline values. Glucose, glycerol and lactate concentrations were analyzed by two-way RM-ANOVA (series 3; Table 2.3). Gene expression, protein abundance and enzyme activity results were analyzed using a two-tailed unpaired t-test to assess the effects of exogenous lactate. Before all tests, normality and homoscedasticity were assessed using the Shapiro-Wilk test and the Levene's test, respectively. When the assumptions of normality or equality of variances were not met, the data were normalized by natural log or square root transformation. If the transformation was unsuccessful, Kruskall-Wallis non-parametric one-way analysis of variance (ANOVA) on ranks (series 1 and 2) or non-parametric Mann-Whitney U test (series 3) were performed. Values presented are means ± s.e.m. and a level of significance of $p<0.05$ was used in all tests.

Results

Series 1: Glucose kinetics

During the measurement of glucose kinetics, exogenous lactate infusion had no effect on plasma glucose concentration ($p>0.05, F=0.890, df=9$; Figure 2.1A), but progressively increased plasma lactate concentration to 10.9 ± 0.4 mM over 180 min

(*p<0.001, F=172.612, df=9*; Figure 2.1B and Table 2.2). Elevating plasma lactate caused an increase in glucose specific activity (*p<0.001, F=3.822, df=9*; Figure 2.2A) and a decrease in hepatic glucose production from a baseline rate of 16.4 ± 2.0 μmol kg^{-1} min^{-1} to a final value of 8.9 ± 1.2 μmol kg^{-1} min^{-1} (*p<0.001, F=6.449, df=9*; Figure 2.2B and Table 2.2).

Series 2: Glycerol kinetics

During the measurement of glycerol kinetics, the infusion of exogenous lactate caused an increase in plasma glycerol concentration (*p<0.001, F=14.337, df=9*; Figure 2.3A) and plasma lactate concentration (*p<0.001, F=71.923, df=9*; Figure 2.3B). Glycerol concentration doubled and lactate concentration reached 10.5 ± 1.4 mM: the same level as in the glucose kinetics experiments (Table 2.2). Increasing the availability of plasma lactate caused minor fluctuations in glycerol specific activity (*p<0.05, df=9;* Figure 2.4A) and glycerol production or lipolytic rate (*p<0.05, df=9*; Figure 2.4B). However, for these 2 parameters, post hoc tests could not identify any means that were significantly different from the baseline (Figure 2.4B and Table 2.2).

Figure 2.1. Circulating glucose (A) and lactate concentrations (B) of rainbow trout while hepatic glucose production (R_a glucose) was quantified during exogenous lactate infusion that started at time 0. Values are means ± s.e.m. (N=8). Significant differences from mean baseline values are indicated by *** (*p<0.001*).

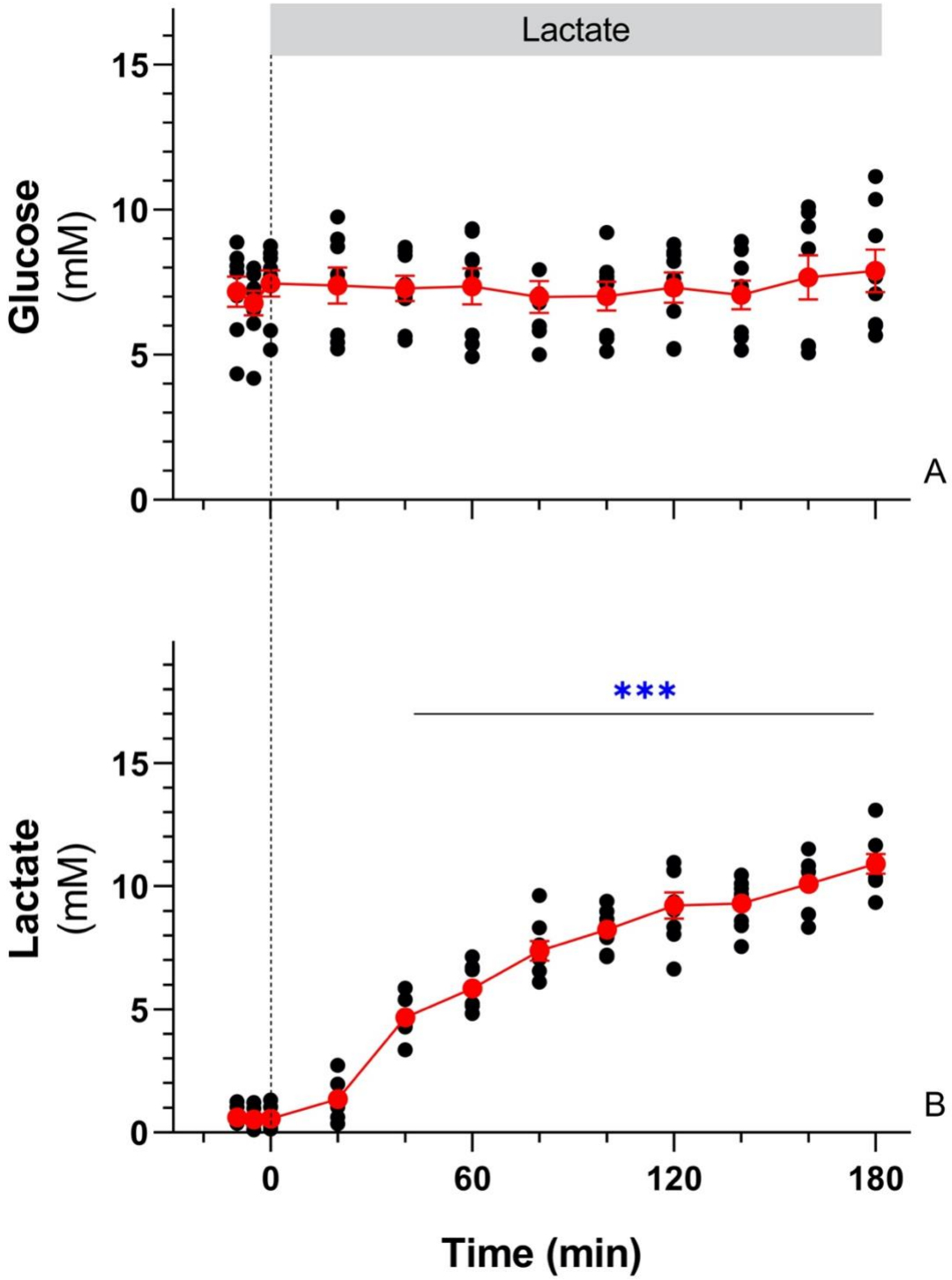
Lactate
Glucose
(mM)
15
10
5
0
A
***
Lactate
(mM)
15
10
5
0
B
0
60
120
180
Time (min)

Figure 2.2. Effects of exogenous lactate on glucose specific activity (A) and hepatic glucose production (R_a glucose) (B) in rainbow trout. Values are means ± s.e.m. (N=7-8). Significant differences from mean baseline values are indicated by * ($p<0.05$), ** ($p<0.01$) and *** ($p<0.001$).

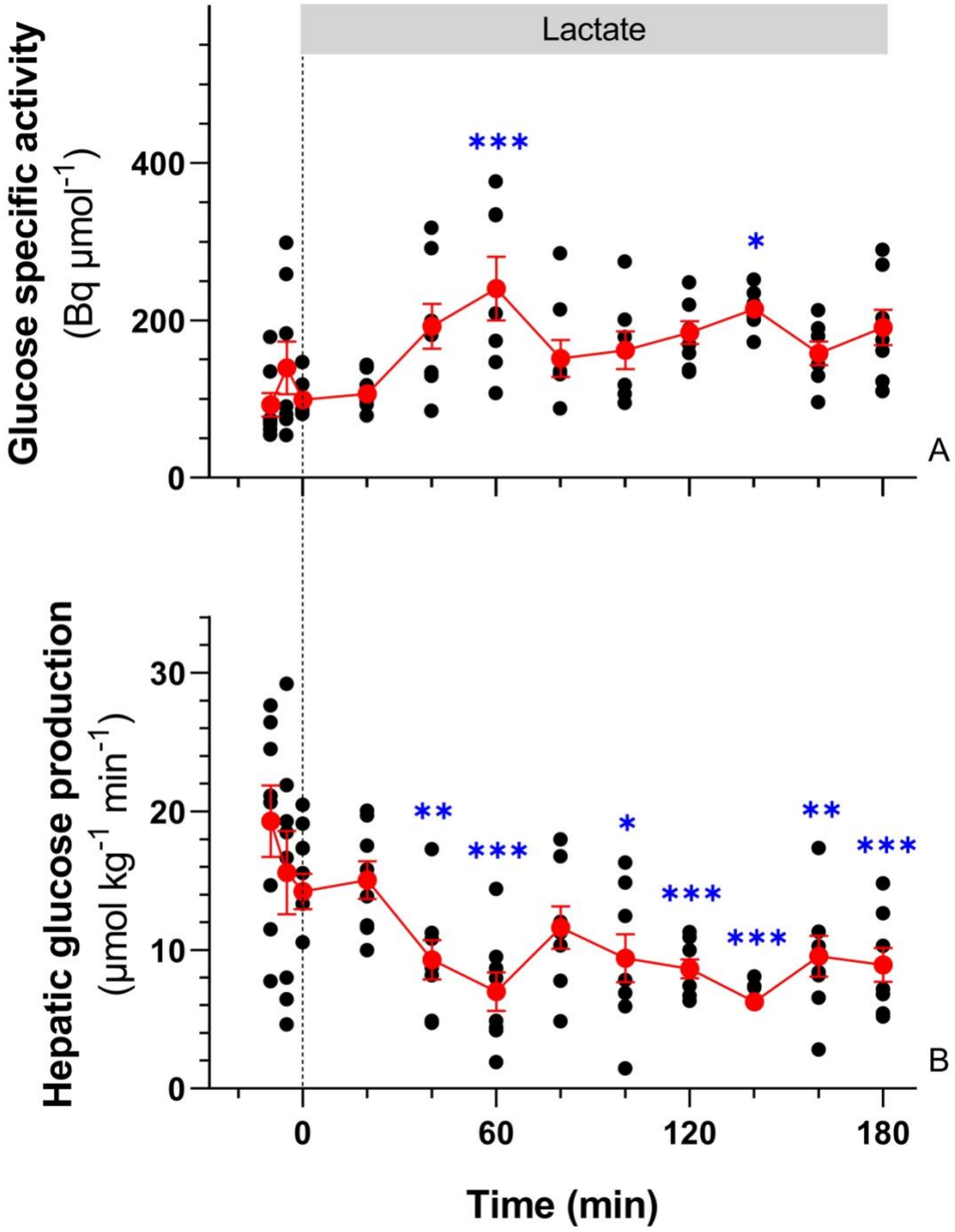
Lactate
Glucose specific activity
(Bq µmol-1)
400
200
0
***
*
A
Hepatic glucose production
(µmol kg-1 min-1)
30
20
10
0
**
***
*
***
***
**
***
B
0
60
120
180
Time (min)

Figure 2.3. Circulating glycerol (A) and lactate concentrations (B) of rainbow trout while lipolytic rate (R_a glycerol) was quantified and during exogenous lactate infusion that starts at time 0. Values are means ± s.e.m. (N=10). Significant differences from mean baseline values are indicated by ** ($p<0.01$) and *** ($p<0.001$).

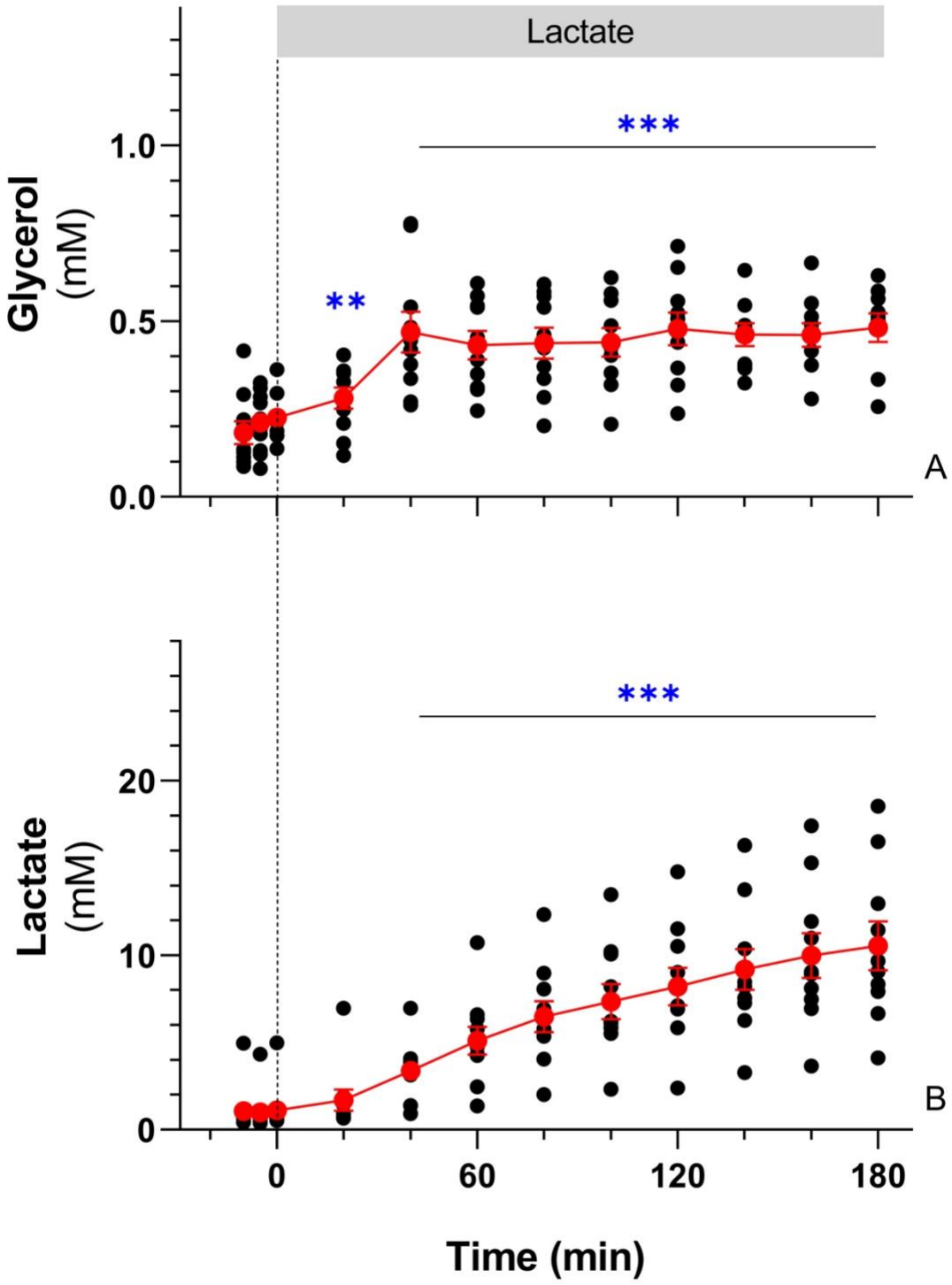
Lactate
***
**
1.0
0.5
0.0
Glycerol
(mM)
A
***
20
10
0
Lactate
(mM)
B
0
60
120
180
Time (min)

Figure 2.4. Effects of exogenous lactate on glycerol specific activity (A) and lipolytic rate (R_a glycerol) (B) in rainbow trout. Values are means ± s.e.m. (N=10).

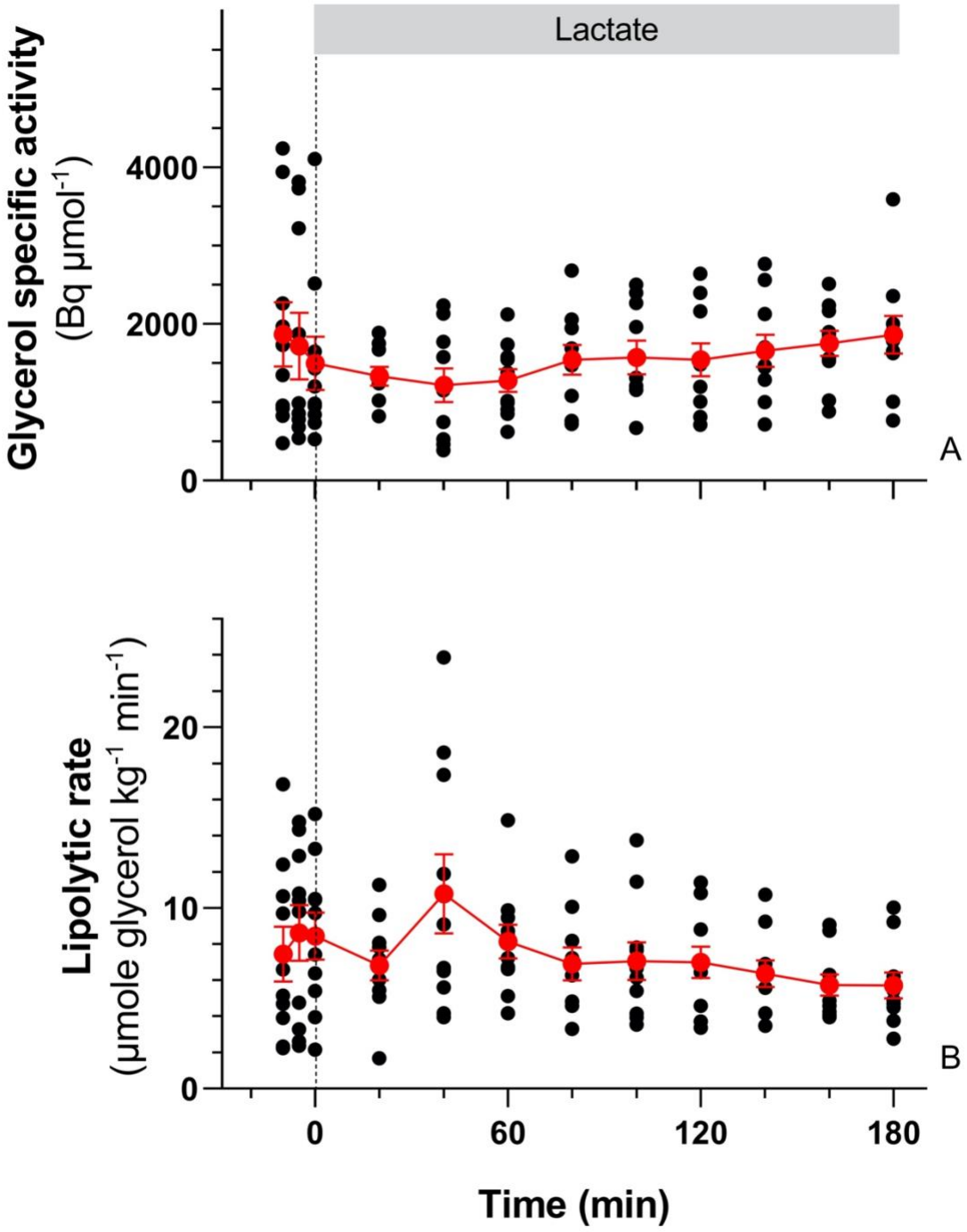
Lactate
Glycerol specific activity
(Bq µmol-1)
4000
2000
0
A
Lipolytic rate
(µmole glycerol kg-1 min-1)
20
10
0
B
0
60
120
180
Time (min)

Table 2.2. Initial (baseline) and final values after 3 h of lactate administration for the kinetics experiments.

	Baseline (0 h)	**Final (3 h)**
Plasma glucose (mM)	7.14 ± 0.45	7.89 ± 0.74
R_a glucose (μmol kg^{-1} min^{-1})	16.42 ± 2.01	8.92 ± 1.22
Plasma lactate (mM)	0.82 ± 0.22	10.90 ± 0.40
Plasma glycerol (mM)	0.21 ± 0.03	0.48 ± 0.04
R_a glycerol (μmol kg^{-1} min^{-1})	8.17 ± 1.39	5.70 ± 0.72
Plasma lactate (mM)	1.06 ± 0.41	10.53 ± 1.40

Values are means ± s.e.m (N=8-10). Hepatic glucose production (R_a glucose) and glycerol production (R_a glycerol) was obtained with the steady-state equation.

Series 3: Gene expression, protein signaling and enzyme activities

Metabolite concentrations

Plasma metabolite concentrations of the fish used for tissue measurements (series 3) are summarized in Table 2.3. Control animals that received a Cortland saline infusion showed no changes in glucose, glycerol or lactate levels. Those given an infusion of exogenous lactate also maintained steady glucose concentration, but more than doubled glycerol concentration. In addition, they showed a large increase in plasma lactate concentration like the animals used to measure *in vivo* metabolite fluxes (series 1 and 2). Interactions between time and treatment effects were significant for glycerol and lactate concentrations.

Table 2.3. Plasma lactate, glucose and glycerol concentration for series 3: molecular experiment.

	Group	Baseline (0 h)	Final (3 h)	Time effect	Treatment effect	Time×treatment interaction
Glucose (mM)	Control	4.52 ± 0.37	4.57 ± 0.64	ns	ns	ns
	Lactate	4.57 ± 0.43	4.12 ± 0.48			
Glycerol (mM)	Control	0.21 ± 0.02	0.24 ± 0.03	ns	ns	*
	Lactate	0.20 ± 0.02	0.51 ± 0.09			
Lactate (mM)	Control	0.67 ± 0.05	0.67 ± 0.06	ns	ns	****
	Lactate	0.64 ± 0.04	14.9 ± 1.16			

Values are means ± s.e.m. ns $p>0.05$, * $p<0.05$, **** $p<0.0001$; ns, no significant difference.

Gene expression

Exogenous lactate reduced the relative mRNA expression of the lactate receptor *hcar1* in red muscle (*p=0.0056, t=3.367, df=12*; Figure 2.5), suggested a non-significant trend to decrease in white muscle (*p=0.0572, t=3.124, df=11*; Figure 2.5), and had no effect in the liver (*p=0.1440, t=1.555, df=13*; Figure 2.5). The impacts of lactate on target genes that play key roles in the regulation of carbohydrate metabolism are shown in Figure 2.6. For carbohydrate metabolism, exogenous lactate decreased the relative mRNA abundance of the glucose transporters *glut4a* and *glut4b* in red muscle (*glut4a: p=0.0011, t=4.270, df=12; glut4b: p=0.0009, t=4.630, df=10*), but was increased in white muscle (*glut4a: p=0.0391, t=2.341, df=11; glut4b: p=0.0227, t=2.691, df=10*). In the liver, lactate reduced the relative expression of *pck1* (*p=0.0282, t=2.611, df=9*), but had no effect on *pck2a* and *pck2b* (*pck2a: p=0.9739, t=0.03336, df=13; pck2b: p=0.5370, t=0.6342, df=13*). For glucose-6-phosphatase, none of its paralogues (*g6pca*, *g6pcb1a* and *g6pcb1b*) were affected by lactate (*g6pca: p=0.1363, t=1.607, df=11; g6pcb1a: p=0.7783, t=0.2879, df=12; g6pcb1b: p=0.3578, t=0.9562, df=12*). In the liver, lactate reduced the relative expression of the *gckb* (*p=0.0049, t=3.506, df=11*), but had no effect on the other paralogue of this glycolytic enzyme (*gcka*: *p=0.2422, t=1.236, df=11*).

The impacts of lactate on target genes that play key roles in the regulation of lipid metabolism are shown in Figure 2.7. The relative transcript abundance of 2 enzymes involved in lipolysis was quantified: *hsl* and *lpl*. The relative mRNA expression of *hsl* was increased in red muscle (*p=0.0024, t=3.911, df=11*), decreased in white muscle (*p=0.0114, t=2.982, df=12*) and had no effect in the liver (*p=0.1382, t=1.588, df=12*). Exogenous lactate had no effect on the relative mRNA expression of *lpl* in the liver, red

or white muscle (*liver: p=0.6528, t=0.4614, df=12; red muscle: p=0.9500, t=0.06408, df=12; white muscle: p=0.6369, t=0.4842, df=12*). The relative transcript abundance of 2 enzymes from the β-oxidation pathway was quantified: *cpt1a* and *hoad*. Lactate did not affect *cpt1a* in the liver, red muscle or white muscle (*liver: p=0.0521, t=2.156, df=12; red muscle: p=0.5906, t=0.5541, df=11; white muscle: p=0.2637, t=1.173, df=12*). The relative expression of *hoad* was stimulated in white muscle (*p=0.0089, t=3.119, df=12*), but remained constant in the liver and red muscle (*liver: p=0.3808, t=0.9100, df=12; red muscle: p=0.2286, t=1.269, df=12*). The relative mRNA expression of the NEFA transporter *cd36* was increased in the liver (*p=0.0334, t=2.430, df=11*), but remained unaffected by lactate in red and white muscle (*red muscle: p=0.6648, t=0.4465, df=10; white muscle: p=0.1520, t=1.522, df=13*). Similarly, exogenous lactate caused no measurable change in the transcript abundance of *fas* and *srebp1c* in the liver (*fas: p=0.0537, t=2.139, df=12; srebp1c: p=0.1956, t=1.378, df=11*).

Figure 2.5. Effects of exogenous lactate on the relative mRNA expression of the hydroxycarboxylic acid receptor 1 (*hcar1*) in rainbow trout tissues. Individual data points and means ± s.e.m. (N=6-7) are presented for the control (white) and lactate (grey) group. Significant effect of lactate is indicated by ** ($p<0.01$).

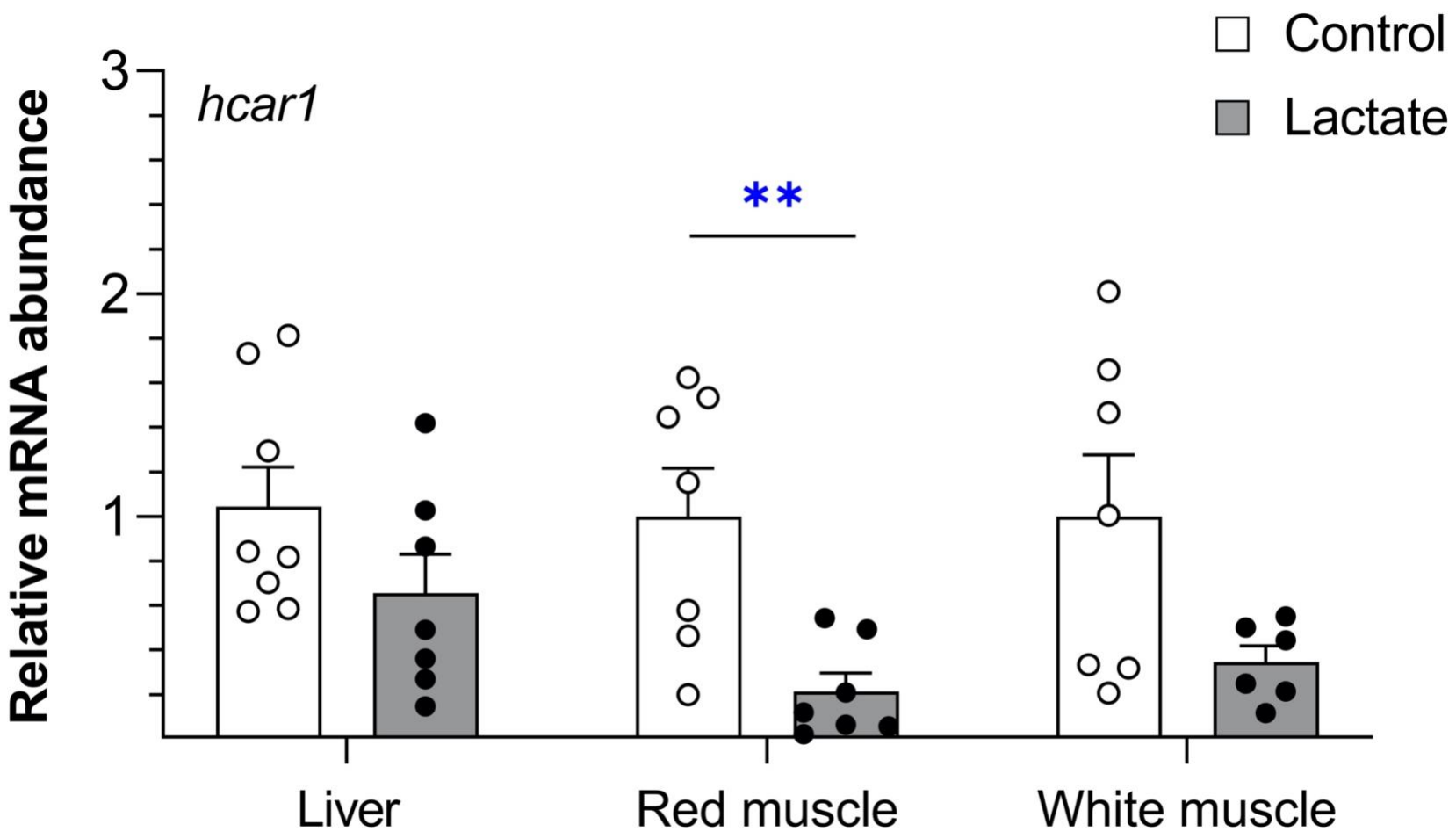
Control
Lactate
hcar1
Relative mRNA abundance
3
2
1
**
Liver
Red muscle
White muscle

Figure 2.6. Effects of exogenous lactate on the relative mRNA expression of genes associated with carbohydrate metabolism in rainbow trout tissues: glucose transport 4 (*glut4a* and *glut4b*), glucokinase (*gcka* and *gckb*), phosphoenolpyruvate carboxykinase (*pck1*, *pck2a* and *pck2b*) and glucose 6 phosphatase (*g6pca*, *g6pcb1a* and *g6pcb1b*). Individual data points and means ± s.e.m. (N=6-8) are presented for the control (white) and lactate (grey) group. Significant effects of lactate are indicated by * (*p<0.05*), ** (*p<0.01*) and *** (*p<0.001*).

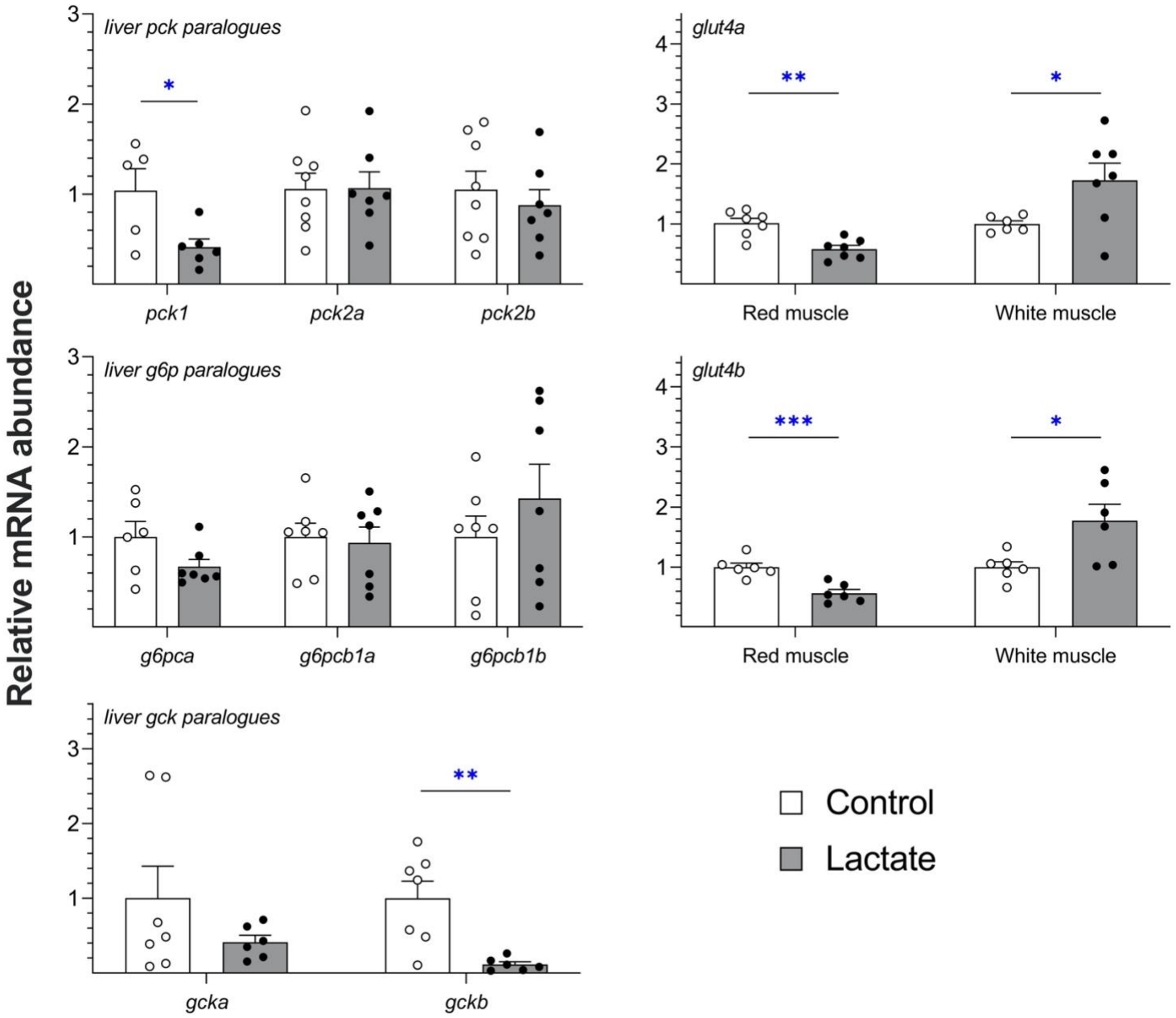
Relative mRNA abundance
liver pck paralogues
*
pck1
pck2a
pck2b
glut4a
**
*
Red muscle
White muscle
liver g6p paralogues
g6pca
g6pcb1a
g6pcb1b
glut4b
***
*
Red muscle
White muscle
liver gck paralogues
**
gcka
gckb
Control
Lactate

Figure 2.7. Effects of exogenous lactate on the relative mRNA expression of genes associated with lipid metabolism in rainbow trout tissues: hormone-sensitive lipase (*hsl*), lipoprotein lipase (*lpl*), carnitine palmitoyltransferase 1a (*cpt1a*), 3-hydroxyacyl dehydrogenase (*hoad*), fatty acid translocase (*cd36*), fatty acid synthase (*fas*) and sterol regulatory element-binding protein 1c (*srebp1c*). Individual data points and means ± s.e.m. (N=5-8) are presented for the control (white) and lactate (grey) group. Significant effects of lactate are indicated by * ($p<0.05$), ** ($p<0.01$) and *** ($p<0.001$).

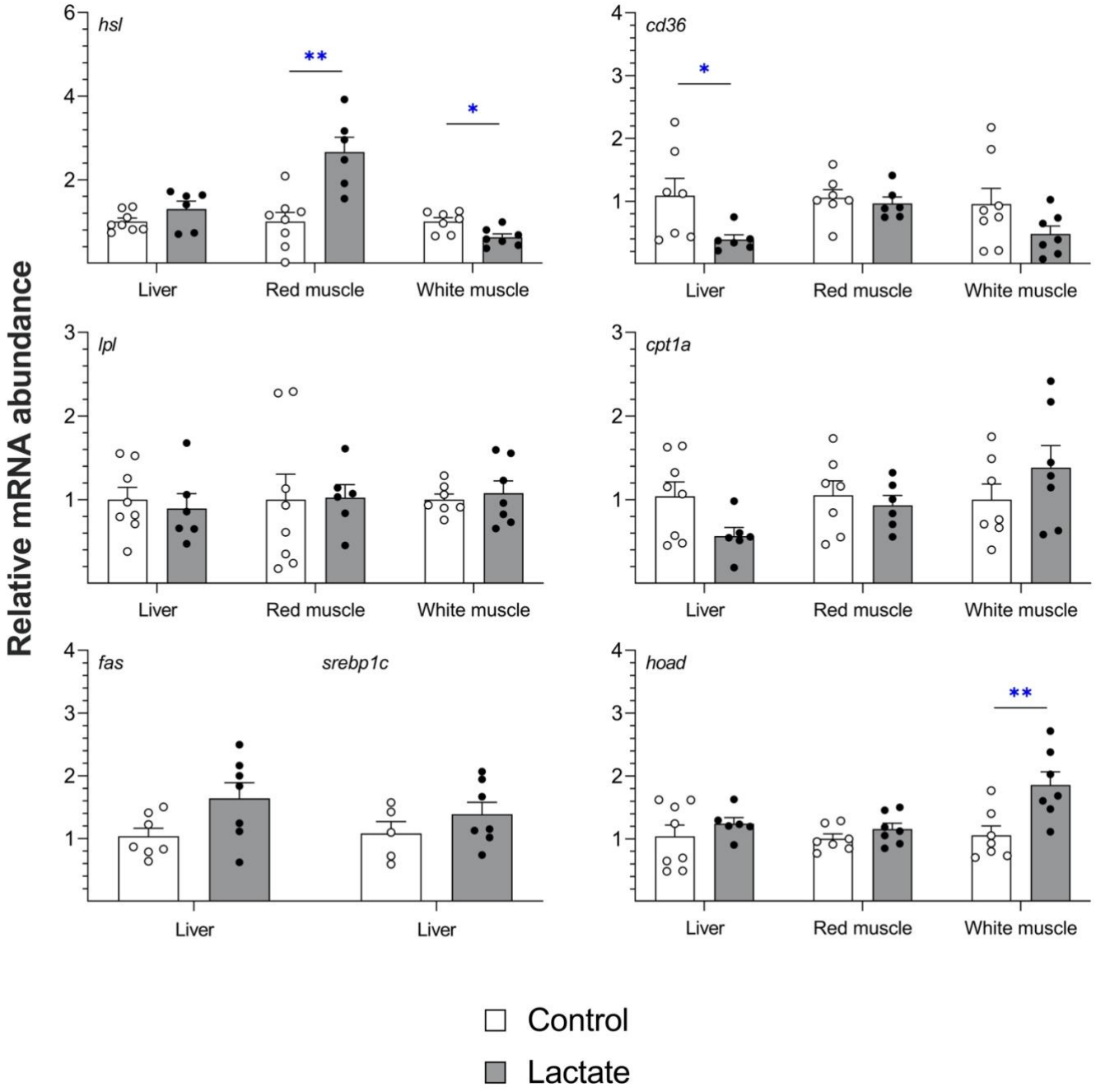
Relative mRNA abundance
hsl
cd36
lpl
cpt1a
fas
srebp1c
hoad
Liver
Red muscle
White muscle
Control
Lactate

Protein expression

The relative protein abundance of Pck1 and Glut4 was quantified by Western blotting (Figure 2.8). Exogenous lactate decreased the protein expression of Pck1 in the liver (*p=0.0260, Mann-Whitney U=4*), echoing what had been observed for the mRNA abundance of the gluconeogenic enzyme (Figure 2.8). However, the expression of Glut4 in red or white muscle was not affected by lactate (*red muscle: p=0.2403, Mann-Whitney U=10; white muscle: p=0.7452, t=0.3341; df=10*).

Enzyme activities

The effects of exogenous lactate on the activities of target enzymes playing key roles in the regulation of carbohydrate and lipid metabolism are presented in Figure 2.9. For carbohydrate metabolism, lactate caused an increase in HK activity in white muscle (*p=0.0121, t=3.001, df=11*), but had no effect on hepatic PCK, HK, or GK (*PCK: p=0.0666, t=2.002, df=13; HK: p=0.1679, t=1.461, df=13; GK: p=0.1433, t=1.566, df=12*). For lipid metabolism, HOAD activity was reduced by lactate in the liver (*p=0.0027, t=3.694, df=13*), but remained constant in red and white muscle (*red muscle: p=0.9062, t=0.1202, df=13; white muscle: p=0.1834, t=1.412, df=12*).

Figure 2.8. Effects of exogenous lactate on the protein expression of liver phosphoenolpyruvate carboxykinase (Pck1) and muscle glucose transporter 4 (Glut4) in rainbow trout. Individual data points and means ± s.e.m. (N=6) are presented for the control (white) and lactate (grey) group. Significant effect of lactate is indicated by * (*$p<0.05$*).

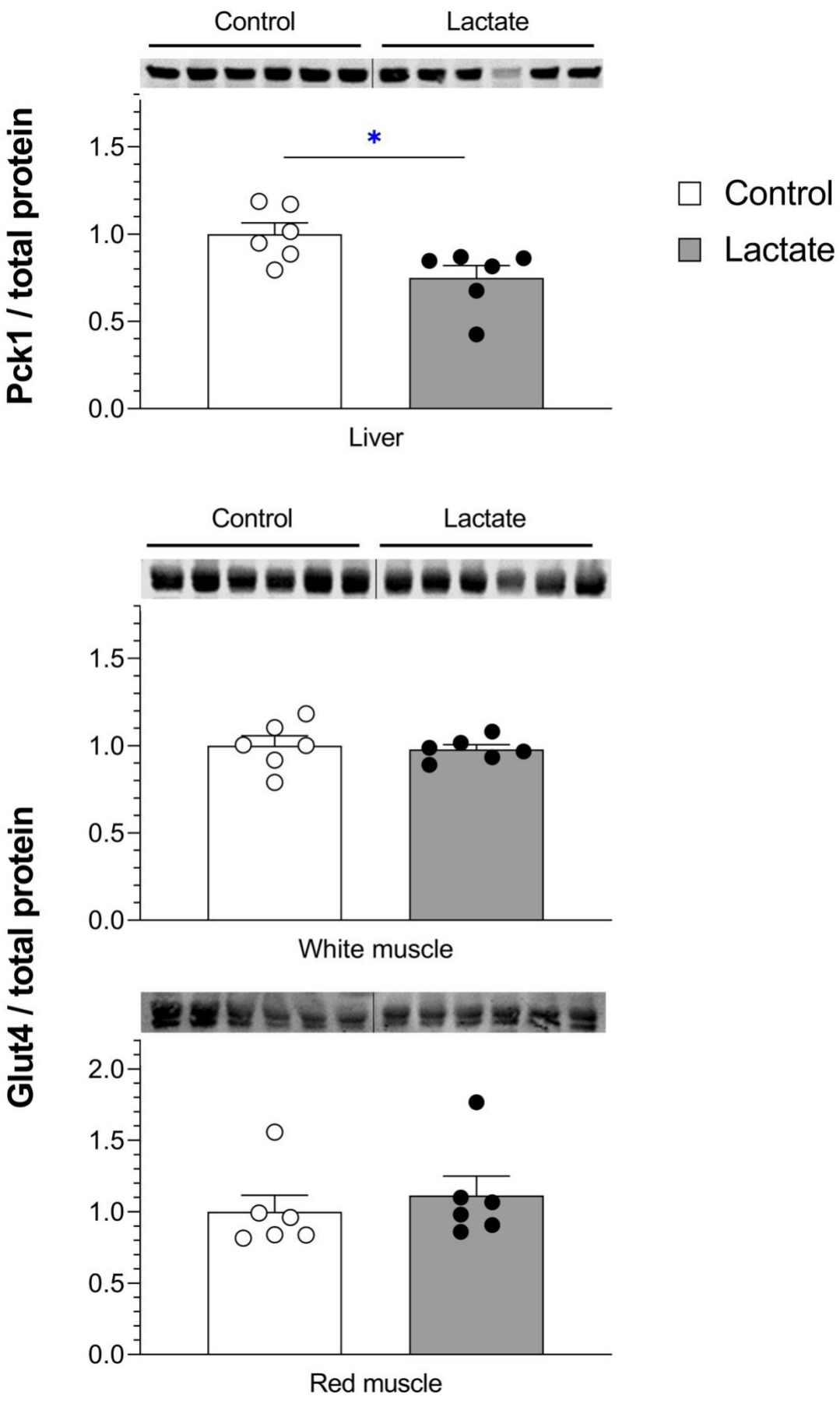
Control
Lactate
Pck1 / total protein
1.5
1.0
0.5
0.0
*
Liver
Control
Lactate
Glut4 / total protein
White muscle
2.0
1.5
1.0
0.5
0.0
Red muscle
Control
Lactate

Figure 2.9. Effects of exogenous lactate on the activity of enzymes involved in carbohydrate and lipid metabolism in rainbow trout tissues: phosphoenolpyruvate carboxykinase (PCK) hexokinase (HK), glucokinase (GK) and 3-hydroxyacyl dehydrogenase (HOAD). Individual data points and means ± s.e.m. (N=7-8) are presented for the control (white) and lactate (grey) group. Significant effects of lactate are indicated by ** ($p<0.01$).

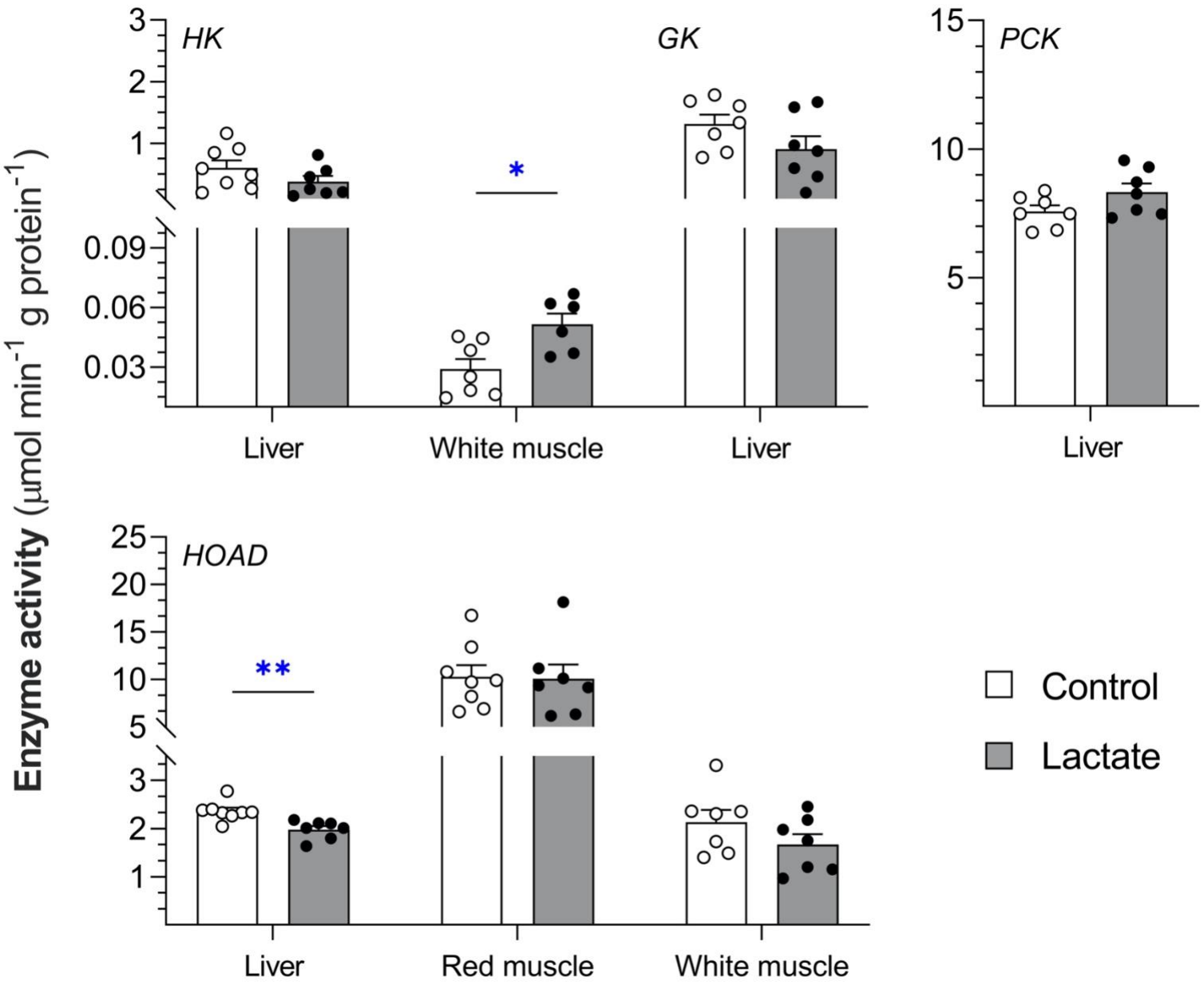
HK
GK
PCK
HOAD
Enzyme activity (µmol min-1 g protein-1)
3
2
1
0.09
0.06
0.03
15
10
5
25
20
15
10
5
3
2
1
*
**
Liver
White muscle
Liver
Liver
Liver
Red muscle
White muscle
Control
Lactate

Discussion

This study shows that high lactate does not inhibit lipolysis in fish as it does in mammals but strongly decreases hepatic glucose production. This lack of effect on trout lipolytic rate may be due to the lack of HCAR1-mediated signaling because the expression of the trout receptor is not modified by elevated lactate except in red muscle where it declines. Therefore, the well-known HCAR1 autocrine feedback that slows lipolysis in mammals does not seem to operate in fish. Trout R_a glucose is greatly reduced by lactate, mainly through a decrease in gluconeogenesis caused by the inhibition of PCK1. The overall need for glucose is reduced because it is replaced by lactate as an oxidative fuel in tissues that readily use carbohydrates like the brain, heart, and liver. Opposite responses in red and white muscle *glut4* expression show that glucose import is reduced in red muscle where it is replaced by lactate, but increased in white muscle: a tissue with a very limited capacity for MCT-mediated transmembrane lactate transport (Omlin and Weber, 2013). These results emphasize the importance of measuring metabolite fluxes directly rather than relying on changes in concentration when investigating metabolic responses (Haman et al., 1997b). Without quantifying glycerol and glucose kinetics, it would have been impossible to demonstrate that lactate does not affect lipolysis (because glycerol concentration increases dramatically) and strongly inhibits hepatic glucose production (because glycemia remains perfectly steady).

Lactate infusion protocol mimics strenuous exercise

Here, I have selected to administer exogenous lactate in the circulation rather than to exercise the animals. Before starting the exogenous supply, the fish showed no

signs of stress and their circulating lactate (~1 mM), glucose (~7 mM) and glycerol levels (~0.2 mM) (Figures 2.1 and 2.3) were well within normal resting values (Forbes et al., 2019a; Teulier et al., 2013; Turenne and Weber, 2018). Lactate was then infused at twice the baseline endogenous rate of release in the circulation (Omlin and Weber, 2010) to reach plasma levels of 10.9 ± 0.4 mM and 10.5 ± 1.4 mM after 3 h in series 1 and 2 experiments, respectively (Figures 2.1B and 2.3B, Table 2.2). The rate of exogenous supply was equal to what rainbow trout would release endogenously in the circulation when they swim at ~3 BL s^{-1}(Teulier et al., 2013). The final plasma lactate concentrations were similar to those measured in previous exogenous supply experiments (Omlin et al., 2014) and adequately mimicked the normal increase in circulating lactate induced by strenuous exercise (Milligan and Girard, 1993; Omlin and Weber, 2013).

High lactate does not inhibit fish lipolysis

The rate of glycerol release in the circulation is the best index of lipolysis (Wolfe, 1992) and it has been widely used to assess *in vivo* lipid mobilization of mammals (Issekutz et al., 1975; McClelland et al., 2001; Weber and Reidy, 2012; Wolfe et al., 1990) as well as fish (Bernard et al., 1999; Magnoni et al., 2008b; Turenne and Weber, 2018; Wolfe et al., 1990). This study is the first to investigate the effects of lactate on whole-organism lipolytic rate in any species. Surprisingly, how lactate modulates glycerol and NEFA fluxes have never been measured in mammals, and this provides an important future research avenue to improve the general understanding of lactate signaling.

Present results show that elevated lactate levels do not affect trout R_a glycerol which remains at an average baseline value of 7.3 ± 0.5 µmol kg^{-1} min^{-1} throughout the experiment (Figure 2.4B). This contrasts greatly with the well-known anti-lipolytic effect of hyperlactatemia reported for mammals (Brooks, 2018; Brooks et al., 2022) and it suggests that other responses of mammalian lipid metabolism to lactate, like triacylglycerol accumulation and the lowering of circulating FA levels (Chen et al., 2021; Sun et al., 2016; Zhou et al., 2021) may also be absent in trout. This idea is supported by the observation that lactate has no effect on the expression of *fas* and *srebp1c* (Figure 2.7), two genes involved in lipogenesis (Girard et al., 1997; Thompson et al., 2010). Similarly, the expression of *lpl* does not respond to lactate and the expression of *hsl* shows opposite responses in red muscle (activation that would prevent lipid storage) and white muscle (inhibition that could promote storage; Figure 2.7). What could then be the underlying physiological reasons why the lipid metabolism of fish remains mostly insensitive to lactate? In mammals, lipolytic suppression is mediated by lactate binding to HCAR1 in adipose tissue and muscle (Ahmed et al., 2010). Even though fish possess the lactate receptor (Kuei et al., 2011; Thomsen et al., 2019), this pathway does not seem to operate in trout because HCAR1 does not respond to lactate and may therefore have a different function than in mammals. Mammalian HCAR1 is regulated via an autocrine feedback loop (Rooney and Trayhurn, 2011) whereby lactate increases the expression of the receptor (Longhitano et al., 2022; Sun et al., 2016). However, lactate has no stimulating effect on trout *hcar1* expression in any tissue, and even suppresses it by 78% in red muscle (Figure 2.5). Overall, rainbow trout always maintain a high lipolytic rate and elevated TAG/NEFA cycling under a wide range of different

physiological conditions that include rising plasma lactate concentrations to ~10 mM in the resting state (Figure 2.4B), endurance exercise lasting several days (Bernard et al., 1999), and graded exercise up to critical swimming speed (Turenne and Weber, 2018). In mammals, lactate inhibits lipolysis (Brooks et al., 2022) and equivalent endurance and strenuous exercise stresses cause major changes in fat mobilization (Klein et al., 1996; Wolfe et al., 1990). The lack of HCAR1 signaling observed here may be responsible for the high lipolytic activity and the lipolytic inertia now well-characterized for fish. This study highlights major functional differences between fish and mammals with respect to the physiological role of lactate and HCAR1 signaling in metabolic fuel selection.

High lactate reduces hepatic glucose production

Elevated lactate causes a large decline in R_a glucose from 16.4 ± 2.0 to 8.9 ± 1.2 μmol kg^{-1} min^{-1} (Figure 2.2B) and this 46% reduction occurs within an hour of exogenous supply. A similar decrease in resting glucose production was reported in endurance-trained humans (Miller et al., 2002a), but not sedentary subjects (Miller et al., 2002b) when circulating lactate was clamped at 4 mM. R_a glucose represents the combined contributions of gluconeogenesis and glycogenolysis, but it does not provide information on the relative importance of each pathway. However, tissue measurements show that a reduction in gluconeogenic flux is most likely responsible for the observed decrease in total glucose production. This is because lactate infusion reduces both *pck1* transcript abundance (-60%; Figure 2.6) and Pck1 protein levels (-24%; Figure 2.8). In mammals, cytosolic Pck1 is considered the first rate-limiting step of gluconeogenesis. It catalyzes the conversion of oxaloacetate to phosphoenolpyruvate that in turn serves as

a substrate for downstream gluconeogenic enzymes, among them fructose 1,6-bisphosphatase and glucose-6-phosphatase which ultimately cause the release of free glucose in the circulation. The Pck1 transcript has a very short half-life (~30 min) and there is no evidence that PCK is subject to covalent modifications or allosteric regulation. Its activity depends on transcription and/or pck1 mRNA degradation (Yu et al., 2021) and the observed inhibition of trout R_a glucose is, therefore, at least in part, caused by a decrease in gluconeogenesis mediated by the downregulation of Pck1.

In trout as well as mammals, the role of mitochondrial Pck2 has recently been the subject of renewed interest, especially in the context of substrate preference for gluconeogenesis (Marandel et al., 2019; Stark and Kibbey, 2014; Yu et al., 2021). Because mitochondrial Pck2 silencing reduces the ability to use lactate as a gluconeogenic substrate (Stark et al., 2014) and hypoxia induces the expression of *pck2b* in rainbow trout alevins, I have also quantified the hepatic expression of *pck2* transcripts but found no effect of lactate (Figure 2.6). The relative expression of cytosolic and mitochondrial Pck appears to be strongly species, tissue, and physiological state-dependent (Mommsen et al., 1985; Yu et al., 2021). Overall hepatic Pck activity did not change following lactate infusion (Figure 2.8) and previous reports show strong compartmentalization of Pck activity to mitochondria in rainbow trout (Mommsen et al., 1985). This suggests that other factors than changes in *pck1* transcript and Pck1 protein abundance are involved in reducing R_a glucose. Further work is needed to establish the exact localization of Pck isozymes and to delineate the relative influence of each isozyme on the regulation of trout gluconeogenesis.

Glucose, lactate and lipid oxidation

In rainbow trout, exogenous lactate had no effect on glycemia (Figure 2.1A), therefore, the lactate-mediated reduction in R_a glucose discussed earlier (Figure 2.2B), also represented a decrease in glucose utilization. At rest, oxidative disposal accounts for ~50% of glucose utilization. However, the availability of other oxidative substrates can alter the relative importance of glucose oxidation (Choi and Weber, 2016). *In vivo* kinetics, suggested a decrease in glucose utilization in trout, especially the liver, where *gck* paralogue expression is suppressed (Figure 2.6) and GK activity is unchanged (Figure 2.9). The expression and activity of GK in trout is a sensitive marker of hepatic glucose concentration (Panserat et al., 2000). Therefore, the maintenance of hepatic GK activity and decrease in paralogue expression suggests lactate may be used as an alternative fuel (Polakof and Soengas, 2008). Overall, glucose was not the preferred fuel under high lactate availability, indicating lactate as a predominant oxidative fuel.

In rainbow trout, plasma lactate concentration, as a result of exogenous infusion, increased to 10.9 ± 0.4 mM and 10.5 ± 1.4 mM in series 1 (Figure 2.1B) and 2 (Figure 2.3B) respectively. An exogenous supply increases lactate availability and consequently utilization in peripheral tissues (Omlin et al., 2014). Of the many fates of circulating lactate, its role as an oxidation fuel dominates lactate utilization (Brooks, 2002; Brooks, 2020; Brooks et al., 2022; Girard and Milligan, 1992; Milligan and Girard, 1993; Pagnotta and Milligan, 1991). In rainbow trout, oxidation is responsible for most lactate utilization observed during high intensity swimming, making oxidation essential for lactate elimination. Rainbow trout have a high baseline R_a lactate, likely as a continuous supply to highly aerobic tissues that favour lactate for oxidative metabolism (Omlin et

al., 2014; Omlin and Weber, 2010; Teulier et al., 2013). *In vitro* measurements in teleost have shown that highly aerobic tissues readily use lactate as a preferred oxidative fuel mediated by transmembrane lactate uptake through MCTs (Bilinski and Jonas, 1972; Lanctin et al., 1980; Milligan and Farrell, 1991; Omlin et al., 2014; Soengas and Aldegunde, 2002). Exogenous lactate has a significant impact on endogenous glucose supply, thus, trout may alter their fuel selection pattern by substituting other oxidative substrates for lactate. In the present study, tissue measurements suggest decreased NEFA mobilization and oxidation in hyperlactatemic trout, especially the liver, where HOAD activity (Figure 2.9) and *cd36* expression (Figure 2.7) were suppressed. Furthermore, mRNA levels of *lpl* and *cpt1a*, both indicators of NEFA mobilization, uptake and oxidation (Du et al., 2019; Rozovski et al., 2015) did not change after lactate treatment. Thus, circulating NEFAs were spared which further supports a substitution for lactate as the preferred oxidative substrate. Together, these findings support lactate as a useful oxidative fuel, replacing other oxidative substrates and suggest trout can modulate their fuel selection to accommodate elevated circulating lactate.

Differential oxidative fuel selection in red and white muscle

In rainbow trout, hyperlactatemia caused a tissue-specific response in red and white muscle. Slow and sustained swimming is maintained by oxidative muscle fibres in red muscle, while the fast-twitch glycolytic muscles fibres of white muscle are responsible for power output during brief periods of exhausting exercise (Domenici and Blake, 1997; Marras et al., 2013; McKenzie, 2011). Glucose and lactate metabolism in rainbow trout is significantly constrained by transmembrane transport through GLUTs and MCTs, respectively (Navale and Paranjape, 2016; Omlin et al., 2014). The

reduction in *glut4* paralogue expression in red muscle (Figure 2.6) may partially explain the decrease in glucose utilization, discussed above. However, no changes were observed in protein abundance (Figure 2.8). Gene expression and protein abundance often show differential responses and direct measurements of Glut4 translocation will be needed to confirm this conclusion. The decrease in glucose uptake in red muscle suggests a decreased requirement for glucose as an oxidative fuel, due to a preference for lactate.

In trout white muscle, exogenous lactate caused an increase in HK activity (Figure 2.9) and *glut4* paralogue expression (Figure 2.6). White muscle carbohydrate metabolism has been characterized as a quasi-closed system due to low lactate disposal from white muscle following exhaustive exercise, which prolongs recovery from intensive exercise (Wang et al., 1997; Watt et al., 1988). This retention of lactate in fish white muscle is explained by: (i) the poor expression of MCTs in trout compared to mammals and other trout tissues and (ii) the failure of exhaustive exercise to upregulate MCT isoform expression and thus lactate permeability in white muscle (Omlin and Weber, 2013). Thus, white muscle has a limited capacity to uptake lactate and may alter its fuel selection pattern to favour glucose uptake for oxidation and glycogen synthesis. Interestingly, the molecular signature in white muscle also suggests downregulation of NEFA mobilization and upregulation oxidation of muscle lipids stored in trout, where *hsl* expression was suppressed and *hoad* expression was induced, However, lactate caused no change in HOAD activity. It is important to note, changes in gene expression precede any changes in function. Overall, the lactate-driven HK activity and *glut4*

paralogue expression in white muscle are likely caused by the inability of white muscle to import and oxidize lactate.

Lipolytic rate cannot be predicted from changes in glycerol concentration

Circulating glycerol concentration was increased 2.3-fold over the first 40 min of exogenous lactate administration (Figure 2.3A). From this response alone (and without direct measurement of R_a glycerol), it could have been tempting to conclude that lipolysis had been greatly stimulated because glycerol concentration and flux are well known to show a strong positive correlation in the context of exercise (Klein et al., 1996; Turenne and Weber, 2018; Weber et al., 1993). This was clearly not the case here because lipolytic rate remained unaffected by hyperlactatemia (Figure 2.4B). This increase in plasma glycerol concentration was caused by a temporary divergence between the rates of glycerol appearance and disappearance (R_a>R_d) in the initial stages of the experiment. However, variability in flux measurements prevented us from showing this difference statistically after calculating R_a and R_d separately with the non-steady state equations of Steele (results not shown) (Steele, 1959). The dissimilar behaviours seen for glycerol concentration and flux illustrate the necessity to quantify fluxes whenever possible when investigating metabolism *in vivo* to avoid making erroneous conclusions based on concentrations (Haman et al., 1997b).

Chapter 3: Mobilization of energy reserves during Intralipid infusion

This chapter is based on a manuscript titled “Mobilization of rainbow trout energy reserves during Intralipid infusion”

Written by
Giancarlo G.M. Talarico, Elie Farhat, Jan A. Mennigen and Jean-Michel Weber

Biology Department, University of Ottawa, Canada

In preparation for
Journal of Experimental Biology

Author contributions: G.G.M.T., J.A.M. and J.-M.W. conception and design of research; G.G.M.T. and E.F. performed experiments; all authors analyzed data and interpreted results; G.G.M.T., J.A.M. and J.-M.W. prepared figures; G.G.M.T. drafted the manuscript; G.G.M.T., J.A.M. and J.-M.W. edited, revised and approved the manuscript.

Introduction

Lipids and their constituent FAs play a critical role in energy distribution at rest and during sustained exercise (Magnoni et al., 2006; McWilliams et al., 2004; Richards et al.; Richards et al., 2002; van Loon et al., 2001; Watanabe 1982). As a result of their high energy density, lipids, stored as TAG, make up the majority of energy reserves (Hurley et al., 1986; Weber, 2011). TAGs are liberated from reserves through lipolysis (3 NEFAs and 1 glycerol), to be oxidized for fuel during prolonged exercise or recycled through lipogenesis (Bou et al., 2016; Edens et al., 1990; Frayn, 2010; Tocher, 2003). Lipids can also circulate as TAG-rich micelles known as lipoproteins. Rainbow trout circulate >90% of lipids as mostly lower density lipoproteins (chylomicrons and VLDL) (Babin and Vernier, 1989; Magnoni and Weber, 2007). Lipids play an important role in mammalian fuel selection by regulating the opposing pathways, gluconeogenesis and glycolysis, stimulating *de novo* gluconeogenesis and inhibiting glucose oxidation (Berry et al., 1993; Jenkins et al., 1988; Thiébaud et al., 1982).

The regulation of metabolic fuel selection in rainbow trout is multifactorial and includes nutritional status, hormonal balance and exercise intensity and duration (Weber et al., 2016). Glucose mobilization (the rate of hepatic glucose production: R_a glucose) is reduced by exogenous carbohydrate loads (Choi and Weber, 2015), alanine (Jubouri et al., 2021), insulin (Forbes et al., 2019b) and prolonged swimming (Shanghavi and Weber, 1999). In fish, the mobilization of lipid reserves (the lipolytic rate or rate of glycerol production: R_a glycerol) is higher relative to their metabolic rate than most mammals (Turenne and Weber, 2018) and remains surprisingly unaffected by exogenous lactate (Chapter 2) and exercise (Bernard et al., 1999). Despite being well-

characterized in mammals, the role of lipids in modulating fish fuel mobilization *in vivo* has never been quantified. Therefore, the aim of this study was to explore how exogenous lipids modulate fuel selection *in vivo* by measuring its effects on hepatic glucose production and lipolytic rate in rainbow trout. My goals were to quantify the effects of Intralipid on: (i) R_a glucose and R_a glycerol, and (ii) strategic tissue parameters involved in carbohydrate and lipid metabolism. This integrative approach could explain the observed changes *in vivo*. The selected tissue indices targeted key carbohydrate and lipid metabolic pathways including: glycolysis, gluconeogenesis, lipolysis, lipogenesis, FA oxidation and fuel transport. I anticipated that exogenous lipids would cause an increase in lipolysis and an inhibition of hepatic glucose production as it does in mammals (Berry et al., 1993). It was predicted that these trout responses would be reflected by corresponding changes in key regulatory proteins of carbohydrate and lipid metabolism.

Methods

Animals

Rainbow trout (*Oncorhynchus mykiss*), with a Fulton's condition factor of 1.63 ± 0.05 (N=31) (Blackwell et al., 2000) of both sexes were purchased from Cedar Crest Trout Farm (Hanover, Ontario, Canada). Three groups of fish were used: (i) for *in vivo* measurements of glycerol and (ii) glucose kinetics, and (iii) for measurements of FA composition, gene expression (*real-time* RT-PCR), protein expression (Western blots) and enzyme activities. The physical characteristics of all experimental groups are presented in Table 3.1. The fish were held in a 1,200-litre flow-through tank supplied with dechloraminated Ottawa tap water at 13°C, on a 12 h:12 h light-dark photoperiod

and were fed Profishnet floating fish pellets 5 days a week. They were acclimated to these conditions for a minimum of 3 weeks before experiments. The results presented are pooled male and female values because no significant sex differences were observed in this study. All the procedures were approved by the Animal Care Committee of the University of Ottawa (protocol BL-1625) and adhered to the guidelines established by the Canadian Council on Animal Care.

Table 3.1. Physical characteristics and hematocrit of the rainbow trout used Intralipid administration.

	Glucose kinetics	Glycerol kinetics	Molecular experiments
Sample size	6	6	19
Body mass (g)	555 ± 78	614 ± 55	625 ± 26
Body length (cm)	31.8 ± 1.5	33.3 ± 1.3	34.1 ± 0.4
Fulton's condition factor (K)	1.64 ± 0.04	1.66 ± 0.06	1.59 ± 0.04
Hematocrit (%)	22.4 ± 1.82	24.0 ± 1.21	24.1 ± 0.9

Trout were used for (i) *in vivo* glucose kinetics measurements, (ii) *in vivo* glycerol kinetics measurements, or (iii) plasma fatty acid composition, tissue gene expression, signaling and enzyme activity. Body mass and length were measured before the surgery. Hematocrit was measured on the second day, after recovery from the surgery to minimize blood loss. Mean values ± s.e.m. are presented.

Catheterizations

Fish were anesthetized with 60 mg l^{-1} MS-222 buffered with 0.2 g l^{-1} $NaHCO_3$ and surgically fitted with 2 catheters in the dorsal aorta (Haman and Weber, 1996). The catheters were kept patent by flushing with Cortland saline containing 50 U ml^{-1} heparin. After catheterization, the fish were left to recover overnight in a 90-litre swim-tunnel where *in vivo* measurements were carried out in resting animals kept at a water velocity of 0.5 BL s^{-1}. This weak current reduces stress and enhances the flow of water over the gills, but does not require swimming to maintain body position (Choi and Weber, 2015). The swim tunnel was supplied with 13°C aerated and dechloraminated Ottawa tap water.

Glycerol and glucose kinetics (series 1 and 2)

The rates of R_a glucose and R_a glycerol were measured by continuous infusion of [6-^{3}H] glucose (2220 GBq $mmol^{-1}$) and [2-^{3}H] glycerol (925 GBq $mmol^{-1}$) respectively. This *in vivo* tracer method has been validated to quantify R_a glucose in fish (Haman et al., 1997a) and thoroughly tested for rainbow trout under a variety of physiological stresses (Choi and Weber, 2016; Haman et al., 1997b; Jubouri et al., 2021; Shanghavi and Weber, 1999; Weber et al., 2016). Similarly, the tracer method used to quantify R_a glycerol has been tested repeatedly for rainbow trout (Bernard et al., 1999; Magnoni et al., 2008b; Turenne and Weber, 2018). Infusates were freshly prepared immediately before each experiment by drying an aliquot of the radiolabelled tracer under N_2 and resuspending in Cortland saline. For glucose kinetics, a priming dose of tracer equivalent to 180 min of infusion was injected as a bolus at the start of each infusion to reach isotopic steady state in <45 min. A priming dose was not necessary for glycerol

kinetics because the high turnover rate relative to pool size allows for rapid equilibration of labelled glycerol within the glycerol pool. For each flux measurement, the infusate was administered continuously at ~1 ml h^{-1} (exact infusion rates were determined individually for each fish to correct for differences in body mass) using a calibrated syringe pump as described in Jubouri et al., 2021. Infusion rates averaged 1230.2 ± 97.7 Bq kg^{-1} min^{-1} (N=6) for labelled glucose and 9689.8 ± 380.1 Bq kg^{-1} min^{-1} (N=6) for labelled glycerol. These trace amounts (labelled and unlabelled) had no effect on glucose or glycerol metabolism, only accounting for <0.0000001% of baseline endogenous R_a glucose and <0.00001% of the baseline endogenous R_a glycerol. Blood samples (~200 µl each) were drawn 50, 55 and 60 min after starting the tracer infusion to determine baseline glucose or glycerol kinetics, and every 30 min thereafter during Intralipid 20% emulsion administration (I141, Sigma-Aldrich; at a rate of 8.4 µmol kg^{-1} min^{-1}). This rate of TAG-rich infusion is equivalent to ~¼ the baseline endogenous rate of TAG appearance into circulation (Magnoni et al., 2008a). A previous study has shown that an equivalent infusion rate causes a doubling in circulating FA concentration (Carneiro et al., 1996). The total amount of blood sampled from each fish accounted for <10% of total blood volume. Blood samples were immediately centrifuged to separate plasma (5 min; 13,000 RPM) and stored at -20ºC until analyses.

Plasma sample analyses

Glycerol and glucose radioactivity was measured by scintillation counting in Bio-Safe II scintillation fluid. To measure glycerol radioactivity in series 1, plasma samples were prepared prior to the scintillation counting by eliminating glucose activity. Tritium from infused [2-^{3}H] glycerol partitions into circulating glycerol, glucose and H_2O

(Bernard et al., 1999). Glucose activity was eliminated by incubating 40 µl of each sample with 1.11 mM ATP and 7 U ml^{-1} HK to phosphorylate and remove free tritiated glucose by ion-exchange column chromatography. The samples were passed through cation and anion 200-400 mesh exchange resins in elution columns, separated with porous polyethylene frits as described in Turenne and Weber, 2018. Samples were washed through the elution column with 7 ml dH_2O allowing only labelled glycerol and tritiated H_2O to pass through. Eluates were dried overnight at 65°C under N_2 to eliminate tritiated H_2O. Residues were resuspended in 1 ml dH_2O and counted. A previous study determined that 10.6% of labelled glycerol was lost during the ion-exchange separation by column chromatography, therefore, glycerol activity was corrected accordingly (Turenne and Weber, 2018). To measure glucose radioactivity in series 2, plasma samples were prepared prior to the scintillation counting by drying 20 µl of each sample under N_2, eliminating tritiated H_2O, and resuspending in 1 ml dH_2O.

Plasma glucose and glycerol concentrations were measured spectrophotometrically. Plasma glucose concentration was determined with 7 U ml^{-1} HK and 0.1 U ml^{-1} G6PDH in a buffer containing 60 mM Trizma base, 40 mM Tris-HCl, 1.01 mM $MgSO_4$, 2.22 mM NAD^+ and 1.11 mM ATP and measured by the absorbance of NADH at 340 nm as described in Jubouri et al., 2021. Plasma glycerol concentration was determined using a colorimetric glycerol assay kit (MAK117, Sigma-Aldrich) following the manufacturer's protocol.

Tissue measurements (series 3)

To avoid analyzing radioactive tissues, these experiments were carried out on different fish than those used to measure glucose and glycerol kinetics. Saline (control

group; N=8) or Intralipid (treatment group; N=11; 8.4 µmol kg^{-1} min^{-1}) was administered at ~1 ml h^{-1} through the catheter for 240 min. Blood samples were taken prior to and following the 240 min infusion. The trout were euthanized by spinal cord transection, whole liver, red muscle (along the lateral line), white muscle (perpendicular to the dorsal fin) and perivisceral adipose tissue were collected and stored at -80°C until analyses.

Fatty acid analysis

Lipids were extracted by mixing 100 µl of plasma or 5 µl of Intralipid in 5 ml of chloroform:methanol (Folch et al., 1957), centrifuging (10 min; 3,000 RPM) and filtering the supernatant into 3.75 ml of 0.25% v/v KCl and repeating the extraction of the pellet in an additional 5 ml of chloroform:methanol as described in Bernard et al., 1999. The resulting mixture was then centrifuged to separate the aqueous and organic phases. The aqueous phase was discarded and the organic phase was collected and dried at 75°C using a rotating evaporator (Büchi RE 121 Rotavapor). Lipids were then resuspended in chloroform and separated by filtration through solid-phase extraction columns (Supelclean 3 ml 500 mg LC-NH2, Sigma-Aldrich) (Bernard et al., 1999; Gonzalez et al., 2015; Magnoni et al., 2006). Neutral lipid (NL), phospholipid (PL) and NEFA fractions were separated by sequential elution using solvents of increasing polarity: chloroform:isopropanol (3:2 v/v), isopropyl ether:acetic acid (98:2 v/v), and methanol (Maillet and Weber, 2006). Plasma FA plasma composition was measured by gas chromatography following methylation (NEFA) or acid transesterification (NL and PL) (Chapelle and Zwingelstein, 1984; Malak et al., 1989). Plasma FA plasma concentration by adding an internal standard before solid-phase column separation, margaric acid (17:0; 0.3 mg ml^{-1}; 51610, Sigma- Aldrich) for the NL and NEFA fraction

and phosphatidylcholine (17:0 PC; 0.4 mg 100 ml^{-1}; 850360, Avanti Polar Lipids; Alabaster, AL, USA) for the PL fraction.

Lipid fractions were analyzed on an Agilent Technologies 6890N gas chromatograph (Mississauga, Ontario, Canada) equipped with a flame-ionization detector and a fused silica capillary column (Supelco DB-23, 60m, 0.25 mm, 0.25 µm; Sigma-Aldrich) using hydrogen as the carrier gas (Magnoni and Weber, 2007). Individual FAs were identified by determining exact retention times with pure standards (Supelco, Bellefonte, PA, USA). Individually, the following FAs accounted for >1% of total FAs: 16:0, 16:1, 18:0, 18:1, 18:2 (omega-6 polyunsaturated; n-6), 20:0, 20:1, 20:2, 20:3 (n-6), 20:4 (n-6), 20:5 (omega-3 polyunsaturated; n-3), 22:1, 22:6 (n-3) and 24:0. FAs accounting for <1% of total FAs in all fractions were not reported. Blank runs were also performed and FA composition was corrected accordingly as described by Farhat et al., 2019.

RNA extraction and gene expression

Total RNA from the liver, red muscle, white muscle and adipose tissue was extracted by homogenizing 50 mg of tissue in TRIzol reagent using a sonicator. RNA concentration was quantified and samples were stored at -80°C. A QuantiTect reverse transcriptase kit was used to generate cDNA using total RNA from the liver, red muscle, white muscle and adipose tissue following the manufacturer's protocol. A no-RT negative control (RT replaced with RNase-free H_2O) and a no-template negative control (RNA replaced with RNase-free H_2O) were included to check for genomic contamination as described in Jubouri et al., 2021. Two-step *real-time* RT-PCR assays were performed to quantify relative fold-changes in mRNA abundances of key glycolytic

genes (*gcka* and *gckb*), gluconeogenic genes (*pck1*, *pck2a*, *pck2b*, *g6pca*, *g6pcb1a*, and *g6pcb1b*) and glucose transporters (*glut4a* and *glut4b*). Additionally, transcripts involved in lipid metabolism, specifically TAG breakdown (*hsl, lpl, atgl* and *plin1*) and synthesis [monoacylglycerol acyltransferase 1 (*mgat1*) and *dgat2*] as well as FA oxidation (*cpt1a* and *hoad*), transport (*cd36*) and synthesis (*fas* and *srebp1c*) were quantified. For each assay, a standard curve consisting of serial dilutions of pooled cDNA samples was run in duplicate for each experiment. The total reaction volume was 20 µl, which consisted of 1 µl of diluted cDNA template, 1 µl of 10 nM specific forward and 1 µl of 10 nM specific reverse primer (Tables S3.1 and S3.2), 10 µl of SsoAdvanced Universal SYBR Green Supermix and 7 µl of H_2O as described in Jubouri et al., 2021. *Real-time* RT-PCR cycling parameters were a 5 min activation step at 95°C, followed by 40 cycles consisting of a 20 s denaturation step at 95°C and a 30 s annealing and extension step at a primer-specific temperature (Tables S3.1 and S3.2). Negative controls (no-RT and no-template) were included in each assay to control for genomic contamination. After each run, melting curves were produced and monitored for single peaks to confirm the specificity of the reaction and the absence of primer dimers. All amplification efficiencies calculated from serially diluted 7-point standard curves were between 92.6-109.0%, with R^2 values >0.950 (Tables S3.1 and S3.2). Relative transcript abundance derived from standard curves was normalized using the NORMA-Gene approach as described in Heckmann et al., 2011. Finally, mRNA fold changes were calculated relative to the control group.

Western blotting

Total protein from the liver, red muscle, white muscle and adipose tissue was extracted by homogenizing 100 mg of tissue in 400 µl of cold homogenization buffer using a sonicator as described in Jubouri et al., 2021. The homogenization buffer (pH 8.0) contained 150 mM NaCl, 1% Triton X-100, 0.5% sodium deoxycholate, 0.1% SDS, 50 mM Tris-HCl, 1 mM EDTA, 100 mM NaF, 4 mM sodium pyrophosphate, 2 mM sodium orthovanadate and a protease inhibitor cocktail. Homogenates were centrifuged (10 min; 15,000 RCF) at 4°C, the resulting supernatants were recovered and stored at -20°C. Protein concentrations were determined using BCA assay with BSA as a standard. Protein samples were denatured (5 min; 95°C), reduced and diluted in 2X Laemmli buffer for a total amount of 25 µg protein in 20 µl of loading volume. Protein samples were loaded along with 5 µl of Page Ruler prestained protein ladder in a 10% resolving gel (5 ml ddH_2O, 2.5 ml buffer B, 2.5 ml 40% Acryl/Bis, 50 µl 10% APS and 20 µl TEMED) and a 4% stacking gel (3.25 ml ddH_2O, 1.25 ml buffer C, 0.5 ml 40% Acryl/Bis, 25 µl 10% APS and 10 µl TEMED) as described in Jubouri et al., 2021. Gels were placed in 1X TGS running buffer consisting of 2.5 mM Tris base, 0.192 M glycine and 0.1% SDS dissolved in dH_2O. Proteins were migrated (2 h; 100 V) and blotted (2 h; 100 V) on nitrocellulose membrane (pore size 0.2 µm) in 20% Western transfer buffer consisting of 250 mM Tris base, 1.92 M glycine dissolved in dH_2O. Membranes were then incubated in Odyssey blocking buffer for 1 h at room temperature.

Membranes were incubated overnight at 4°C in rabbit-raised Pck1 or Fas (3189S, Cell Signaling Technology, Danvers, MA, USA) antibodies (diluted 1:1000 in Odyssey blocking buffer), previously validated in rainbow trout (Jubouri et al., 2021).

Following incubation in primary antibodies, membranes were washed with PBST [PBS and 0.01% (v/v) Tween 20] and incubated with IRDye 800 CW goat-anti-rabbit secondary antibody (diluted 1:5000 in Odyssey blocking buffer; 925-32211, LI-COR) for 1.5 h at room temperature on the shaker protected from light. Following incubation in secondary antibodies, membranes were washed with PBST followed by PBS as described in Jubouri et al., 2021. Membranes were visualized by infrared fluorescence using the Odyssey Imaging System and band intensity was quantified by Odyssey Infrared Imaging System software. Protein intensities were normalized to Revert 700 Total Protein Stain intensity. Finally, fold changes were calculated relative to the control group.

Enzyme activities

Tissue homogenate for the liver, white muscle and adipose tissue was prepared by sonicating 100 mg of tissue in 1 ml of cold homogenization buffer 1. Homogenates were centrifuged (5 min; 2400 RCF) at 4°C, the resulting supernatants were recovered and stored at -80°C. Homogenization buffer 1 (pH 7.5) contained 25 mM Tris-HCl, 1 mM EDTA, 5 mM DTT and 0.05% Triton X-100. Tissue homogenate for liver and adipose tissue (specifically to quantify FAS activity) was prepared by sonicating 100 mg of tissue in 1 ml of cold homogenization buffer 2. Homogenates were centrifuged (20 min; 17,000 RCF) at 4°C, the resulting supernatants were recovered and stored at -80°C. Homogenization buffer 2 (pH 7.4) contained 20 mM Tris-HCl, 250 mM sucrose (S9378, Sigma-Aldrich), 100 mM NaF, 2 mM EDTA, 0.5 mM phenylmethylsufonyl fluoride (55748121, Roche, Basel, Switzerland) and 10 mM β-mercaptoethanol (M6250, Sigma-Aldrich). Protein concentrations were determined using Bradford reagent assay with

BSA as a standard. Enzyme activity was determined kinetically by measuring the oxidation of NADH/NADPH or reduction of $NADP^+$ at 340 nm using a microplate reader, expressed as µmol min^{-1} g^{-1} protein and assayed in triplicate. Control reactions were run for 10-15 min for each enzyme assay after adding reagents. Background activity was subtracted from enzyme activity. The conditions of the individual enzyme assay were as detailed below (final concentration in the well). HK (EC 2.7.1.1) and GK (EC 2.7.1.2) assay mixture contained 300 mM imidazole (I202, Sigma-Aldrich, pH 8.1), 100 mM KCl (P5405, Sigma-Aldrich), 10 mM $MgCl_2$ (M8266, Sigma-Aldrich), 1 mM $NADP^+$ (N0505, Sigma-Aldrich), 5 U ml^{-1} G6PDH, 5 mM ATP and 5 or 50 mM glucose (G7021, Sigma-Aldrich; omitted for control) for HK and GK respectively. PCK (EC 4.1.1.32) reaction mixture contained 50 mM imidazole, 20 mM $NaHCO_3$ (S6014, Sigma-Aldrich), 1 mM $MnCl_2$, 0.5 mM PEP · Na_3), 0.12 mM NADH, 6 U ml^{-1} malate dehydrogenase and 0.2 mM dGDP (omitted for control). HOAD (EC 1.1.1.35) reaction mixture contained 50 mM imidazole, 5 mM EDTA, 1 mM KCN, 0.05 mM NADH and 0.1 mM acetoacetyl CoA (omitted for control). FAS (EC 2.3.1.85) assay mixture contained 20 mM sodium phosphate dibasic (S0876, Sigma-Aldrich, pH 6.8), 0.1 mM acetyl CoA, 0.5 mM NADPH (58124426, Roche) and 0.2 mM malonyl CoA (M4263, Sigma-Aldrich; omitted for control) (Chakrabarty and Leveille, 1969).

Calculations and statistics

The Fulton's condition factor, *K*, was calculated using the equation,

$$K = \frac{10^5 \cdot m_b}{L^3}$$

Here m_b is body mass and *L* is fork length (Blackwell et al., 2000). Total circulating NL, PL and NEFA concentration is given by:

$$[\mathrm{NL}] = \sum \frac{m_{FA}}{V_{plasma} \cdot 3} = \sum \frac{A_{FA} \cdot m_{17:0}}{A_{17:0} \cdot V_{plasma} \cdot 3}$$

$$[\mathrm{PL}] = \sum \frac{m_{FA}}{V_{plasma} \cdot 2} = \sum \frac{A_{FA} \cdot m_{17:0PC}}{A_{17:0PC} \cdot V_{plasma} \cdot 2}$$

$$[\mathrm{NEFA}] = \sum \frac{m_{FA}}{V_{plasma}} = \sum \frac{A_{FA} \cdot m_{17:0}}{A_{17:0} \cdot V_{plasma}}$$

Here *m* and *A*, are the mass and area of each FA (or internal standard; NL/NEFA: 17:0; PL: 17:0 PC), present in a volume of plasma, V_{plasma}. Total PL and NL concentration was corrected to account for the number of FA in PL (2) and NL (3). Rates of *in vivo* R_a glucose and R_a glycerol were calculated over time using the steady-state equation of Steele (Steele, 1959). Statistical comparisons for metabolite kinetics (series 1 and 2) were performed using one-way RM-ANOVA with the Dunnett's post hoc test to determine which time points were statistically different from mean baseline values. Glucose and glycerol concentrations were analyzed by two-way RM-ANOVA (series 3; Table 3.3). Gene expression, protein expression and enzyme activity results were analyzed using a two-tailed unpaired t-test to assess the effects of Intralipid. Before all tests, normality and homoscedasticity were assessed using the Shapiro-Wilk test and the Levene's test, respectively. When the assumptions of normality or equality of variances were not met, the data were normalized by natural log, square root or arcsine transformation. If the transformation was unsuccessful, Kruskall-Wallis non-parametric one-way ANOVA on ranks (series 1 and 2) or non-parametric Mann-Whitney U test (series 3) were performed. Values presented are means ± s.e.m. and a level of significance of $p<0.05$ was used in all tests.

Results

Fatty acid composition of circulating lipids

The lipid composition and relative distribution FAs in different lipid classes for Intralipid are presented in Table S3.3. In Intralipid, the vast majority of FAs (88%) were NL. PL and NEFA accounted for 4% and 8% of all FAs respectively. The infusion of Intralipid caused an increase in total circulating lipid concentration from a baseline concentration of 12.54 ± 1.99 μmol ml^{-1} to a final value of 16.55 ± 4.25 μmol ml^{-1} (*p=0.0362, F=3.433, df=4*; Figure 3.1A). Elevating plasma lipids increased NL concentration from a baseline concentration of 0.93 ± 0.19 μmol ml^{-1} to a final value of 3.27 ± 0.97 μmol ml^{-1} (*p=0.0115, F=5.527, df=4*; Figure 3.1A), but had no effect on plasma PL and NEFA concentration (mean value of 11.25 ± 1.42 and 1.91 ± 0.37 μmol ml^{-1}, respectively; *p>0.05*; Figure 3.1A). Intralipid increased NL plasma composition from a baseline percentage of 7.4 to a final percentage of 18.9 and decreased PL plasma composition from a baseline percentage of 79.5 to a final percentage of 67.6. However, it had no effect on plasma NEFA composition (mean value of 13.3%). The Intralipid infusion significantly decreases the n-3/n-6 ratio in total FA, PL and NL.

Figure 3.1. Effects of Intralipid on circulating fatty acid concentration (A) and omega-3 omega-6 ratio (B) in rainbow trout. Total fatty acids: Total; Neutral lipids: NL; phospholipids: PL; non-esterified fatty acids: NEFA. Values are means ± s.e.m. (N=11). Significant differences from mean baseline values are indicated by * (*p<0.05*) and *** (*p<0.001*).

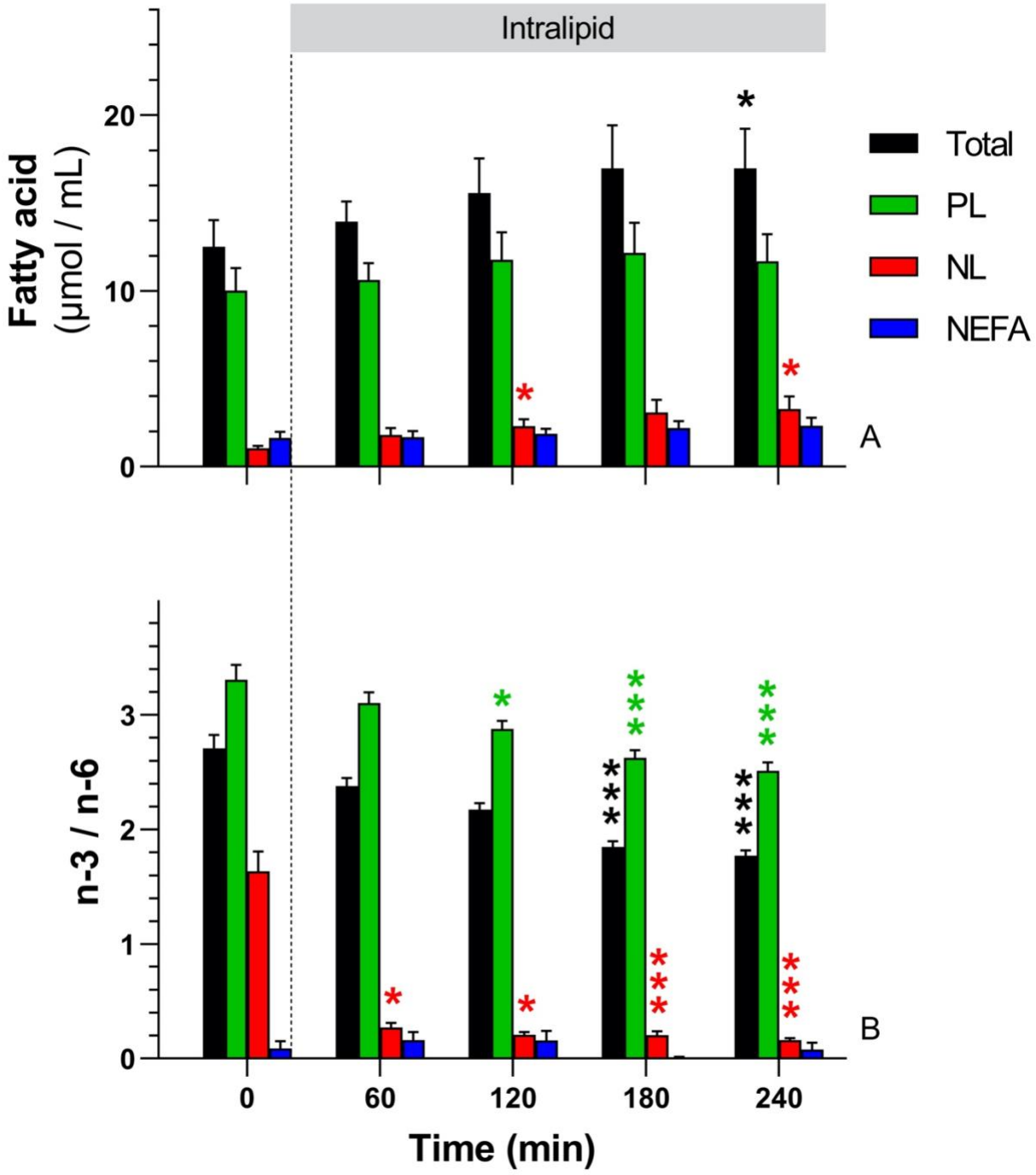
Intralipid
Fatty acid
(µmol / mL)
20
10
0
Total
PL
NL
NEFA
A
n-3 / n-6
3
2
1
0
B
0
60
120
180
240
Time (min)

Series 1: Glycerol kinetics

During the measurement of glycerol kinetics, the infusion of Intralipid caused an increase in plasma glycerol concentration (*p<0.001, F=54.655, df=8*; Figure 3.2A). Glycerol concentration increased by a factor of 8 from 0.15 ± 0.02 mM to 1.13 ± 0.09 mM (Table 3.2). Elevating plasma lipids caused a decrease in glycerol specific activity (*p<0.001, F=18.492, df=8*; Figure 3.2B) and lipolytic rate doubled from a baseline rate of 2.53 ± 0.50 μmol kg^{-1} min^{-1} to a final value of 5.28 ± 0.32 μmol kg^{-1} min^{-1} (*p<0.001, F=8.547, df=8*; Figure 3.2C and Table 3.2).

Series 2: Glucose kinetics

During the measurement of glucose kinetics, the infusion of Intralipid had no effect on plasma glucose concentration (*p>0.05, df=8*; Figure 3.3A). Elevating plasma lipids caused an increase in glucose specific activity (*df=8, p>0.05* at 180 min and *p<0.01* at 240 min; Figure 3.3B) and a decrease in hepatic glucose production from a baseline rate of 7.33 ± 0.91 μmol kg^{-1} min^{-1} to a final value of 4.74 ± 0.44 μmol kg^{-1} min^{-1} (*p=0.010, F=2.984, df=8*; Figure 3.3C).

Figure 3.2. Effects of Intralipid on circulating glycerol concentration (A), glycerol specific activity (B) and lipolytic rate (R_a glycerol) (C) in rainbow trout. Values are means ± s.e.m. (N=6). Significant differences from mean baseline values are indicated by ** ($p<0.01$) and *** ($p<0.001$).

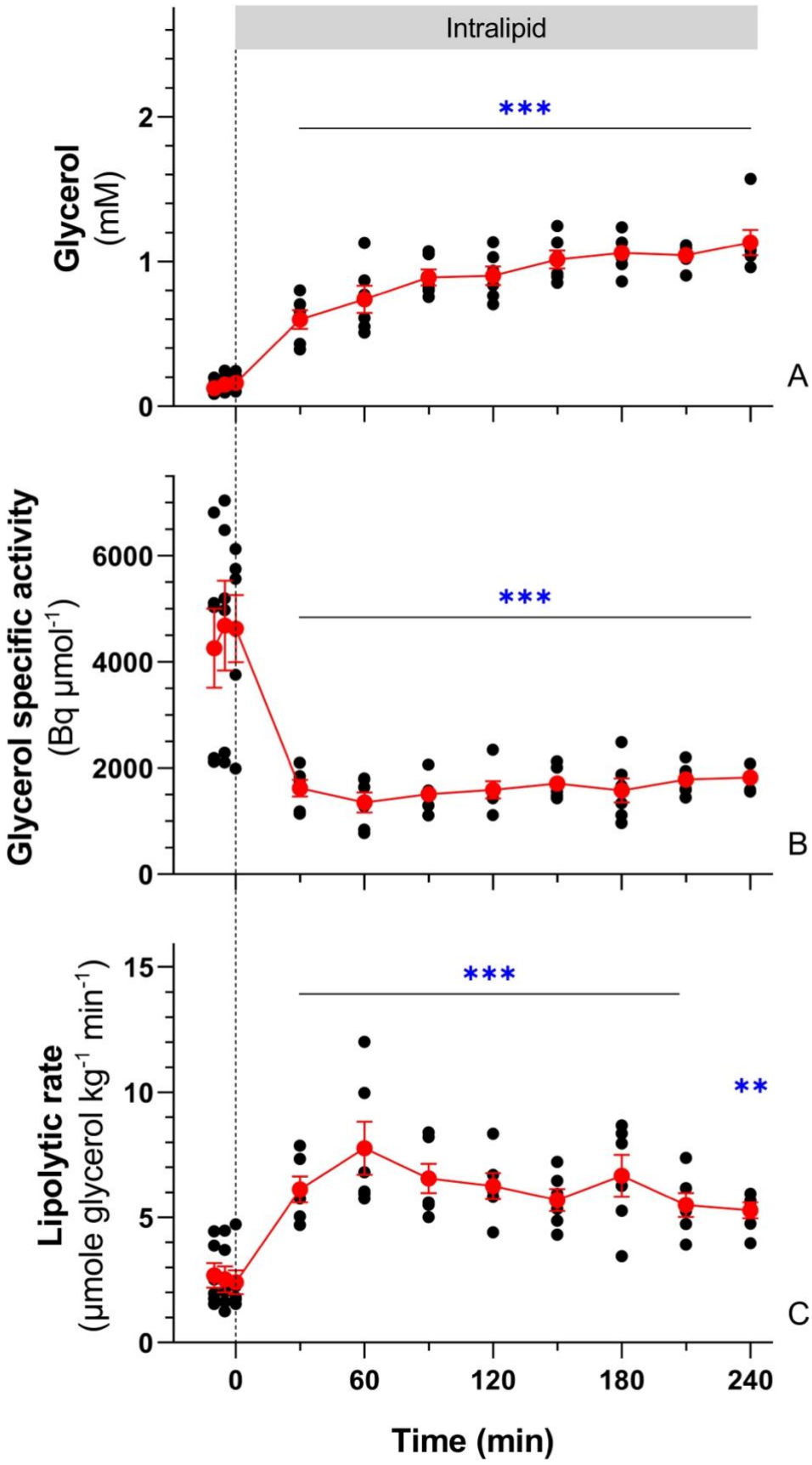
Intralipid
Glycerol
(mM)
***
A
Glycerol specific activity
(Bq µmol-1)
***
B
Lipolytic rate
(µmole glycerol kg-1 min-1)
***
**
C
Time (min)

Figure 3.3. Effects of Intralipid on circulating glucose concentration (A), glucose specific activity (B) and hepatic glucose production rate (R_a glucose) (C) in rainbow trout. Values are means ± s.e.m. (N=6). Significant differences from mean baseline values are indicated by * ($p<0.05$) and ** ($p<0.01$).

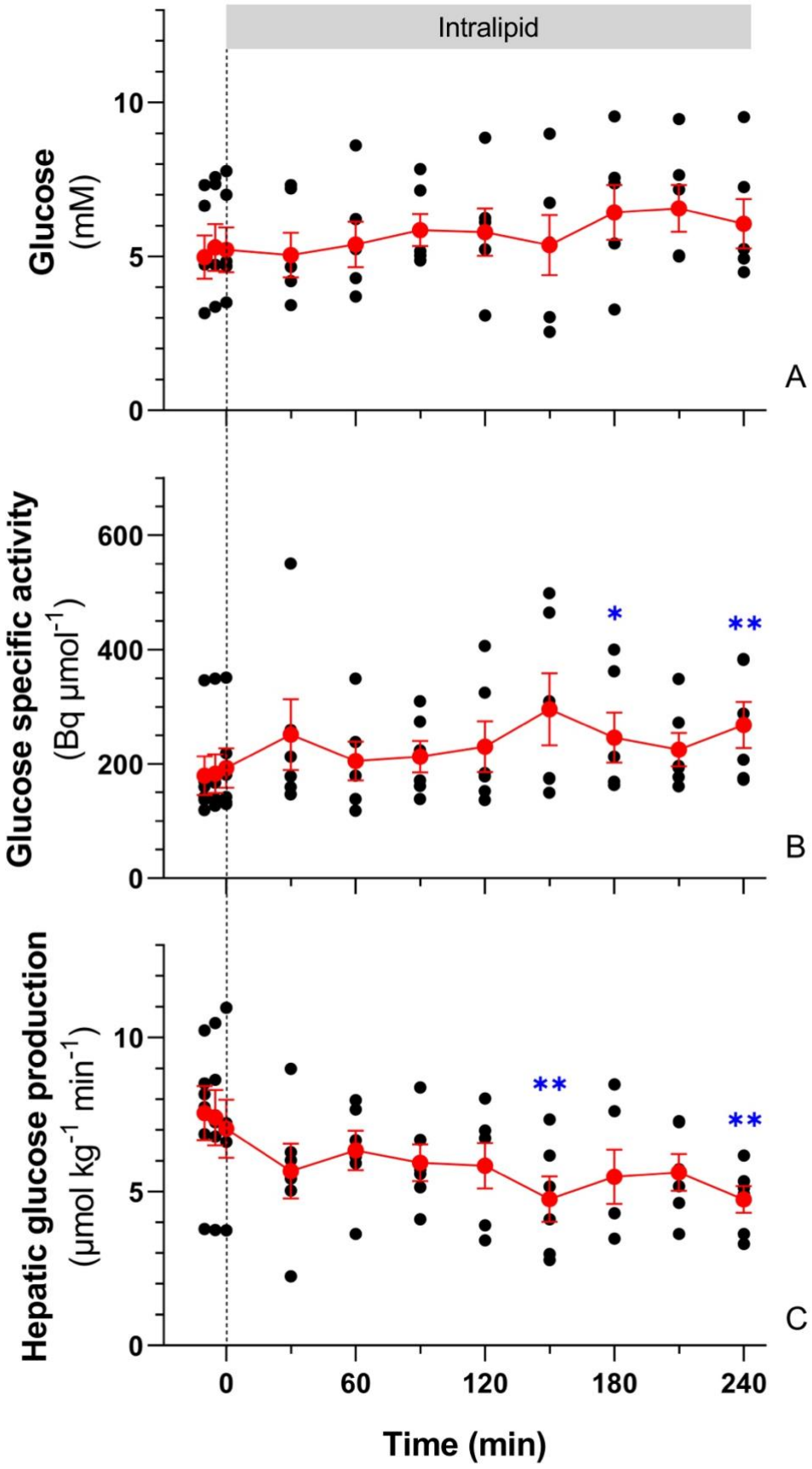
Intralipid
Glucose
(mM)
10
5
0
A
Glucose specific activity
(Bq µmol-1)
600
400
200
0
*
**
B
Hepatic glucose production
(µmol kg-1 min-1)
10
5
0
**
**
C
0
60
120
180
240
Time (min)

Table 3.2. Initial (baseline) and final values after 4 h of Intralipid administration for the kinetics experiments.

	Baseline (0 h)	Final (4 h)
Plasma glucose (mM)	5.16 ± 0.73	6.06 ± 0.80
R_a glucose (μmol kg^{-1} min^{-1})	7.33 ± 0.91	4.74 ± 0.44
Plasma glycerol (mM)	0.15 ± 0.02	1.13 ± 0.09
R_a glycerol (μmol kg^{-1} min^{-1})	2.53 ± 0.50	5.28 ± 0.32

Values are means ± s.e.m (N=6). Hepatic glucose production (R_a glucose) and glycerol production (R_a glycerol) was obtained with the steady-state equation.

Series 3: Gene expression, protein signaling and enzyme activities

Metabolite concentrations

Plasma metabolite concentrations of the fish used for tissue measurements are summarized in Table 3.3. Control animals that received a Cortland saline infusion showed no changes in glucose or glycerol levels. Those given an infusion of Intralipid also maintained steady glucose concentration, but more than quintupled glycerol concentration, like the animals used to measure *in vivo* metabolite fluxes. Interactions between time and treatment effects were significant for glycerol concentration.

Table 3.3. Plasma glucose and glycerol concentration for series 3: molecular experiment.

	Group	Baseline (0 h)	Final (3 h)	Time effect	Treatment effect	Time×treatment interaction
Glucose (mM)	Control	7.16 ± 0.63	6.75 ± 0.57	ns	ns	ns
	Intralipid	6.40 ± 0.39	7.15 ± 0.48			
Glycerol (mM)	Control	0.10 ± 0.01	0.09 ± 0.01	ns	ns	**
	Intralipid	0.14 ± 0.03	0.76 ± 0.10			

Values are means ± s.e.m. ns $p>0.05$, ** $p<0.01$; ns, no significant difference.

Gene expression

The impacts of Intralipid on target genes that play key roles in the regulation of lipid metabolism are shown in Figure 3.4. The relative transcript abundance of 4 enzymes involved in lipolysis was quantified: *hsl*, *lpl*, *plin1* and *atgl*. Intralipid increased the relative mRNA expression of *hsl* in muscle (*red muscle: p=0.0007, t=4.360, df=14; white muscle: p=0.0094, t=3.087, df=12*) and suggested a non-significant trend to decrease in adipose tissue (*p=0.0648, t=2.004, df=14*) while having no effect in the liver (*p=0.1233, t=1.640, df=14*). Intralipid decreased the relative mRNA expression of *lpl* in the liver and adipose tissue (*liver: p=0.0068, t=3.209, df=13; adipose tissue: p=0.0128, t=2.883, df=1*3) and suggested a non-significant trend to increase it in muscle (*red muscle: p=0.0742, t=1.929, df=14; white muscle: p=0.0669, t=2.000, df=13*). Intralipid decreased the relative mRNA expression of *plin1* (*p=0.0047, t=3.408, df=13*) and suggested a non-significant decrease in *atgl* (*p=0.0635, t=2.028, df=13*).

The relative transcript abundance of 2 enzymes from the β-oxidation pathway were quantified: *cpt1a* and *hoad*. The relative expression of *cpt1a* was stimulated in the liver (*p=0.0025, t=3.894, df=11*) but decreased in red muscle (*p=0.0274, t=2.485, df=13*). The relative expression of *hoad* was stimulated in the liver (*p=0.0276, t=2.458, df=14*), but remained constant in red and white muscle (*red muscle: p=0.9202, t=0.1020, df=14; white muscle: p=0.3398, t=0.9979, df=11*). The relative mRNA expression of the NEFA transporter, *cd36*, was increased in white muscle (*p=0.0421, t=2.299, df=11*), but remained unaffected by Intralipid in the liver, red muscle and adipose tissue (*liver: p=0.1939, t=1.365, df=14; red muscle: p=0.8406, t=0.2049, df=14; adipose tissue: p=0.1975, t=1.353, df=14*). The relative transcript abundance of 2

enzymes involved in TAG synthesis was quantified: *dgat2* and *mgat1*. Intralipid decreased the relative mRNA expression of *dgat2* (*p=0.0002, t=5.404, df=12*) while *mgat1* was unaffected (*p=0.2351, t=1.250, df=12*). The relative transcript abundance of 2 enzymes involved in FA synthesis was quantified: *fas* and *srebp1c*. Intralipid decreased the relative mRNA expression of *fas* in the liver (*p=0.0023, t=3.857, df=12*) and adipose tissue (*p=0.0399, t=2.266, df=14*) while *srebp1c* was unaffected (*liver: p=0.6376, t=0.4823, df=13; adipose tissue: p=0.2133, t=1.304, df=14*).

The impacts of Intralipid on target genes that play key roles in the regulation of carbohydrate metabolism are shown in Figure 3.5. For glucose transporters, Intralipid increased the relative mRNA abundance of the glucose transporters *glut4a* and *glut4b* in white muscle (*glut4a: p=0.0118, t=2.894, df=14; glut4b: p=0.0396, t=2.308, df=12*) but decreased only *glut4a* abundance in adipose tissue (*glut4a: p=0.0098, t=3.022, df=13; glut4b: p=0.4038, t=0.8630, df=13*). Relative *glut4a* and *glut4b* abundance remained constant in red muscle (*glut4a: p=0.4270, t=0.8181, df=14; glut4b: p=0.2680, t=1.162, df=12*). The relative transcript abundance of 5 key gluconeogenic enzymes was quantified: *pck1*, *pck2a*, *pck2b*, *g6pca*, *g6pcb1a* and *g6pcb1b*. In the liver, Intralipid increased the relative expression of the *pck1* (*p=0.0034, t=3.630, df=12*), but had no effect on other paralogues (*pck2a: p=0.1450, t=1.543, df=14; pck2b: p=0.4379, t=0.7985, df=14*). For glucose-6-phosphatase, *g6pca* and *g6pcb1b* relative mRNA abundance was increased by Intralipid (*g6pca: p=0.0005, t=4.459, df=14; g6pcb1b: p<0.0001, t=8.848, df=12*), while *g6pcb1a* remained unaffected (*p=0.7725, t=0.2947, df=14*). The relative transcript abundance of glucokinase paralogues (*gcka* and *gckb*) was quantified. In the liver, Intralipid decreased the relative expression of both

paralogues of this glycolytic enzyme (*gcka: p=0.0003, t=4.973, df=13; gckb: p=0.0002, t=5.362, df=12*).

Figure 3.4. Effects of Intralipid on the relative mRNA expression of genes associated with lipid metabolism in rainbow trout tissues: hormone-sensitive lipase (*hsl)*, lipoprotein lipase *(lpl*), adipose triglyceride lipase (atgl), perilipin 1 (*plin1*), monoacylglycerol acyltransferase 1 (*mgat1*), diacylglycerol acyltransferase 2 (*dgat2*), carnitine palmitoyltransferase 1a (*cpt1a*), 3-hydroxyacyl dehydrogenase (*hoad*), fatty acid translocase (*cd36*), fatty acid synthase (*fas*) and sterol regulatory element-binding protein 1c (*srebp1c*). Individual data points and means ± s.e.m. (N=6-8) are presented for the control (white) and Intralipid (grey) group. Significant effects of Intralipid are indicated by * ($p<0.05$), ** ($p<0.01$) and *** ($p<0.001$).

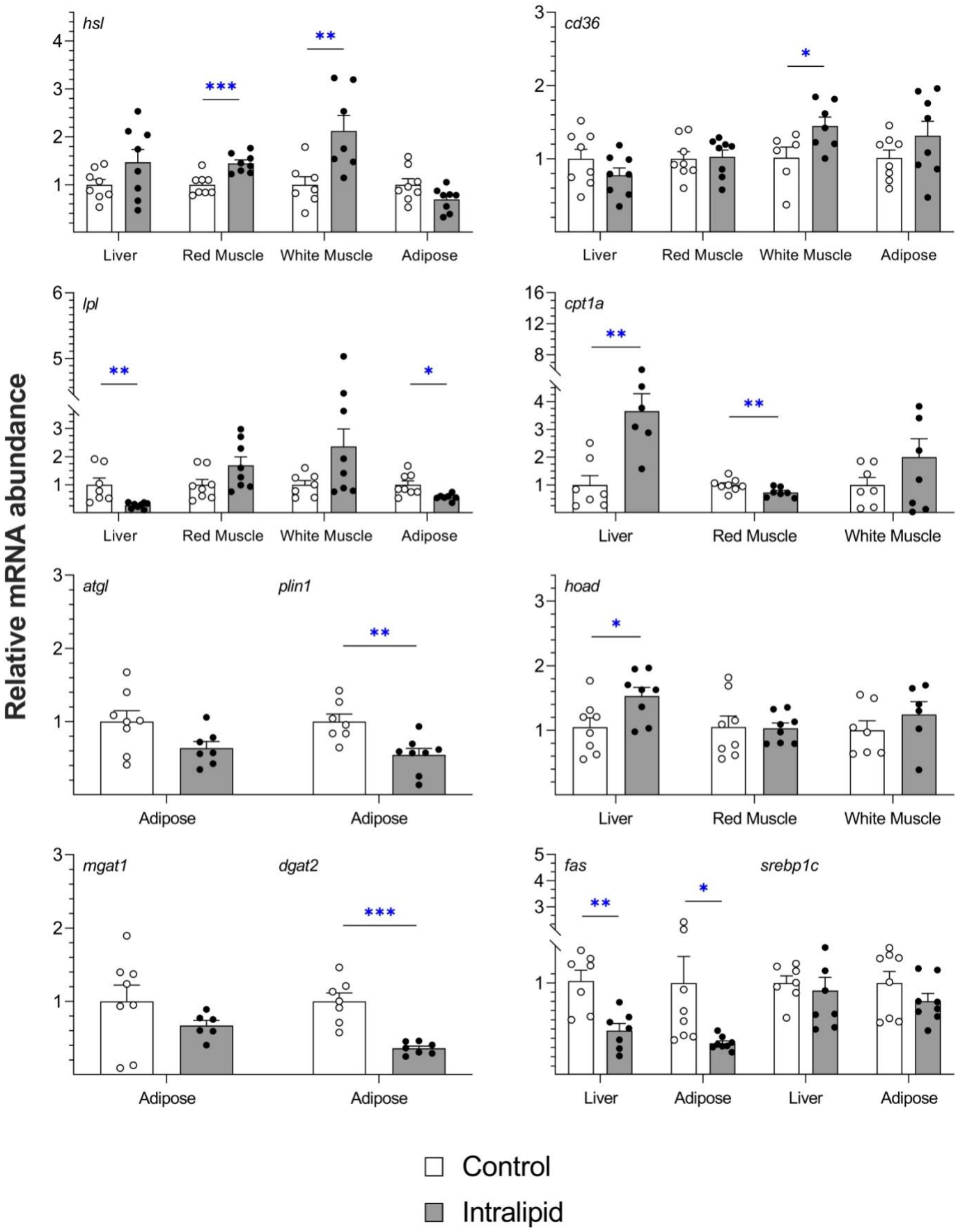
Relative mRNA abundance
hsl
cd36
lpl
cpt1a
atgl
plin1
hoad
mgat1
dgat2
fas
srebp1c
Liver
Red Muscle
White Muscle
Adipose
Control
Intralipid

Figure 3.5. Effects of Intralipid on the relative mRNA expression of genes associated with carbohydrate metabolism in rainbow trout tissues: glucose transport 4 (*glut4a* and *glut4b*), glucokinase (*gcka* and *gckb*), phosphoenolpyruvate carboxykinase (*pck1*, *pck2a* and *pck2b*) and glucose 6 phosphatase (*g6pca*, *g6pcb1a* and *g6pcb1b*). Individual data points and means ± s.e.m. (N=6-8) are presented for the control (white) and Intralipid (grey) group. Significant effects of Intralipid are indicated by * (*p<0.05*), ** (*p<0.01*), *** (*p<0.001*) and **** (*p<0.0001*).

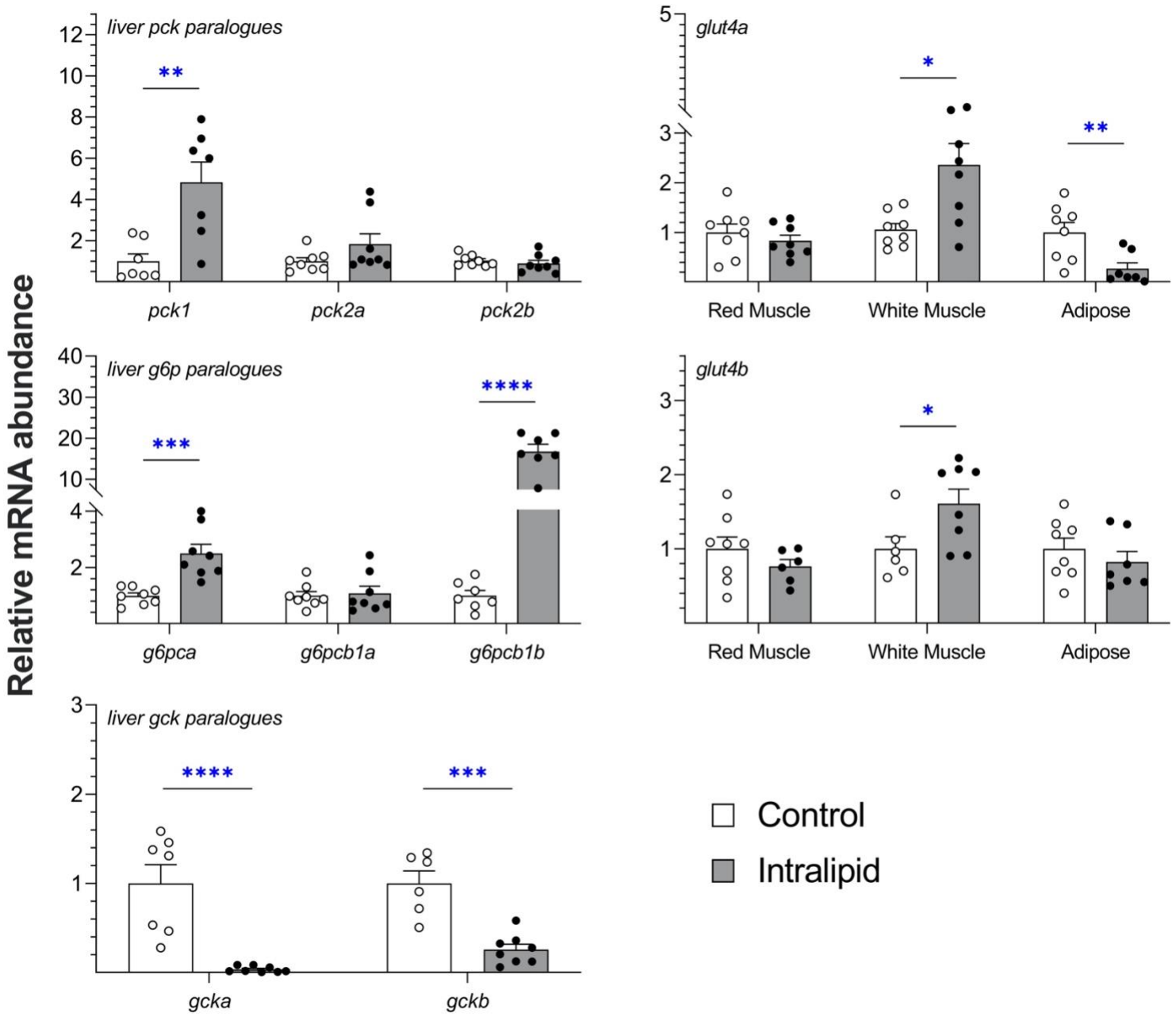
Relative mRNA abundance
liver pck paralogues
**
pck1
pck2a
pck2b
liver g6p paralogues
***
****
g6pca
g6pcb1a
g6pcb1b
liver gck paralogues
****
***
gcka
gckb
glut4a
*
**
Red Muscle
White Muscle
Adipose
glut4b
*
Red Muscle
White Muscle
Adipose
Control
Intralipid

Protein expression

The relative protein abundance of Pck1 and Fas was quantified by Western blotting (Figure 3.6). Intralipid had no effect on the protein expression of Pck1 in the liver (*p=0.2343, Mann-Whitney U=12*) and Fas in the liver and adipose tissue (*liver: p=0.1106, t=1.735, df=11; adipose tissue: p=0.9372, Mann-Whitney U=17)*.

Enzyme activities

The effects of Intralipid on the activities of target enzymes playing key roles in the regulation of carbohydrate and lipid metabolism are presented in Figure 3.7. For carbohydrate metabolism, Intralipid caused a decrease in HK activity in adipose tissue (*p=0.0002, t=5.884, df=10*), but had no effect on liver and white muscle (*liver: p=0.2930, t=1.093, df=14; white muscle: p=0.1508, t=1.535, df=12*). Intralipid also had no effect on hepatic GK and PCK activity (*GK: p=0.1356, t=1.584, df=14; PCK: p=0.6732, t=0.4307, df=14*). For lipid metabolism, FAS activity decreased in adipose tissue (*p=0.0031, t=3.616, df=13*) while liver HOAD activity was reduced by Intralipid (*p=0.0121, t=2.913, df=13*). Liver FAS, white muscle and adipose HOAD activity remained constant (*liver FAS: p=0.7590, t=0.3146, df=11; white muscle HOAD: p=0.6173, t=0.5120, df=13; adipose tissue HOAD: p=0.0870, t=1.864, df=12*).

Figure 3.6. Effects of Intralipid on the protein expression of liver phosphoenolpyruvate carboxykinase (Pck1) and liver and adipose fatty acid synthase (Fas) in rainbow trout. Individual data points and means ± s.e.m. (N=6-7) are presented for the control (white) and Intralipid (grey) group.

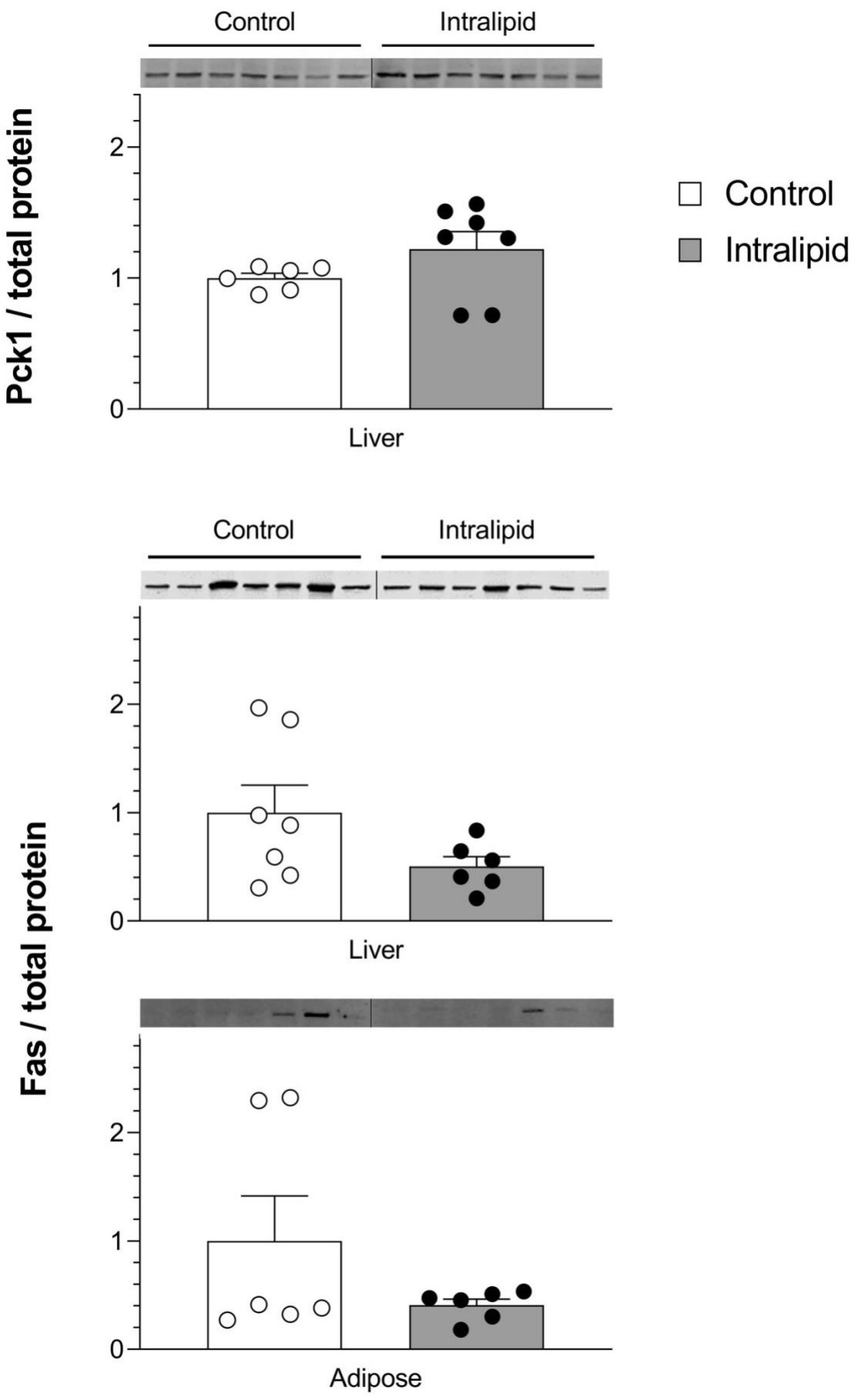
Control
Intralipid
Pck1 / total protein
2
1
0
Liver
Control
Intralipid
Fas / total protein
2
1
0
Liver
2
1
0
Adipose

Figure 3.7. Effects of Intralipid on the activity of enzymes involved in carbohydrate and lipid metabolism in rainbow trout tissues: hexokinase (HK), glucokinase (GK), phosphoenolpyruvate carboxykinase (PCK), fatty acid synthase (FAS) and 3-hydroxyacyl dehydrogenase (HOAD). Individual data points and means ± s.e.m. (N=5-8) are presented for the control (white) and Intralipid (grey) group. Significant effects of Intralipid are indicated by * ($p<0.05$), and ** ($p<0.01$) and *** ($p<0.001$).

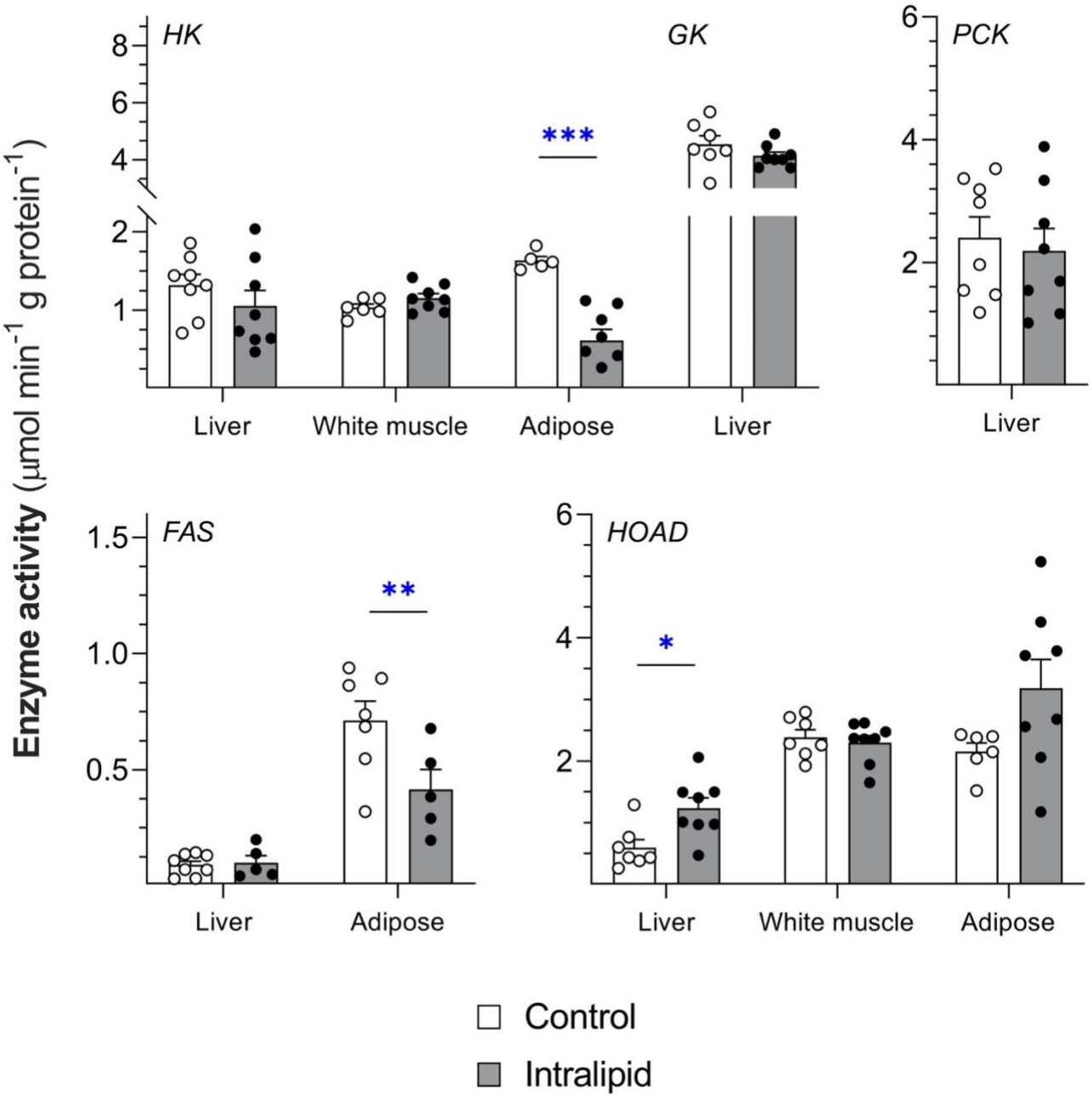
Enzyme activity (µmol min-1 g protein-1)
HK
GK
PCK
FAS
HOAD
***
**
*
Liver
White muscle
Adipose
Liver
Liver
Liver
Adipose
Liver
White muscle
Adipose
Control
Intralipid

Discussion

Intralipid induces hyperlipidemia and alters fatty acid composition in trout

In salmonids, adipose tissue, liver and muscle serve as the main fat depots and all play a critical role in lipid metabolism, including uptake, oxidation and synthesis of FAs (Kiessling et al., 1991; Kozlova, 1998; Rodríguez et al., 2004). Intralipid is a lipid emulsion designed for parenteral nutrition of human patients. It is made of a mixture of FAs (88% NL; 4% PL; 8% NEFA; Table S3.3) that coalesce as artificial lipoproteins of different sizes (77% VLDL; 17% HDL; 16% LDL) (Magnoni et al., 2008a). In rainbow trout, >90% of circulating lipids are also lipoproteins of varying densities, including chylomicrons, VLDL, LDL and HDL (Babin and Vernier, 1989; Magnoni and Weber, 2007). In this study, the administration Intralipid caused a 26% increase in the circulating concentration of total FAs, mostly due to the tripling of NL of which 90% is TAG (Figure 3.1A). Because Intralipid is mostly derived from soy that contains practically no n-3 FAs (Table S3.3), the infusion of this emulsion also caused a 35% decrease in the n-3/n-6 ratio of total FAs in the circulation (-90% in NL and -24% in PL) (Figure 3.1B). This ratio is often considered a major index of metabolic signaling by FAs because n-3 acids mostly reduce inflammation processes whereas n-6 acids play the opposite physiological role (Hulbert, 2021; Surette, 2008). Therefore, it is important to keep in mind that the changes triggered by exogenous Intralipid infusion observed in the present study result from: (i) the increase in blood lipid concentration (Figure 3.1A), (ii) the important changes in circulating FA composition (Figure 3.1B; Table S3.4-S3.7), or (iii) a combination of both.

Effects of Intralipid on lipolytic rate

The continuous infusion of Intralipid resulted in a rapid increase in R_a glycerol from 2.5 ± 0.5 μm kg^{-1} min^{-1} to 7.8 ± 1.1 μm kg^{-1} min^{-1} within 60 min (Figure 3.2C). Mammals regulate R_a glycerol to meet the requirements of energy metabolism, while trout sustain stable fluxes of glycerol and NEFAs that far exceed their energy demand (Bernard et al., 1999; Magnoni et al., 2008a; Magnoni et al., 2008b; Turenne and Weber, 2018; Weber et al., 2003). The rapid decrease of labelled glycerol from the circulating pool observed within 30 min (Figure 3.2B) suggests infused TAG from Intralipid are immediately hydrolyzed. Under basal conditions, circulating lipases in trout are unsaturated, thus, through mass action effects, high circulating lipids could increase TAG hydrolysis without upregulating lipase activity. Temporal responses and abundance of lipase enzymes vary between tissues and species (Albalat et al., 2006; Nayak et al., 2003), however, research regarding the regulation of teleost lipase activity remains scarce. As lipase activity or phosphorylation state was not measured in the current study it is difficult to conclude whether an increase in R_a glycerol is a result of changes in lipase activity or by mass action effect.

In rainbow trout, continuous Intralipid infusion also increased circulating glycerol from 0.1 ± 0.02 mM to 1.1 ± 0.09 mM (Figure 3.2A). This increase was likely due to a divergence between the rates of glycerol appearance and utilization in the initial stages of the experiment. However, variability in flux measurements prevented statistically significant differences after calculating R_a and R_d separately with the non-steady state equations of Steele (results not shown) (Steele, 1959). After 90 min of Intralipid infusion, circulating glycerol and R_a glycerol stabilized at approximately 1.0 mM (Figure 3.2A) and

5.9 μm kg^{-1} min^{-1} (Figure 3.2C), respectively. These longer-term changes suggest that acute hyperglycerolemia may trigger counter-regulatory responses to prevent further elevations in R_a glycerol and concentration. When fish experience hyperglycerolemia, hepatic glycerol kinase activity has a tendency to increase thus suggesting increased glycerol utilization, however, fish are generally considered poor regulators of glycerol kinase (da Costa et al., 2015; Panserat et al., 2020).

Suppression of endogenous lipid metabolism in response to Intralipid

In the present study, Intralipid infusion resulted in a suppression of lipid metabolism in trout liver and adipose tissue. Lipid deposition is determined by a balance between lipolytic and lipogenic pathways (Sheridan, 1988; Tocher, 2003). Elevated R_a glycerol, resulted in transcriptional suppression of the lipolytic genes, *plin1* and *lpl* as well as the lipogenic genes, *dgat2* and *fas* in trout liver and adipose tissue (Figure 3.4). Elevated plasma lipids also resulted in no change of *atgl*, *hsl*, *mgat1*, *cd36 and srebp1c* expression in these tissues (Figure 3.4). Although expressed in muscle, these lipolytic and lipogenic genes are most abundant in the major lipid depositing sites in salmonids (liver and adipose tissue) and their activity is required to restrain lipid loss (Ahmadian et al., 2009; Corraze and Kaushik, 1999; Dai et al., 2018; Kittilson et al., 2011; Sheridan, 1988). Therefore, the resilience and suppression of these lipolytic and lipogenic markers suggest Intralipid prevents the hydrolytic breakdown and synthesis of TAG from major lipid deposits at the transcriptional level. In addition to this transcriptional suppression of lipid metabolism, exogenous lipids caused a decrease in FAS activity in adipose tissue (Figure 3.7). This decrease suggests trout acutely suppress lipogenesis in response to Intralipid. This is in accordance with previous long-term hyperlipidemic studies, where

trout downregulate FAS expression and activity when fed high-lipid diets (Figueiredo-Silva et al., 2012; Mennigen et al., 2014). Therefore, despite an increase in circulating lipids trout may suppress lipid deposition, however, the suppression of both lipolytic and lipogenic markers makes it unclear whether Intralipid causes trout to accumulate intracellular lipids. The mammalian GPRs, FFAR1 and FFAR4 suppress lipogenic and lipolytic activity respectively (Anthonsen et al., 1998; Husted et al., 2020; Pollak et al., 2015; Strålfors et al., 1984). While the absence of *ffar4* in the rainbow trout genome makes the inhibitory expression of these lipolytic genes unclear (Chapter 4), I correctly annotate a previously misannotated trout GPR gene as *ffar1* (Chapter 4). The precise localization of this receptor in fish tissues and the underlying mechanism is unknown in fish. Thus, future studies are warranted to explore the regulatory mechanisms of teleost lipogenesis and lipolysis.

How Intralipid modulates glycerol and lipid utilization

In rainbow trout, circulating glycerol concentration stabilizes after 90 min (Figure 3.2A) which represents an increase in glycerol utilization. In trout, glycerol utilization is typically low compared to other oxidative fuels such as lactate and NEFAs especially in contracting muscles due to their low rates of glycerol kinase activity trout (Kam and Milligan, 2006; Newsholme and Taylor, 1969). However, in Nile tilapia, hepatic glycerol kinase activity, though low, tends to increase with increasing dietary glycerol over long-term, while juveniles can catabolize it for energy (da Costa et al., 2017; da Costa et al., 2015). However, there is currently no evidence that acute changes in circulating glycerol upregulate glycerol oxidation (Bortz et al., 1972; Newsholme and Taylor, 1969; Panserat et al., 2020; Sjarif et al., 2000). Therefore, it is unclear whether trout can

rapidly alter their fuel selection pattern to substitute other oxidative substrates for glycerol. Despite their conventionally poor glycerol oxidative capacity, trout readily oxidize NEFA to meet the energy requirements of the liver and contracting muscles. In the present study, hepatic HOAD activity (Figure 3.7) as well as *cpt1a* and *hoad* expression (Figure 3.4) were upregulated in hyperlipidemic trout. Thus, based on activity and expression profiles, the liver oxidizes NEFA presumably available from (i) an exogenous source and (ii) a rapidly hydrolyzed supply from Intralipid. Although NEFA kinetics were not quantified in the present study, these changes in lipid oxidative markers suggest a reliance on circulating lipids as an oxidative fuel.

In trout red and white muscle, Intralipid caused an increase in *hsl* expression, while *lpl* expression (Figure 3.4) remained unchanged. Furthermore, *cd36* expression increased in white muscle and did not change in red muscle (Figure 3.4). This data suggests that *hsl* and *lpl* expression is regulated in a tissue-specific manner. In teleosts, *hsl* transcript abundance is correlated to β-oxidation capacity, thus the highly oxidative fibres in red muscle express more *hsl* than the glycolytic fibres of white muscle (Langfort et al., 2003; Stubhaug et al., 2005). In resting trout, red muscle mitochondria utilize NEFA to maintain energy production, while oxidation in white muscle is relatively low (Albalat et al., 2006; Kiessling and Kiessling, 1993). Interestingly, changes in *hsl* and *cd36* expression, occur in the absence of changes in β-oxidation activity and gene expression for white muscle (Figures 3.4 and 3.7), while, in red muscle changes in *hsl* expression, occur with a simultaneous decrease in *cpt1a* expression (Figure 3.4). Thus, the increase in *hsl* expression in trout muscle may not contribute to lipid oxidation in trout muscle, however, may contribute to the high TAG/NEFA cycling typically seen in

trout. At rest, teleosts elevate *lpl* expression to serve increased energy demands and maintain a high reserve capacity to induce LPL activity (Magnoni and Weber, 2007; Saera-Vila et al., 2005). The maintenance of *lpl* expression in red and white muscle and HOAD activity in white muscle suggests Intralipid may not upregulate lipid uptake and oxidation. Therefore, based on gene expression profiles, hyperlipidemic trout may increase hepatic lipid oxidation and intramuscular lipid mobilization.

Inhibition of hepatic glucose production

In rainbow trout, Intralipid had no effect on glycemia (Figure 3.3A) and caused a reduction in R_a glucose from a baseline of 7.3 ± 0.9 to 4.7 ± 0.4 μm kg^{-1} min^{-1} (Figure 3.3C). The liver plays a central role in the regulation of R_a glucose due to the contribution of two hepatic processes, gluconeogenesis and glycogenolysis (Haman et al., 1997a; Jones, 2016). In hyperlipidemic trout, gluconeogenic gene expression was strongly induced, specifically a 5.0-fold, 2.6-fold and 16.5-fold increase in *pck1*, *g6pca* and *g6pcb1b* expression, respectively (Figure 3.5). Interestingly, the expression of *pck2*, the mitochondrial isoform, remained unchanged (Figure 3.5) contradicting the previous finding in rainbow trout where *pck2* expression significantly increased in fish fed high-lipid diets (Ducasse-Cabanot et al., 2007). In carnivorous fish, glycerol competes with other endogenous gluconeogenic precursors for hepatic gluconeogenesis and Pck localization gives rise to differential precursor preference (Mauerwerk et al., 2020; Rito et al., 2019; Stark and Kibbey, 2014). In the canonical linear gluconeogenic pathway, glycerol is an indiscriminate intermediate and its use is predicated on the activity of glycerol kinase, which increases in Nile tilapia fed dietary glycerol (da Costa et al., 2015; da Costa et al., 2017; Leithner, 2021; Stark and Kibbey, 2014). Interestingly, in a

nutritional study in seabass, some glycerol was shown to be converted to glucose via the hepatic TCA cycle suggesting Pck2 may influence glucose production from glycerol (Rito et al., 2019). Thus, the increase in circulating glycerol (Figure 3.2A) may stimulate a long-term gluconeogenic response to aid in glycerol clearance, similar to mammals (Kulyté et al., 2022).

The maintenance of enzymatic activity of total PCK (Figure 3.7) and Pck1 protein abundance (Figure 3.6) in response to elevated plasma lipids may indicate a slower regulatory response and explain the divergence in kinetics and gene expression data. Changes in transcript abundance may not yet be effective but represent induction of temporally delayed responses compared to acute effects on activity. Thus, the functional contribution to glycerol use and hepatic glucose production is likely not seen within the experimental design. Given the observed lipid-dependent reduction of R_a glucose in the absence of changes in PCK activity, it is possible Intralipid inhibited hepatic glycogenolysis, as short-term changes in R_a glucose are likely a result of changes in glycogen breakdown. While the hepatic glycogenolytic rate was not quantified in this study, in carnivorous fish, high-lipid diets increase hepatic glycogen content (Borges et al., 2014; Figueiredo-Silva et al., 2012). Therefore, the slight decrease in R_a glucose over 4 hours of Intralipid infusion is likely due to a suppression in glycogenolysis, whereas, the changes in gluconeogenic gene expression may be an initiation of a compensatory response to induce R_a glucose and buildup glycogen reserves.

How Intralipid modulates glucose utilization

In rainbow trout, Intralipid had no effect on glycemia (Figure 3.3A), therefore, the Intralipid-mediated 35% reduction in R_a glucose discussed earlier (Figure 3.3C), also represented a slight decrease in glucose utilization. Oxidative disposal accounts for most glucose utilization, however in trout as in many species, the relative importance of glucose oxidation changes with the availability of other oxidative substrates (Choi and Weber, 2016). In hyperlipidemic trout, hepatic *gck* paralogue expression (Figure 3.5) is strongly suppressed, while hepatic GK activity is unchanged (Figure 3.7). The expression of *gck* paralogues in trout is a sensitive marker of hepatic glucose concentration and uptake (Panserat et al., 2000). Therefore, the complete suppression of *gck* paralogue expression may be a long-term compensatory response by the liver to react to the suppression of R_a glucose. Along with induction of gluconeogenic genes, trout may suppress glycolytic genes to promote long-term glucose and glycogen production and limit their utilization. However, the maintenance of GK activity suggests there are few acute changes to hepatic glucose utilization.

Elevated circulating lipids suppressed both *glut4a* expression (Figure 3.5) and HK activity (Figure 3.7) in trout adipose tissue. Interestingly, hyperlipidemic trout upregulated *glut4* paralogue expression in white muscle (Figure 3.5). In muscle, short-term glucose uptake is regulated by Glut4 translocation (Marín-Juez et al., 2013; Navale and Paranjape, 2016), while long-term glucose uptake has been attributed to *glut4* expression (Corrêa-Giannella and Machado, 2013). Thus, the increase in *glut4* paralogue expression in white muscle is suggestive of an increase in long-term glucose uptake in this glycolytic tissue. The induction of glucose uptake in white muscle may be

to accumulate glycogen while energy demands at rest are low (Omlin and Weber, 2013; Richards et al., 2002). Similar to muscle, glucose uptake in adipose tissue is facilitated by Glut4 (Klip, 2009; Simpson et al., 2001). Thus, based on gene expression profiles, it is plausible the suppression of *glut4a* expression indicates inhibition of glucose uptake into adipose tissue. While transcriptional responses may precede functional roles, this data suggests that less import into adipose tissue may reflect reduced glucose fluxes following Intralipid infusion, which is further supported by observed reductions in HK activity in the same tissue (Figure 3.7). Changes in *gck* and *glut4* paralogue expression and HK activity in the liver and adipose tissue supports the overall suppression in glucose utilization reported suggestive of impaired glucose import and utilization in the liver and adipose tissue. While changes in white muscle *glut4* paralogue expression are suggestive of enhanced glucose import and utilization in this glycolytic tissue. Therefore, decreased glycolytic activity and impaired glucose uptake suggest hyperlipidemic trout do not utilize glucose.

Chapter 4: General Conclusions and Future Directions

This chapter is based on a manuscript titled “Metabolic signaling in rainbow trout: a potential explanation for hyperlipolysis”

Written by
Giancarlo G.M. Talarico[1], Dapeng Zhang[2], Jean-Michel Weber[1] and Jan A. Mennigen[1]

[1]Biology Department, University of Ottawa, Canada
[2]Biology Department, Saint Louis University, USA

In preparation for
Journal of Experimental Biology

Author contributions: all authors conception; G.G.M.T., D.Z. and J.A.M investigation and data curation; G.G.M.T. and J.A.M formal analysis of research and prepared figures; G.G.M.T. and J.A.M drafted, edited, revised and approved the manuscript.

Insights into fuel mobilization and selection in rainbow trout

The goal of this thesis was to research *in vivo* fuel mobilization in adult rainbow trout and investigate how it plays a role in regulating key carbohydrate and lipid metabolic pathways. By measuring *in vivo* fluxes and enzyme activities as well as using *real-time* RT-PCR and Western blotting approaches, I provided novel insights into energy mobilization under experimental conditions linked to carbohydrate and lipid synthesis, oxidation and metabolic signaling.

Lactate administration, at twice the baseline endogenous rate of appearance in the circulation (Omlin and Weber, 2010), greatly increased circulating lactate (~1mM to >10mM) similar to concentrations induced by strenuous exercise (Milligan and Girard, 1993; Omlin and Weber, 2013). *In vivo* measurements of metabolic fuel kinetics show that lactate strongly reduced hepatic glucose production (16.4 ± 2.0 to 8.9 ± 1.2 μm kg^{-1} min^{-1}) by suppressing gluconeogenesis (by downregulating Pck1 and *pck1* expression). Hyperlactatemia also suppressed whole-animal glucose utilization (by downregulating *gck* and *glut4* expression, in the liver and red muscle respectively) in most peripheral tissues, due to the significant impact exogenous lactate had on endogenous glucose supply. However, increased glycolytic capacity in white muscle (by upregulating HK activity and *glut4* expression) suggests this tissue has a preference for glucose due to its very limited capacity for MCT-mediated transmembrane lactate transport (Omlin et al., 2013). Therefore, overall trout may alter their fuel selection pattern by substituting glucose for lactate, excluding in white muscle. Additionally, in contrast to mammals, trout exhibited no lipolytic suppression during lactate administration (no change in the rate of appearance of glycerol: mean value of 7.3 ± 0.5 μm kg^{-1} min^{-1}), suggesting

HCAR1 signaling is weak in trout (no response of gene expression in white muscle and liver; inhibition in red muscle).

Intralipid-infusion, at ~¼ of the baseline endogenous rate of release of TAG in the circulation (Magnoni et al., 2008a), increased total circulating FA concentration (12.6 ± 2.0 to 16.5 ± 4.3 μmol ml^{-1}) and altered FA composition. *In vivo* measurements of metabolic fuel kinetics show that exogenous lipids strongly increased lipolysis (2.5 ± 0.5 to 5.3 ± 0.3 μm kg^{-1} min^{-1}; peak of 7.8 ± 1.1 μm kg^{-1} min^{-1} after 60 min) and suppressed lipogenesis (by downregulating FAS activity as well as *fas* and *dgat2* expression). Intralipid also caused an acute reduction in hepatic glucose production (7.3 ± 0.9 to 4.7 ± 0.4 μm kg^{-1} min^{-1}), compensated by transcriptional upregulation of gluconeogenesis (*pck1*, *g6pca* and *g6pcb1b*) and suppression of hepatic glycolytic gene expression (*gcka* and *gcka*). Changes in energy mobilization can be explained by the substitution of glucose for NEFAs in the liver (by upregulating HOAD activity as well as *cpt1a* and *hoad* expression, respectively). The systematic upregulation of glycolytic flux capacity in white muscle (by upregulating HK activity and *glut4* expression, in the liver and red muscle respectively) suggests trout white muscle utilize glucose as an oxidative fuel or to replenish glycogen stores.

G-protein coupled receptors as molecular mediators of fuel selection

Recently, a novel mechanistic basis for fuel selection has been explored in mammals in the form of deorphaned GPRs. Relevant to metabolic fuels investigated in this thesis (Chapter 2), a GPR (GPR81), with the capacity to bind lactate and subsequently induce cell signaling cascades, was found expressed in several tissues particularly relevant to energy metabolism. These include the liver, muscle, adipose

tissue and brain, among others (Liu et al., 2009). Now termed hydroxycarboxylic acid receptor 1 (HCAR1), this receptor has more recently been shown to (i) stimulate β-oxidation in the liver under fasting conditions (Wu et al., 2022), (ii) stimulate NL retention and increase mitochondrial content in skeletal muscle (Sun et al., 2016; Chen et al., 2021; Zhou et al., 2021) and (iii) suppress lipolytic activity in white adipose tissue (Liu et al., 2009). Similarly, the GPRs, FFAR1 and FFAR4 have been reported to be selective for LCFAs (Kimura et al., 2020), a relevant metabolic fuel in rainbow trout. This is in contrast to FFAR2 and FFAR3 which exhibit a high affinity for SCFAs, metabolites relevant to microbiome signaling and ketone body production (Kimura et al., 2020).

Interestingly, the presence of both HCAR1, as well as FFAR1 and FFAR4, have been reported in rainbow trout, albeit based on different lines of evidence. The expression of *hcar1* has been quantified in rainbow trout, where it was particularly highly expressed in the (first branch) of the gill and ubiquitously but lowly expressed in tissues relevant to this thesis, including the liver, muscle, and adipose tissue (Thomsen et al., 2019). The evolutionary origin of HCAR1 was hypothesized to be in early vertebrate evolution (Thomsen et al., 2019). Conversely, evidence for the presence of FFAR1 and FFAR4 in rainbow trout has been based on pharmacological approaches using intracerebroventricular injection of mammalian-validated endogenous agonist oleate and mammalian FFAR-specific agonists/antagonists to probe the role of central FA sensing mechanisms in the hypothalamic regulation of feed intake in this species (Velasco et al., 2020). Potent anorexigenic responses coincided with the induction of anorexigenic transcripts such as proopiomelanocortin (*pomc*) and the downregulation of orexigenic transcripts such as neuropeptide Y (*npy*). Despite evidence for teleost FFAR

signaling regulating feed intake, recent studies in rainbow trout have put into question the presence of the mammalian-like *ffar1* and *ffar4* receptors in rainbow trout based on genome-sequence information (Roy et al., 2022). Specifically, Roy and colleagues reported low expression of a *ffar1*-like transcript in rainbow trout and did not identify *ffar4* in the rainbow trout genome. Therefore, given these conflicting data and to clarify the potential role of lactate and LCFA metabolite GPR signaling in rainbow trout as potential (acute) signaling systems involved in fuel selection, I conducted a detailed *in silico* analysis to assess the presence of *hcar1*, *ffar1* and *ffar4* in key teleosts which hold key positions in fish evolution, are important research models and/or are relevant to aquaculture. Because comparative information on these GPRs remains scarce in vertebrates in general, I subsequently extended the analysis to key Sarcopterygian species, albeit at a lower level of resolution.

The molecular evolution of lactate and long chain fatty acid metabolite sensing in vertebrates with a focus on teleost fish

The hcar1 receptor

While detailed information on the structure and ligand binding kinetics for GPRs exist in mammals in the form of mutational analyses and/or *in silico* modelling approaches, comparable studies are generally lacking in fish. Interestingly, an early study harnessing the (comparative) zebrafish model to identify and functionally characterize conserved Hcar1 residues with regard to mammalian models represents a notable and useful exception in this regard (Kuei et al., 2011). Through *in silico* approaches and heterologous expression studies of mutated zebrafish receptors to assess lactate binding, this important study revealed that Hcar1 is not only present but

also binds lactate in fish with ~4 mM affinities comparable to characterized mammalian receptors (Liu et al., 2009). Importantly, the study also uncovered highly conserved amino acid residues critically involved in lactate-specific binding in zebrafish. These are, specifically, a cysteine, glutamate, serine and phenylalanine (CESF) motif in the second extracellular loop of the Hcar1 receptor, as well as several arginine residues believed to form part of the lactate binding pocket. By applying this functional insight to derived amino acid sequencing from genome sequence data in fish and other vertebrates (Figure 4.1), I identified *hcar1* in all fish, including elasmobranchs and sarcopterygian species excluding reptiles and birds (Figure 4.2). However, a search of the Japanese lamprey genome failed to identify *hcar1* in this species, similar to the situation in invertebrate species. In line with this scenario, microsynteny analysis of these assigned *hcar1* genes revealed an overall deep conservation of the *hcar1* gene locus (Figure 4.3A-B), with notable exceptions in some fish species. As such, *hcar1* sequences in elasmobranchs form part of a larger cluster of *hcar*-like receptors (Figure 4.3A), some of which are known to respond to ketone bodies such as β-hydroxybutyrate (Abdelrahman et al., 2022). This possibly reflects the unique metabolism of elasmobranches characterized by a reliance on ketone rather than FA oxidation to meet energetic needs (Speers-Roesch and Treberg, 2010). Future studies are warranted to explore the elasmobranch *hcar* gene family in this context. In line with teleost genome duplication events and genome reorganization events within and between teleost families, a second genome locus containing *hcar1* genes was identified in neoteleostei (Figure 4.3A). Conversely, *hcar1* genes are absent from these loci in reptiles and birds (Figure 4.3B) and are also not identified in whole genome searches. Together, these findings confirm

the presence of *hcar1* in rainbow trout as in most vertebrates, however with a notable exception in reptiles and birds (Figure 4.2).

Figure 4.1. Genome-derived amino acid sequences of HCAR-like receptors from fish and other vertebrates were identified as HCAR1 receptors based on conserved critical residues and functionally tested as being crucially involved in mediating lactate binding specificity across species including zebrafish (Kuei et al., 2011). All sequences were retrieved from Pubmed NCBI and aligned using ClustalOmega. Amino acids identified as critical for ligand binding are highlighted as follows: critical cysteine-disulphide bond forming residues (magenta), lactate interacting residues (green) and remaining residues of Hcar motif critical to lactate specificity (yellow).

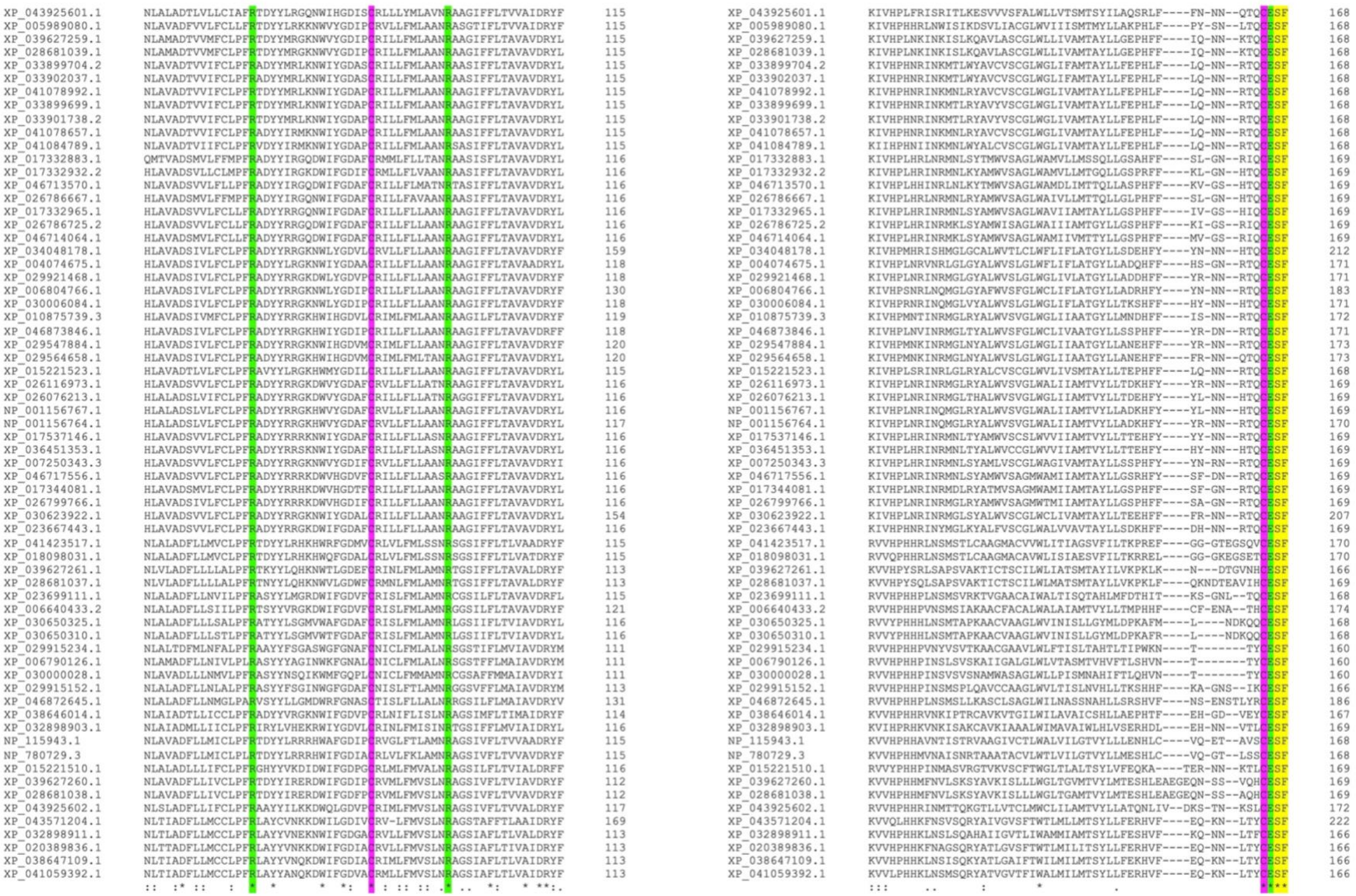
XP_043925601.1 NLALADTLVLLCIAFRTDYYLRGQNWIHGDISCRLLLYMLAVNRAAGIFFLTVVAIDRYF 115
XP_005989080.1 NLAVADFVVLFCLLFRTDYYLRKKNWVYGDIPCRVLLFMLAANRASGTIFLTVVAIDRYF 115
XP_039627259.1 NLAMADTVVMFCLPFRTDYYMRGKNWVYGDIPCRILLFMLAANRAAGIFFLTAVAVDRYL 115
XP_028681039.1 NLAMADTVVMFCLPFRTDYYMRGKNWVYGDIPCRILLFMLAANRAAGIFFLTAVAVDRYL 115
XP_033899704.2 NLAVADTVVIFCLPFRADYYMRLKNWIYGDASCRILLFMLAANRAASIFFLTAVAVDRYL 115
XP_033902037.1 NLAVADTVVIFCLPFRADYYMRLKNWIYGDASCRILLFMLAANRAASIFFLTAVAVDRYL 115
XP_041078992.1 NLAVADTVVIFCLPFRTDYYMRLKNWIYGDAPCRILLFMLAANRAAGIFFLTAVAVDRYL 115
XP_033899699.1 NLAVADTVVIFCLPFRTDYYMRLKNWIYGDAPCRILLFMLAANRAAGIFFLTAVAVDRYL 115
XP_033901738.2 NLAVADTVVIFCLPFRTDYYMRLKNWIYGDAPCRILLFMLAANRAAGIFFLTAVAVDRYL 115
XP_041078657.1 NLAVADTVVIFCLPFRADYYIRMKNWIYGDAPCRILLFMLAANRAASIFFLTAVAVDRYI 115
XP_041084789.1 NLAVADTVIIFCLPFRVDYYIRMKNWIYGDAPCRILLFMLAANRSASIFFLTAVAVDRYL 115
XP_017332883.1 QMTVADSMVLFFMPFRADYYIRGQDWIFGDAFCRMMLFLLTANRAASISFLTAVAVDRYL 116
XP_017332932.2 HLAVADSVLLCLMPFRADYYIRGKDWIFGDIFCRMLLFLVAANRAASIFFLTAVAVDRYL 116
XP_046713570.1 NLAVADSVVLFLLPFRADYYIRGQDWIFGDAFCRILLFLMATNRTASIFFLTAVAVDRYL 116
XP_026786667.1 HLAVADSMVLFFMPFRADYYIRGQNWIFGDAFCRILLFAVAANRAASIFFLTAVAVDRYL 116
XP_017332965.1 HLAVADSVVLFCLLFRADYYRRGQNWIFGDAFCRILLFLLAANRAAGIFFLTAVAVDRYL 116
XP_026786725.2 HLAVADSVVLFCLLFRADYYRRGQDWIFGDAFCRILLFLLAANRAAGIFFLTAVAVDRYL 116
XP_046714064.1 HLAVADSMVLFCLLFRADYYRRGQDWIFGDAFCRILLFLLAANRAAGIFFLTAVAVDRYL 116
XP_034048178.1 HLAVADSIVLFCLPFRADYYRRGKNWLYGDVLCRVLLFLLAANRAAGIFFLTAVAVDRYF 159
XP_004074675.1 HLAVADSIVLFCLPFRADYYLRGKNWIYGDAACRILLFLLAANRAAGIFFLTAVAADRYL 118
XP_029921468.1 HLAVADSIVLFCLPFRADYYRRGKDWLYGDVPCRILLFLLAANRAAGIFFLTAVAVDRYF 118
XP_006804766.1 HLAVADSIVLFCLPFRADYYRRGKNWLYGDIPCRILLFLLAANRAAGIFFLTAVAVDRYF 130
XP_030006084.1 HLAVADSIVLFCLPFRADYYRRGKNWLYGDIPCRILLFLLAANRAAGIFFLTAVAVDRYF 118
XP_010875739.3 HLAVADSIVMFCLPFRADYYRRGKHWIHGDVLCRIMLFMLAANRAAGILFLTAVAVDRYF 119
XP_046873846.1 HLAVADSIVLFCLPFRADYYRRGKHWIYGDIPCRILLFLLAANRAAGIFFLTAVADRFF 118
XP_029547884.1 HLAVADSIVLFCLPFRADYYRRGKNWIHGDVMCRIMLFLLAANRAAGIFFLTAVAVDRYF 120
XP_029564658.1 HLAVADSIVLFCLPFRADYYRRGKHWIHGDVMCRIMLFMLTANRAAGIFFLTAVAVDRYL 120
XP_015221523.1 HLAVADTLVLFCLPFRAVYYLRGKNWIYGDILCRILLFLLAANRAAGIFFLTAVAVDRYL 116
XP_026116973.1 HLAVADSVVLFCLPFRADYYRRGKDWVYGDAFCRVLLFLLATNRAAGIFFLTAVAVDRYL 116
XP_026076213.1 HLALADSLVIFCLPFRADYYRRGKDWVYGDAFCRILLFLLATNRAGGIFFLTAVADRYL 116
NP_001156767.1 HLALADSLVLFCLPFRADYYRRGKHWVYGDAFCRVLLFLLAANRAAGIFFLTAVAVDRYL 116
NP_001156764.1 HLALADSLVLFCLPFRADYYRRGKHWVYGDAFCRVLLFLLAANRAAGIFFLTAVAVDRYL 117
XP_017537146.1 HLAVADSVVLFCLPFRADYYRRRKNWIYGDAFCRILLFLLASNRAAGIFFLTAVAVDRYL 116
XP_036451353.1 HLAVADSVVLFCLPFRADYYRRSKNWIYGDAFCRILLFLLASNRAAGIFFLTAVAVDRYL 116
XP_007250343.3 HLAVADSVVLFCLPFRADYYRRGKNWVYGDIFCRVLLFLLAANRAAGIFFLTAVAVDRYI 116
XP_046717556.1 HLAVADSVVLFCLPFRADYYRRRKDWVHGDVFCRILLFLLAASRAAGIFFLTAVAVDRYL 116
XP_017344081.1 HLAVADSMVLFCLPFRADYYRRHKDWVHGDTFCRILLFLLAANRAAGIFFLTAVAVDRYL 116
XP_026799766.1 HLAVADSIVLFCLPFRADYYRRRKDWVHGDIFCRILLFLLAANRAAGIFFLTAVAVDRYL 116
XP_030623922.1 HLAVADSVVLFCLPFRADYYRRGKNWIYGDALCRILLFLLAANRAAGIFFLTAVAVDRYL 154
XP_023667443.1 HLAVADSVVLFCLPFRADYYRRGKDWIFGDAFCRILLFLLAANRAAGIFFLTAVAVDRYL 116
XP_041423517.1 NLALADFLLMVCLPFRTDYYLRHKHWRFGDMVCRLVLFMLSSNRSGSIFFLTLVAADRYF 115
XP_018098031.1 NLALADFLLMVCLPFRTDYYLRHKHWQFGDALCRLVLFMLSSNRSGSIFFLTLVATDRYF 115
XP_039627261.1 NLVLADFLLLLALPFRTKYYLQHKNWTLGDEFCRINLFMLAMNRTGSIFFLTAVALDRYF 113
XP_028681037.1 NLVLADFLLLLALPFRTNYYLQHKNWVLGDWFCRMNLFMLAMNRTGSIFFLTAVALDRYF 113
XP_023699111.1 NLALADFLLNVILPFRASYYLMGRDWIFGDVFCRISLFMLAMNRCGSILFLTAVAVDRFL 115
XP_006640433.2 NLALADFLLSIILPFRTSYYVRGKDWIFGDVFCRISLFMLAMNRGGSILFLTAVAVDRYF 121
XP_030650325.1 NLALADFLLLSALPFRATYYLSGMVWAFGDAFCRISLFMLAMNRLGSIIFLTVIAVDRYL 116
XP_030650310.1 NLALADFLLLSTLPFRATYYLSGMVWTFGDAFCRISLFMLAMNRLGSIIFLTVIAVDRYL 116
XP_029915234.1 NLALTDFMLNFALPFRAAYYFSGASWGFGNAFCNICLFMLALNRSGSTIFLMVIAVDRYM 111
XP_006790126.1 NLAMADFLLNIVLPLRASYYYAGINWKFGNALCNICLFMLALNRSGSTFFLMAIAVDRYM 111
XP_030000028.1 NLAVADLLLNMVLPFRASYYNSQIKWMFGQPLCNICLFMMAMNRCGSAFFMMAIAVDRYI 111
XP_029915152.1 NLALADFLLNLALPFRASYYFSGINWGFGDAFCNISLFTLAMNRGGSVFFLMAIAVDRYM 113
XP_046872645.1 NLALADFLLNMGLPARVSYYLLGMDWRFGNASCTISLFLLALNRRGSILFLMAIAVDRYV 131
XP_038646014.1 NLAIADTLLICCLPFRADYYVRGKNWIFGDVPCRLNIFLISLNRAGSIMFLTIMAIDRYF 114
XP_032898903.1 NLAIADMLLIICLPFRIRYLVHEKRWIYGDVLCRINLFMISINRTGSIFFLMVIAIDRYL 116
NP_115943.1 NLAVADFLLMICLPFRTDYYLRRRHWAFGDIPCRVGLFTLAMNRAGSIVFLTVVAADRYF 115
NP_780729.3 NLAVADFLLMICLPLRTDYYLRRRHWIFGDIACRLVLFKLAMNRAGSIVFLTVVAVDRYF 115
XP_015221510.1 NLALADLLLIFCLPFRGHYYVKDIDWIFGDPGCRLMLFMVALNRAGSILFLTVIALDRFF 116
XP_039627260.1 NLAVADFLLIVCLPFRTDYYIRERDWIFGDIPCRVMLFMVSLNRAGSIVFLTVIAVDRYF 112
XP_028681038.1 NLAVADFLLIVCLPFRTDYYIRERDWIFGDFPCRVMLFMVSLNRAGSIVFLTVVAVDRYF 112
XP_043925602.1 NLSLADFLLIFCLPFRAAYYILKKDWQLGDVPCRIMLFMVSLNRAGSIVFLTVVALDRYF 117
XP_043571204.1 NLTIADFLLMCCLPFRLAYCVNKKDWILGDIVCRV-LFMVSLNRAGSTAFFTLAAIDRYF 169
XP_032898911.1 NLTLADFLLMCCLPFRLAYYVNEKNWIFGDGACRVLLFMVSLNRAGSIAFLTLVALDRYF 113
XP_020389836.1 NLTTADFLLMCCLPFRLAYYVNKKDWIFGDIACRVLLFMVSLNRAGSIAFLTIVAIDRYF 113
XP_038647109.1 NLTIADFLLMCCLPFRLAYYVNQKDWIFGDIACRIMLFMVSLNRAGSIAFLTLVAIDRYF 113
XP_041059392.1 NLTIADFLLMCCLPFRLAYYANQKDWIFGDVACRMLLFMVSLNRAGSIAFLTLVAIDRYF 113
:: :* :: : * * * *: * : :: :: .* .. *: * **:.
XP_043925601.1 KIVHPLFRISRITLKESVVVSFALWLLVTSMTSYILAQSRLF----FN-NN--QTQCESF 168
XP_005989080.1 KIVHPHHRLNWISIKDSVLIACGLWVIIISMTMYLLAKPHLF----PY-SN--LTQCESF 168
XP_039627259.1 KIVHPLNKINKISLKQAVLASCGLWLLIVAMTAYLLGEPHFF----IQ-NN--KTQCESF 168
XP_028681039.1 KIVHPLNKINKISLKQAVLASCGLWLLIVAMTAYLLGEPHFF----IQ-NN--KTQCESF 168
XP_033899704.2 KIVHPHNRINKMTLWYAVCVSCGLWGLIFAMTAYLLFEPHLF----LQ-NN--RTQCESF 168
XP_033902037.1 KIVHPHNRINKMTLWYAVCVSCGLWGLIFAMTAYLLFEPHLF----LQ-NN--RTQCESF 168
XP_041078992.1 KIVHPHNRINKMNLRYAVCVSCGLWGLIVAMTAYLLFEPHLF----LQ-NN--RTQCESF 168
XP_033899699.1 KIVHPHNRINKMTLRYAVYVSCGLWGLIVAMTAYLLFEPHLF----LQ-NN--RTQCESF 168
XP_033901738.2 KIVHPHNRINKMTLRYAVYVSCGLWGLIVAMTAYLLFEPHLF----LQ-NN--RTQCESF 168
XP_041078657.1 KIVHPHNRINKMNLRYAVCVSCGLWGLIVAMTAYLLFEPHLF----LQ-NN--RTQCESF 168
XP_041084789.1 KIIHPHNIINKMNLWYALCVSCGLWGLIVAMTAYLLFEPHLF----LQ-NN--RTQCESF 168
XP_017332883.1 KIVHPLHRLNRMNLSYTMWVSAGLWAMVLLMSSQLLGSAHFF----SL-GN--RIQCESF 169
XP_017332932.2 KIVHPLHRINRMNLKYAMWVSAGLWAMVLLMTGQLLGSPRFF----KL-GN--HTQCESF 169
XP_046713570.1 KIVHPLHHINRLNLKYTMWVSAGLWAMDLIMTTQLLASPHFF----KV-GS--HTQCESF 169
XP_026786667.1 KIVHPLHRLNRMNLRYAMWVSAGLWAIVLLMTTQLLGLPHFF----SL-GN--HTQCESF 169
XP_017332965.1 KIVHPLHRINRMNLSYAMWVSAGLWAVIIAMTAYLLGSPHFF----IV-GS--HIQCESF 169
XP_026786725.2 KIVHPLHRINRMKLSYAMWISAGLWAIIIAMTGYLLGSPHFF----KI-GS--RIQCESF 169
XP_046714064.1 KIVHPLHRINRMKLSYAMWVSAGLWAMIIVMTTYLLGSPHFF----MV-GS--RIQCESF 169
XP_034048178.1 KIVHPMHRISHMGLGCALWVTLCLWFLIFLATGYLLSDEHFY----YN-NN--HTQCESF 212
XP_004074675.1 KIVHPLNRVNRLGLGYALWVSLGLWFLIFLATGYLLADQHFF----HS-GN--RTQCESF 171
XP_029921468.1 KIVHPLNRINRMGLGYALWVSLGLWGLIVLATGYLLADDHFF----YR-NN--RTQCESF 171
XP_006804766.1 KIVHPSNRLNQMGLGYAFWVSFGLWCLIFLATGYLLADRHFY----YN-NN--RTQCESF 183
XP_030006084.1 KIVHPRNRINQMGLVYALWVSLGLWGLIFLATGYLLTKSHFF----HY-NN--HTQCESF 171
XP_010875739.3 KIVHPMNTINRMGLRYALWVSVGLWGLIIAATGYLLMNDHFF----IS-NN--RTQCESF 172
XP_046873846.1 KIVHPLNVINRMGLTYALWVSFGLWCLIVAATGYLLSSPHFF----YR-DN--RTQCESF 171
XP_029547884.1 KIVHPMNKINRMGLNYALWVSLGLWGLIIAATGYLLANEHFF----YR-NN--RTQCESF 173
XP_029564658.1 KIVHPMNKINRMGLNYALWVSLGLWGLIIAATGYLLANEHFF----FR-NN--QTQCESF 173
XP_015221523.1 KIVHPLSRINRLGLRYALCVSCGLWVLIVSMTAYLLTEPHFF----LQ-NN--RTQCESF 168
XP_026116973.1 KIVHPLNRINRMGLRYALWVSVGLWALIIAMTVYLLTDKHFY----YR-NN--RTQCESF 169
XP_026076213.1 KIVHPLNRINRMGLTHALWVSVGLWGLIIAMTVYLLTDEHFY----YL-NN--HTQCESF 169
NP_001156767.1 KIVHPLNRINQMGLRYALWVSVGLWALIIAMTVYLLADKHFY----YL-NN--HTQCESF 169
NP_001156764.1 KIVHPLNRINQMGLRYALWVSVGLWALIIAMTVYLLADKHFY----YR-NN--RTQCESF 170
XP_017537146.1 KIVHPLHRINRMNLTYAMWVSCSLWVVIIAMTVYLLTTEHFY----YY-NN--RTQCESF 169
XP_036451353.1 KIVHPLHRINRMNLTYALWVCCGLWVVIIAMTVYLLTTEHFY----HY-NN--HTQCESF 169
XP_007250343.3 KIVHPLHRINRMNLSYAMLVSCGLWAGIVAMTAYLLSSPHFY----YN-RN--RTQCESF 169
XP_046717556.1 KIVHPLNRINRMNLSYAMWVSAGMWAMIIAMTAYLLGSRHFY----SF-DN--RTQCESF 169
XP_017344081.1 KIVHPLNRINRMDLRYATMVSAGMWAMIIAMTAYLLGSPHFF----SF-GN--RTQCESF 169
XP_026799766.1 KIVHPLNRINRMGLRYAMWVSAGMWTMIIAMTAYLLGSPHFF----SA-GN--RTQCESF 169
XP_030623922.1 KIVHPLNRINRMGLSYALWVSCGLWCLIVAMTAYLLTEEHFF----FR-NN--RTQCESF 207
XP_023667443.1 KIVHPHNRINYMGLKYALFVSCGLWALVVAVTAYLLSDKHFF----DH-NN--RTQCESF 169
XP_041423517.1 RVVHPHHRLNSMSTLCAAGMACVVWLITIAGSVFILTKPREF----GG-GTEGSQVCESF 170
XP_018098031.1 RVVQPHHRLNSMSTLCAAGMACAVWLISIAESVFILTKRREL----GG-GKEGSETCESF 170
XP_039627261.1 KVVHPYSRLSAPSVAKTICTSCILWLIATSMTAYILVKPKLK----N---DTGVNHCESF 166
XP_028681037.1 KVVHPYSQLSAPSVAKTICTSCILWLMATSMTAYLLVKPKLF----QKNDTEAVIHCESF 169
XP_023699111.1 RVVHPHHPLNSMSVRKTVGAACAIWALTISQTAHLMFDTHIT----KS-GNL--TQCESF 168
XP_006640433.2 RVVHPHHPVNSMSIAKAACFACALWALAIAMTVYLLTMPHHF----CF-ENA--THCESF 174
XP_030650325.1 RVVYPHHHLNSMTAPKAACVAAGLWVINISLLGYMLDPKAFM----L----NDKQQCESF 168
XP_030650310.1 RVVYPHHHLNSMTAPKAACVAAGLWVINISLLGYMLDPKAFR----L----NDKQQCESF 168
XP_029915234.1 RVVHPHHPVNYVSVTKAACGAAVLWLFTISLTAHTLTIPWKN----T-------TYCESF 160
XP_006790126.1 RVVHPHHPINSLSVSKAIIGALGLWLVTASMTVHVFTLSHVN----T-------TYCESF 160
XP_030000028.1 RVVHPHHPINSVSVSNAMWASAGLWLLPISMNAHIFTLQHVN----T-------TYCESF 160
XP_029915152.1 RVVHPHHPINSMSPLQAVCCAAGLWVLTISLNVHLLTKSHHF----KA-GNS--IKCESF 166
XP_046872645.1 RVVHPHHPLNSMSLLKASCLSAGLWILNASSNAHLLSRSHVF----NS-ENSTLYRCESF 186
XP_038646014.1 KVVHPHHRVNKIPTRCAVKVTGILWILAVAICSHLLAEPHTF----EH-GD--VEYCESF 167
XP_032898903.1 KVIHPRHKVNKISAKCAVKIAAALWIMAVAIWLHLVSERHDL----EH-NN--VTLCESF 169
NP_115943.1 KVVHPHHAVNTISTRVAAGIVCTLWALVILGTVYLLLENHLC----VQ-ET--AVSCESF 168
NP_780729.3 KVVHPHHMVNAISNRTAAATACVLWTLVILGTVYLLMESHLC----VQ-GT--LSSCESF 168
XP_015221510.1 RVVYPHHPINMASVRGTVKVSCFTWGLTLALTSYLVFEQKA----TER-NN--KTLCESF 169
XP_039627260.1 KVVHPHHMFNVLSKSYAVKISLLLWGLTGVMTVYLMTESHLEAEGEQN-SS--VQHCESF 169
XP_028681038.1 KVVHPHHMFNVLSKSYAVKISLLLWGLTGAMTVYLMTESHLEAEGEQN-SS--AQHCESF 169
XP_043925602.1 RVVHPHHRINMTTQKGTLLVTCLMWCLILAMTVYLLATQNLIV--DKS-TN--KSLCESF 172
XP_043571204.1 KVVQLHHKFNSVSQRYAIVGVSFTWTLMLLMTSYLLFERHVF----EQ-KN--LTYCESF 222
XP_032898911.1 KVVHPHHKLNSLSQAHAIIGVTLIWAMMIAMTSYLLFESHVF----KQ-NN--LTFCESF 166
XP_020389836.1 KVVHPHHKFNAGSQRYATLGVSFTWTLMLILTSYLLFERHVF----EQ-NN--LTYCESF 166
XP_038647109.1 KVVHPHHKLNSISQKYATLGAIFTWILMILMTSYLLFEKHVF----EQ-KN--LTYCESF 166
XP_041059392.1 KVVLPHHKLNSMSQRYATVGVTFIWALMILMTSYLLFERHVF----EQ-KN--LTYCESF 166
::: .. : * . *****

Figure 4.2. Proposed evolution of lactate (HCAR1) and long-chain fatty acid receptor (FFAR1 and FFAR4) in vertebrates. Filled circles indicate the appearance of *hcar1* (yellow), *ffar1* (green) and *ffar4* (blue).

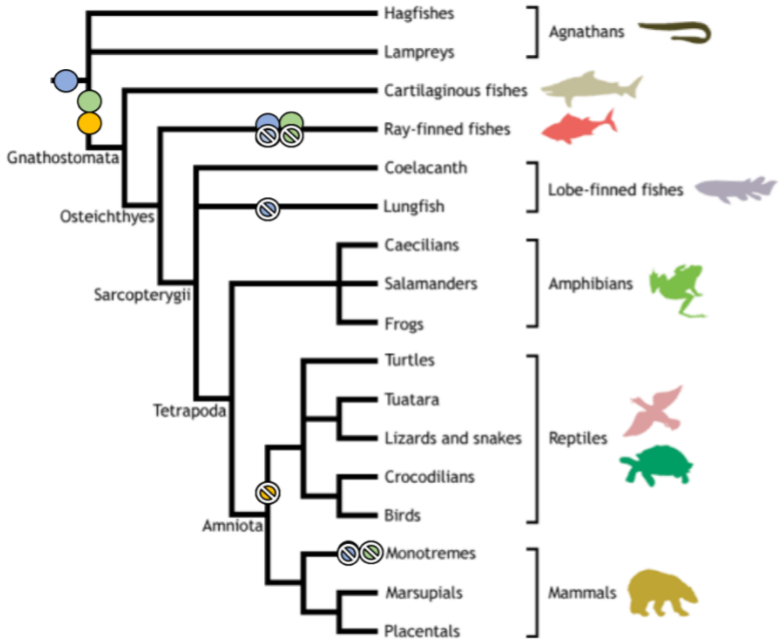

Proposed evolutionary history of the lactate receptor *hcar1 (gpr81)* in vertebrates

Proposed evolutionary history of the long-chain fatty acid receptor *ffar1 (gpr40)* in vertebrates

Proposed evolutionary history of the long-chain fatty acid receptor *ffar4 (gpr120)* in vertebrates

Figure 4.3. Genome sequence-derived microsynteny analysis of the *hcar1* locus in select Elasmobranchii + Actinopterygii (A) and Sarcopterygii (B). *hcar*-like receptors are indicated in red, while *hcar1* receptors are indicated in red with a black pattern fill. All synteny information was retrieved from Pubmed NCBI.

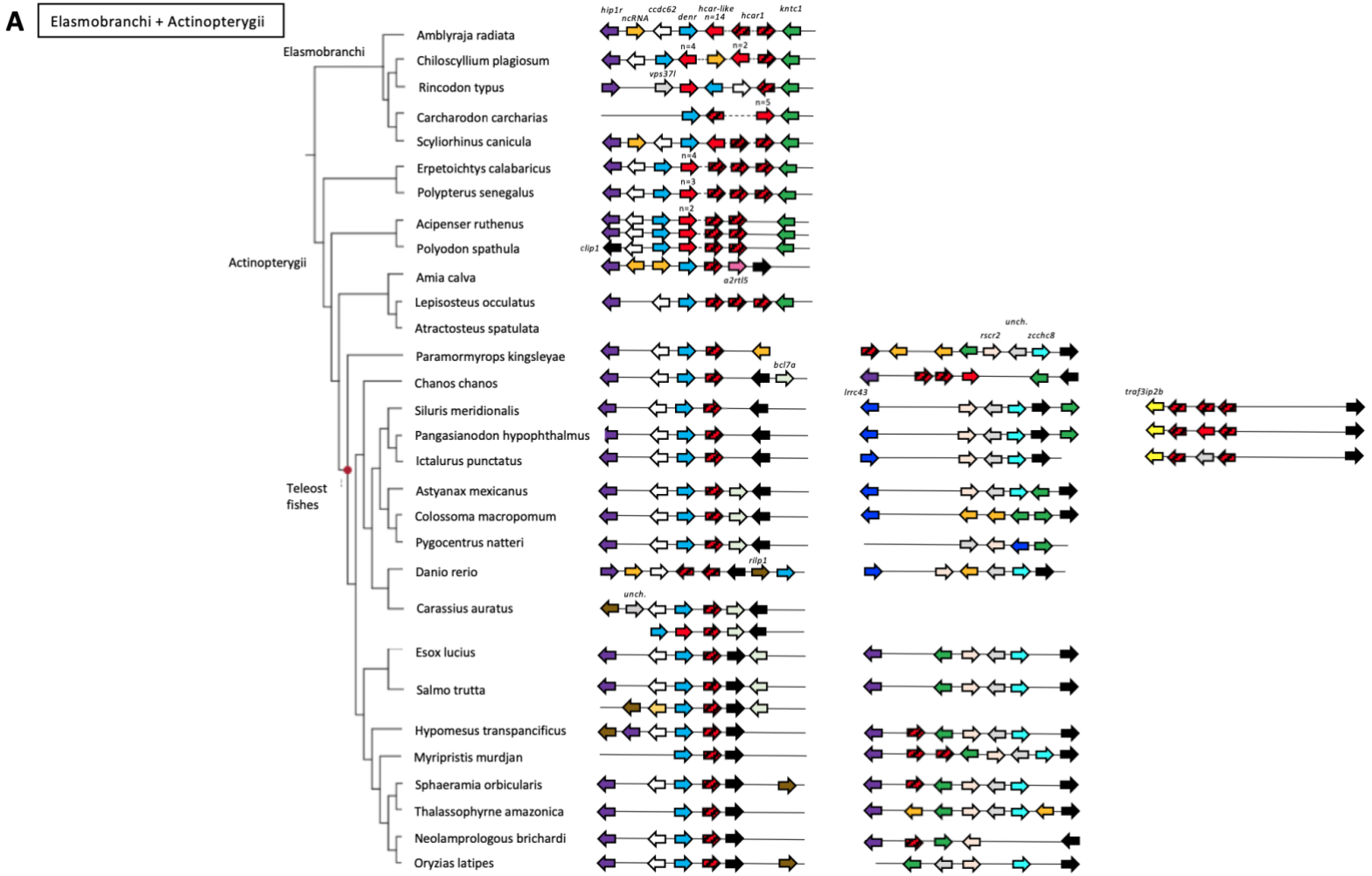

B Sarcopterygii

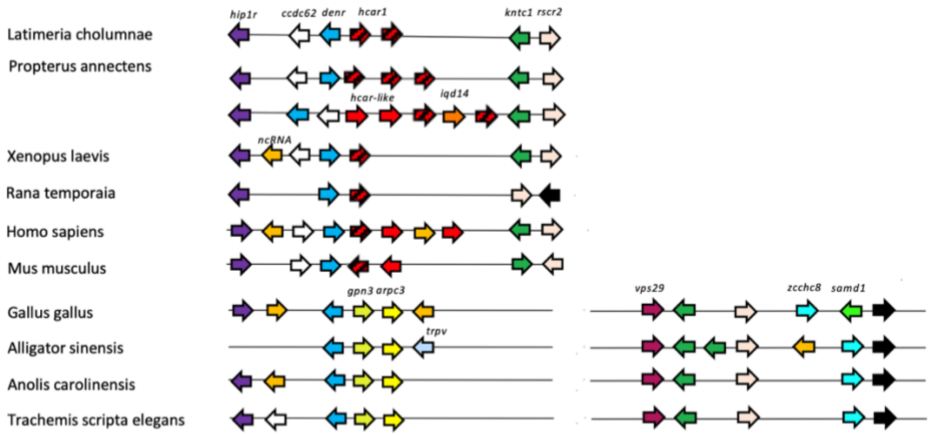

The long chain fatty acid receptors ffar1 and ffar4

In mammals, LCFA receptors FFAR1 and FFAR4 are expressed in several metabolic tissues relevant to the investigation of fuel selection, including the liver, pancreas and adipose tissue (Secor et al., 2021). FFAR1 knockout mice reveal several metabolic alterations, including hepatic steatosis (Steneberg et al., 2005). At the tissue level, FFAR1 is involved in mediating the anti-lipogenic effects of unsaturated LCFAs (22:6) in hepatocytes (On et al., 2019). In the pancreas, FFAR1 has been shown to promote insulin secretion (Itoh et al., 2003). Conversely, FFAR4 function is best understood in white adipose tissue, where FFAR4 inhibits lipolysis via an autocrine negative feedback loop involving non-esterified LCFAs (Husted et al., 2020). In addition, FFARs in general have been shown to modulate macrophage function and other inflammatory responses (Al Mahri et al., 2022), suggesting the potential for secondary effects on energy metabolism via modulation of inflammatory pathways.

In contrast to the situation for the lactate-binding HCAR1 receptor, no functional analysis of specific amino acids involved in LCFA binding of FFARs exists in fish. Indeed, the modelling and functional analysis of key amino acid residues forming LCFA binding pockets in FFARs continues to be an area of active investigation in mammalian species (Teng et al., 2022; Tikhonova, 2017). Thus, functional extrapolation remains limited to microsynteny, amino acid similarity and residue conservation analyses. Investigation of (i) microsynteny of the mammalian *ffar1* locus across vertebrates (Figure 4.4), (ii) overall amino acid sequence similarity between FFARs in this locus (Figure 4.5) and (iii) residues involved in mammalian FFAR1 ligand binding (Figure 4.6), suggest that FFAR1 emerged early within the vertebrate lineage (Figure 4.2). While

overall conservation of the gene locus containing multiple FFARs is relatively conserved across vertebrate species, phylogenetic analysis of all FFARs (except FFAR4) reveals that individual FFAR genes annotated as FFAR2-like and FFAR3-like in several vertebrates (including rainbow trout) cluster distinctly with known FFAR1 or FFAR1-like annotated proteins, suggesting they are indeed FFAR1 receptors (Figure 4.5). This notion is further supported by shared critical residues for the mammalian FFAR1 binding pocket (Figure 4.6), which suggests these receptors bind LCFAs and are indeed FFAR1 receptors. However, formal analyses in non-mammalian vertebrate 'FFAR1-like' receptors are needed to functionally validate this finding through heterologous expression and binding assay similar to what has been reported for the HCAR1 receptor. Together these findings confirm that *ffar1* emerged early in vertebrate evolution, although it is not present in lampreys (data not shown). It is thus present in trout, but not zebrafish fish, *Danio rerio*, and future detailed analyses in fish are warranted to assess potential lineage-specific losses of *ffar1* in more detail.

In contrast, synteny analysis reveals an early origin of FFAR4 at the base of vertebrate evolution. Present in lamprey, elasmobranchs and sarcopterygians except for the West African lungfish, *Protopterus annectens*, *ffar4* appears to have originated early in vertebrate evolution and retained across classes (Figure 4.7A-B). In line with this finding, identified residues considered to form part of the binding pocket (Hudson et al., 2014; Moniri, 2016) are highly conserved between lamprey and all vertebrate groups (Figure 4.8). However, microsynteny analysis of *ffar4* reveals a somewhat complex evolutionary history in bony fish: In some non-teleost bony fish such as the spotted gar, *Lepisosteus oculatus*, and the bowfin, *Amia calva*, *ffar4* is lost (Figure 4.7A). Teleost-

specific duplication of this group of genes resulted in the loss of *ffar4* in one locus in all teleost fish, while some widely studied and cultivated fish species including cyprinids such as zebrafish, goldfish, *Carassius auratus*, and salmonids such as river trout, *Salmo trutta*, as well as the acanthomorph Japanese ricefish, *Oryzias latipes*, lost *ffar4* in both loci (Figure 4.7A; Figure 4.9). While these findings thus confirm the absence of *ffar4* in rainbow trout, the unusual evolution of *ffar4* in teleost fish does not follow known relationships between species in fish evolution (Hughes et al., 2018) and warrants comparative functional investigation.

Overall, evidence suggests the presence of the lactate receptor, *hcar1*, and the LCFA receptor, *ffar1* in rainbow trout and fish in general, while rainbow trout lack *ffar4*, contrary to reports in the literature. The evolutionary loss of *ffar4* appears to be linked to a unique evolutionary history in fish, as it originated early in vertebrate evolution (present in lamprey, elasmobranchs and basal teleost fish). Indeed, rainbow trout, salmonids and other (largely fish) species appear to have lost *ffar4* secondarily, resulting in the absence of mammalian-like FFAR4 receptors in rainbow trout. Given the diversity of (uncharacterized) GPRs, it remains however possible that rainbow trout may express other receptors capable of responding to LCFAs.

Figure 4.4. Microsynteny analysis of the mammalian FFAR1 locus across selected vertebrate species. All synteny information was retrieved from Pubmed NCBI.

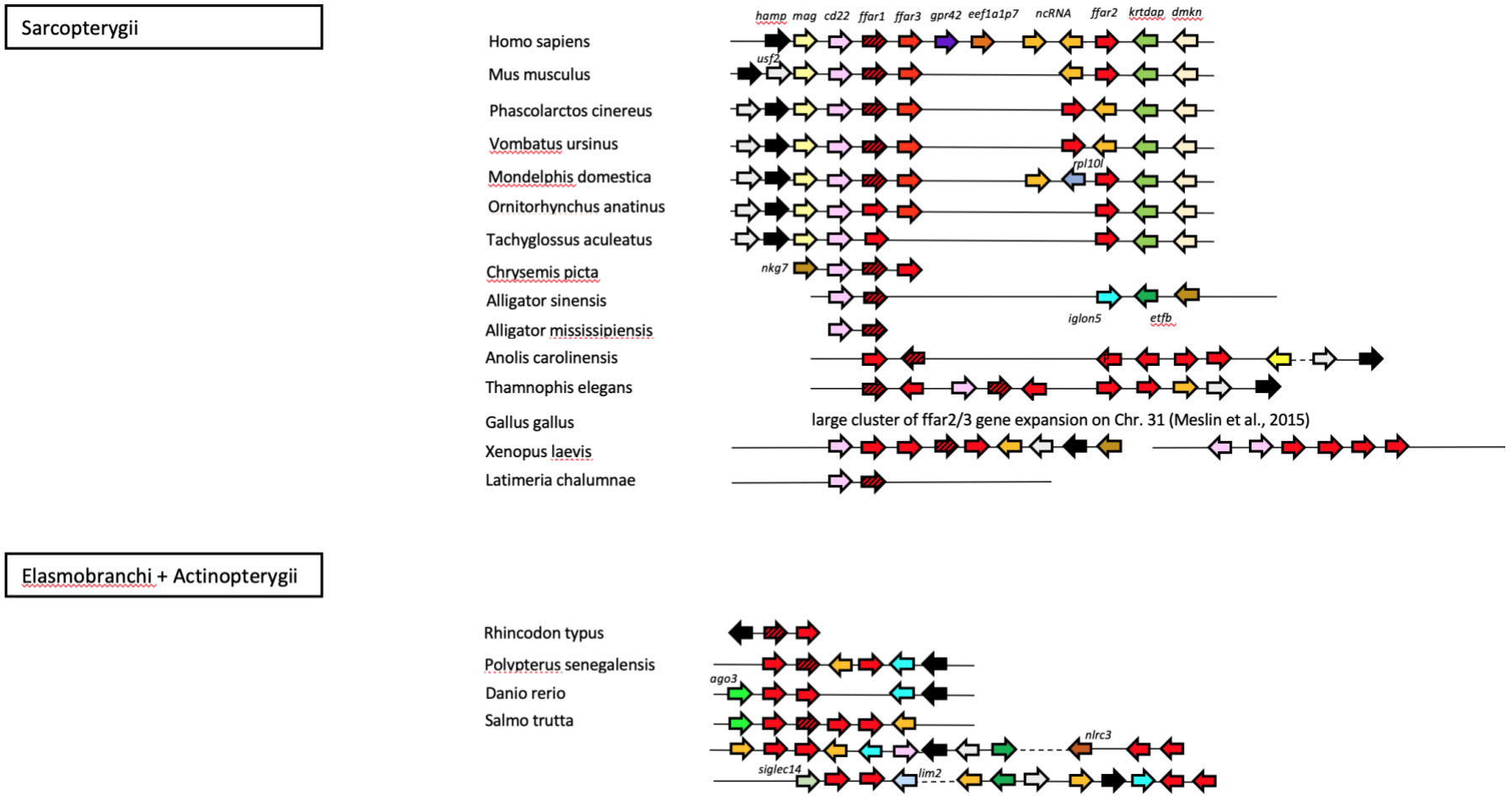

Figure 4.5. Overall amino acid sequence similarity of FFAR1(-like), FFAR2(-like) and FFAR3(-like) receptors across vertebrates in relevant loci. Genome-derived amino acid sequences of these receptors were obtained from NCBI in FASTA format and subsequently analyzed using the 'one click' mode of the Phylogeny.fr pipeline (Dereeper et al., 2008) with standard parameters using the G-blocks program to eliminate poorly aligned positions and divergent regions.


XP_025049972.1_free_fatty_acid_receptor_1_Alligator_sinensis
XP_019352189.1_PREDICTED_free_fatty_acid_receptor_1_Alligator_mi
XP_032083603.1_G-protein_coupled_receptor_42-like_Thamnophis_ele
XP_032083601.1_G-protein_coupled_receptor_42-like_Thamnophis_ele
XP_003225139.1_PREDICTED_free_fatty_acid_receptor_2-like_Anolis
XP_042703733.1_free_fatty_acid_receptor_1-like_Chrysemys_picta_b
NP_005294.1_free_fatty_acid_receptor_1_Homo_sapiens
NP_918946.2_free_fatty_acid_receptor_1_Mus_musculus
XP_003341098.1_PREDICTED_free_fatty_acid_receptor_1_Monodelphis
XP_020833099.1_free_fatty_acid_receptor_1_Phascolarctos_cinereus
XP_027711341.1_free_fatty_acid_receptor_3-like_Vombatus_ursinus
XP_048476477.1_free_fatty_acid_receptor_1-like_Rhincodon_typus
XP_018080387.1_free_fatty_acid_receptor_2_Xenopus_laevis
XP_029586936.1_free_fatty_acid_receptor_2-like_Salmo_trutta
XP_039627319.1_free_fatty_acid_receptor_2_Polypterus_senegalus
XP_006011340.2_PREDICTED_free_fatty_acid_receptor_2-like_Latimer
XP_029573699.1_free_fatty_acid_receptor_2-like_Salmo_trutta
XP_029593465.1_free_fatty_acid_receptor_2-like_Salmo_trutta
XP_029574501.1_free_fatty_acid_receptor_2-like_Salmo_trutta
XP_018080389.1_free_fatty_acid_receptor_2_Xenopus_laevis
XP_041426679.1_free_fatty_acid_receptor_3-like_Xenopus_laevis
XP_018080388.2_free_fatty_acid_receptor_3_Xenopus_laevis
XP_005312793.1_free_fatty_acid_receptor_3-like_Chrysemys_picta_b
XP_008174842.1_free_fatty_acid_receptor_2-like_Chrysemys_picta_b
XP_005312791.2_free_fatty_acid_receptor_2-like_Chrysemys_picta_b
XP_005315540.1_free_fatty_acid_receptor_2-like_partial_Chrysemys
XP_025072255.1_free_fatty_acid_receptor_2-like_Alligator_sinensi
XP_014450019.1_PREDICTED_free_fatty_acid_receptor_2_Alligator_mi
XP_028920755.1_free_fatty_acid_receptor_3-like_Ornithorhynchus_a
XP_038623549.1_G-protein_coupled_receptor_42-like_Tachyglossus_a
XP_001369770.2_PREDICTED_free_fatty_acid_receptor_3_Monodelphis
XP_020833146.1_free_fatty_acid_receptor_3_Phascolarctos_cinereus
XP_027711354.1_free_fatty_acid_receptor_1_Vombatus_ursinus
NP_001028488.1_free_fatty_acid_receptor_3_Mus_musculus
NP_005295.1_free_fatty_acid_receptor_3_Homo_sapiens
NP_001335124.1_G-protein_coupled_receptor_42_Homo_sapiens
XP_028921127.1_free_fatty_acid_receptor_2_Ornithorhynchus_anatin
XP_038622817.1_free_fatty_acid_receptor_2-like_Tachyglossus_acul
NP_001161981.1_free_fatty_acid_receptor_2_Mus_musculus
XP_016278122.1_PREDICTED_free_fatty_acid_receptor_2_Monodelphis
XP_020833122.1_LOW_QUALITY_PROTEIN_free_fatty_acid_receptor_2_Ph
XP_027711111.1_free_fatty_acid_receptor_2_Vombatus_ursinus
XP_005314353.1_free_fatty_acid_receptor_3-like_Chrysemys_picta_b
XP_006034574.1_free_fatty_acid_receptor_2-like_Alligator_sinensi
XP_006276909.1_PREDICTED_free_fatty_acid_receptor_2_Alligator_mi
XP_006034573.3_free_fatty_acid_receptor_2-like_Alligator_sinensi
XP_014457957.1_PREDICTED_free_fatty_acid_receptor_2_Alligator_mi
XP_019348779.1_PREDICTED_LOW_QUALITY_PROTEIN_free_fatty_acid_rec
XP_018098244.2_free_fatty_acid_receptor_2_Xenopus_laevis
XP_032084228.1_free_fatty_acid_receptor_2-like_Thamnophis_elegan
XP_032083600.1_free_fatty_acid_receptor_2-like_Thamnophis_elegan
XP_003225138.1_PREDICTED_free_fatty_acid_receptor_2-like_Anolis
XP_016851582.1_PREDICTED_LOW_QUALITY_PROTEIN_free_fatty_acid_rec
XP_003225140.2_PREDICTED_free_fatty_acid_receptor_2_Anolis_carol
XP_006011226.1_PREDICTED_free_fatty_acid_receptor_3-like_Latimer
XP_005995728.1_PREDICTED_free_fatty_acid_receptor_2-like_Latimer
XP_039626507.1_free_fatty_acid_receptor_3-like_Polypterus_senega
XP_005312792.1_free_fatty_acid_receptor_2-like_Chrysemys_picta_b
XP_032083598.1_free_fatty_acid_receptor_3-like_Thamnophis_elegan
XP_008115500.1_PREDICTED_free_fatty_acid_receptor_2_Anolis_carol
XP_041427634.1_free_fatty_acid_receptor_2_Xenopus_laevis
XP_041426003.1_free_fatty_acid_receptor_2-like_Xenopus_laevis
XP_020381493.2_free_fatty_acid_receptor_2-like_Rhincodon_typus
XP_005995736.2_PREDICTED_free_fatty_acid_receptor_2-like_Latimer
XP_039626509.1_free_fatty_acid_receptor_3-like_Polypterus_senega
XP_029587278.1_free_fatty_acid_receptor_3-like_Salmo_trutta
XP_029593446.1_free_fatty_acid_receptor_2-like_Salmo_trutta
XP_029593608.1_free_fatty_acid_receptor_2-like_isoform_X1_Salmo
XP_017206899.1_free_fatty_acid_receptor_3-like_Danio_rerio
XP_029587273.1_free_fatty_acid_receptor_3-like_Salmo_trutta
XP_029593598.1_free_fatty_acid_receptor_2-like_Salmo_trutta
XP_029593272.1_free_fatty_acid_receptor_2-like_Salmo_trutta
XP_021322753.1_free_fatty_acid_receptor_3-like_Danio_rerio
0.4

Figure 4.6. Conservation of amino acid residues critically involved in the mammalian FFAR1 binding pocket in protein sequences extrapolated from genome sequences of FFAR1 and neighbouring FFAR-like genes across vertebrates. Amino acids identified as critical for ligand binding (Hudson et al., 2014; Moniri, 2016) are highlighted in green.

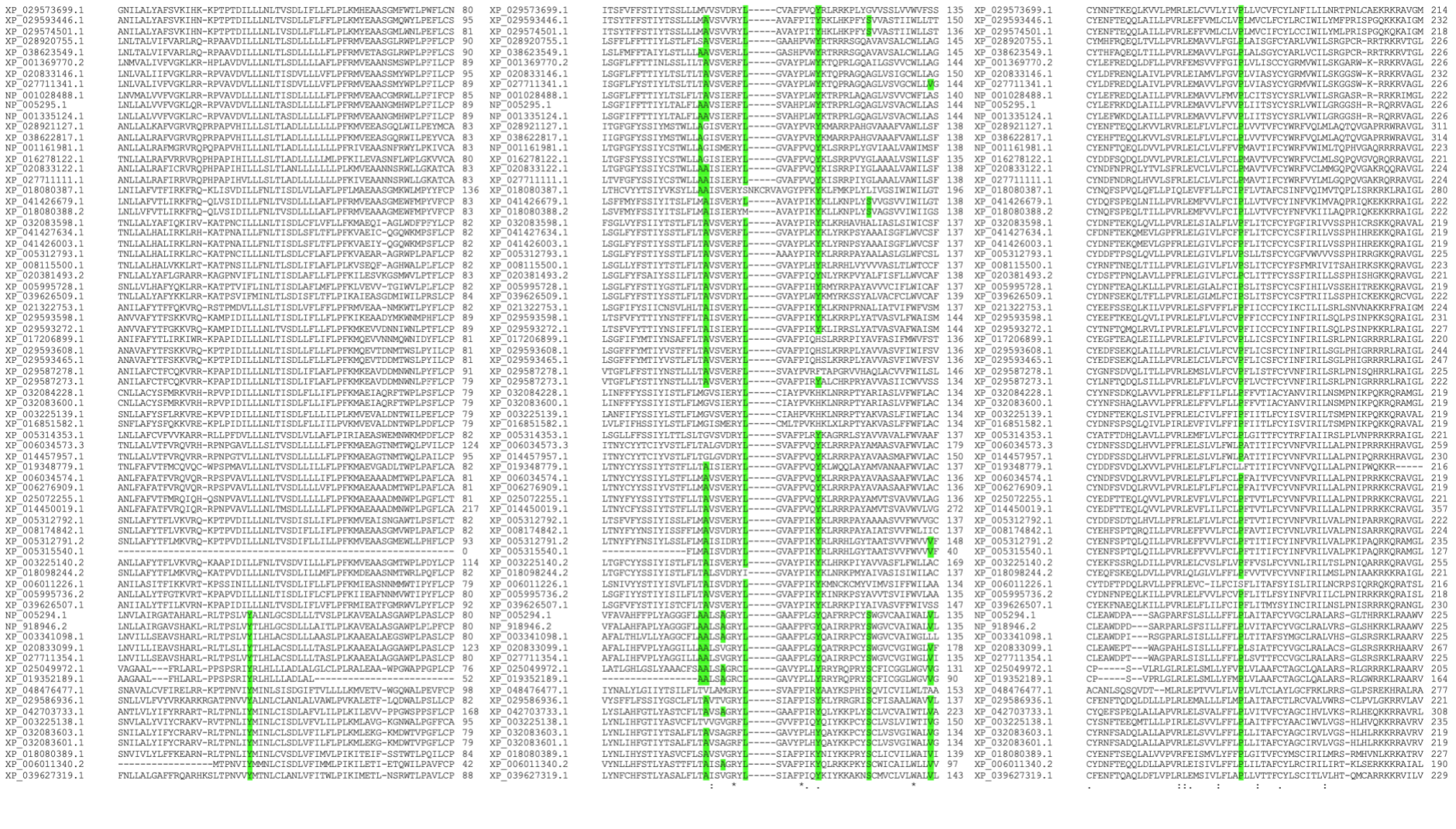

Figure 4.7. Genome sequence-derived microsynteny analysis of the *ffar4* locus in select Elasmobranchii + Actinopterygii (A) and Sarcopterygii (B). The *ffar4* gene is indicated in red. All synteny information was retrieved from Pubmed NCBI and Ensembl.

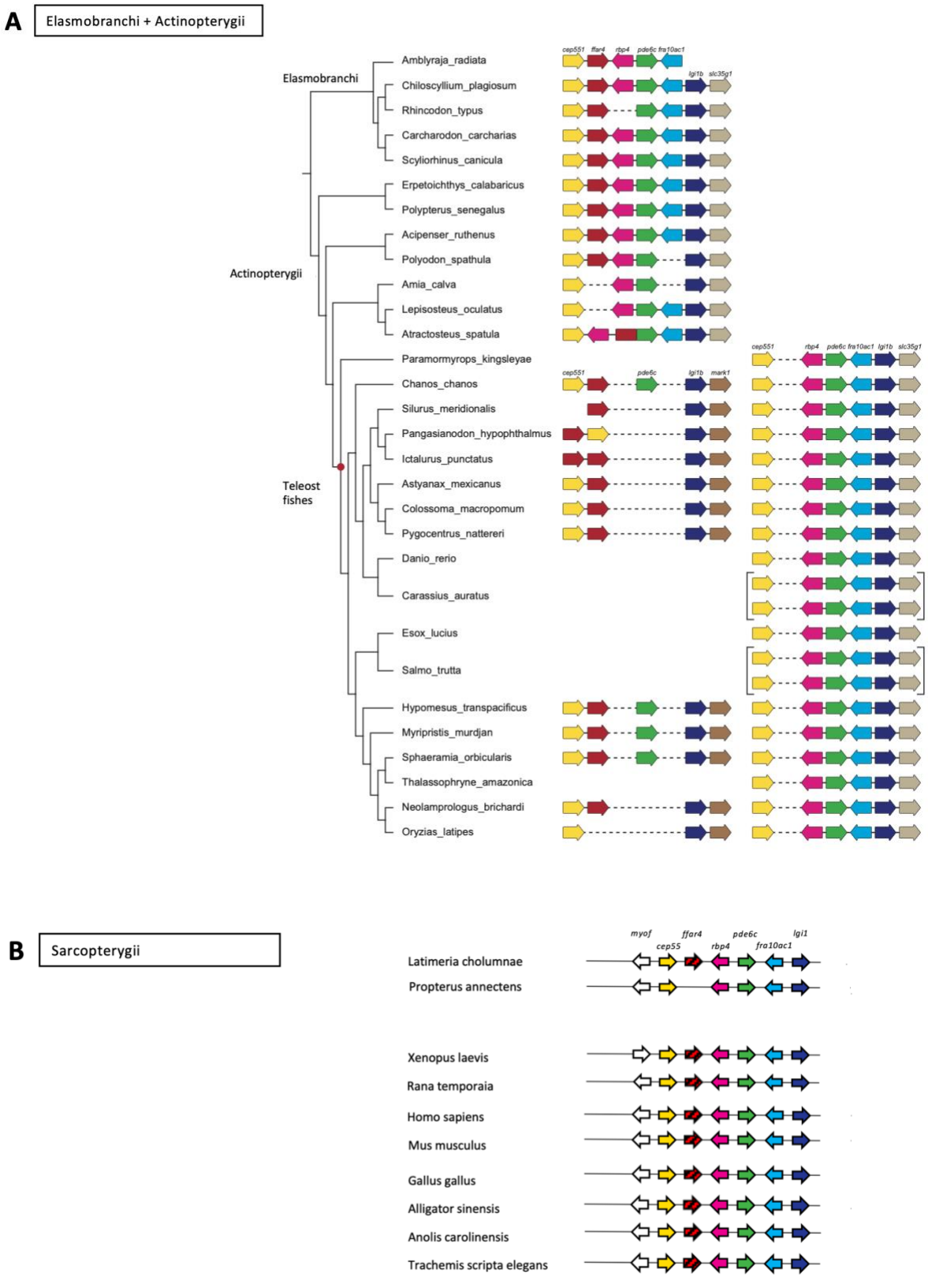
A
Elasmobranchi + Actinopterygii
Elasmobranchi
Actinopterygii
Teleost fishes
Amblyraja_radiata
Chiloscyllium_plagiosum
Rhincodon_typus
Carcharodon_carcharias
Scyliorhinus_canicula
Erpetoichthys_calabaricus
Polypterus_senegalus
Acipenser_ruthenus
Polyodon_spathula
Amia_calva
Lepisosteus_oculatus
Atractosteus_spatula
Paramormyrops_kingsleyae
Chanos_chanos
Silurus_meridionalis
Pangasianodon_hypophthalmus
Ictalurus_punctatus
Astyanax_mexicanus
Colossoma_macropomum
Pygocentrus_nattereri
Danio_rerio
Carassius_auratus
Esox_lucius
Salmo_trutta
Hypomesus_transpacificus
Myripristis_murdjan
Sphaeramia_orbicularis
Thalassophryne_amazonica
Neolamprologus_brichardi
Oryzias_latipes
cep551
ffar4
rbp4
pde6c
fra10ac1
lgi1b
slc35g1
mark1
B
Sarcopterygii
myof
cep55
lgi1
Latimeria cholumnae
Propterus annectens
Xenopus laevis
Rana temporaia
Homo sapiens
Mus musculus
Gallus gallus
Alligator sinensis
Anolis carolinensis
Trachemis scripta elegans

Figure 4.8. Genome-derived amino acid sequences of FFAR4 from fish and other vertebrates. All sequences were retrieved form Pubmed NCBI and aligned using ClustalOmega. Amino acids identified as critical for ligand binding (Hudson et al., 2014; Moniri, 2016) are highlighted in green.

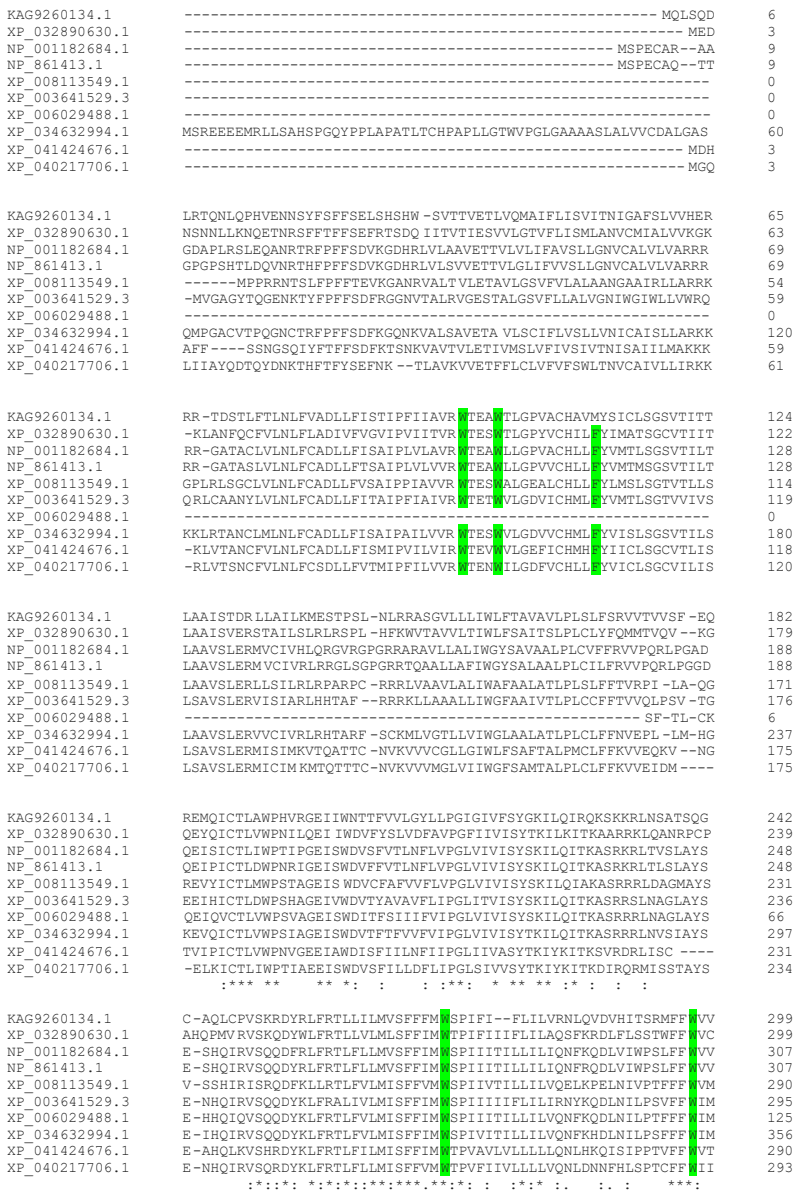

Figure 4.9. Phylogenetic analysis of *ffar4* (A) and neighbouring genes *rbp4* (B) *cep551* (C) and *Igilb* (D) in relevant loci in key fish species.

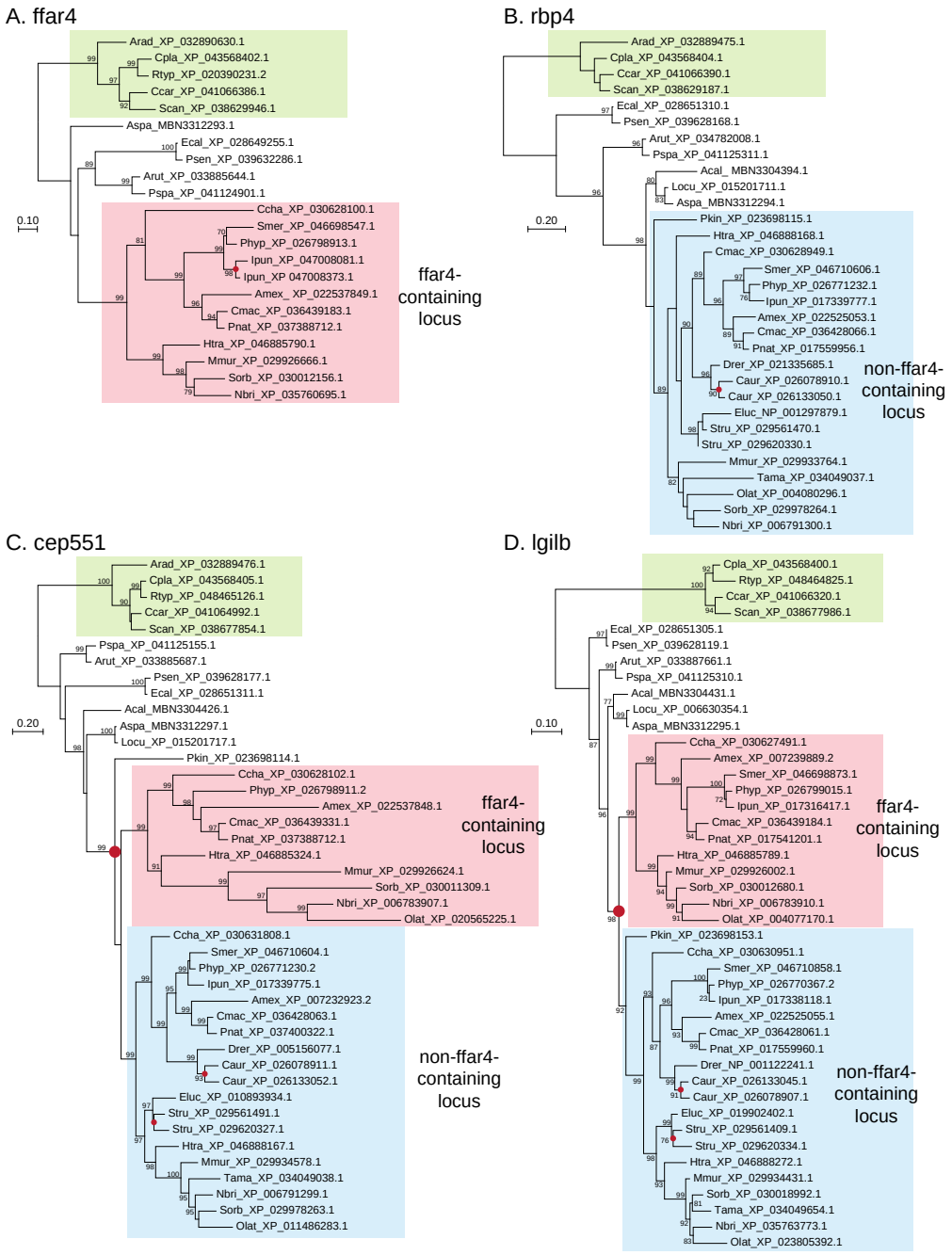

Novel insights into G-protein coupled receptors may explain hyperlipolysis in rainbow trout

Changes in organismal lipolytic flux capacity in rainbow trout treated with exogenous lactate (Chapter 2) and Intralipid (Chapter 3) contrast greatly with the well-known anti-lipolytic effect of lactate and LCFAs reported in mammalian adipose tissue (Brooks et al., 2022; Husted et al., 2020). By measuring *in vivo* lipolytic rate and using *real-time* RT-PCR, I have provided evidence for a major functional difference between fish and mammals with respect to the physiological role of lactate as a signal. Moreover, by assessing microsynteny, amino acid conservation and critical residues in the binding of *ffar4*, I have provided evidence for the absence of *ffar4* in the rainbow trout genome, contrary to reports in the literature. Despite transcriptional suppression of lipolytic genes (Chapter 3), the phosphorylation status of ATGL and HSL is currently unknown in hyperlipidemic trout. Given that mammals use FFAR4 to mediate autocrine negative feedback suppression of lipolysis via ATGL and HSL (London et al., 2020), it is clear such mechanistic controls could not exist in trout. Overall, the lack of HCAR1 signaling and the absence of *ffar4* in the rainbow trout genome may give insights into the high lipolytic inertia characteristic of rainbow trout, while mammals modulate lipolytic rate to meet energy expenditures.

Limitations

While in this thesis, changes in carbohydrate and lipid metabolic pathways by lactate and Intralipid infusion were identified, several limitations should be acknowledged. Firstly, while I show that lactate and LCFAs, which induce lipolytic suppression in mammalian tissues, did not decrease R_a glycerol, the question of

whether this lack of anti-lipolytic effect is a result of the PKA signaling pathway cannot be determined by this experimental approach. Additionally, emerging research on guanylyl cyclase, phosphodiesterase and adipokine regulation of energy-expenditure and secondary inflammatory responses cannot be excluded (Al Mahri et al., 2022; Ceddia and Collins, 2020; Liu et al., 2022; Tang et al., 2021). Secondly, while I show changes in R_a glucose and R_a glycerol in response to exogenous lactate and Intralipid, differences in R_a (rate of appearance) and R_d (rate of disappearance) for both metabolites could not be quantified statistically due to high variability between individuals. However, these changes are distinguishable qualitatively when compared to changes in circulating concentration.

Integrating whole-body fluxes with measurements of gene expression, protein abundance and enzyme activities, help us to understand the underlying mechanisms that lead to the observed changes in energy metabolism. However, a limitation of this experimental approach is that parameters for tissue measurement analysis were only assessed prior to and following the 3 h lactate (Chapter 2) or 4 h Intralipid (Chapter 3) infusion. Changes in transcript abundance represent a delayed induction of metabolic pathways due to slow transcriptional processes. Conversely, changes in activity or translation (protein abundance) are more rapidly induced by post-translational modifications (covalent modifications or allosteric regulation) (Yu et al., 2021). With regard to experimental design, tissue measurements from two time points may not capture changes in complex transcriptional, translational and post-translational processes, especially given transcript half-life and allosteric regulation varies between genes and gene products, respectively (Chan et al., 2018; Yu et al., 2021). Additionally,

emerging epigenetic regulation of metabolism including deoxyribonucleic acid (DNA) methylation and histone modifications cannot be excluded (Farhat et al., 2022).

Future directions and final remarks

The scope of this thesis was to investigate how key carbohydrate and lipid metabolic pathways regulate *in vivo* fuel mobilization in adult rainbow trout. However, it is clear from previous research that in mammals, GPRs play an essential role in regulating energy metabolism (Ahmed et al., 2010; Chen et al., 2021; Husted et al., 2020). Therefore, studies are clearly required and should prioritize the precise localization of these GPRs in trout tissues and their functional involvement in the metabolic fuel selection of this freshwater species. Given the well-characterized mammalian GPR-PKA signaling cascade (Ahmed et al. 2010; Chen et al., 2021; Mizuta et al., 2019) and conserved critical residue of trout *hcar1* and *ffar1*, the functional probing of this pathway is warranted. It is unclear whether the lack of anti-lipolytic effects (Chapter 2) and induced anti-lipogenic effects (Chapter 3) are caused by PKA dephosphorylation via HCAR1 and FFAR1, respectively. Additionally, in mammals, FFAR1 plays a significant role in regulating glucose-stimulated insulin secretion in acute and long-term exposure (Kristinsson et al., 2013). The complete functional probing of the PKA signaling cascade using cultured cells (adipocytes, myocytes and hepatocytes) and well-established PKA inhibitor peptides (Liu et al., 2020; London et al., 2020), should reveal the involvement of PKA dephosphorylation in trout lipolysis, lipogenesis and insulin secretion. In addition to regulating lipid mobilization circulating lactate, as a metabolic product of anaerobic glycolysis, is essential in tissue regeneration and neuronal cell proliferation via the HCAR1 signaling pathway in mammals (Kennedy et

al., 2022). The unorthodox HCAR1 signaling of rainbow trout (Chapter 2) may give insights into their hypoxia intolerance (Omlin et al., 2010; Thomsen et al., 2019), while research focused on hypoxic tolerant species should further our understanding of the role of HCAR1 signaling during tissue repair and regeneration. Thus, future studies are required to determine (i) the precise localization of this receptor in the brain and (ii) the cellular role of this receptor as a key transcription regulator of pathways promoting tissue regeneration in hypoxic tolerant (goldfish and naked mole rats) (Farhat et al., 2021a; Farhat et al., 2021b) and intolerant (rainbow trout) species.

This thesis is the first to quantify the effects of lactate or Intralipid on *in vivo* energy mobilization in rainbow trout and provides important insights into potential mechanisms governing hyperlipolysis in this aquaculture species. In this thesis, I show that lactate is a preferred metabolic fuel and HCAR1 signaling is likely weak in trout (Chapter 2). I also show that elevated FA concentration and decreased n-3 content (by Intralipid) strongly induced lipolysis, while transcriptional induction of gluconeogenesis compensates for the acute reduction in hepatic glucose production (Chapter 3). Finally, in Chapter 4, I identify the presence (*hcar1* and *ffar1*) and unique absence (*ffar4*) of key GPRs genes important to metabolic signaling. Overall, the unique metabolic regulation in this freshwater species makes it a useful comparative model to study fuel mobilization and metabolic signaling, especially in the context of aquaculture.

SUPPLEMENTAL

Table S2.1. *Real-time* RT-PCR primer sequences and reaction parameters of gene targets involved in glucose transport (*glut4a* and *glut4b*), glycolysis (*gcka* and *gckb*) and gluconeogenesis (*pck1, pck2a, pck2b, g6pca, g6pb1a* and *g6pb1b*).

Gene target	Primer pair (5' to 3')	Tissue	Annealing temperature (°C); Efficiency (%); R^2	Reference
glut4a	F: CATCTTTGCAGTGCTCCTTG R: CAGCTCTGTACTCTGCTTGC	Red muscle White muscle	56; 104.7; 0.997 57; 101.8; 0.992	Liu et al., 2017
glut4b	F: TCGGCTTTGGCTTCCAATATG R: GTTTGCTGAAGGTGTTGGAG	Red muscle White muscle	57; 107.3; 0.968 56; 106.4; 0.987	Liu et al., 2017
gka	F: CTGCCCACCTACGTCTGT R: GTCATGGCGTCCTCAGAGAT	Liver	54; 101.8; 0.964	Designed
gkb	F: TCTGTGCTAGAGACAGCCC R: CATTTTGACGCTGGACTCCT	Liver	56; 104.0; 0.995	Designed
pck1	F: ACAGGGTGAGGCAGATGTAGG R: CTAGTCTGTGGAGGTCTAAGGGC	Liver	55; 100.4; 0.992	Marandel et al., 2015
pck2a	F: ACAATGAGATGATGTGACTGCA R: TGCTCCATCACCTACAACCT	Liver	55; 101.8; 0.987	Marandel et al., 2015
pck2b	F: AGTAGGAGCAGGGACAGGAT R: CCGTTCAGCAAAGGTTAGGC	Liver	55; 102.5; 0.968	Marandel et al., 2015
g6pca	F: GATGGCTTGACGTTCTCCT R: AGATCCAGGAGAGTCCTCC	Liver	55; 99.8; 0.992	Marandel et al., 2015
g6pcb1a	F: GCAAGGTCCAAAGATCAGGC R: GCCAATGTGAGATGTGATGGG	Liver	59; 106.5; 0.983	Marandel et al., 2015
g6pcb1b	F: GCTACAGTGCTCTCCTTCTG R: TCACCCCATAGCCCTGAAA	Liver	55; 108.7; 0.991	Marandel et al., 2015

Table S2.2. *Real-time* RT-PCR primer sequences and reaction parameters of gene targets involved in lipolytic regulation (*hcar1*, *hsl* and *lpl*), fatty acid oxidation (*cpt1a* and *hoad*), transport (*cd36*) and synthesis (*fas* and *srebp1c*) in hyperlactatemic rainbow trout.

Gene target	Primer pair (5' to 3')	Tissue	Annealing temperature (°C); Efficiency (%); R^2	Reference
hcar1	F: CGGCTTATGCTGTTCCTGTT R: GCCCATCCTGTTGATCTTGT	Liver Red muscle White muscle	63; 107.3; 0.995 64; 92.8; 0.950 64; 107.8; 0.951	Designed
hsl	F: TGCCTTCCTGTACTCGCAAG R: GCAAGAAAGGCAAGGGTGTT	Liver Red muscle White muscle	55; 96.7; 0.984 55; 102.2; 0.989 55; 100.1; 0.990	Kostyniuk et al., 2019b
lpl	F: ACATGAGCCGGAAAGAGAAA R: GGTTGGGAGGCAGAACATAC	Liver Red muscle White muscle	60; 106.6; 0.991 60; 103.2; 0.950 60; 99.0; 0.972	Designed
cd36	F: GATTCTCTGCGCCCATCTAC R: GGGTTCTTCCACGACTCAAA	Liver Red muscle White muscle	60; 104.7; 0.954 60; 102.0; 0.983 62; 94.7; 0.994	Designed
hoad	F: GGACAAAGTGGCACCAGCAC R: GGGACGGGGTTGAAGAAGTG	Liver Red muscle White muscle	60; 104.4; 0.989 60; 107.3; 0.991 59; 103.3; 0.983	Polakof et al., 2010
cpt1a	F: TCGATTTTCAAGGGTCTTCG R: GGTGAAACGACTAGCAACAC	Liver Red muscle White muscle	61; 98.2; 0.989 61; 108.2; 0.993 61; 108.7; 0.989	Kostyniuk et al., 2019a
fas	F: TGATCTGAAGGCCCGTGTCA R: TATGGTGCGTTGCAGTGGG	Liver	58; 106.3; 0.985	Kostyniuk et al., 2019a
srebp1c	F: GACAAGGTGGTCCCAGTTGCT R: CACACGTTAGTCCGCATCAC	Liver	54; 95.1; 0.984	Kostyniuk et al., 2019a

Table S3.1. *Real-time* RT-PCR primer sequences and reaction parameters of gene targets involved in glucose transport (*glut4a* and *glut4b*), glycolysis (*gcka* and *gckb*) and gluconeogenesis (*pck1, pck2a, pck2b, g6pca, g6pb1a* and *g6pb1b*) in hyperlactatemic rainbow trout.

Gene target	Primer pair (5' to 3')	Tissue	Annealing temperature (°C); Efficiency (%); R^2	Reference
glut4a	F: CATCTTTGCAGTGCTCCTTG R: CAGCTCTGTACTCTGCTTGC	Red muscle White muscle Adipose	56; 104.6; 0.997 57; 101.8; 0.992 56; 94.2; 0.988	Lui et al., 2017
glut4b	F: TCGGCTTTGGCTTCCAATATG R: GTTTGCTGAAGGTGTTGGAG	Red muscle White muscle Adipose	57; 107.3; 0.968 56; 106.4; 0.987 57; 98.4; 0.998	Lui et al., 2017
gka	F: CTGCCCACCTACGTCTGT R: GTCATGGCGTCCTCAGAGAT	Liver	54; 101.8; 0.964	Designed
gkb	F: TCTGTGCTAGAGACAGCCC R: CATTTTGACGCTGGACTCCT	Liver	56; 104.0; 0.995	Designed
pck1	F: ACAGGGTGAGGCAGATGTAGG R: CTAGTCTGTGGAGGTCTAAGGGC	Liver	55; 100.2; 0.999	Marandel et al., 2015
pck2a	F: ACAATGAGATGATGTGACTGCA R: TGCTCCATCACCTACAACCT	Liver	55; 101.9; 0.999	Marandel et al., 2015
pck2b	F: AGTAGGAGCAGGGACAGGAT R: CCGTTCAGCAAAGGTTAGGC	Liver	55; 102.5; 0.981	Marandel et al., 2015
g6pca	F: GATGGCTTGACGTTCTCCT R: AGATCCAGGAGAGTCCTCC	Liver	55; 99.8; 0.992	Marandel et al., 2015
g6pcb1a	F: GCAAGGTCCAAAGATCAGGC R: GCCAATGTGAGATGTGATGGG	Liver	59; 105.4; 0.995	Marandel et al., 2015
g6pcb1b	F: GCTACAGTGCTCTCCTTCTG R: TCACCCCATAGCCCTGAAA	Liver	55; 108.6; 0.995	Marandel et al., 2015

Table S3.2. *Real-time* RT-PCR primer sequences and reaction parameters of gene targets involved in TAG breakdown (*hsl, lpl, atgl* and *plin1*) and synthesis (*mgat1* and *dgat2*), fatty acid oxidation (*cpt1a* and *hoad*), transport (*cd36*) and synthesis (*fas* and *srebp1c*) in Intralipid-infused rainbow trout.

Gene target	Primer pair (5' to 3')	Tissue	Annealing temperature (°C); Efficiency (%); R^2	Reference
hsl	F: TGCCTTCCTGTACTCGCAAG R: GCAAGAAAGGCAAGGGTGTT	Liver Red muscle White muscle Adipose	55; 96.7; 0.984 55; 102.2; 0.989 55; 100.1; 0.990 55; 102.7; 0.987	Kostyniuk et al., 2019b
lpl	F: ACATGAGCCGGAAAGAGAAA R: GGTTGGGAGGCAGAACATAC	Liver Red muscle White muscle Adipose	60; 106.6; 0.991 60; 103.2; 0.950 60; 99.0; 0.972 60; 102.5; 0.986	Designed
atgl	F: TCCAAGGAGTGCGTTATGTG R: TCGTGGAAGTTGAAGGAGGT	Adipose	59; 105.8; 0.997	Designed
plin1	F: GGGAGGAGCAGAGAGACAAA R: AGATGCTGTTCACCACACGA	Adipose	60; 99.8; 0.989	Designed
dgat2	F: CTTTGGGGAGAACGATGTGT R: ATGGTGGTGATGGGTTTGTT	Adipose	59; 105.2; 0.996	Designed
mgat1	F: TGACCCTTCCTCTGCTCTGT R: GTTGAGCGGGATATTCAAGG	Adipose	60; 105.9; 0.994	Designed
cd36	F: GATTCTCTGCGCCCATCTAC R: GGGTTCTTCCACGACTCAAA	Liver Red muscle White muscle Adipose	60; 101.4; 0.958 60; 92.8; 0.998 62; 94.7; 0.994 62; 92.6; 0.989	Designed
hoad	F: GGACAAAGTGGCACCAGCAC R: GGGACGGGGTTGAAGAAGTG	Liver Red muscle White muscle	60; 104.4; 0.989 60; 107.3; 0.999 59; 103.5; 0.999	Polakof et al., 2010
cpt1a	F: TCGATTTTCAAGGGTCTTCG R: GGTGAAACGACTAGCAACAC	Liver Red muscle White muscle	61; 98.2; 0.989 61; 108.2; 0.993 61; 108.7; 0.999	Kostyniuk et al., 2019a
fas	F: TGATCTGAAGGCCCGTGTCA R: TATGGTGCGTTGCAGTGGG	Liver Adipose	58; 108.4; 0.992 58; 109.0; 0.996	Kostyniuk et al., 2019a
srebp1c	F: GACAAGGTGGTCCCAGTTGCT R: CACACGTTAGTCCGCATCAC	Liver Adipose	54; 95.1; 0.984 58; 108.2; 0.991	Kostyniuk et al., 2019a

Table S3.3. Intralipid fatty acid composition of the three lipids classes (NL, PL, NEFA). Composition is expressed as a percentage of total fatty acids within each class. Total fatty acid concentration (μmol ml^{-1}) is also presented.

Fatty acids	NL	PL	NEFA
16:0	11.4 ± 2.8	34.2 ± 1.7	**–**
18:0	**–**	21.9 ± 2.4	**–**
18:1	27.3 ± 1.0	23.1 ± 1.5	30.1 ± 1.1
18:2	53.6 ± 5.6	15.8 ± 1.4	48.9 ± 2.5
20:0	5.4 ± 0.5	**–**	6.0 ± 0.2
20:4	**–**	5.7 ± 0.1	3.1 ± 0.6
20:5	**–**	**–**	4.5 ± 0.3
22:1	**–**	**–**	1.7 ± 0.3
22:3	**–**	**–**	4.0 ± 0.3
22:6	**–**	**–**	1.7 ± 0.1
Total [FA]	223.6 ± 24.7	8.8 ± 1.8	19.8 ± 4.5

Values are means ± s.e.m (N=5). Neutral lipids: NL; phospholipids: PL; non-esterified fatty acids: NEFA.

Table S3.4. Composition of the total fatty acids from trout plasma expressed as a percentage of total fatty acids. Total fatty acid concentration (μmol ml^{-1}) is also presented.

Fatty acids	0h	1h	2h	3h	4h
16:0	25.5 ± 3.6	22.3 ± 3.4	22.1 ± 3.6	23.7 ± 3.9	24.1 ± 5.9
16:1	1.0 ± 0.3	0.9 ± 0.4	0.9 ± 0.3	1.3 ± 0.5	1.1 ± 0.4
18:0	10.9 ± 2.5	9.4 ± 2.2	8.4 ± 1.9	8.1 ± 1.6	9.2 ± 2.7
18:1	15.4 ± 2.6	16.5 ± 2.5	17.9 ± 3.0	18.8 ± 3.7	19.2 ± 4.2
18:2	5.1 ± 1.0	9.6 ± 1.7	11.7 ± 2.2	12.5 ± 2.5	13.5 ± 2.5
20:0	0.2 ± 0.1	0.8 ± 0.2	1.0 ± 0.3	1.1 ± 0.3	1.2 ± 0.3
20:1	1.3 ± 0.2	1.2 ± 0.2	1.1 ± 0.2	1.3 ± 0.3	1.2 ± 0.3
20:2	0.9 ± 0.2	1.3 ± 0.3	1.1 ± 0.3	1.2 ± 0.3	1.2 ± 0.4
20:3	1.75 ± 0.3	1.6 ± 0.2	1.5 ± 0.2	1.5 ± 0.3	2.0 ± 0.9
20:4	2.9 ± 0.4	2.9 ± 0.3	2.7 ± 0.3	2.5 ± 0.3	2.4 ± 0.7
20:5	4.5 ± 0.6	4.2 ± 0.5	4.0 ± 0.6	3.6 ± 0.6	3.2 ± 0.8
22:3	1.4 ± 0.2	1.3 ± 0.2	1.2 ± 0.2	1.2 ± 0.2	1.0 ± 0.3
22:5	1.5 ± 0.2	1.5 ± 0.2	1.4 ± 0.2	1.2 ± 0.2	1.2 ± 0.4
22:6	25.6 ± 3.3	24.3 ± 2.2	23.0 ± 3.1	20.5 ± 2.9	18.1 ± 5.1
24:0	1.6 ± 0.2	1.6 ± 0.2	1.6 ± 0.2	1.3 ± 0.1	1.2 ± 0.3
Total [FA]	12.6 ± 2.0	14.0 ± 2.1	15.6 ± 2.6	17.1 ± 3.0	16.5 ± 4.3

Values are means ± s.e.m (N=11). Individual fatty acids accounting for <1% are not included.

Table S3.5. Composition of the neutral lipids (NLs) from trout plasma expressed as a percentage of total fatty acids.

Fatty acids	0h	1h	2h	3h	4h
16:0	15.1 ± 2.0	12.1 ± 1.1	12.2 ± 0.6	13.5 ± 0.8	12.4 ± 0.8
16:1	2.3 ± 0.9	1.1 ± 0.5	1.8 ± 0.5	1.8 ± 0.5	1.6 ± 0.5
18:0	8.9 ± 2.8	6.8 ± 2.4	6.0 ± 1.6	6.3 ± 1.5	5.2 ± 0.9
18:1	38.1 ± 3.0	31.6 ± 2.1	31.6 ± 1.5	31.4 ± 1.4	31.2 ± 2.0
18:2	8.0 ± 0.5	26.2 ± 2.1	29.3 ± 2.4	28.3 ± 2.0	29.5 ± 2.2
20:0	1.3 ± 0.4	3.3 ± 0.2	3.6 ± 0.2	3.5 ± 0.2	3.4 ± 0.4
20:1	4.2 ± 0.4	2.4 ± 0.2	2.2 ± 0.2	3.3 ± 1.4	2.8 ± 0.7
20:2	0.2 ± 0.2	5.4 ± 1.4	4.6 ± 1.5	3.3 ± 0.9	4.5 ± 1.4
20:5	3.3 ± 0.5	2.2 ± 0.4	2.0 ± 0.3	1.5 ± 0.2	1.3 ± 0.3
22:0	1.0 ± 0.6	0.9 ± 0.6	0.6 ± 0.4	1.5 ± 0.9	0.4 ± 0.2
22:1	3.0 ± 0.2	1.9 ± 0.7	0.9 ± 0.4	0.7 ± 0.3	0.3 ± 0.2
22:6	11.4 ± 1.1	6.0 ± 0.7	4.8 ± 0.5	4.4 ± 0.6	3.6 ± 0.6

Values are means ± s.e.m (N=11). Individual fatty acids accounting for <1% are not included.

Table S3.6. Composition of the phospholipids (PLs) from trout plasma expressed as a percentage of total fatty acids.

Fatty acids	0h	1h	2h	3h	4h
16:0	24.1 ± 0.6	22.8 ± 0.9	23.3 ± 1.0	24.9 ± 0.4	24.4 ± 0.8
16:1	1.0 ± 0.2	0.8 ± 0.2	0.8 ± 0.2	1.0 ± 0.3	0.9 ± 0.2
18:0	6.8 ± 0.5	7.2 ± 0.4	7.7 ± 0.6	7.6 ± 0.3	7.8 ± 0.4
18:1	13.2 ± 0.4	13.4 ± 0.2	14.2 ± 0.3	14.9 ± 0.2	15.0 ± 0.2
18:2	5.0 ± 0.2	5.5 ± 0.1	6.1 ± 0.1	6.6 ± 0.1	6.9 ± 0.2
20:1	1.3 ± 0.1	1.3 ± 0.1	1.0 ± 0.2	1.1 ± 0.1	1.0 ± 0.1
20:2	1.0 ± 0.1	1.0 ± 0.1	0.8 ± 0.2	0.8 ± 0.1	0.8 ± 0.1
20:3	2.2 ± 0.1	2.1 ± 0.1	2.1 ± 0.1	2.0 ± 0.1	1.9 ± 0.1
20:4	3.5 ± 0.1	3.7 ± 0.2	3.8 ± 0.2	3.7 ± 0.1	3.9 ± 0.2
20:5	5.3 ± 0.2	5.2 ± 0.2	4.9 ± 0.2	4.6 ± 0.2	4.6 ± 0.2
22:3	1.6 ± 0.1	1.6 ± 0.1	1.4 ± 0.2	1.6 ± 0.1	1.5 ± 0.1
22:5	1.9 ± 0.1	2.0 ± 0.1	1.9 ± 0.2	1.7 ± 0.1	1.8 ± 0.1
22:6	31.1 ± 0.8	31.0 ± 1.0	29.8 ± 0.9	27.8 ± 0.6	27.6 ± 0.9
24:0	2.0 ± 0.1	2.1 ± 0.1	2.1 ± 0.1	1.9 ± 0.1	1.9 ± 0.1

Values are means ± s.e.m (N=11). Individual fatty acids accounting for <1% are not included.

Table S3.7. Composition of the non-esterified fatty acids (NEFAs) from trout plasma expressed as a percentage of total fatty acids.

Fatty acids	0h	1h	2h	3h	4h
16:0	43.3 ± 5.0	25.6 ± 5.4	24.1 ± 5.0	33.1 ± 4.5	31.9 ± 1.7
18:0	31.3 ± 5.5	16.9 ± 5.6	14.0 ± 4.7	12.3 ± 3.4	15.7 ± 4.7
18:1	15.3 ± 3.8	22.4 ± 3.9	24.5 ± 3.9	22.4 ± 3.2	22.8 ± 2.9
18:2	4.1 ± 2.0	21.6 ± 3.9	25.9 ± 3.5	26.6 ± 3.5	22.5 ± 2.3
20:0	1.2 ± 0.7	4.8 ± 0.9	4.6 ± 0.8	4.7 ± 1.4	3.8 ± 0.4
22:6	1.6 ± 0.8	2.1 ± 0.9	3.1 ± 2.4	0.3 ± 0.3	0.5 ± 0.3

Values are means ± s.e.m (N=11). Individual fatty acids accounting for <1% are not included.

APPENDIX

Prior to pivoting my research to study fuel selection in rainbow trout, I aimed to use the same integrative approach to investigate the effects of amino acids on glucose regulation and metabolism. I proposed to use a novel technique in fish to inhibit the insulin signaling cascade using the mammalian insulin receptor antagonist, S961 (Vikram and Jena, 2010). The complete functional probing of the insulin signaling cascade would identify how amino acids affect glucose fluxes and potential mechanisms that could explain the observed changes in glucose fluxes. Preliminary experiments included testing the efficacy of S961 as an insulin receptor antagonist in rainbow trout. My findings are summarized in the following manuscript.

The mammalian insulin antagonist S961 does not exhibit insulin receptor antagonism in rainbow trout *in vivo*

This is based on a manuscript titled “The mammalian insulin antagonist S961 does not exhibit insulin receptor antagonist in rainbow trout *in vivo*”

Written by
Giancarlo Talarico, Mélissa Grégoire, Jean-Michel Weber and Jan A. Mennigen

Biology Department, University of Ottawa, Canada

Submitted to
Journal of Fish Biology, under review

Author contributions: G.G.M.T., J.-M.W. and J.A.M. conception; G.G.M.T. and M.G. investigation and data curation; G.G.M.T., J.-M.W. and J.A.M. formal analysis of research and prepared figures; G.G.M.T. and J.A.M. drafted the manuscript; G.G.M.T., J.-M.W. and J.A.M. edited, revised and approved the manuscript.

Abstract

Due to their ‘glucose intolerance’, rainbow trout have been the focus of comparative studies probing the role of insulin, an important glucoregulatory hormone, and its interaction with macronutrients at the organismal, tissue and molecular level. A limiting factor is a current lack of reliable assays to quantify circulating, bioactive insulin. To circumvent this limitation, tissue-specific responsiveness to postprandial or exogenous insulin has been quantified. These studies revealed that cell signaling proteins and their post-translational modifications are evolutionarily conserved and thus provide useful and quantifiable proxy indices to investigate insulin function in rainbow trout. While specific branches of the intracellular insulin signaling pathway have been successfully probed through pharmacological approaches, it would be useful to have a functionally validated insulin receptor antagonist to characterize the glucoregulatory role of insulin in its entirety. I used two separate *in vivo* experiments to test the ability of the mammalian insulin receptor antagonist, S961, to block insulin signaling in the liver and muscle in response to postprandial and exogenous insulin. I found that irrespective of dose concentration or experimental treatment, insulin signaling was not inhibited by S961, showing that its antagonistic effect on the mammalian insulin receptor does not extend to rainbow trout.

Introduction

Rainbow trout are an important freshwater aquaculture and recreational species, which has been introduced to almost every continent. The ‘glucose intolerant’ phenotype of carnivorous trout has been well described (Blasco et al., 1996; Polakof et al., 2012; Moon, 2001). The physiology of this species has been particularly well studied

because of its importance for aquaculture and angling (Cresswell, 1981; Fornshell, 2002) and its usefulness as a comparative model (Krishnan and Rohner, 2019). The comparative role of the glucoregulatory hormone, insulin, and its interaction with dietary macronutrients has been investigated in great detail (Forbes et al., 2019b; Polakof et al., 2010), but progress in fish has been hampered by the lack of a reliable assay to quantify circulating mature, and thus bioactive, insulin. While mammalian insulin is bioactive in fish, it is immunologically different, making it impossible to measure with commercially available mammalian RIAs (Plisetskaya, 1989). While studies using non-mammalian insulin RIAs revealed salmonids are not insulin deficient, it remains unknown whether released proinsulin contributes to measured concentrations and whether it is biologically active (Plisetskaya, 1998).

To probe piscine insulin function at the tissue level, the quantification of cell signaling pathways has proven a useful alternative to direct insulin concentration measurements (Plagnes-Juan et al., 2008; Seiliez et al., 2011a). Macronutrient-dependent regulation (Lansard et al., 2010; Seiliez et al., 2011a), time courses (Mennigen et al., 2012; Seiliez et al., 2011a) and downstream regulation of targets involved in glucoregulation (Blanco et al., 2020; Dai et al., 2013) have been investigated in diverse tissues such as the liver, muscle and brain. However, current approaches to block trout insulin signaling remain limited *in vivo*. When targeting only specific signaling branches, such as mTOR inhibition (Dai et al., 2013), highly conserved transcription factors, such as FoxO1 or GSK3 remain active. These proteins exert well-described roles in the mammalian regulation of hepatic gluconeogenic gene expression (Gross et al., 2008) and skeletal muscle glycogen synthase regulation and glucose clearance

(Henriksen and Dokken, 2006; Patel and Woodgett, 2017). The functional, *in vivo* validation of an insulin receptor antagonist in trout, would greatly improve the capacity for comparative mechanistic investigation of insulin function. The goal of this study is to examine the possibility to use the selective insulin receptor antagonist, S961, to induce insulin resistance in rainbow trout as previously shown in rodent models (Okamoto et al., 2017; Schäffer et al., 2008; Vikram and Jena, 2010).

Methods

Animals

Rainbow trout (*Oncorhynchus mykiss*), with a body mass of ~200g and a Fulton's condition factor K of 1.07 ± 0.02 (N=26) (Blackwell et al., 2000), were purchased from Linwood Acres Trout Farm (Campbellcroft, Ontario, Canada). They were randomly divided into experimental groups for two separate experiments. These experiments were designed to measure the efficacy of S961 as an insulin receptor antagonist testing the effects of (i) feeding status and endogenous insulin release (full factorial design N=4 experimental groups) and (ii) exogenous insulin (dose-response N=5 experimental groups). The fish were held in a 1,200 litre flow-through tank supplied with dechlorinated Ottawa tap water at 13°C, on a 12 h:12 h light-dark photoperiod and were fed commercial trout pellets (Zeigler Finfish Silver, Gardners, PA, USA) 5 days a week. They were acclimated to these conditions for a minimum of 3 weeks before experiments. All the procedures were approved by the Animal Care Committee of the University of Ottawa (Protocol #3407) and adhered to the guidelines established by the Canadian Council on Animal Care.

Feeding status experiment (series 1)

Physical characteristics and injection information of the four groups of rainbow trout (N=4) used in the feeding experiment are shown in Table 5.1. After acclimation, fish assigned to this experiment were further separated into four groups using a full-factorial experimental design to study the effects of S961 injected intraperitoneally (factor 1), feeding status (factor 2), and their interaction (factor 1 × factor 2) on postprandial activation of the hepatic and muscle insulin signaling pathway. All fish were fasted for 2 days to ensure the emptying of the digestive tract. Groups 1 and 2 were injected with Cortland saline 4 h prior to terminal anesthesia and tissue collection. Groups 3 and 4 were injected with S961 at a concentration of 0.01 μM kg^{-1} prior to terminal anesthesia and tissue collection. The concentration was chosen based on single intraperitoneal injection studies demonstrating functional insulin receptor antagonism in Sprague-Dawley rats and C57/BL6 mice (Vikram and Jena et al., 2010; Okamoto et al., 2017). Groups 2 and 4 were refed a single meal 4 h prior to terminal anesthesia and tissue collection to stimulate postprandial insulin release and cell signaling activation (Mennigen et al., 2012). In all cases, fish were anesthetized with 60 mg l^{-1} MS-222 buffered with 0.2 g l^{-1} $NaHCO_3$ and blood samples were collected using caudal puncture with heparinized syringes. Following blood sampling, fish were euthanized by spinal cord transection and feeding status was confirmed by the absence/presence of food pellets in the stomach and intestinal tract. Whole liver and muscle tissue (dissected along the lateral line) were collected and stored at -80°C until analysis. Plasma glucose concentrations were measured spectrophotometrically by

measuring the absorbance of NADH at 340 nm (Jubouri et al., 2021). The experimental design is summarized in Figure 5.1A.

Insulin infusion experiment (series 2)

Fish were anesthetized with 60 mg l^{-1} MS-222 buffered with 0.2 g l^{-1} $NaHCO_3$ and surgically fitted with a single catheter in the dorsal aorta as described in Haman and Weber, 1996. The catheter was kept patent by flushing with Cortland saline containing 50 U ml^{-1} heparin. After catheterization, the fish were left to recover overnight in a 90 litre swim-tunnel (Loligo Systems, Viborg, Denmark) where all measurements were carried out on resting animals kept at a water velocity of 0.5 body length per second. This weak current reduces stress and enhances the flow of water over the gills, but does not require swimming to maintain body position (Choi and Weber 2015). The swim tunnel was supplied with 13 °C aerated and dechlorinated Ottawa tap water. S961 was injected as a bolus at the start of each infusion and five different concentrations (0, 0.01, 0.1, 1 and 10 µM kg^{-1}; N=2 per group). Following, the S961 bolus injection, exogenous insulin was then administered continuously at ~1 ml h^{-1} (1.5 µg kg^{-1} min^{-1}; exact infusion rates were determined individually for each fish to correct for differences in body mass) (Forbes et al., 2019). A blood sample was taken at 0 h, prior to the S961 bolus injection and another following the 4 h insulin infusion (~400 µl each). The fish were euthanized by spinal cord transection. Whole liver and muscle tissue (dissected along the lateral line) were collected and stored at -80 °C until analysis. Plasma glucose concentrations were measured as previously described by Jubouri et al., 2021. The experimental design is summarized in Figure 5.1B. Physical characteristics and injection information of the 5 groups used in the insulin infusion experiment are shown in Table 5.2.

Western blot analysis of insulin signaling pathway

Total protein from the liver and muscle was extracted, quantified and prepared as previously described (Farhat et al., 2022). Proteins were migrated and blotted for 2 h at 100 V on nitrocellulose membrane (pore size 0.2 µm, Bio-Rad Laboratories, Hercules, CA, USA) in 20% Western transfer buffer. The membranes were incubated in Odyssey blocking buffer (LI-COR Biosciences, Lincoln, NE, USA) for 1 h at room temperature. Membranes were then incubated overnight at 4°C in rabbit-raised p-Akt (S473, Cell Signaling Technologies) and p-S6 (S235/236, Cell Signaling Technologies) antibodies. Membranes were washed and incubated with IRDye 800 CW goat-anti-rabbit secondary antibody (925-32211, LI-COR) for 1.5 h at room temperature, protected from light. Following incubation, the membranes were washed and visualized by infrared fluorescence using the Odyssey Imaging System (LI-COR Biosciences) (Farhat et al., 2022; Jubouri et al., 2021). Band intensity was quantified by Odyssey Infrared Imaging System software (v.3.0; LI-COR Biosciences). Both p-Akt and p-S6 protein intensity were normalized to rabbit β-tubulin (#2146; Cell Signaling Technologies) intensity and expressed as fold change compared with control groups for liver and muscle. The phosphorylated proteins p-Akt and p-S6 were targeted because they represent the active form of the proteins and are activated in response to insulin in trout liver and muscle tissue (Forbes et al., 2019b; Mennigen et al., 2012; Seiliez et al., 2008).

Glucose concentration analysis

Plasma glucose concentrations were measured spectrophotometrically using a Spectra Max Plus 384 Microplate Spectrophotometer (Molecular Devices, Sunnyvale, CA, USA). Plasma glucose concentration was determined with 7 U ml^{-1} HK and 0.1 U

ml^{-1} G6PDH (G5885, Sigma-Aldrich) in a buffer containing 60 mM Trizma base (T6066, Sigma-Aldrich), 40 mM Tris-HCl (TRS004, BioShop Canada Inc., Burlington, ON, Canada), 1.01 mM $MgSO_4$ (M7506, Sigma-Aldrich), 2.22 mM NAD^+ and 1.11 mM ATP. All concentrations were determined in duplicates by measuring the reduction of NAD^+ at 340 nm.

In silico characterization of rainbow trout insulin receptor paralogues

Gene sequence-derived insulin receptor amino acid sequences and gene location information were retrieved from Genome sequences deposited in Pubmed NCBI (www.pubmed/gene) for rainbow trout, Atlantic salmon, zebrafish, rat and human. The inclusion of two closely related salmonids, rainbow trout and Atlantic salmon, and a more distant teleost, zebrafish, in my sequence analysis, will allow for better interpretation in the context of salmonid lineage and teleost-specific genome duplication. Mammalian sequences were included due to their detailed functional characterization. To annotate functional residues and domains involved in insulin binding and cell signaling, mammalian model-based annotations derived from structural and alanine-substitution mutagenesis studies reviewed in (de Meyts et al., 2016) were highlighted in Clustal Omega (www.ebi.ac.uk/Tools/msa/clustalo/) aligned amino acid sequences. To infer evolutionary relationships between fish paralogues and mammalian homologies, I created an amino-acid sequence-based phylogeny using Phylogeny.fr program (www.phylogeny.fr/) and compared gene loci using Pubmed NCBI deposited microsyntenies.

Calculations and statistics

The Fulton's condition factor, *K*, was calculated using the equation,

$$K = \frac{10^5 \cdot m_b}{L^3}$$

Here m_b is body mass and L is fork length (Blackwell et al., 2000). All data were analyzed and visualized using Prism V8 (Graphpad, San Diego, CA, USA). Data obtained from the feeding experiment were assessed for normality using the Shapiro-Wilk test and homoscedasticity by the Levene's test. When the assumptions of normality or equality of variances were not met, the data were normalized by natural log or square root transformation. Data were analyzed using a two-way ANOVA to assess the effects of antagonist treatment and feeding status, as well as their interaction on cell signaling activity assessed by post-translation modifications (phosphorylation of Akt and S6) and on blood glucose concentrations. Where appropriate, Tukey's post hoc tests were conducted. Data obtained from the insulin infusion experiment were analyzed using simple linear regression analysis to test the potential dose-dependency effects of S961 on glucose concentration and insulin-induced activation of the insulin signaling pathway in the liver and muscle tissue. In all tests, a level of significance of $p<0.05$ was used.

Results

Postprandial insulin signaling is not attenuated by S961

In the liver, feeding status affected Akt (*df=1, F=12.466, p=0.004*) and S6 (*df=1, F=37.502, p<0.001*) phosphorylation status. In both cases, feeding significantly increased Akt and S6 phosphorylation status ($p<0.05$) compared to unfed animals (Figure 5.2A-B). Neither S961 treatment alone, nor its interaction with feeding status had effects on Akt (*S961 treatment: df=1, F=0.0758, p=0.407; S961 treatment × feeding status: df=1, F=0.580, p=0.461*) or S6 (*S961 treatment: df=1, F=0.396, p=0.541; S961*

treatment × feeding status: df=1, F=0.008, p=0.952) phosphorylation status (Figure 5.2A-B). In muscle tissue, neither feeding status, S961 treatment, nor their interaction resulted in changes in Akt (*feeding status: df=1, F=0.175, p=0.685; S961 treatment: df=1, F=0.759, p=0.410; S961 treatment × feeding status: df=1, F=1.605, p=0.229*) or S6 (*feeding status: df=1, F=0.526, p=0.482; S961 treatment: df=1, F=0.253, p=0.624; S961treatment × feeding status: df=1, F=0.029, p=0.869*) phosphorylation status (Figure 5.3A-B). Circulating glucose concentration (Figure 5.4) was not affected by feeding status (*df=1, F=2.091, p=0.167*), S961 treatment (*df=1, F=0.040, p=0.844*) or their interaction (*df=1, F=0.223, p=0.643*).

Bolus S961 injection and exogenous insulin do not attenuate insulin signaling and fail to increase circulating glucose concentration

Hepatic (Figure 5.5A) and muscle (Figure 5.6A) Akt phosphorylation status was not dose-dependently attenuated in response to bolus S961 infusion prior to 4 h insulin infusion (*liver: df=4, F=1.085, p=0.45; muscle: df=4, F=0.0916, p=0.98*). Simple linear regression analyses of liver and muscle Akt-p over bolus-infused S961 concentrations revealed slopes of 0.027 for both tissues. In both cases slopes were not significantly different from zero (*liver: df=1, F=1.317, p=0.284; muscle: df=1, F=0.0409, p=0.84*). Similarly, hepatic and muscle S6 phosphorylation status (Figure 5.5B and Figure 5.6B) was not dose-dependently attenuated in response to the S961 bolus infusion prior to 4 h insulin infusion (*liver: df=4, F=0.2561, p=0.8943; muscle: df=4, F=0.5702, p=0.70*). Simple linear regression analysis of liver and muscle Akt-p over insulin antagonist bolus concentrations preceding bovine insulin infusion revealed a slope of -0.024 and 0.038,

respectively. In both cases, slopes were not significantly different from 0 (*liver: df=1, F=0.7598, p=0.41; muscle df=1, F=0.0137, p=0.91*).

Circulating glucose (Figure 5.7) was affected by S961 treatment (*df=4, F=10.29, p=0.0125*). While post-hoc analysis revealed that the S961 bolus infusion treatment prior to insulin infusion never significantly changed glucose concentrations compared to insulin infusion alone (*p<0.05*), glucose concentration was increased in fish bolus-injected with 10 μM kg^{-1} prior to insulin infusion compared to fish bolus-injected with 0.01 and 0.1 μM kg^{-1} prior to insulin infusion (*p<0.05*). Simple linear regression analysis of blood glucose concentration over S961 bolus concentrations preceding insulin infusion (Figure 5.7) revealed a slope of 0.12, which was not different from zero (*df=1, F=11.49, p=0.0095*).

In silico analysis reveals sequential duplication events of insulin receptor loci in teleost fish and conservation of key residues involved in insulin binding

Alignment of amino acid sequences reveals that across rainbow trout and fish insulin receptor paralogues and homologues analyzed, key amino acid residues involved in mammalian insulin receptor binding of insulin, also believed to be targeted by S961, are highly conserved (Figure 5.8A; Figure 5.9). A particularly high degree of conservation is seen in the intracellular signaling domain and functional residues involved in autophosphorylation loops and their stabilization. A notable exception is the only partial conservation of the functionally important alphaCT chain, which reveals differences in its C terminal sequence (Figure 5.8A, bold letters). *In silico* analysis of genome derived amino acid sequences of rainbow trout insulin receptors revealed that four paralogues exist in rainbow trout. These paralogues cluster with four salmon

specific insulin receptor sequences, while two paralogues cluster with zebrafish Insa and the other with zebrafish Insb sequences. This finding supports that a salmonid-lineage specific duplication event of teleost *insa* and *insb* receptors led to the evolution and retention of two *insa* and two *insb* paralogues in rainbow trout (Figure 5.8B), a finding furthermore supported by synteny analysis (Figure 5.8C).

Figure 5.1. Schematic representation of the experimental designs used to probe the efficacy of the mammalian insulin receptor antagonist S961 in attenuating key nodes of the hepatic and muscular rainbow trout insulin cell signaling pathway. Experimental design to probe efficacy of S961 to attenuate postprandial endogenous insulin-dependent activation of the hepatic and muscle insulin cell signaling pathway (**A**). Experimental design to probe to probe efficacy of S961 to attenuate exogenous insulin dependent activation of the hepatic and muscle insulin cell signaling pathway using a bolus infusion of different concentrations of S961 followed by continuous infusion of exogenous bovine insulin (**B**).

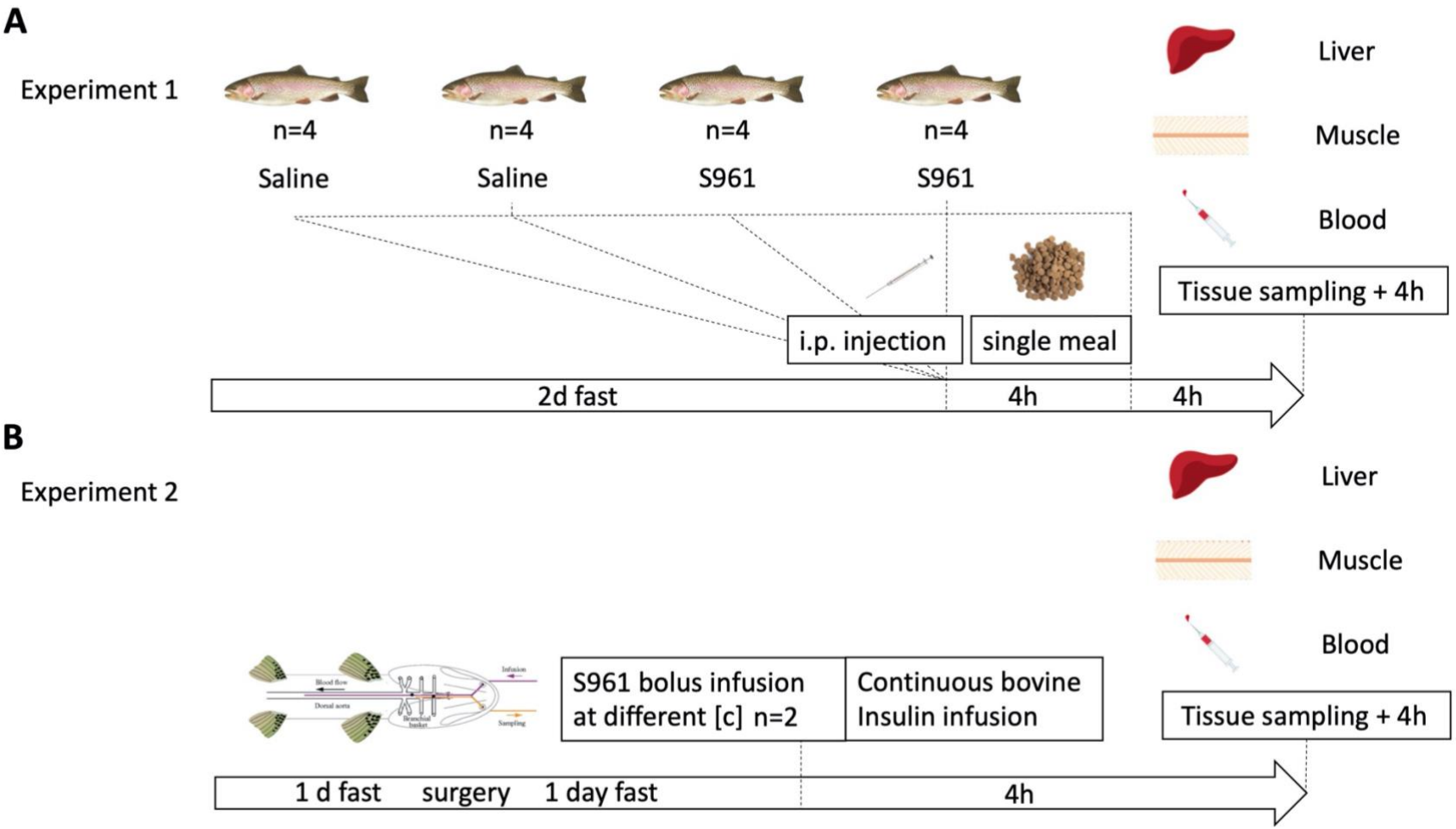
A
Experiment 1
n=4
Saline
n=4
Saline
n=4
S961
n=4
S961
Liver
Muscle
Blood
Tissue sampling + 4h
i.p. injection
single meal
2d fast
4h
4h
B
Experiment 2
Liver
Muscle
Blood
Tissue sampling + 4h
S961 bolus infusion
at different [c] n=2
Continuous bovine
Insulin infusion
1 d fast
surgery
1 day fast
4h

Figure 5.2. Postprandial activation of hepatic Akt (**A**) and S6 (**B**) assessed by Western Blot quantification of known activating phosphorylation sites normalized to beta-tubulin abundance. Individual data points, means and s.e.m. are presented for all treatment groups (N=4 per group). Data were analyzed using a two-way ANOVA with feeding status and antagonist treatment as factors. Representative images of visualized Western Blots (N=2 samples per treatment group) are shown for each group.

A

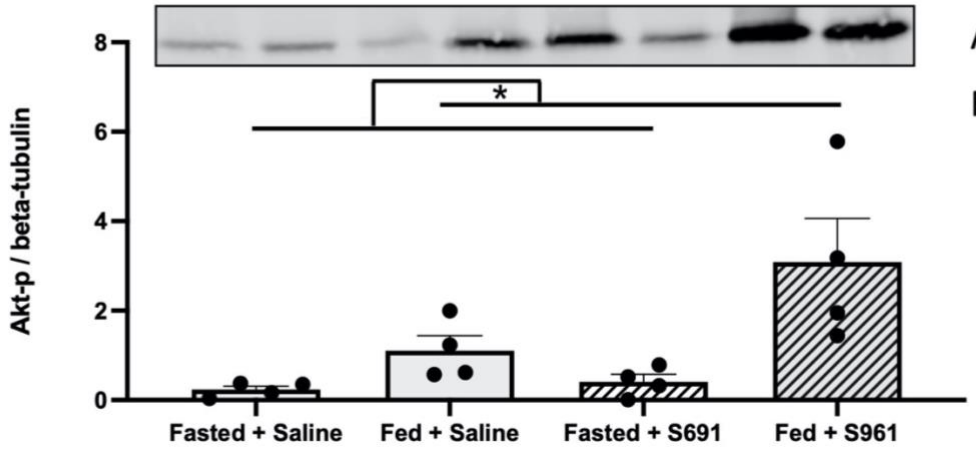

Akt-p Ser^{473} 60 kDa

Feeding status: Fed > Fasted

B

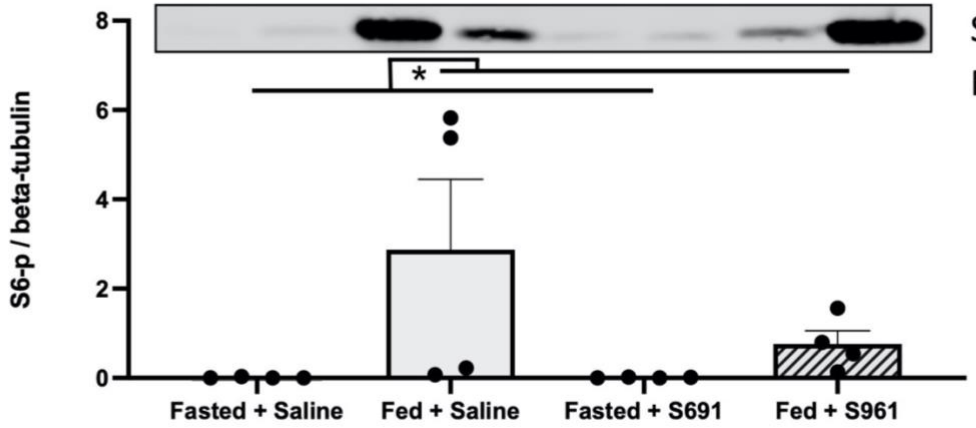

S6-p Ser$^{235/236}$ 32 kDa

Feeding status: Fed > Fasted

Figure 5.3. Postprandial activation of muscle Akt and S6 assessed by Western Blot quantification of known activating phosphorylation sites normalized to beta-tubulin abundance. Individual data points, means and s.e.m. are presented for all treatment groups (N=4 per group). Data were analyzed using a two-way ANOVA with feeding status and antagonist treatment as factors. Representative images of visualized Western Blots (N=2 samples per treatment group) are shown for each group.

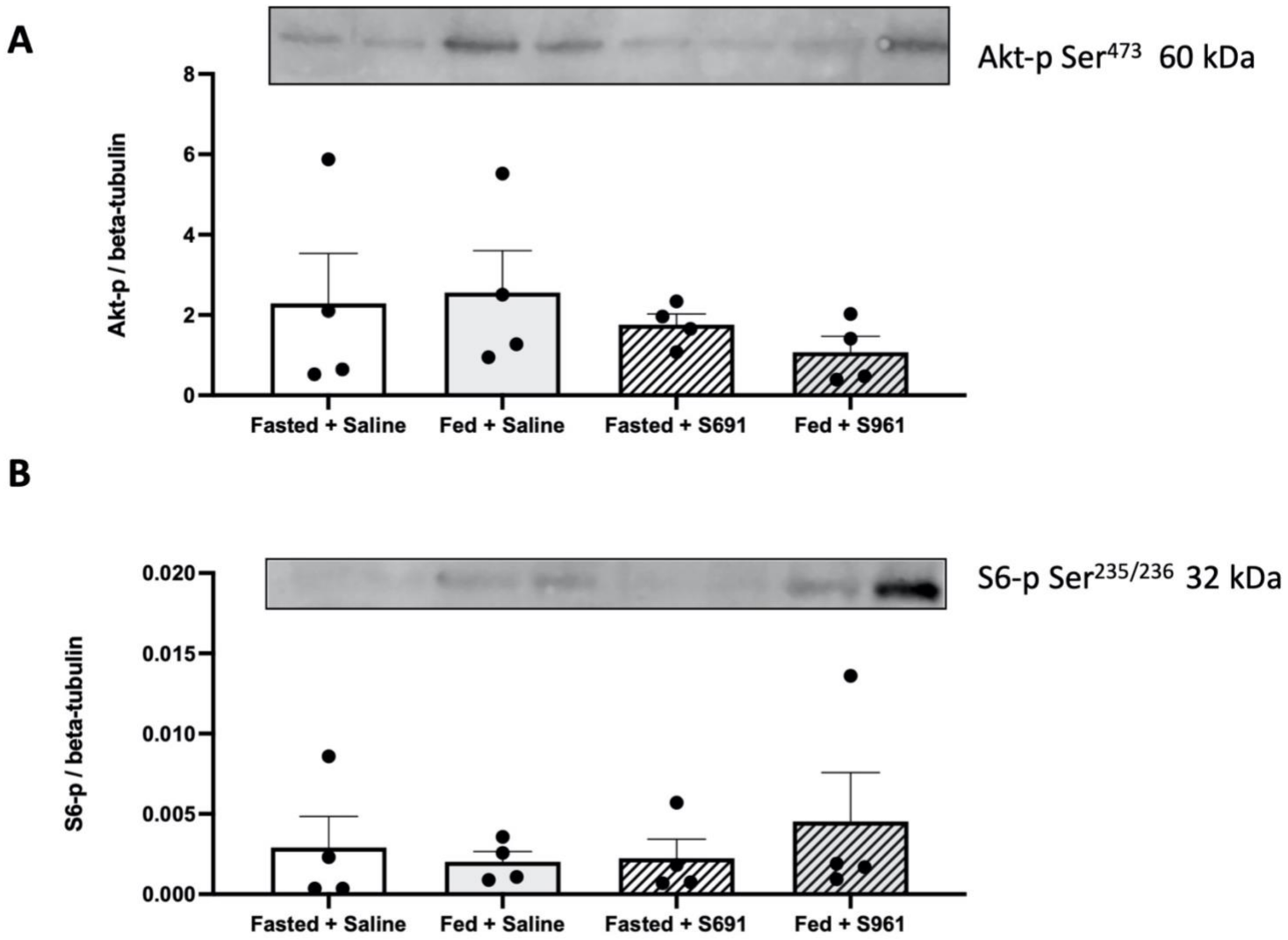
A
Akt-p Ser473 60 kDa
Akt-p / beta-tubulin
8
6
4
2
0
Fasted + Saline
Fed + Saline
Fasted + S691
Fed + S961
B
S6-p Ser235/236 32 kDa
S6-p / beta-tubulin
0.020
0.015
0.010
0.005
0.000
Fasted + Saline
Fed + Saline
Fasted + S691
Fed + S961

Figure 5.4. Postprandial blood glucose concentrations in caudal vein blood samples. Individual data points, means and s.e.m. are presented for all treatment groups (N=4 per group). Data were analyzed using a two-way ANOVA with feeding status and antagonist treatment as factors.

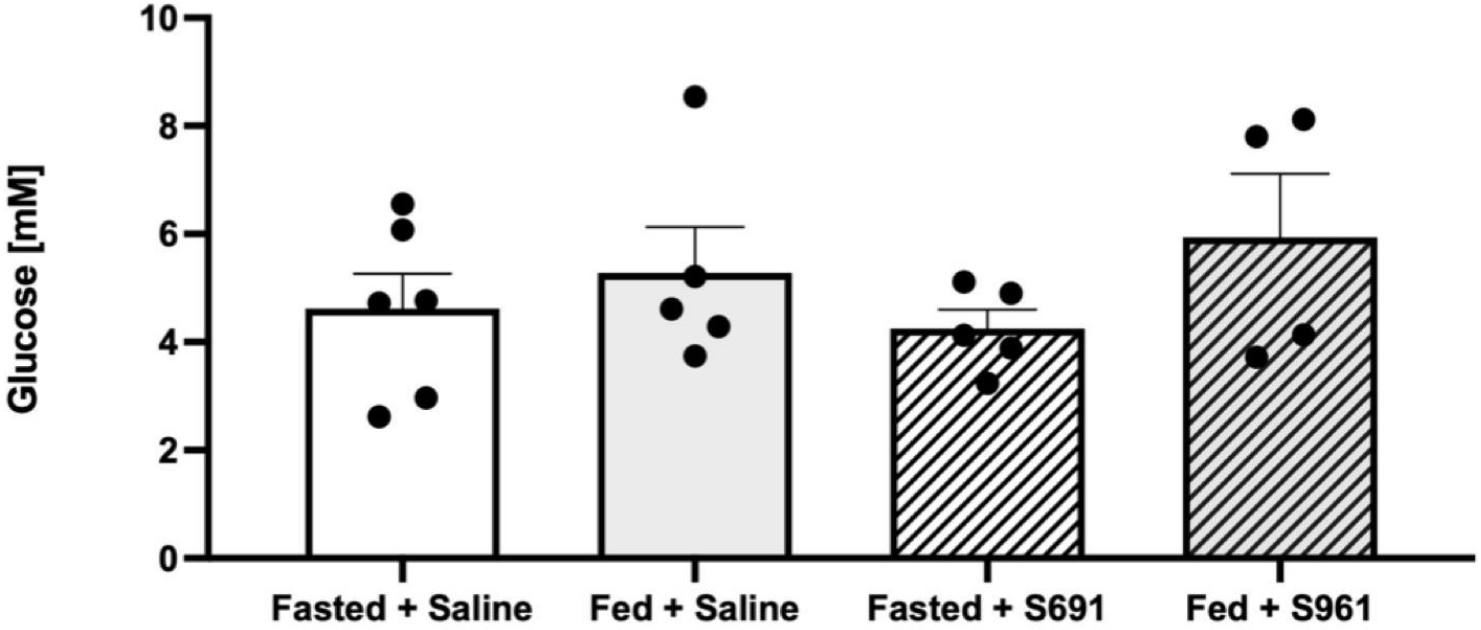
Glucose [mM]
10
8
6
4
2
0
Fasted + Saline
Fed + Saline
Fasted + S691
Fed + S961

Figure 5.5. Exogenous bovine insulin infusion-dependent activation of hepatic Akt (**A**) and S6 (**B**) following bolus infusion of S961 antagonist at concentrations of 0, 0.01, 0.1, 1 and 10 μM kg^{-1} assessed by Western Blot quantification of known activating phosphorylation sites normalized to beta-tubulin abundance. Individual data points, means and s.e.m. are presented for all treatment groups (N=2 per group). Data were analyzed using a one-way ANOVA with feeding status and antagonist treatment as factors. Representative images of visualized Western Blots (N=2 samples per treatment group) are shown for each group (left panel). Means, s.e.m. and 95% confidence intervals were plotted over S961 antagonist concentration on a log scale, and a line was fit using simple linear regression analysis (right panel).

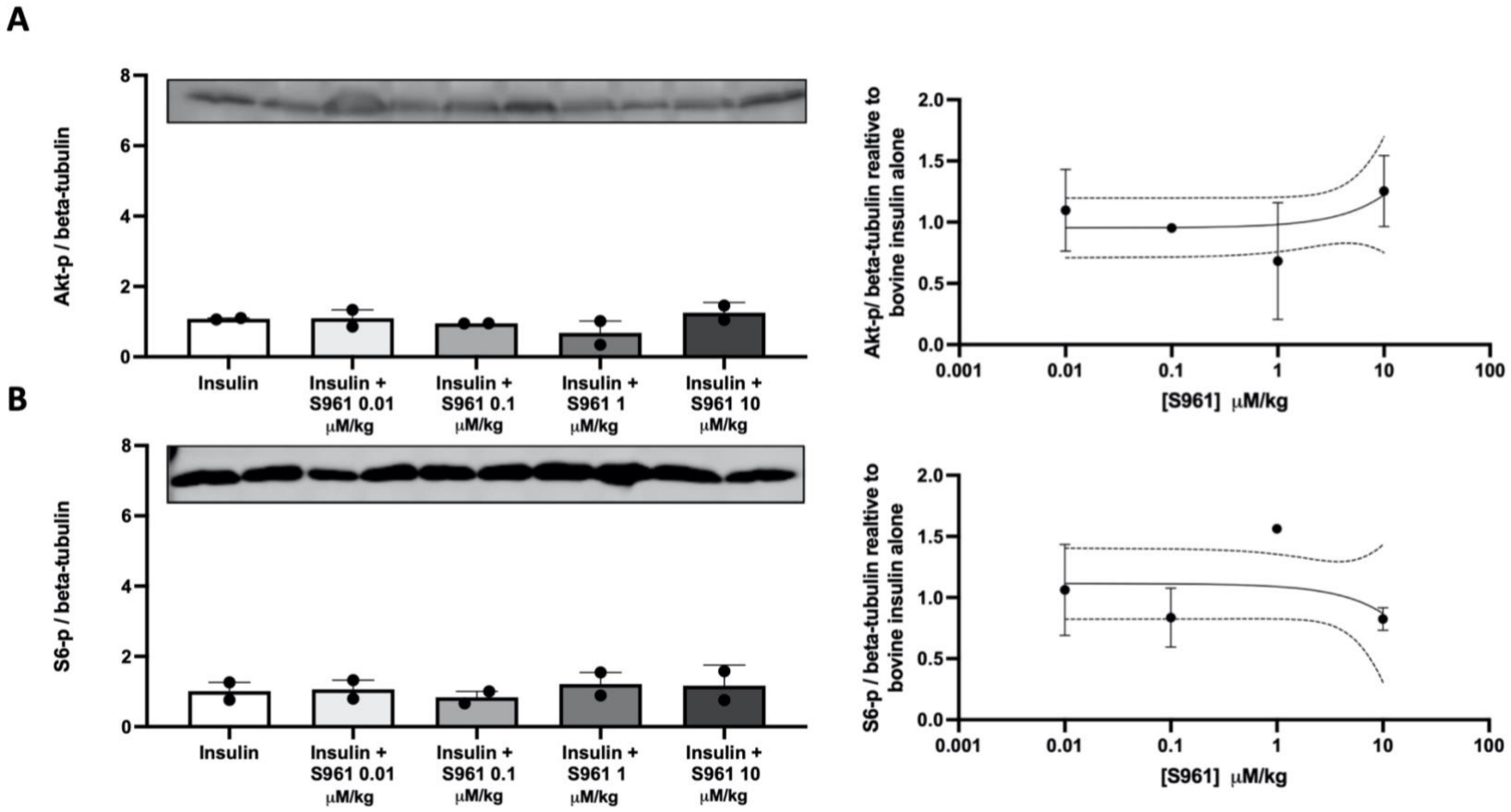
A
Akt-p / beta-tubulin
8
6
4
2
0
Insulin
Insulin + S961 0.01 μM/kg
Insulin + S961 0.1 μM/kg
Insulin + S961 1 μM/kg
Insulin + S961 10 μM/kg
Akt-p/ beta-tubulin realtive to bovine insulin alone
2.0
1.5
1.0
0.5
0.0
0.001
0.01
0.1
1
10
100
[S961] μM/kg
B
S6-p / beta-tubulin
8
6
4
2
0
Insulin
Insulin + S961 0.01 μM/kg
Insulin + S961 0.1 μM/kg
Insulin + S961 1 μM/kg
Insulin + S961 10 μM/kg
S6-p / beta-tubulin realtive to bovine insulin alone
2.0
1.5
1.0
0.5
0.0
0.001
0.01
0.1
1
10
100
[S961] μM/kg

Figure 5.6. Exogenous bovine insulin infusion-dependent activation of muscle Akt (**A**) and S6 (**B**) following bolus infusion of S961 antagonist at concentrations of 0, 0.01, 0.1, 1 and 10 μM kg^{-1} assessed by Western Blot quantification of known activating phosphorylation sites normalized to beta-tubulin abundance. Individual data points, means and s.e.m. are presented for all treatment groups (N=2 per group). Data were analyzed using a one-way ANOVA with feeding status and antagonist treatment as factors. Representative images of visualized Western Blots (N=2 samples per treatment group) are shown for each group (left panel). Means, s.e.m. and 95% confidence intervals were plotted over S961 antagonist concentration on a log scale, and a line was fit using simple linear regression analysis (right panel).

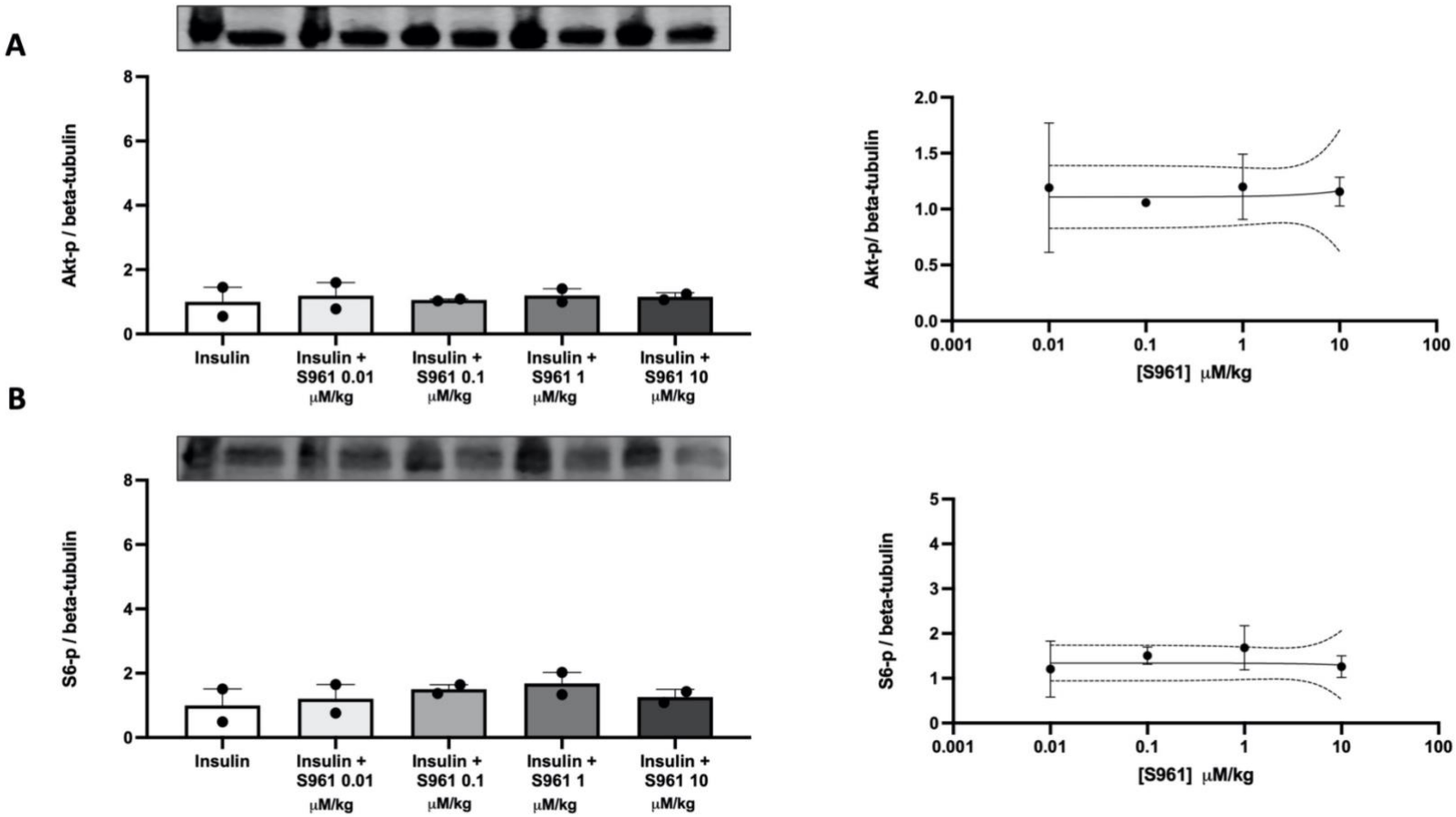
A
Akt-p / beta-tubulin
0
2
4
6
8
Insulin
Insulin + S961 0.01 μM/kg
Insulin + S961 0.1 μM/kg
Insulin + S961 1 μM/kg
Insulin + S961 10 μM/kg
Akt-p/ beta-tubulin
0.0
0.5
1.0
1.5
2.0
0.001
0.01
0.1
1
10
100
[S961] μM/kg
B
S6-p / beta-tubulin
0
2
4
6
8
Insulin
Insulin + S961 0.01 μM/kg
Insulin + S961 0.1 μM/kg
Insulin + S961 1 μM/kg
Insulin + S961 10 μM/kg
S6-p / beta-tubulin
0
1
2
3
4
5
0.001
0.01
0.1
1
10
100
[S961] μM/kg

Figure 5.7. Exogenous bovine insulin infusion-dependent circulating glucose concentration 4h following bolus infusion of S961 antagonist at concentrations of 0, 0.01, 0.1, 1 and 10 μM kg^{-1}. Individual data points, means and s.e.m. are presented for all treatment groups (N=2 per group). Data were analyzed using a one-way ANOVA with feeding status and antagonist treatment as factors (left panel). Means, s.e.m. and 95% confidence intervals were plotted over S961 antagonist concentration on a log scale, and a line was fit using simple linear regression analysis (right panel).

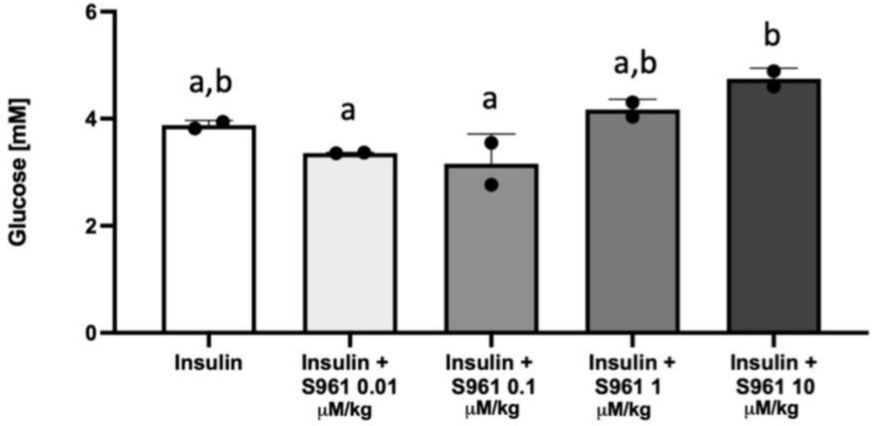
Glucose [mM]
6
4
2
0
a,b
a
a
a,b
b
Insulin
Insulin + S961 0.01 μM/kg
Insulin + S961 0.1 μM/kg
Insulin + S961 1 μM/kg
Insulin + S961 10 μM/kg

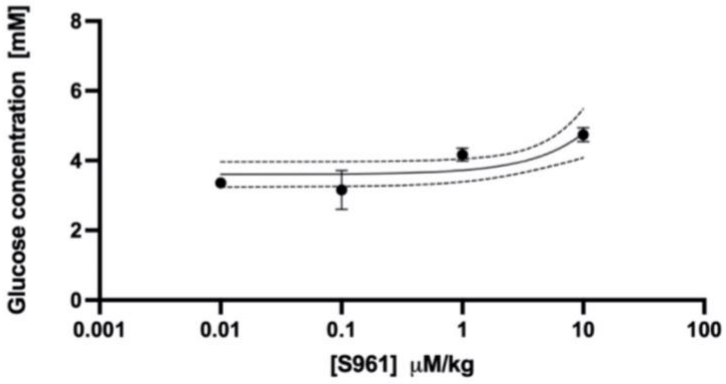
Glucose concentration [mM]
8
6
4
2
0
0.001
0.01
0.1
1
10
100
[S961] μM/kg

Figure 5.8. Clustal Omega alignment of human, rat, zebrafish, Atlantic salmon and rainbow trout and insulin receptor amino acid sequences (**A**). Key sequence features are highlighted according to de Meyts (2016) as follows: L1 and L2 domains (light grey), CR domain (dark grey), FN 1-3 domains (dark green) with alpha CT (bright green), intramembrane domain (red) and intracellular signaling domain (blue). Throughout domains, key functional amino acid residues are involved in insulin site 1 (yellow) and site 2 binding (brown) as well as autophosphorylation (light blue). NCBI genome sequence-derived insulin receptor amino acid sequence-derived phylogeny (**B**) and insulin receptor microsynteny analysis (**C**).

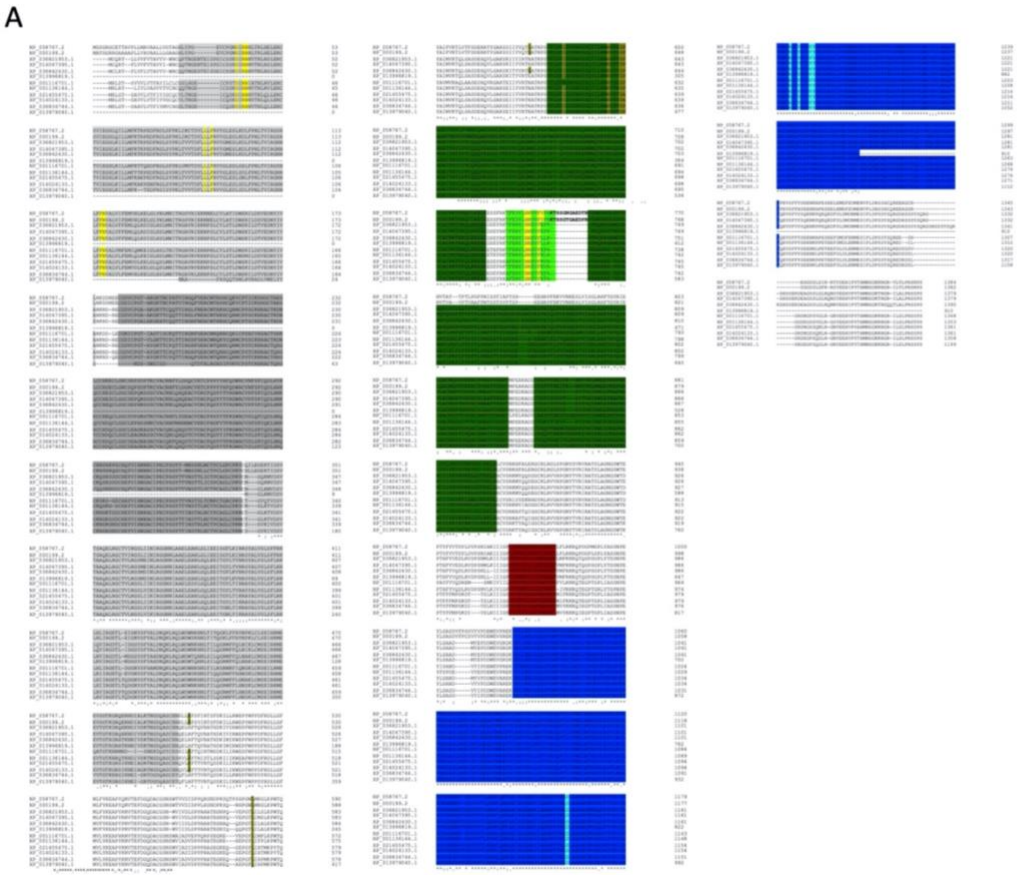
A

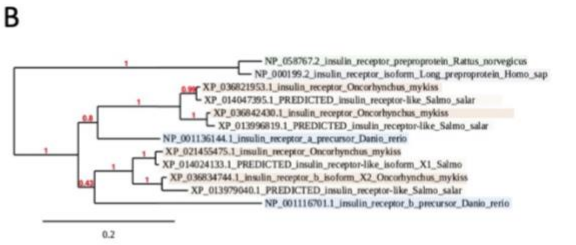
B
NP_058767.2_insulin_receptor_preproprotein_Rattus_norvegicus
NP_000199.2_insulin_receptor_isoform_Long_preproprotein_Homo_sap
XP_036821953.1_insulin_receptor_Oncorhynchus_mykiss
XP_014047395.1_PREDICTED_insulin_receptor-like_Salmo_salar
XP_036842430.1_insulin_receptor_Oncorhynchus_mykiss
XP_013996819.1_PREDICTED_insulin_receptor-like_Salmo_salar
NP_001136144.1_insulin_receptor_a_precursor_Danio_rerio
XP_021455475.1_insulin_receptor_Oncorhynchus_mykiss
XP_014024133.1_PREDICTED_insulin_receptor-like_isoform_X1_Salmo
XP_036834744.1_insulin_receptor_b_isoform_X2_Oncorhynchus_mykiss
XP_013979040.1_PREDICTED_insulin_receptor-like_Salmo_salar
NP_001116701.1_insulin_receptor_b_precursor_Danio_rerio
0.2

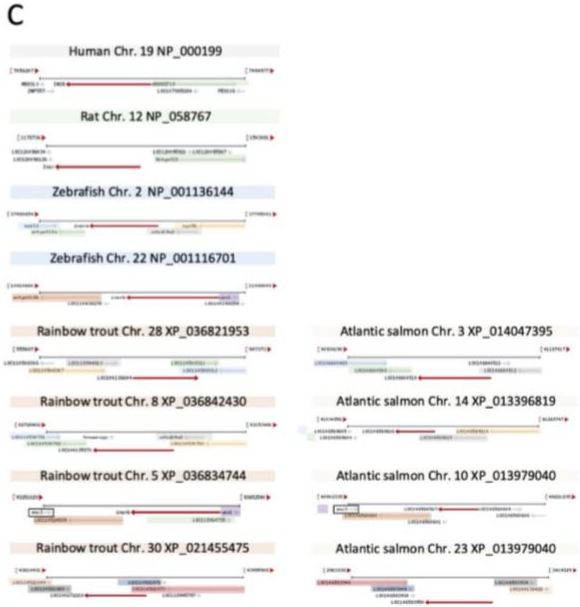
C
Human Chr. 19 NP_000199
Rat Chr. 12 NP_058767
Zebrafish Chr. 2 NP_001136144
Zebrafish Chr. 22 NP_001116701
Rainbow trout Chr. 28 XP_036821953
Rainbow trout Chr. 8 XP_036842430
Rainbow trout Chr. 5 XP_036834744
Rainbow trout Chr. 30 XP_021455475
Atlantic salmon Chr. 3 XP_014047395
Atlantic salmon Chr. 14 XP_013396819
Atlantic salmon Chr. 10 XP_013979040
Atlantic salmon Chr. 23 XP_013979040

Figure 5.9. Clustal Omega alignment of human, rat, zebrafish, Atlantic salmon and rainbow trout and insulin amino acid sequences obtained from Pubmed NCBI Genbank (**A**). Key sequence features are highlighted according to de Meyts (2016) as follows: Signaling peptide (orange font), A and B chains (light grey). Cytosine residues involved in disulphide bridges are shown in bold, basic AA residue peptide chain cleavage sites are shown in red font. Throughout domains key functional amino acid residues of insulin receptor interacting sites 1 (yellow) and site 2 (brown) are shown. NCBI genome sequence-derived insulin receptor amino acid sequence-derived phylogeny (**B**) and insulin receptor microsynteny analysis (**C**).

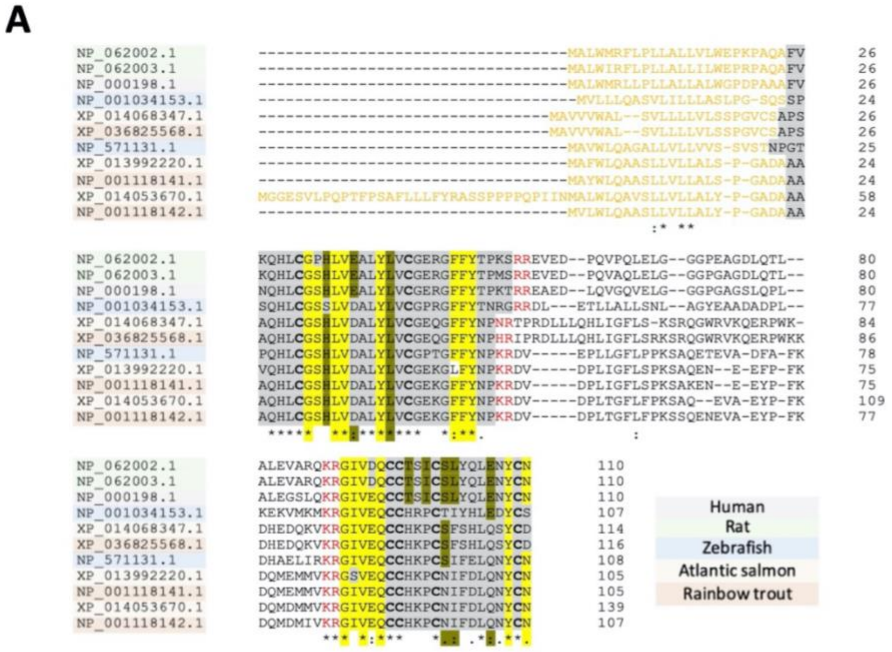
A
NP_062002.1
NP_062003.1
NP_000198.1
NP_001034153.1
XP_014068347.1
XP_036825568.1
NP_571131.1
XP_013992220.1
NP_001118141.1
XP_014053670.1
NP_001118142.1
Human
Rat
Zebrafish
Atlantic salmon
Rainbow trout

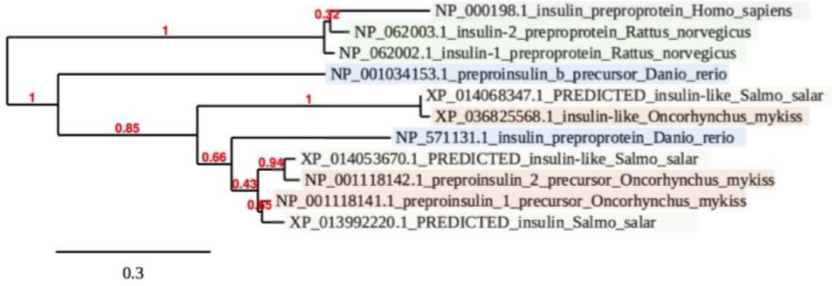
B
NP_000198.1_insulin_preproprotein_Homo_sapiens
NP_062003.1_insulin-2_preproprotein_Rattus_norvegicus
NP_062002.1_insulin-1_preproprotein_Rattus_norvegicus
NP_001034153.1_preproinsulin_b_precursor_Danio_rerio
XP_014068347.1_PREDICTED_insulin-like_Salmo_salar
XP_036825568.1_insulin-like_Oncorhynchus_mykiss
NP_571131.1_insulin_preproprotein_Danio_rerio
XP_014053670.1_PREDICTED_insulin-like_Salmo_salar
NP_001118142.1_preproinsulin_2_precursor_Oncorhynchus_mykiss
NP_001118141.1_preproinsulin_1_precursor_Oncorhynchus_mykiss
XP_013992220.1_PREDICTED_insulin_Salmo_salar
0.3


C
Human Chr. 11 NP_000198
Rat Chr. 1 NP_062002
Rat Chr. 1 NP_062003
Zebrafish Chr. 5 NP_571131
Zebrafish Chr. 14 NP_001034153
Rainbow trout Chr. 10 NP_001118142
Rainbow trout Chr. 12 NP_001118141
Rainbow trout Chr. 31 XP_036825568
Atlantic salmon Chr. 4 XP_014053670
Atlantic salmon Chr. 13 XP_013992220
Atlantic salmon Chr. 9 XP_014068347

Table 5.1. Physical characteristics and experimental parameters of four groups of rainbow trout used in the feeding status experiment.

	Group 1: Saline & Fasted	**Group 2:** Saline & Fed	**Group 3:** S961 & Fasted	**Group 4:** S961 & Fed
Sample size	4	4	4	4
Body mass (g)	219.3 ± 31.3	211.6 ± 16.3	199.2 ± 39.1	212.8 ± 47.2
Body length (cm)	27.1 ± 1.9	27.5 ± 1.5	26.6 ± 1.5	26.9 ± 1.9
Fulton's condition factor (K)	1.10 ± 0.02	1.02 ± 0.01	1.06 ± 0.02	1.09 ± 0.02
Injection volume (µl)	109.7 ± 15.6	105.8 ± 8.1	99.6 ± 19.5	106.4 ± 23.6
Pellets eaten	0	11.2 ± 6.5	0	22.5 ± 4.4

Saline or S961 was administered via intraperitoneal injection. Body mass and length were measured before the surgery. Pellets eaten were measured following euthanasia by the number of pellets in the stomach and intestinal tract. Mean values ± s.e.m. are presented.

Table 5.2. Physical characteristics and experimental parameters of rainbow trout used in the insulin infusion experiments.

	Group 1: 0 µM kg^{-1} S961	**Group 2:** 0.01 µM kg^{-1} S961	**Group 3:** 0.1 µM kg^{-1} S961	**Group 4:** 1 µM kg^{-1} S961	**Group 5:** 10 µM kg^{-1} S961
Sample size	2	2	2	2	2
Body mass (g)	275.0 ± 15.0	205.0 ± 20.0	234.0 ± 12.0	204.0 ± 6.0	244.0 ± 11.0
Body length (cm)	30.0 ± 0.0	27.0 ± 0.0	26.9 ± 2.1	26.75 ± 0.8	29.3 ± 0.3
Hematocrit (%)	31.5 ± 11.5	18.85 ± 3.1	17.0 ± 3.0	19.40 ± 8.5	19.6 ± 6.6
Fulton's condition factor (K)	0.94 ± 0.06	1.04 ± 0.10	0.97 ± 0.22	0.98 ± 0.12	0.93 ± 0.07
Insulin infusion rate (ml h^{-1})	0.70 ± 0.04	0.59 ± 0.06	0.62 ± 0.03	0.63 ± 0.02	0.62 ± 0.03
S961 injection volume (µl)	137.5 ± 7.5	102.5 ± 10.0	117.0 ± 6.0	102.0 ± 3.0	122.0 ± 5.5

Body mass and length were measured before the surgery. Hematocrit was measured on the second day, after recovery from the surgery to minimize blood loss. Mean values ± s.e.m. are presented.

Discussion

S961 does not induce signaling or metabolic changes indicative of insulin receptor antagonism in rainbow trout

Our findings strongly support the lack of efficacy of the mammalian insulin antagonist, S961 in rainbow trout. S961 does not attenuate the activation of the insulin signaling pathway in response to: (i) feeding-induced endogenous insulin release or (ii) exogenous bovine insulin infusion. In both experiments, S961 does not induce hyperglycemia compared to experimental control groups, supporting a lack of antagonistic effect *in vivo*. Commercially available diets used in the feeding status experiment, contained carbohydrate concentration (<20%) below the threshold to induce postprandial hyperglycemia (Kostyniuk et al., 2019a). Similarly, in the insulin infusion experiment, S961 was bolus injected prior to continuous insulin infusion in short-term fasted trout, thus eliminating potential interaction between simultaneously absorbed carbohydrates and insulin in the postprandial state (Mennigen et al., 2012; Seiliez et al., 2011b). Nevertheless, because exogenous insulin infusion in the absence of S961 was previously shown to significantly lower circulating glucose concentrations (Forbes et al., 2019b), my data supports a lack of antagonistic effect of S961. While S961 successfully binds to insulin receptors in multiple mammalian models to induce hyperglycemia (Galsgaard et al., 2019; Okamoto et al., 2017; Schäffer et al., 2008; Vikram and Jena, 2010), this effect was not observed in rainbow trout. This lack of effect does not appear to be linked to the tested concentrations. Monotonous and non-monotonous dose-dependency for metabolic and mitogenic insulin-dependent endpoints, have been described for S961 in mammals (Knudsen et al., 2012; Vikram

and Jena, 2010). Therefore, I employed an experimental design to test concentration ranges spanning several orders of magnitude including concentrations exceeding reported thresholds (10-30 nM) to induce hyperglycemia (Schäffer et al., 2008; Vikram and Jena, 2010).

Differences in S961 peptide half-life between rainbow trout and mammalian models cannot be formally excluded in the experiments and may thus exist in-between both models. This scenario appears unlikely, as exogenous injection of insulin has previously reported to be bioactive in rainbow trout over timeframes similar to the current experiment (Forbes et al., 2019b; Mennigen et al., 2012). Thus, the consistent selection of timeframes between reported *in vivo* mammalian (Vikram and Jena, 2010) and trout experiments (Mennigen et al., 2012; Mennigen et al., 2014) is unlikely to have resulted in differences. Overall, using two routes of administration (feeding status design: intraperitoneal injection; insulin infusion design: bolus injection) and different concentrations (0, 0.01, 0.1, 1, 10 μM kg^{-1}), biologically active in mammalian models (Galsgaard et al., 2019; Okamoto et al., 2017; Schäffer et al., 2008; Vikram and Jena, 2010), suggests that concentration and/or kinetics are unlikely to be the principal reason in the observed lack of antagonistic effect of S961 on insulin signaling and glucoregulation in rainbow trout.

In silico analysis identifies differences in the fish insulin receptor as a possible reason for the lack of S961 activity in rainbow trout

Structural differences between fish and mammalian insulin receptor, may be exacerbated by the fact that the genome of rainbow trout and other salmonid fish, such as Atlantic salmon, contain four genes coding for the insulin receptor (Figure 5.8).

Potential S961 binding site diversity between insulin receptor paralogues may explain the lack of antagonistic effects observed in the experiments. Retrieval of amino acid sequences and annotations derived from mammalian studies (de Meyts et al., 2016) confirmed the characterization of four encoded and expressed insulin receptor paralogues in rainbow trout. These paralogues exhibit differential expression across development, between tissues and in response to nutritional and endocrine factors (Caruso et al., 2010; Caruso and Sheridan, 2012; Caruso and Sheridan, 2014). Exogenous insulin binds to rainbow trout insulin receptors (Gutiérrez et al., 1991), to stimulate rainbow trout insulin receptor signaling and gene expression (Mennigen et al., 2012; Plagnes-Juan et al., 2008) and to regulate rainbow trout energy metabolism *in vivo* and *in vitro* (Forbes et al., 2019b; Mennigen et al., 2014; Pereira et al., 1995). S961 was specifically developed to target insulin 1 and 2 binding sites (Figure 5.9) in humans and to displace insulin in competitive binding (Schäffer et al., 2008). These binding sites are largely conserved between rainbow trout paralogues and mammalian homologues (Figure 5.8). Overall, *in silico* evidence does support a role for differential S961 binding in trout and mammals, supporting the lack of antagonistic effect of S961 reported (Figure 5.8A). A notable exception is the alphaCT helix domain, which is involved in insulin binding and receptor conformation changes linked to negative cooperativity and heterodimer-dependent autophosphorylation (de Meyts et al., 2016). In contrast to mammals, the insulin receptor in fish does not involve differential splicing of exon 11 to yield *Insa* and *Insb* type receptors from a single gene product (Hernández-Sánchez et al., 2008). Therefore, terminal residues of the alphaCT chain are not conserved between rainbow trout and mammals (Figure 5.8A).

Unlike mammals, teleosts evolved separate paralogues for the insulin receptor, *insra* and *insrb*, which is supported at both the microsynteny (Figure 5.8B) and amino acid level (Figure 5.8C). Zebrafish *insra* and *insrb* paralogue specific knockouts have shown differential metabolic roles in glucose and lipid metabolism indicative of sub-functionalization (Yang et al., 2018). While S961 binds to both mammalian homologues, *Insa* and *Insb* (Schäffer et al., 2008), reduced interaction between S961 and the alphaCT helix in rainbow trout may be responsible for the lack of antagonistic effects of S961. Other, less conserved parts of the insulin receptor may differentially interact with S961 in rainbow trout. Finally, targets other than the insulin receptor may sequester S961 and abolish its insulin receptor antagonism. Indeed, while highly selective for insulin, compared to mammalian IGF1R receptors, S961 also effectively binds insulin and IGF1R heterodimers (Schäffer et al., 2008). The IGF1 receptor and IGF-binding protein family experienced significant diversification in teleost fish evolution (Alzaid et al., 2016; Garcia de la Serrana and Macqueen, 2018). Differential binding may contribute to the lack of antagonistic effect of S961 observed in rainbow trout. However, neither the existence nor function of insulin receptor heterodimers has been investigated in teleosts to date.

This study demonstrates that S961 is not a functional insulin receptor antagonist in rainbow trout. However, the inhibition of the insulin signaling pathway remains a desirable experimental tool for comparative studies. Upstream acting agents such as Wortmannin employed to inhibit insulin signaling at the central Akt node (Blanco et al., 2020; Bouraoui et al., 2010; Castillo et al., 2004) should be prioritized for testing to

extend pharmacological inhibition of salmonid insulin receptor signaling. It is however important to note that Wortmannin also may act non-specifically.

REFERENCES

Abdelrahman, A., Powell, F., Jadeja, R., Jones, M., Thounaojam, M., Bartoli, M., Al-Shabrawey, M. and Martin, P. (2022). Expression and activation of the ketone body receptor HCAR2/GPR109A promotes preservation of retinal endothelial cell barrier function. *Exp Eye Res.* **221**, 109129.

Ahmadian, M., Duncan, R., Varady, K., Frasson, D., Hellerstein, M., Birkenfeld, A., Samuel, V., Shulman, G., Yuhui, W., Chulho, K. et al. (2009). Adipose overexpression of desnutrin promotes fatty acid use and attenuates diet-induced obesity. *Diabetes.* **58**, 855-66.

Ahmed, K. (2011). Biological roles and therapeutic potential of hydroxy-carboxylic acid receptors. *Front Endocrinol (Lausanne).* **2**.

Ahmed, K., Tunaru, S., Tang, C., Müller, M., Gille, A., Sassmann, A., Hanson, J. and Offermanns, S. (2010). An autocrine lactate loop mediates insulin-dependent inhibition of lipolysis through GPR81. *Cell Metab.* **11**, 311-9.

Al Mahri, S., Malik, S., Al Ibrahim, M., Haji, E., Dairi, G. and Mohammad, S. (2022). Free Fatty Acid Receptors (FFARs) in Adipose: Physiological Role and Therapeutic Outlook. *Cells.* **11**, 750.

Albalat, A., Sánchez-Gurmaches, J., Gutiérrez, J. and Navarro, I. (2006). Regulation of lipoprotein lipase activity in rainbow trout (*Oncorhynchus mykiss*) tissues. *Gen Comp Endocrinol.* **146**, 226-35.

Alzaid, A., Martin, S. and Macqueen, D. (2016). The complete salmonid *IGF-IR* gene repertoire and its transcriptional response to disease. *Sci Rep.* **6**.

Andoh, A., Tsujikawa, T. and Fujiyama, Y. (2003). Role of dietary fibre and short-chain fatty acids in the colon. *Curr Pharm Des.* **9**, 347-58.

Anthonsen, M., Rönnstrand, L., Wernstedt, C., Degerman, E. and Holm, C. (1998). Identification of novel phosphorylation sites in hormone-sensitive lipase that are phosphorylated in response to isoproterenol and govern activation properties in vitro. *J Biol Chem.* **273**, 215-21.

Babin, P. and Vernier, J. (1989). Plasma lipoproteins in fish. *J Lipid Res.* **30**, 467-89.

Bechmann, L., Hannivoort, R., Gerken, G., Hotamisligil, G., Trauner, M. and Canbay, A. (2012). The interaction of hepatic lipid and glucose metabolism in liver diseases. *J Hepatol.* **56**, 952-64.

Bernard, S., Reidy, S., Zwingelstein, G. and Weber, J. (1999). Glycerol and fatty acid kinetics in rainbow trout: effects of endurance swimming. *J Exp Biol.* **202**, 279-88.

Berry, M., Phillips, J., Henly, D. and Clark, D. (1993). Effects of fatty acid oxidation on glucose utilization by isolated hepatocytes. *FEBS Lett.* **319**, 26-30.

Bilinski, E. and Jonas, R. (1972). Oxidation of lactate to carbon dioxide by rainbow trout (*Salmo gairdneri)* tissue. *J Fish Res Board Can.*

Blackwell, B., Brown, M. and Willis, D. (2000). Relative Weight (Wr) Status and Current Use in Fisheries Assessment and Management. *Rev Fish Sci.* **8**, 1-44.

Blanco, A., Bertucci, J., Soengas, J. and Unniappan, S. (2020). *In vitro* insulin treatment reverses changes elicited by nutrients in cellular metabolic processes that regulate food intake in fish. *J Exp Biol.* **223**.

Blasco, J., Fernàndez-Borràs, J., Marimon, I. and Requena, A. (1996). Plasma glucose kinetics and tissue uptake in brown trout in vivo: effect of an intravascular glucose load. *J Comp Physiol B.* **165**, 534-541.

Bortz, W., Paul, P., Haff, A. and Holmes, W. (1972). Glycerol turnover and oxidation in man. *J Clin Invest.* **51**, 1537-46.

Bou, M., Todorčević, M., Torgersen, J., Škugor, S., Navarro, I. and Ruyter, B. (2016). De novo lipogenesis in Atlantic salmon adipocytes. *Biochim Biophys Acta.* **1860**, 86-96.

Bouraoui, L., Capilla, E., Gutiérrez, J. and Navarro, I. (2010). Insulin and insulin-like growth factor I signaling pathways in rainbow trout (*Oncorhynchus mykiss*) during adipogenesis and their implication in glucose uptake. *Am J Physiol Regul Integr Comp Physiol.* **299**, R33-41.

Briscoe, C., Tadayyon, M., Andrews, J., Benson, W., Chambers, J., Eilert, M., Ellis, C., Elshourbagy, N., Goetz, A., Minnick, D. et al. (2003). The orphan G protein-coupled receptor GPR40 is activated by medium and long chain fatty acids. *J Biol Chem.* **278**, 11303-11.

Brooks, G. (1998). Mammalian fuel utilization during sustained exercise. *Comp Biochem Physiol B Biochem Mol Biol.* **120**, 89-107.

Brooks, G. (2002). Lactate shuttles in Nature. *Biochem Soc Trans.* **30**, 258-64.

Brooks, G. (2020). Lactate as a fulcrum of metabolism. *Redox Biol.* **35**.

Brooks, G., Arevalo, J., Osmond, A., Leija, R., Curl, C. and Tovar, A. (2022). Lactate in contemporary biology: a phoenix risen. *J Physiol.* **600**, 1229-1251.

Brown, A., Goldsworthy, S., Barnes, A., Eilert, M., Tcheang, L., Daniels, D., Muir, A., Wigglesworth, M., Kinghorn, I., Fraser, N. et al. (2003). The Orphan G protein-coupled receptors GPR41 and GPR43 are activated by propionate and other short chain carboxylic acids. *J Biol Chem.* **278**, 11312-9.

Cai, T., Ren, N., Jin, L., Cheng, K., Kash, S., Chen, R., Wright, S., Taggart, A. and Waters, M. (2008). Role of GPR81 in lactate-mediated reduction of adipose lipolysis. *Biochem Biophys Res Commun.* **377**, 987-91.

Capilla, E., Díaz, M., Gutiérrez, J. and Planas, J. (2002). Physiological regulation of the expression of a GLUT4 homolog in fish skeletal muscle. *Am J Physiol Endocrinol Metab.* **283**, E44-9.

Carneiro, N., Eilertson, C. and Sheridan, M. (1996). Lipid-stimulated somatostatin secretion in rainbow trout, *Oncorhynchus mykiss*. *Fish Physiol Biochem.* **15**, 447-52.

Caruso, M., Blaufuss, P., Kittilson, J., Raine, J. and Sheridan, M. (2010). Isolation and characterization of a mRNA encoding a novel insulin receptor (IR) subtype, IR2, from rainbow trout (*Oncorhynchus mykiss*) and patterns of expression of the four IR subtypes, IR1-IR4, in tissues and during embryonic development. *Gen Comp Endocrinol.* **169**, 258-68.

Caruso, M. and Sheridan, M. (2012). The expression of insulin and insulin receptor mRNAs is regulated by nutritional state and glucose in rainbow trout (Oncorhynchus mykiss). *Gen Comp Endocrinol.* **175**, 321-8.

Caruso, M. and Sheridan, M. (2014). Differential regulation of the multiple insulin and insulin receptor mRNAs by somatostatin. *Mol Cell Endocrinol.* **384**, 126-33.

Castillo, J., Codina, M., Martínez, M., Navarro, I. and Gutiérrez, J. (2004). Metabolic and mitogenic effects of IGF-I and insulin on muscle cells of rainbow trout. *Am J Physiol Regul Integr Comp Physiol.* **286**, R935-41.

Ceddia, R. and Collins, S. (2020). A compendium of G-protein-coupled receptors and cyclic nucleotide regulation of adipose tissue metabolism and energy expenditure. *Clin Sci (Lond).* **134**, 473-512.
Chakrabarty, K. and Leveille, G. (1969). Acetyl CoA carboxylase and fatty acid synthetase activities in liver and adipose tissue of meal-fed rats. *Proc Soc Exp Biol Med.* **131**, 1051-4.
Chan, L., Mugler, C., Heinrich, S., Vallotton, P. and Weis, K. (2018). Non-invasive measurement of mRNA decay reveals translation initiation as the major determinant of mRNA stability. *Elife.* **7**.
Chapelle, S. and Zwingelstein, G. (1984). Phospholipid composition and metabolism of crustacean gills as related to changes in environmental salinities: Relationship between Na+-ATPase activity and phospholipids. *Comp Biochem Physiol B, Biochem Mol Biol.* **78**, 363-372.
Chen, S., Zhou, L., Sun, J., Qu, Y. and Chen, M. (2021). The Role of cAMP-PKA Pathway in Lactate-Induced Intramuscular Triglyceride Accumulation and Mitochondria Content Increase in Mice. *Front Physiol.* **12**, 709135.
Chitraju, C., Walther, T. and Farese, R. J. (2019). The triglyceride synthesis enzymes DGAT1 and DGAT2 have distinct and overlapping functions in adipocytes. *J Lipid Res.* **60**, 1112-20.
Choi, K. and Weber, J.-M. (2015). Pushing the limits of glucose kinetics: how rainbow trout cope with a carbohydrate overload. *J Exp Biol.* **218**, 2873-80.
Choi, K. and Weber, J.-M. (2016). Coping with an exogenous glucose overload: glucose kinetics of rainbow trout during graded swimming. *Am J Physiol Regul Integr Comp Physiol.* **310**, R493-501.
Chung, S., Chacko, S., Sunehag, A. and Haymond, M. (2015). Measurements of gluconeogenesis and glycogenolysis: a methodological review. *Diabetes.* **64**, 3996-4010.
Corraze, G. and Kaushik, S. (1999). Lipids from marine and freshwater fish. *Oleagineux Corps Gras Lipides.* **6**, 111-5.
Corrêa-Giannella, M. and Machado, U. (2013). SLC2A4gene: a promising target for pharmacogenomics of insulin resistance. *Pharmacogenomics.* **14**, 847-50.
Cresswell, R. (1981). Post-stocking movements and recapture of hatchery-reared trout released into flowing waters—a review. *J Fish Biol.* **18**, 429-442.
da Costa, D., Dias, J., Colen, R., Rosa, P. and Engrola, S. (2017). Partition and metabolic fate of dietary glycerol in muscles and liver of juvenile tilapia. *Arch Anim Nutr.* **71**, 165-174.
da Costa, D., Paulino, R. and Okamura, D. (2015). Growth and energy metabolism of Nile tilapia juveniles fed glycerol. *Pesqui.* **50**, 347-54.
Dai, W., Panserat, S., Mennigen, J., Terrier, F., Dias, K., Seiliez, I. and Skiba-Cassy, S. (2013). Post-prandial regulation of hepatic glucokinase and lipogenesis requires the activation of TORC1 signaling in rainbow trout (*Oncorhynchus mykiss*). *J Exp Biol.* **216**, 4483-92.
Dai, Y., Liu, W., Li, X., Zhou, M., Xu, C., Qian, Y. and Jiang, G. (2018). Molecular cloning of adipose triglyceride lipase (ATGL) gene from blunt snout bream and its expression after LPS-induced TNF-α factor. *Fish Physiol Biochem.* **44**, 1143-1157.

de Meyts, P., Feingold, K., Anawalt, B., Boyce, A., Chrousos, G., de Herder, W., Dhatariya, K., Dungan, K., Hershman, J., Hofland, J. et al. (2016). The Insulin Receptor and Its Signal Transduction Network. *Endotext*.

Dereeper, A., Guignon, V., Blanc, G., Audic, S., Buffet, S., Chevenet, F., Dufayard, JF., Guindon, S., Lefort, V., Lescot, M. et al. (2008). Phylogeny.fr: robust phylogenetic analysis for the non-specialist. *Nucleic Acids Res.* **36**

Domenici, P. and Blake, R. (1997). The kinematics and performance of fish fast-start swimming. *J Exp Biol.* **200**, 1165-78.

Du, Q., Tan, Z., Shi, F., Tang, M., Xie, L., Zhao, L., Li, Y., Hu, J., Zhou, M., Bode, A. et al. (2019). PGC1α/CEBPB/CPT1A axis promotes radiation resistance of nasopharyngeal carcinoma through activating fatty acid oxidation. *Cancer Sci.* **110**, 2050-62.

Ducasse-Cabanot, S., Zambonino-Infante, J., Richard, N., Medale, F., Corraze, G., Mambrini, M., Robin, J., Cahu, C., Kaushik, S. and Panserat, S. (2007). Reduced lipid intake leads to changes in digestive enzymes in the intestine but has minor effects on key enzymes of hepatic intermediary metabolism in rainbow trout (*Oncorhynchus mykiss*). *Animal.* **1**, 1272-82.

Díaz, M., Capilla, E. and Planas, J. (2007). Physiological regulation of glucose transporter (GLUT4) protein content in brown trout (*Salmo trutta*) skeletal muscle. *J Exp Biol.* **210**, 2346-51.

Edens, N., Leibel, R. and Hirsch, J. (1990). Mechanism of free fatty acid re-esterification in human adipocytes in vitro. *J Lipid Res.* **31**, 1423-31.

Enes, P., Panserat, S., Kaushik, S. and Oliva-Teles, A. (2009). Nutritional regulation of hepatic glucose metabolism in fish. *Fish Physiol Biochem.* **35**, 519-39.

Farhat, E., Cheng, H., Romestaing, C., Pamenter, M. and Weber, J. (2021a). Goldfish Response to Chronic Hypoxia: Mitochondrial Respiration, Fuel Preference and Energy Metabolism. *Metabolites.* **11**, 187.

Farhat, E., Devereaux, M., Cheng, H., Weber, J. and Pamenter, M. (2021b). Na+/K+-ATPase activity is regionally regulated by acute hypoxia in naked mole-rat brain. *Neurosci Lett.* **764**, 136244.

Farhat, E., Talarico, G., Grégoire, M., Weber, J.-M. and Mennigen, J. (2022). Epigenetic and post-transcriptional repression support metabolic suppression in chronically hypoxic goldfish. *Sci Rep.* **12**, 5576.

Figueiredo-Silva, A., Panserat, S., Kaushik, S., Geurden, I. and Polakof, S. (2012). High levels of dietary fat impair glucose homeostasis in rainbow trout. *J Exp Biol.* **215**, 169-78.

Folch, J., Lees, M. and Sloane Stanley, G. (1957). A simple method for the isolation and purification of total lipides from animal tissues. *J Biol Chem.* **226**, 497-509.

Forbes, J., Kostyniuk, D., Mennigen, J. and Weber, J.-M. (2019a). Glucagon regulation of carbohydrate metabolism in rainbow trout: *in vivo* glucose fluxes and gene expression. *J Exp Biol.* **222**.

Forbes, J., Kostyniuk, D., Mennigen, J. and Weber, J.-M. (2019b). Unexpected effect of insulin on glucose disposal explains glucose intolerance of rainbow trout. *Am J Physiol Regul Integr Comp Physiol.* **316**, R387-R394.

Fornshell, G. (2002). Rainbow Trout - Challenges and Solutions. *Rev Fish Sci.* **10**, 545-557.

Frayn, K. (2010). Fat as a fuel: emerging understanding of the adipose tissue-skeletal muscle axis. *Acta Physiol (Oxf).* **199**, 509-18.
Galsgaard, K., Winther-Sørensen, M., Pedersen, J., Kjeldsen, S., Rosenkilde, M., Wewer Albrechtsen, N. and Holst, J. (2019). Glucose and amino acid metabolism in mice depend mutually on glucagon and insulin receptor signaling. *Am J Physiol Endocrinol Metab.* **316**, E660-E673.
Garcia de la Serrana, D. and Macqueen, D. (2018). Insulin-Like Growth Factor-Binding Proteins of Teleost Fishes. *Front Endocrinol (Lausanne).* **9**, 80.
Gerich, J. (2010). Role of the kidney in normal glucose homeostasis and in the hyperglycaemia of diabetes mellitus: therapeutic implications. *Diabet Med.* **27**, 136-42.
Girard, J., Ferré, P. and Foufelle, F. (1997). Mechanisms by which carbohydrates regulate expression of genes for glycolytic and lipogenic enzymes. *Annu Rev Nutr.* **17**, 325-52.
Girard, S. and Milligan, C. (1992). The Metabolic Fate of Blood-Borne Lactate in Winter Flounder (*Pseudopleuronectes americanus*) during Recovery from Strenuous Exercise. *Physiol Zool.* **65**, 1114-34.
Gonzalez, A., Pagé, B. and Weber, J.-M. (2015). Membranes as a possible pacemaker of metabolism in cypriniform fish: does phylogeny matter? *J Exp Biol.* **218**, 2563-72.
Gotoh, C., Hong, Y., Iga, T., Hishikawa, D., Suzuki, Y., Song, S., Choi, K., Adachi, T., Hirasawa, A., Tsujimoto, G. et al. (2007). The regulation of adipogenesis through GPR120. *Biochem Biophys Res Commun.* **354**, 591-7.
Gross, D., van den Heuvel, A. and Birnbaum, M. (2008). The role of FoxO in the regulation of metabolism. *Oncogene* **27**, 2320-36.
Gutiérrez, J., Asgård, T., Fabbri, E. and Plisetskaya, E. (1991). Insulin-receptor binding in skeletal muscle of trout. *Fish Physiol Biochem.* **9**, 351-60.
Haman, F., Powell, M. and Weber, J.-M. (1997a). Reliability of continuous tracer infusion for measuring glucose turnover rate in rainbow trout. *J Exp Biol.* **200**, 2557-63.
Haman, F. and Weber, J.-M. (1996). Continuous tracer infusion to measure in vivo metabolite turnover rates in trout. *J Exp Biol.* **199**, 1157-62.
Haman, F., Zwingelstein, G. and Weber, J.-M. (1997b). Effects of hypoxia and low temperature on substrate fluxes in fish: plasma metabolite concentrations are misleading. *Am J Physiol Regul Integr Comp Physiol.* **273**, R2046-R2054.
Hatting, M., Tavares, C., Sharabi, K., Rines, A. and Puigserver, P. (2018). Insulin regulation of gluconeogenesis. *Ann N Y Acad Sci.* **1411**, 21-35.
Heckmann, L., Sørensen, P., Krogh, P. and Sørensen, J. (2011). NORMA-Gene: a simple and robust method for qPCR normalization based on target gene data. *BMC Bioinformatics.* **12**, 250.
Henderson, R. and Tocher, D. (1987). The lipid composition and biochemistry of freshwater fish. *Prog Lipid Res.* **26**, 281-347.
Henriksen, E. and Dokken, B. (2006). Role of glycogen synthase kinase-3 in insulin resistance and type 2 diabetes. *Curr Drug Targets.* **7**, 1435-41.

Hernández-Sánchez, C., Mansilla, A., de Pablo, F. and Zardoya, R. (2008). Evolution of the insulin receptor family and receptor isoform expression in vertebrates. *Mol Biol Evol.* **25**, 1043-53.

Hirasawa, A., Tsumaya, K., Awaji, T., Katsuma, S., Adachi, T., Yamada, M., Sugimoto, Y., Miyazaki, S. and Tsujimoto, G. (2005). Free fatty acids regulate gut incretin glucagon-like peptide-1 secretion through GPR120. *Nat Med.* **11**, 90-4.

Hudson, B., Shimpukade, B., Milligan, G. and Ulven, T. (2014). The molecular basis of ligand interaction at free fatty acid receptor 4 (FFA4/GPR120). *J Biol Chem.* **289**, 20345-58.

Hughes, L., Ortí, G., Huang, Y., Sun, Y., Baldwin, C., Thompson, A., Arcila, D., Betancur-R, R., Li, C., Becker, L. et al. (2018). Comprehensive phylogeny of ray-finned fishes (Actinopterygii) based on transcriptomic and genomic data. *Proc Natl Acad Sci U S A.* **115**, 6249-54.

Hulbert, A. (2021). The under-appreciated fats of life: the two types of polyunsaturated fats. *J Exp Biol.* **224**.

Hultman, E. (1995). Fuel selection, muscle fibre. *Proc Nutr Soc.* **54**, 107-21.

Hurley, B., Nemeth, P., Martin, W., Hagberg, J., Dalsky, G. and Holloszy, J. (1986). Muscle triglyceride utilization during exercise: effect of training. *J Appl Physiol.* **60**, 562-7.

Husted, A., Ekberg, J., Tripp, E., Nissen, T., Meijnikman, S., O'Brien, S., Ulven, T., Acherman, Y., Bruin, S., Nieuwdorp, M. et al. (2020). Autocrine negative feedback regulation of lipolysis through sensing of NEFAs by FFAR4/GPR120 in WAT. *Mol Metab.* **42**, 101103.

Ichimura, A., Hirasawa, A., Poulain-Godefroy, O., Bonnefond, A., Hara, T., Yengo, L., Kimura, I., Leloire, A., Liu, N., Iida, K. et al. (2012). Dysfunction of lipid sensor GPR120 leads to obesity in both mouse and human. *Nature.* **483**, 350-4.

Ishizawa, R., Masuda, K., Sakata, S. and Nakatani, A. (2015). Effects of different fatty acid chain lengths on fatty acid oxidation-related protein expression levels in rat skeletal muscles. *J Oleo Sci.* **64**, 415-21.

Issekutz, B., Shaw, W. and Issekutz, T. (1975). Effect of lactate on FFA and glycerol turnover in resting and exercising dogs. *J Appl Physiol.* **39**, 349-53.

Itoh, Y., Kawamata, Y., Harada, M., Kobayashi, M., Fujii, R., Fukusumi, S., Ogi, K., Hosoya, M., Tanaka, Y., Uejima, H. et al. (2003). Free fatty acids regulate insulin secretion from pancreatic beta cells through GPR40. *Nature.* **422**, 173-6.

Jenkins, A., Storlien, L., Chisholm, D. and Kraegen, E. (1988). Effects of nonesterified fatty acid availability on tissue-specific glucose utilization in rats in vivo. *J Clin Invest.* **82**, 293-9.

Jones, J. (2016). Hepatic glucose and lipid metabolism. *Diabetologia.* **59**, 1098-103.

Jubouri, M., Talarico, G., Weber, J.-M. and Mennigen, J. (2021). Alanine alters the carbohydrate metabolism of rainbow trout: glucose flux and cell signaling. *J Exp Biol.* **224**.

Kam, J. and Milligan, C. (2006). Fuel use during glycogenesis in rainbow trout (*Oncorhynchus mykiss* Walbaum) white muscle studied in vitro. *J Exp Biol.* **209**, 871-80.

Karaki, S., Mitsui, R., Hayashi, H., Kato, I., Sugiya, H., Iwanaga, T., Furness, J. and Kuwahara, A. (2006). Short-chain fatty acid receptor, GPR43, is expressed by enteroendocrine cells and mucosal mast cells in rat intestine. *Cell Tissue Res.* **324**, 353-60.

Kennedy, L., Glesaaen, E., Palibrk, V., Pannone, M., Wang, W., Al-Jabri, A., Suganthan, R., Meyer, N., Austbø, M., Lin, X. et al. (2022). Lactate receptor HCAR1 regulates neurogenesis and microglia activation after neonatal hypoxia-ischemia. *Elife.* **11**, e76451.

Kiessling, A., Storebakken, T., Åsgård, T. and Kiessling, K. (1991). Changes in the structure and function of the epaxial muscle of rainbow trout (*Oncorhynchus mykiss*) in relation to ration and age: I. Growth dynamics. *Aquaculture* **93**, 335-56.

Kiessling, K.-H. and Kiessling, A. (1993). Selective utilization of fatty acids in rainbow trout (*Oncorhynchus mykiss* Walbaum) red muscle mitochondria. *Can J Zoo.* **71**, 248-51.

Kim, I., Park, S., Kim, Y., Chang, Y., Choi, C., Suh, S. and Wolfe, R. (2020). *In Vivo* and *In Vitro* Quantification of Glucose Kinetics: From Bedside to Bench. *Endocrinol Metab (Seoul).* **35**, 733-49.

Kimura, I., Ichimura, A., Ohue-Kitano, R. and Igarashi, M. (2020). Free Fatty Acid Receptors in Health and Disease. *Physiol Rev.* **100**, 171-210.

Kirchner, S., Panserat, S., Lim, P., Kaushik, S. and Ferraris, R. (2008). The role of hepatic, renal and intestinal gluconeogenic enzymes in glucose homeostasis of juvenile rainbow trout. *J. Comp. Physiol. B Biochem. Syst. Environ. Physiol.* **178**, 429-38.

Kittilson, J., Reindl, K. and Sheridan, M. (2011). Rainbow trout (*Oncorhynchus mykiss*) possess two hormone-sensitive lipase-encoding mRNAs that are differentially expressed and independently regulated by nutritional state. *Comp Biochem Physiol A Mol Integr Physiol.* **158**, 52-60.

Klein, S., Weber, J.-M., Coyle, E. and Wolfe, R. (1996). Effect of endurance training on glycerol kinetics during strenuous exercise in humans. *Metabolism.* **45**, 357-61.

Klip, A. (2009). The many ways to regulate glucose transporter 4. *Appl Physiol Nutr Metab.* **34**, 481-7.

Knudsen, L., Hansen, B., Jensen, P., Pedersen, T., Vestergaard, K., Schäffer, L., Blagoev, B., Oleksiewicz, M., Kiselyov, V. and De Meyts, P. (2012). Agonism and antagonism at the insulin receptor. *PLoS One.* **7**.

Kostyniuk, D., Culbert, B., Mennigen, J. and Gilmour, K. (2018). Social status affects lipid metabolism in rainbow trout, *Oncorhynchus mykiss*. *Am J Physiol Regul Integr Comp Physiol.* **315**, R241-R255.

Kostyniuk, D., Marandel, L., Jubouri, M., Dias, K., de Souza, R., Zhang, D., Martyniuk, C., Panserat, S. and Mennigen, J. (2019a). Profiling the rainbow trout hepatic miRNAome under diet-induced hyperglycemia. *Physiol Genomics* **51**, 411-31.

Kostyniuk, D., Zhang, D., Martyniuk, C., Gilmour, K. and Mennigen, J. (2019b). Social status regulates the hepatic miRNAome in rainbow trout: Implications for posttranscriptional regulation of metabolic pathways. *PLoS One.* **14**, e0217978.

Kozlova, T. (1998). Lipid class composition of benthic-pelagic fishes (*Cottocomephorus, Cottoidei*) from Lake Baikal. *Fish Physiol Biochem.* **19**, 211-216.
Krishnan, J. and Rohner, N. (2019). Sweet fish: Fish models for the study of hyperglycemia and diabetes. *J Diabetes.* **11**, 193-203.
Kristinsson, H., Smith, D., Bergsten, P. and Sargsyan, E. (2013). FFAR1 is involved in both the acute and chronic effects of palmitate on insulin secretion. *Endocrinology.* **154**, 4078-88.
Kuei, C., Yu, J., Zhu, J., Wu, J., Zhang, L., Shih, A., Mirzadegan, T., Lovenberg, T. and Liu, C. (2011). Study of GPR81, the lactate receptor, from distant species identifies residues and motifs critical for GPR81 functions. *Mol Pharmacol.* **80**, 848-58.
Kulyté, A., Lundbäck, V., Arner, P., Strawbridge, R. and Dahlman, I. (2022). Shared genetic loci for body fat storage and adipocyte lipolysis in humans. *Sci Rep.* **12**, 3666.
Ladu, M., Kapsas, H. and Palmer, W. (1991). Regulation of lipoprotein lipase in muscle and adipose tissue during exercise. *J Appl Physiol.* **71**, 404-9.
Lanctin, H., McMorran, L. and Driedzic, W. (1980). Rates of glucose and lactate oxidation by the perfused isolated trout (*Salvelinus fontinalis*) heart. *Can J Zool.*
Langfort, J., Donsmark, M., Ploug, T., Holm, C. and Galbo, H. (2003). Hormone-sensitive lipase in skeletal muscle: regulatory mechanisms. *Acta Physiol Scand.* **178**, 397-403.
Lansard, M., Panserat, S., Plagnes-Juan, E., Seiliez, I. and Skiba-Cassy, S. (2010). Integration of insulin and amino acid signals that regulate hepatic metabolism-related gene expression in rainbow trout: role of TOR. *Amino Acids.* **39**, 801-10.
Lauff, R. and Wood, C. (1997). Effects of training on respiratory gas exchange, nitrogenous waste excretion, and fuel usage during aerobic swimming in juvenile rainbow trout (O*ncorhynchus mykiss)*. *Can J Fish Aquat Sci.* **54**, 566-71.
Lech, J. (1970). Glycerol kinase and glycerol utilization in trout (*Salmo gairdneri*) liver. *Comp Biochem Physiol.* **34**, 117-24.
Legate, N., Bonen, A. and Moon, T. (2001). Glucose tolerance and peripheral glucose utilization in rainbow trout (*Oncorhynchus mykiss*), American eel (*Anguilla rostrata*), and black bullhead catfish (*Ameiurus melas*). *Gen Comp Endocrinol.* **122**, 48-59.
Li, R.-X., Zhou, W.-H., Ren, J., Wang, J., Qiao, F., Zhang, M.-L. and Du, Z.-Y. (2022). Dietary sodium lactate promotes protein and lipid deposition through increasing energy supply from glycolysis in Nile tilapia (*Oreochromis niloticus*). *Aquaculture* **550**.
Liemburg-Apers, D., Imamura, H., Forkink, M., Nooteboom, M., Swarts, H., Brock, R., Smeitink, J., Willems, P. and Koopman, W. (2011). Quantitative glucose and ATP sensing in mammalian cells. *Pharm Res.* **28**, 2745-57.
Liu, C., Ke, P., Zhang, J., Zhang, X. and Chen, X. (2020). Protein Kinase Inhibitor Peptide as a Tool to Specifically Inhibit Protein Kinase A. *Front Physiol.* **25**, 574030.

Liu, C., Wu, J., Zhu, J., Kuei, C., Yu, J., Shelton, J., Sutton, S., Li, X., Yun, S., Mirzadegan, T. et al. (2009). Lactate inhibits lipolysis in fat cells through activation of an orphan G-protein-coupled receptor, GPR81. *J Biol Chem.* **284**, 2811-2822.

Liu, J., Plagnes-Juan, E., Geurden, I., Panserat, S. and Marandel, L. (2017). Exposure to an acute hypoxic stimulus during early life affects the expression of glucose metabolism-related genes at first-feeding in trout. *Sci Rep.* **7**, 363.

Liu, Z., Zhang, L., Qian, C., Zhou, Y., Yu, Q., Yuan, J., Lv, Y., Zhang, L., Chang, X., Li, Y. et al. (2022). Recurrent hypoglycemia increases hepatic gluconeogenesis without affecting glycogen metabolism or systemic lipolysis in rat. *Metabolism.* **136**.

London, E., Bloyd, M. and Stratakis, C. (2020). PKA functions in metabolism and resistance to obesity: lessons from mouse and human studies. *J Endocrinol.* **246**, R51-R64.

Longhitano, L., Vicario, N., Tibullo, D., Giallongo, C., Broggi, G., Caltabiano, R., Barbagallo, G., Altieri, R., Baghini, M., Di Rosa, M. et al. (2022). Lactate Induces the Expressions of MCT1 and HCAR1 to Promote Tumor Growth and Progression in Glioblastoma. *Front Oncol.* **12**, 871798.

Magnoni, L., Patterson, D., Farrell, A. and Weber, J.-M. (2006). Effects of long-distance migration on circulating lipids of sockeye salmon (O*ncorhynchus nerka)*. *Can. J. Fish. Aquat. Sci.* **63**, 1822 - 1829.

Magnoni, L., Vaillancourt, E. and Weber, J.-M. (2008a). High resting triacylglycerol turnover of rainbow trout exceeds the energy requirements of endurance swimming. *Am J Physiol Regul Integr Comp Physiol.* **295**, R309-15.

Magnoni, L., Vaillancourt, E. and Weber, J.-M. (2008b). In vivo regulation of rainbow trout lipolysis by catecholamines. *J Exp Biol.* **211**, 2460-6.

Magnoni, L. and Weber, J.-M. (2007). Endurance swimming activates trout lipoprotein lipase: plasma lipids as a fuel for muscle. *J Exp Biol.* **210**, 4016-23.

Maillet, D. and Weber, J.-M. (2006). Performance-enhancing role of dietary fatty acids in a long-distance migrant shorebird: the semipalmated sandpiper. *J Exp Biol.* **209**, 2686-95.

Malak, N., Brichon, G., Meister, R. and Zwingelstein, G. (1989). Environmental temperature and metabolism of the molecular species of phosphatidylcholine in the tissues of the rainbow trout. *Lipids* **24**, 318-324.

Marandel, L., Kostyniuk, D., Best, C., Forbes, J., Liu, J., Panserat, S. and Mennigen, J. (2019). Pck-ing up steam: Widening the salmonid gluconeogenic gene duplication trail. *Gene.* **698**, 129-40.

Marras, S., Killen, S., Domenici, P., Claireaux, G. and McKenzie, D. (2013). Relationships among traits of aerobic and anaerobic swimming performance in individual European sea bass, *Dicentrarchus labrax*. *PLoS One.* **8**.

Marín-Juez, R., Diaz, M., Morata, J. and Planas, J. (2013). Mechanisms regulating GLUT4 transcription in skeletal muscle cells are highly conserved across vertebrates. *PLoS One.* **8**, e80628.

Mauerwerk, M., Zadinelo, I. and Meurer, F. (2020). Use of glycerol in fish nutrition: a review. *Rev Aquac.* **13**, 853-61.

McClelland, G. (2004). Fat to the fire: the regulation of lipid oxidation with exercise and environmental stress. *Comp Biochem Physiol B Biochem Mol Biol.* **139**, 443-60.
McClelland, G., Hochachka, P., Reidy, S. and Weber, J. (2001). High-altitude acclimation increases the triacylglycerol/fatty acid cycle at rest and during exercise. *Am J Physiol.* **281**, E537-44.
McKenzie, D. (2011). Swimming and other activities | Energetics of Fish Swimming. *Fish Physiol.* **3**, 1636-44.
McWilliams, S., Guglielmo, C., Pierce, B. and Klaassen, M. (2004). Flying, fasting, and feeding in birds during migration: a nutritional and physiological ecology perspective. *J. Avian Biol.* **35**, 377-93.
Mennigen, J., Panserat, S., Larquier, M., Plagnes-Juan, E., Medale, F., Seiliez, I. and Skiba-Cassy, S. (2012). Postprandial regulation of hepatic microRNAs predicted to target the insulin pathway in rainbow trout. *PLoS One.* **7**.
Mennigen, J., Plagnes-Juan, E., Figueredo-Silva, C., Seiliez, I., Panserat, S. and Skiba-Cassy, S. (2014). Acute endocrine and nutritional co-regulation of the hepatic omy-miRNA-122b and the lipogenic gene *fas* in rainbow trout, *Oncorhynchus mykiss*. *Comp Biochem Physiol B Biochem Mol Biol.* **169**, 16-24.
Miller, B., Fattor, J., Jacobs, K., Horning, M., Navazio, F., Lindinger, M. and Brooks, G. (2002a). Lactate and glucose interactions during rest and exercise in men: effect of exogenous lactate infusion. *J Physiol.* **544**, 963-75.
Miller, B., Fattor, J., Jacobs, K., Horning, M., Suh, S., Navazio, F. and Brooks, G. (2002b). Metabolic and cardiorespiratory responses to "the lactate clamp". *Am J Physiol Endocrinol Metab. 2002 Nov;283(5):E889-98* **283**, E889-98.
Milligan, C. and Farrell, A. (1991). Lactate Utilization by an *In Situ* Perfused Trout Heart: Effects of Workload and Blockers of Lactate Transport. *J Exp Biol.* **155**, 357-73.
Milligan, C. and Girard, S. (1993). Lactate metabolism in rainbow trout *J Exp Biol.* **180**, 175-193.
Modaressi, S., Brechtel, K., Christ, B. and Jungermann, K. (1998). Human mitochondrial phosphoenolpyruvate carboxykinase 2 gene. Structure, chromosomal localization and tissue-specific expression. *Biochem J.* **333**, 359-66.
Moon, T. (2001). Glucose intolerance in teleost fish: fact or fiction? *Comp Biochem Physiol B Biochem Mol Biol.* **129**, 243-9.
Mommsen, T. P., Walsh, P. and Moon, T. (1985). Gluconeogenesis in hepatocytes and kidneys of Atlantic salmon. *Mol Physiol.* **8**, 89-100.
Moniri, N. (2016). Free-fatty acid receptor-4 (GPR120): Cellular and molecular function and its role in metabolic disorders. *Biochem Pharmacol.* **110-111**, 1-15.
Méndez-Lucas, A., Duarte, J., Sunny, N., Satapati, S., He, T., Fu, X., Bermúdez, J., Burgess, S. and Perales, J. (2013). PEPCK-M expression in mouse liver potentiates, not replaces, PEPCK-C mediated gluconeogenesis. *J Hepatol.* **59**, 105-13.
Navale, A. and Paranjape, A. (2016). Glucose transporters: physiological and pathological roles. *Biophys Rev.* **8**, 5-9.

Nayak, J., Viswanathan Nair, P., Ammu, K. and Mathew, S. (2003). Lipase activity in different tissues of four species of fish: rohu (*Labeo rohita* Hamilton), oil sardine (*Sardinella longiceps* Linnaeus), mullet (*Liza subviridis* Valenciennes) and Indian mackerel (*Rastrelliger kanagurta* Cuvier). *J Sci Food Agric.* **83**, 1139-42.

Naylor, R., Hardy, R., Bureau, D., Chiu, A., Elliott, M., Farrell, A., Forster, I., Gatlin, D., Goldburg, R., Hua, K. et al. (2009). Feeding aquaculture in an era of finite resources. *Proc Natl Acad Sci U S A.* **106**, 15103-10.

Newsholme, E. and Taylor, K. (1969). Glycerol kinase activities in muscles from vertebrates and invertebrates. *Biochem J.* **112**, 465-74.

Offermanns, S. (2014). Free fatty acid (FFA) and hydroxy carboxylic acid (HCA) receptors. *Annu Rev Pharmacol Toxicol.* **54**, 407-34.

Offermanns, S., Colletti, S., Lovenberg, T., Semple, G., Wise, A. and Ijzerman, A. (2011). Nomenclature and Classification of Hydroxy-carboxylic Acid Receptors (GPR81, GPR109A, and GPR109B). *Pharmacol Rev.* **63**, 269-90.

Okamoto, H., Cavino, K., Na, E., Krumm, E., Kim, S., Cheng, X., Murphy, A., Yancopoulos, G. and Gromada, J. (2017). Glucagon receptor inhibition normalizes blood glucose in severe insulin-resistant mice. *Proc Natl Acad Sci U S A.* **114**, 2753-2758.

Omlin, T., Langevin, K. and Weber, J.-M. (2014). Exogenous lactate supply affects lactate kinetics of rainbow trout, not swimming performance. *Am J Physiol Regul Integr Comp Physiol.* **307**, R1018-24.

Omlin, T. and Weber, J.-M. (2010). Hypoxia stimulates lactate disposal in rainbow trout. *J Exp Biol.* **213**, 3802-9.

Omlin, T. and Weber, J.-M. (2013). Exhausting exercise and tissue-specific expression of monocarboxylate transporters in rainbow trout. *Am J Physiol Regul Integr Comp Physiol.* **304**, R1036-43.

On, S., Kim, HY., Kim, HS., Park, J. and Kang, KW. (2019). Involvment of G-protein-coupled receptor 40 in the inhibitory effects of docosahexaenoic acid on SREBP1-mediated lipogenic enzyme expression in primary hepatocytes. *Int. J. Mol. Sci.* **20**, 2625

Pagnon, J., Matzaris, M., Stark, R., Meex, R., Macaulay, S., Brown, W., O'Brien, P., Tiganis, T. and Watt, M. (2012). Identification and functional characterization of protein kinase A phosphorylation sites in the major lipolytic protein, adipose triglyceride lipase. *Endocrinology.* **153**, 4278-89.

Pagnotta, A. and Milligan, C. (1991). The role of blood glucose in the restoration of muscle glycogen during recovery from exhaustive exercise in rainbow trout (*Oncorhynchus mykiss*) and winter flounder (*Pseudopleuronectes americanus*). *J Exp Biol.* **161**, 489-508.

Panserat, S., Médale, F., Blin, C., Brèque, J., Vachot, C., Plagnes-Juan, E., Gomes, E., Krishnamoorthy, R. and Kaushik, S. (2000). Hepatic glucokinase is induced by dietary carbohydrates in rainbow trout, gilthead seabream, and common carp. *Am J Physiol Regul Integr Comp Physiol.* **278**, R1164-70.

Panserat, S., Plagnes-Juan, E., Gazzola, E., Palma, M., Magnoni, L., Marandel, L. and Viegas, I. (2020). Hepatic Glycerol Metabolism-Related Genes in Carnivorous Rainbow Trout (*Oncorhynchus mykiss*): Insights Into Molecular Characteristics, Ontogenesis, and Nutritional Regulation. *Front Physiol.* **31**, 882.

Patel, P. and Woodgett, J. (2017). Glycogen Synthase Kinase 3: A Kinase for All Pathways? *Curr Top Dev Biol.* **123**, 277-302.

Pereira, C., Vijayan, M., Storey, K., Jones, R. and Moon, T. (1995). Role of glucose and insulin in regulating glycogen synthase and phosphorylase activities in rainbow trout hepatocytes. *J Comp Physiol B.* **165**, 62-70.

Petersen, M., Vatner, D. and Shulman, G. (2017). Regulation of hepatic glucose metabolism in health and disease. *Nat Rev Endocrinol.* **13**, 572-87.

Philp, A., Macdonald, A. and Watt, P. (2005). Lactate--a signal coordinating cell and systemic function. *J Exp Biol.* **208**, 4561-75.

Pierce, K., Premont, R. and Lefkowitz, R. (2002). Seven- transmembrane receptors. *Nat Rev Mol Cell Biol.* **3**, 639-50.

Plagnes-Juan, E., Lansard, M., Seiliez, I., Médale, F., Corraze, G., Kaushik, S., Panserat, S. and Skiba-Cassy, S. (2008). Insulin regulates the expression of several metabolism-related genes in the liver and primary hepatocytes of rainbow trout (*Oncorhynchus mykiss*). *J Exp Biol.* **211**, 2510-8.

Plisetskaya, E. (1989). Physiology of fish endocrine pancreas. *Fish Physiol Biochem.* **7**, 39-48.

Plisetskaya, E. (1998). Some of my not so favorite things about insulin and insulin-like growth factors in fish. *Comp Biochem Physiol B Biochem Mol Biol.* **121**, 3-11.

Polakof, S., Moon, T., Aguirre, P., Skiba-Cassy, S. and Panserat, S. (2010). Effects of insulin infusion on glucose homeostasis and glucose metabolism in rainbow trout fed a high-carbohydrate diet. *J Exp Biol.* **213**, 4151-7.

Polakof, S., Panserat, S., Soengas, J. and Moon, T. (2012). Glucose metabolism in fish: a review. *J Comp Physiol B.* **182**, 1015-45.

Polakof, S. and Soengas, J. (2008). Involvement of lactate in glucose metabolism and glucosensing function in selected tissues of rainbow trout. *J Exp Biol.* **211**, 1075-86.

Pollak, N., Jaeger, D., Kolleritsch, S., Zimmermann, R., Zechner, R., Lass, A. and Haemmerle, G. (2015). The interplay of protein kinase A and perilipin 5 regulates cardiac lipolysis. *J Biol Chem.* **290**, 1295-306.

Psichas, A., Larraufie, P., Goldspink, D., Gribble, F. and Reimann, F. (2017). Chylomicrons stimulate incretin secretion in mouse and human cells. *Diabetologia.* **60**, 2475-85.

Ranganathan, G., Unal, R., Pokrovskaya, I., Yao-Borengasser, A., Phanavanh, B., Lecka-Czernik, B., Rasouli, N. and Kern, P. (2006). The lipogenic enzymes DGAT1, FAS, and LPL in adipose tissue: effects of obesity, insulin resistance, and TZD treatment. *J Lipid Res.* **47**, 2444-50.

Richards, J., Mercado, A., Clayton, C., Heigenhauser, G. and Wood, C. Substrate utilization during graded aerobic exercise in rainbow trout. *J Exp Biol.* **205**, 2067-77.

Richards, J., Mercado, A., Clayton, C., Heigenhauser, G. and Wood, C. (2002). Substrate utilization during graded aerobic exercise in rainbow trout. *J Exp Biol.* **205**, 2067-77.

Rito, J., Viegas, I., Pardal, M., Meton, I., Baanante, I. and Jones, J. (2019). Utilization of glycerol for endogenous glucose and glycogen synthesis in seabass (*Dicentrarchus labrax*): A potential mechanism for sparing amino acid catabolism in carnivorous fish. *Aquac.* **498**, 488-95.

Roberts, T., Weber, J., Hoppeler, H., Weibel, E. and Taylor, C. (1996). Design of the oxygen and substrate pathways. II. Defining the upper limits of carbohydrate and fat oxidation. *J Exp Biol.* **199**, 1651-8.

Rodríguez, C., Acosta, C., Badía, P., Cejas, J., Santamaría, F. and Lorenzo, A. (2004). Assessment of lipid and essential fatty acids requirements of black seabream (*Spondyliosoma cantharus*) by comparison of lipid composition in muscle and liver of wild and captive adult fish. *Comp Biochem Physiol B Biochem Mol Biol.* **139**, 619-29.

Romijn, J., Coyle, E., Sidossis, L., Rosenblatt, J. and Wolfe, R. (2000). Substrate metabolism during different exercise intensities in endurance-trained women. *J Appl Physiol.* **88**, 1707-14.

Rooney, K. and Trayhurn, P. (2011). Lactate and the GPR81 receptor in metabolic regulation: implications for adipose tissue function and fatty acid utilisation by muscle during exercise. *Br J Nutr.* **106**, 1310-6.

Roy, J., Barank, E., Mercier, Y., Larroquet, L., Surget, A., Ganot, A., Sandres, F., Lanuque, A., Terrier, F. and Braind, L. (2022). Involvement of Taste Receptors in the Oro-Sensory Perception of Nutrients in Rainbow Trout (*Oncorhynchus mykiss*) Fed Diets with Different Fatty Acid Profiles. *Aquac Nutr.*, 1152463.

Rozovski, U., Grgurevic, S., Bueso-Ramos, C., Harris, D., Li, P., Liu, Z., Wu, J., Jain, P., Wierda, W., Burger, J. et al. (2015). Aberrant LPL Expression, Driven by STAT3, Mediates Free Fatty Acid Metabolism in CLL Cells. *Mol Cancer Res.* **13**, 944-53.

Saera-Vila, A., Calduch-Giner, J., Gómez-Requeni, P., Médale, F., Kaushik, S. and Pérez-Sánchez, J. (2005). Molecular characterization of gilthead sea bream (*Sparus aurata*) lipoprotein lipase. Transcriptional regulation by season and nutritional condition in skeletal muscle and fat storage tissues. *Comp Biochem Physiol B Biochem Mol Biol.* **142**, 224-32.

Satapati, S., Qian, Y., Wu, M., Petrov, A., Dai, G., Wang, S., Zhu, Y., Shen, X., Muise, E., Chen, Y. et al. (2017). GPR120 suppresses adipose tissue lipolysis and synergizes with GPR40 in antidiabetic efficacy. *J Lipid Res.* **58**, 1561-78.

Schäffer, L., Brand, C., Hansen, B., Ribel, U., Shaw, A., Slaaby, R. and Sturis, J. (2008). A novel high-affinity peptide antagonist to the insulin receptor. *Biochem Biophys Res Commun.* **376**, 380-3.

Secor, J., Fligor, S., Tsikis, S., Yu, L. and Puder, M. (2021). Free Fatty Acid Receptors as Mediators and Therapeutic Targets in Liver Disease. *Front Physiol.* **12**, 656441.

Seidelin, K. (1995). Fatty acid composition of adipose tissue in humans. Implications for the dietary fat-serum cholesterol-CHD issue. *Prog Lipid Res.* **34**, 199-217.

Seiliez, I., Gabillard, J., Skiba-Cassy, S., Garcia-Serrana, D., Gutiérrez, J., Kaushik, S., Panserat, S. and Tesseraud, S. (2008). An in vivo and in vitro assessment of TOR signaling cascade in rainbow trout (*Oncorhynchus mykiss*). *Am J Physiol Regul Integr Comp Physiol.* **295**, R329-35.

Seiliez, I., Panserat, S., Lansard, M., Polakof, S., Plagnes-Juan, E., Surget, A., Dias, K., Larquier, M., Kaushik, S. and Skiba-Cassy, S. (2011a). Dietary carbohydrate-to-protein ratio affects TOR signaling and metabolism-related gene expression in the liver and muscle of rainbow trout after a single meal. *Am J Physiol Regul Integr Comp Physiol.* **300**, R733-43.

Seiliez, I., Panserat, S., Skiba-Cassy, S. and Polakof, S. (2011b). Effect of acute and chronic insulin administrations on major factors involved in the control of muscle protein turnover in rainbow trout (*Oncorhynchus mykiss*). *Gen Comp Endocrinol.* **172**, 363-70.

Shanghavi, D. and Weber, J.-M. (1999). Effects of sustained swimming on hepatic glucose production of rainbow trout. *J Exp Biol.* **202**, 2161-2166.

Sheridan, M. (1988). Lipid dynamics in fish: aspects of absorption, transportation, deposition and mobilization. *Comp Biochem Physiol B.* **90**, 679-90.

Simpson, F., Whitehead, J. and James, D. (2001). GLUT4--at the cross roads between membrane trafficking and signal transduction. *Traffic.* **2**, 2-11.

Sjarif, D., Ploos van Amstel, J., Duran, M., Beemer, F. and Poll-The, B. (2000). solated and contiguous glycerol kinase gene disorders: a review. *J Inherit Metab Dis.* **23**, 529-47.

Soengas, J. and Aldegunde, M. (2002). Energy metabolism of fish brain. *Comp Biochem Physiol B Biochem Mol Biol.* **131**, 271-96.

Sohn, J., Lee, Y., Han, J., Jeon, Y., Kim, J., Choe, S., Kim, S., Yoo, H. and Kim, J. (2018). Perilipin 1 (Plin1) deficiency promotes inflammatory responses in lean adipose tissue through lipid dysregulation. *J Biol Chem.* **293**, 13974-13988.

Speers-Roesch, B. and Treberg, J. (2010). The unusual energy metabolism of elasmobranch fishes. *Comp Biochem Physiol A Mol Integr Physiol.* **155**, 417-34.

Stark, R. and Kibbey, R. (2014). The mitochondrial isoform of phosphoenolpyruvate carboxykinase (PEPCK-M) and glucose homeostasis: has it been overlooked? *Biochim Biophys Acta.* **1840**, 1313-30.

Steele, R. (1959). Influences of glucose loading and of injected insulin on hepatic glucose output. *Ann N Y Acad Sci.* **82**, 420-30.

Steneberg, P., Rubins, N., Bartoov-Shifman, R., Walker, M. and Edlund, H. (2005). The FFA receptor GPR40 links hyperinsulinemia, hepatic steatosis, and impaired glucose homeostasis in mouse. *Cell Metab.* **1**, 245-58.

Strålfors, P., Björgell, P. and Belfrage, P. (1984). Hormonal regulation of hormone-sensitive lipase in intact adipocytes: identification of phosphorylated sites and effects on the phosphorylation by lipolytic hormones and insulin. *Proc Natl Acad Sci U S A.* **81**, 3317-21.

Stubhaug, I., Frøyland, L. and Torstensen, B. (2005). beta-Oxidation capacity of red and white muscle and liver in Atlantic salmon (*Salmo salar L.*)--effects of increasing dietary rapeseed oil and olive oil to replace capelin oil. *Lipids.* **40**, 39-47.

Sun, J., Ye, X., Xie, M. and Ye, J. (2016). Induction of triglyceride accumulation and mitochondrial maintenance in muscle cells by lactate. *Scientific Reports* **6**, 33732.
Sun, S., Li, H., Chen, J. and Qian, Q. (2017). Lactic Acid: No Longer an Inert and End-Product of Glycolysis. *Physiology (Bethesda)* **32**, 453-463.
Surette, M. (2008). The science behind dietary omega-3 fatty acids. *CMAJ.* **178**, 177-80.
Tang, N., Zhang, X., Chen, D. and Li, Z. (2021). The Controversial Role of Adiponectin in Appetite Regulation of Animals. *Nutrients.* **13**, 3387.
Teng, D., Zhou, Y., Tang, Y., Liu, G. and Tu, Y. (2022). Mechanistic Studies on the Stereoselectivity of FFAR1 Modulators. *J Chem Inf Model.* **62**, 3664-75.
Terjung, R. and Kaciuba-Usciłko, H. (1986). Lipid metabolism during exercise: influence of training. *Diabetes Metab Rev.* **2**, 35-51.
Teulier, L., Omlin, T. and Weber, J.-M. (2013). Lactate kinetics of rainbow trout during graded exercise: do catheters affect the cost of transport? *J Exp Biol.* **216**, 4549-56.
Thiébaud, D., DeFronzo, R., Jacot, E., Golay, A., Acheson, K., Maeder, E., Jéquier, E. and Felber, J. (1982). Effect of long chain triglyceride infusion on glucose metabolism in man. *Metabolism* **31**, 1128-36.
Thompson, B., Lobo, S. and Bernlohr, D. (2010). Fatty acid flux in adipocytes: the in's and out's of fat cell lipid trafficking. *Mol Cell Endocrinol.* **318**, 24-33.
Thomsen, M., Lefevre, S., Nilsson, G., Wang, T. and Bayley, M. (2019). Effects of lactate ions on the cardiorespiratory system in rainbow trout (*Oncorhynchus mykiss*). *Am J Physiol Regul Integr Comp Physiol.* **316**.
Tikhonova, I. (2017). Application of GPCR Structures for Modelling of Free Fatty Acid Receptors. *Handb Exp Pharmacol.* **236**, 57-77.
Tocher, D. (2003). Metabolism and Functions of Lipids and Fatty Acids in Teleost Fish. *Rev Fish Sci.* **11**, 107-184.
Turenne, E. and Weber, J.-M. (2018). Lean, mean, lipolytic machines: lipid mobilization in rainbow trout during graded swimming. *J Exp Biol.* **221**.
van Loon, L., Greenhaff, P., Constantin-Teodosiu, D., Saris, W. and Wagenmakers, A. (2001). The effects of increasing exercise intensity on muscle fuel utilisation in humans. *J Physiol.* **536**, 295–304.
Velasco, C., Conde-Sieira, M., Comesaña, S., Chivite, M., Díaz-Rúa, A., Míguez, J. and Soengas, J. (2020). The long-chain fatty acid receptors FFA1 and FFA4 are involved in food intake regulation in fish brain. *J Exp Biol.* **223**, jeb227330.
Vikram, A. and Jena, G. (2010). S961, an insulin receptor antagonist causes hyperinsulinemia, insulin-resistance and depletion of energy stores in rats. *Biochem Biophys Res Commun.* **398**, 260-5.
Wahren, J., Felig, P., Ahlborg, G. and Jorfeldt, L. (1971). Glucose metabolism during leg exercise in man. *J Clin Invest.* **50**, 2715-25.
Wang, Y., Wright, P., Heigenhauser, G. and Wood, C. (1997). Lactate transport by rainbow trout white muscle: kinetic characteristics and sensitivity to inhibitors. *Am J Physiol Regul Integr Comp Physiol.* **272**, R1577-87.
Watanabe, T. (1982). Lipid nutrition in fish. *Comp Biochem Physiol B, Biochem Mol Biol* **73**, 3-15.

Watt, P., MacLennan, P., Hundal, H., Kuret, C. and Rennie, M. (1988). L(+)-lactate transport in perfused rat skeletal muscle: kinetic characteristics and sensitivity to pH and transport inhibitors. *Biochim Biophys Acta.* **944**, 213-22.

Weber, JM, Roberts, TJ, Vock, R, Weibel, ER and Taylor, C. (1996). Design of the oxygen and substrate pathways. III. Partitioning energy provision from carbohydrates. *J Exp Biol.* **199**, 1659-66.

Weber, J.-M. (2011). Metabolic fuels: regulating fluxes to select mix. *J Exp Biol.* **214**.

Weber, J.-M., Brichon, G. and Zwingelstein, G. (2003). Fatty acid metabolism in rainbow trout (*Oncorhynchus mykiss*) tissues: differential incorporation of palmitate and oleate. *Can J Fish Aquat.* .

Weber, J.-M., Choi, K., Gonzalez, A. and Omlin, T. (2016). Metabolic fuel kinetics in fish: swimming, hypoxia and muscle membranes. *J Exp Biol.* **219**, 250-8.

Weber, J.-M. and Reidy, S. (2012). Extending food deprivation reverses the short-term lipolytic response to fasting: role of the triacylglycerol/fatty acid cycle. *J Exp Biol.* **215**, 1484-90.

Weber, J.-M., Roberts, T. and Taylor, C. (1993). Mismatch between lipid mobilization and oxidation: glycerol kinetics in running African goats. *Am J Physiol.* **264**, R797-803.

Weber, J.-M. and Shanghavi, D. (2000). Regulation of glucose production in rainbow trout: role of epinephrine in vivo and in isolated hepatocytes. *Am J Physiol Regul Integr Comp Physiol.* **278**, R956-63.

Weber, J.-M. and Zwingelstein, G. (1995). Chapter 2 Circulatory substrate fluxes and their regulation. *Biochem Mol Biol Fishes.* **4**, 15-32.

Wolfe, R. (1992). Radioactive and stable isotope tracers in biomedicine: Principles and practice of kinetic analysis. *New York: Wiley-Liss.* .

Wolfe, R., Klein, S., Carraro, F. and Weber, J.-M. (1990). Role of triglyceride-fatty acid cycle in controlling fat metabolism in humans during and after exercise. *Am J Physiol.* **258**, E382-9.

Wu, G., Dai, Y., Yan, Y., Zheng, X., Zhang, H., Li, H. and Chen, W. (2022). The lactate receptor GPR81 mediates hepatic lipid metabolism and the therapeutic effect of metformin on experimental NAFLDs. *Eur J Pharmacol.* **924**, 174959.

Yang, B., Zhai, G., Gong, Y., Su, J., Peng, X., Shang, G., Han, D., Jin, J., Liu, H., Du, Z. et al. (2018). Different physiological roles of insulin receptors in mediating nutrient metabolism in zebrafish. *Am J Physiol Endocrinol Metab.* **315**, E38-E51.

Yu, S., Meng, S., Xiang, M. and Ma, H. (2021). Phosphoenolpyruvate carboxykinase in cell metabolism: Roles and mechanisms beyond gluconeogenesis. *Mol Metab.* **53**.

Zhang, X., Yang, S., Chen, J. and Su, Z. (2019). Unraveling the regulation of hepatic gluconeogenesis. *Front Endocrinol (Lausanne)* **9**.

Zhou, L., Chen, S., Han, H. and Sun, J. (2021). Lactate augments intramuscular triglyceride accumulation and mitochondrial biogenesis in rats. *J Biol Regul Homeost Agents.* **35**, 105-115.